Glutathione and the Cytosolic Heme Pool

Rawlinson, Rosemary Julia

Awarding institution:
King's College London

Glutathione and the Cytosolic Heme Pool

Rosemary Rawlinson

In fulfillment of the requirement

for the degree of Doctor of Philosophy (PhD)

in Pharmaceutical Sciences

Institute of Pharmaceutical Science

King's College London

London

SE1 9NH

September 2017

Acknowledgments

Firstly, my upmost thanks and gratitude goes to my supervisors for their continued support and guidance throughout this project. To Professor Robert Hider for his tireless support throughout my time at King's, his unwavering trust in my scientific capabilities and his assistance with the writing of this thesis. To Dr. Gladys Latunde-Dada for taking me on as a student and for her help with all biological aspects of this project.

My thanks go to all members of Hider's group working in lab 5.119, Franklin-Wilkins Building, especially Dr. Yu-Lin Chen for his help with affinity constants. I am also thankful to my fellow students in the chemical biology group, and my colleagues in labs 3.109 and 3.31 Franklin-Wilkins Building for their help and support throughout this project.

To my friends and family for their understanding and support throughout my time at King's. To Nadine, LIDo course administrator, for going above and beyond to help keep my PhD on track, and for the excellent socials organised, reminding us that time spend outside the lab can be just as important as time spent at the bench. To Xenia for our regular lunches that helped keep both our projects on track and our sanity intact.

Lastly, but by no means least, my heartfelt thanks goes to my partner, Alec, who has been my rock and personal cheerleader throughout my PhD journey, all whilst accomplishing his own. Without his help, support, guidance, grounding and patience this journey would not have been completed.

Thank you to the BBSRC who funded the PhD through LIDo (grant number BB/J014567/1).

Abstract

Recently glutathione (GSH) has been proposed as a key component of the cytosolic iron pool, possessing a buffering role for cytosolic iron(II), protecting it from autoxidation. However the chemical nature of the cytosolic heme pool is unknown. We have investigated whether GSH binds heme iron. If so, the resulting complex would be expected to have increased stability and solubility in aqueous solutions, compared to the extremely hydrophobic heme molecule, thereby reducing its ability to partition into membranes.

An interaction between glutathione and hematin was established with the affinity constant (K_a) of glutathione for hematin determined by absorption spectroscopy to be $5x10^4$ M^{-1}. Using standard bioassays the influence of GSH on heme oxidase activity and the partitioning of hematin into lipid bilayers was assessed. GSH was found to stabilise hematin in the presence of H_2O_2 and was found to have a profound effect on the partitioning of hematin into lipid bilayers, reducing partitioning into prepared liposomes by < 70%. The presence of hematin ligated to GSH within the lysate of mammalian cells was established using synthesised [^{59}Fe]hematin, Caco-2 cells and size exclusion HPLC. These results suggest that GSH could be the predominant ligand for the cytosolic heme pool.

The effect of glutathione on absorption and catabolism of hematin in Caco-2 cells showed an initial decrease in hematin uptake and a decrease in heme oxygenase 1 expression.

Hematin when ligated to GSH, in the presence of ascorbic acid and O_2, was found to be rapidly degraded and whilst GSH decreases hematin partitioning into erythrocyte plasma membranes, the effect was not as dramatic as was observed in liposomes. These results did not provide further support for glutathione serving as the predominant ligand for the organic iron pool and led to the conclusion that heme is chaperoned (not by glutathione) and encapsulated within endosomes in the cytosol. It is proposed that GSH and ascorbic acid function cooperatively to rapidly ligate and degrade any heme which escapes from the endosome system into the cytosol, hence preventing ferroptosis.

Contents

List of Figures

List of Tables

Abbreviations

AA	Ascorbic Acid
ALA	δ-Aminolevulinic acid
ALAS	δ-Aminolevulinic acid synthase
AMP	Adenosine monosphate
ANOVA	Analysis of variance
Arg	Arginine
ATP	Adenosine triphosphate
bp	Base pair
BSA	Bovine serum albumin
C	Cholesterol
Caco-2	Heterogeneous human epithelial colorectal adenocarcinoma cell line
cDNA	Complementary DNA
CPM	Counts per minute
Cys	Cysteine
Cys.Hematin	Hematin ligated to cysteine
DAB	Diaminobenzidine
Dcytb	Duodenal cytochrome b
ddH_2O	Double distilled water
DHA	Dehydroascorbic acid
DMEM	Dulbecco's modified Eagle media
DMSO	Dimethyl sulfoxide
DMT1	Divalent metal transporter 1
DNA	Deoxyribonucleic acid
DP	Dicetyl phosphate
EDTA	Ethylenediaminetetraacetic acid
FABP1	Fatty acid-binding protein 1
FBS	Fetal bovine serum
FLVCR1	Feline leukemia virus subgroup C receptor
Fpn1	Ferriportin 1
Ft	Ferritin
GaPPIX	Gallium Protoporphyrin
GI	Gastrointestinal

GLUTs	Na^+-independent facilitative glucose transporters
Gly	Glycine
GPX4	Glutathione peroxidase 4
GS.hematin	Hematin ligated to glutathione
GSH	Reduced glutathione
GSSG	Glutathione disulphide (oxidised glutathione)
GSTs	Glutathione S-transferases
H	Heavy
HBP1	Heme-binding protein 1
HBP23	23 kDa heme-binding protein
HEL-R	Human mature erythroid cell line
HepG2	Human liver carcinoma cells
His	Histidine
HMGB1	High mobility group box 1
HO-1	Heme oxygenase 1
Hp	Hephaestin
HPLC	High-performance liquid chromatography
HRP	Horseradish peroxidase
K562	Human erythroleukemia cell line
K_a	Affinity constant
K_d	Dissociation constant
L	Light
Maf	Musculoaponeurotic fibrosarcoma
MAREs	Maf recognition elements
MEM	Minimum essential media Eagle
MTT	3-(4,5-Dimethylthiazol-2-yl)-2,5-diphenyltetrazolium bromide
Mw	Molecular Weight
NADPH	Reduced nicotinamide adenine dinucleotide phosphate
NRK	Normal rat kidney cell line
PBS	Phosphate buffered saline
PC	Phosphatidylcholine
PCFT/HCP1	Proton-coupled folate transporter/heme carrier protein
PE	Phosphatidylethanolamine
PPIX	Protoporphyrin IX

PS	Phosphatidylserine
qPCR	Real time polymerase chain reaction
RNA	Ribonucleic acid
ROS	Reactive Oxygen Species
rpm	Revolutions per minute
SDS	Sodium dodecyl sulfate
SEM	Standard error of the mean
Sph	Sphingomyelin
SVCTs	Na^{+}-dependant vitamin C transporters
TEA	Triethylamine
TEER	Transepithelial electrical resistance
TfR1	Transferrin receptor
$tfr^{hpx/hpx}$	Homozygous hypotransferrinemia
TPL	Total phospholipid
Tris	Tris(hydroxymethyl)aminomethane
UV/vis	Ultra violet and visible
ZnMP	Zinc mesoporphyrin

1 Introduction – Iron Transport and Storage in Mammalian Cells

1.1 Background

Recently there has been interest in glutathione as a ligand for the inorganic labile iron in both the cytosol and mitochondria or mammalian cells (Hider & Kong, 2011; Hider & Kong 2012). It is postulated that a second labile iron pool is present in mammalian cells, the organic labile iron pool (Garrick *et al*., 1999; Ryter & Tyrrell, 2000; Yuan *et al*., 2016; Hanna *et al*., 2017), as organic iron is extremely important for the general management of cells. However, the chemical nature of the organic labile iron pool has not be characterised, for instance is it a low molecular weight conjugate, is it partitioned away from the cytosol or is it always ligated to proteins within the cytosol of mammalian cells.

Clearly the chemical nature of the pool can't be heme itself due to heme being a highly hydrophobic and planar molecular meaning it quickly partitions into lipid bilayers resulting in ferroptosis if the resulting lipid peroxidation is not revered. In principle heme could be ligated to glutathione due to the two vacant co-ordination sites on the heme molecule, meaning in principle glutathione could be heme in a 1:1 or 2:1 complex. Such a complex would increase heme solubility and decrease the planarity of the compound whilst stabilising the charge of the iron in the centre of the heme molecule.

This thesis investigates the possibility of glutathione ligating heme under physiological conditions. To place in a wider context the introduction chapter centres on iron, both organic and inorganic, transport and storage within mammalian cells.

1.2 Distribution of Iron in the Human

Iron is the most abundant essential micronutrient and is found in almost all living organisms. Besides oxygen transport, iron is involved in a range of cellular processes including DNA synthesis, electron transport and the regulation of transcription and translation. Furthermore it is a co-enzyme for over 400 enzymes. Cytosolic iron is found in two major forms; inorganic and organic, iron bound to the centre of protoporphyrin IX (PPIX). Inorganic iron is predominantly found in the ferrous (iron(II)) state however ferric (iron(III)), is also present. Organic iron can be found in the reduced state, heme, or oxidised state hematin, (-OH ligand) or hemin, (-Cl ligand), (Figure 1-1).

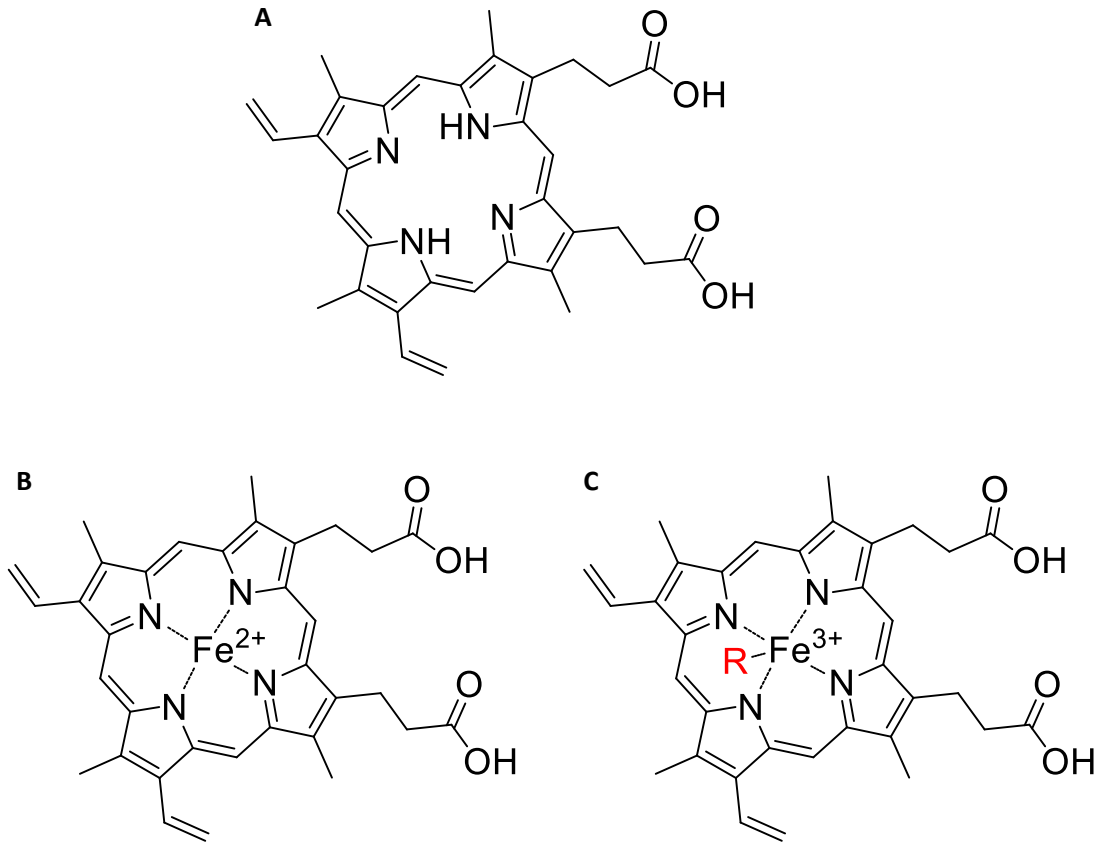

Figure 1-1. Structure of organic iron. **A** – PPIX, **B** – heme and **C** – hematin R = -OH, hemin R = -Cl.

Ninety five percent of the adult human body (70 kg) is comprised of oxygen, carbon, hydrogen and nitrogen, (Emsley, 1998; Emsley, 2011; Prashanth *et al.,* 2015). Electrolytes, the main four being; calcium, phosphorus, sulphur and potassium comprise 3.2% of the body whilst the remainder, 1.8%, is comprised of trace elements otherwise known as micronutrients.

Essential trace elements are nutrients which are required in small quantities for the healthy function of the human body. However, a small imbalance, either an excess or deficit, of essential trace elements can result in the impairment of normal biological activity leading to severe health defects (Prashanth *et al.,* 2015). Essential trace elements include; iron, copper, zinc, cobalt, manganese, selenium, fluorine and iodine. The average amount of micronutrients in a 70 kg adult and the major functions of each trace element are summarised in Table 1-1.

Table 1-1 Average Amount and Daily Intake of Trance Elements and their Main Function in the Human Body

Trace element	**Average amount in human**	**Average daily intake**	**Major functions in the body**	**Reference**
Iron	3-5 g	0.5-2 mg	Oxygen transport, electron transport, DNA synthesis, Redox centres, regulation of transcription and translation	
Copper	100 mg	2-5 mg	Cellular metabolism, including haemoglobin synthesis	
Zinc	2-3 g	15-20 mg	Spermatogenesis and maturation, neurotransmitter function, thymus development, epithelialization in wound healing, taste sensation and enzyme secretion from pancreas and stomach	Prashanth *et al.,* 2015
Chromium	6 mg	5 ng	There is currently controversy over the function of chromium but it was originally thought to be required for the biosynthesis of the glucose tolerance factor	Maret & Wedd, 2014
Cobalt	1.1 g	0.1 ng	Component of Vitamin B12	Prashanth *et al.,* 2015
Manganese	12-15 mg	2-5 mg	Component of metalloenzymes involved with the metabolism of cell signalling molecules	Prashanth *et al.,* 2015
Iodine	12-20 mg	0.1-0.5 mg	Constituent of thyroid hormones thyroxine (tetraiodothyronine and triiodothyronine).	Ahad & Ganie, 2010
Selenium	10-60 mg	0.006-0.2 mg	Selenocysteine is the 21st amino acid that is incorporated into proteins, for example glutathione peroxidases.	Maret & Wedd, 2014
Fluorine	2.6 g	0.3-0.5 mg	Bone and teeth formation	Emsley, 1998

The bone marrow produces approximately 2 million erythrocytes per second (Korolnek & Hamza, 2015). This equates to the adult human body requiring 25 mg of iron per day for erythropoiesis, however only 0.5 to 2 mg of iron is absorbed daily from the diet (Zhao & Enns 2012; Korolnek & Hamza, 2015). The remaining iron requirement is obtained from reticuloendothelial macrophages that phagocytose and degrade senescent erythrocytes, recycling the iron back to the bone marrow for erythropoiesis (Korolnek & Hamza, 2015). The relatively small amount of iron absorbed daily, predominantly in the duodenum, replaces the iron lost through urine, faeces, sweat and the sloughing of endothelial cells, predominantly those found in the gastrointestinal (GI) tract (Zhao & Enns, 2012). Within the body approximately 65-70% of iron is incorporated into haemoglobin (Andrews, 2000), 4% in myoglobin and 2% in iron-containing enzymes (Bowman & Rand, 1980). The remaining 24-29% of iron is found within the liver and spleen, reticuloendothelial macrophages and bone marrow (Andrews, 2000). The liver and spleen contain a large reservoir of iron, sequestered into ferritin, in case of a sudden increase in demand for iron. The bone marrow contains a large quantity of iron as it is the site for erythrocyte production and maturation therefore the progenitor cells for erythrocytes contain a large concentration of iron for the production of haemoglobin (Korolnek & Hamza, 2015). Iron is delivered to the bone marrow by macrophages that have engulfed and degraded senescent erythrocytes, this usually occurs 120 days after erythrocyte maturation. The macrophages engulf the erythrocytes; catabolise the haemoglobin, releasing the inorganic iron, to apo-transferrin (Andrews, 2000).

1.3 Major Functions of Iron

1.3.1 Mitochondrial Iron

Inorganic iron has many functions within the body, a major function being incorporation into protoporphyrin IX (PPIX) resulting in organic iron (heme) and the production of iron-sulfur ([Fe-S]) clusters (Figure 1-2). Organic iron synthesis is an eight step process, with the first step being the synthesis of δ-aminolevulinic acid (ALA) from glycine and succinyl-CoA in the matrix of the mitochondria (Scotto *et al*. 1982). This first step is rate limiting and catalysed by by δ-aminolevulinic acid synthase (ALAS) (Scotto *et al*. 1982; Ryter & Tyrrell, 2000). ALA is exported out of the mitochondria into the cytosol where four subsequent steps result in the formation of coproporphyrinogen III. Coprophorphyrinogen III is imported into the mitochondria for the penultimate stages in organic iron synthesis, the

oxidation and dehydrogenation of the porphyrin ring. The enzymes that catalyse the final stages of heme synthesis are associated with the inner membrane of the mitochondria (Ponka, 1997). The final step is the incorporation of Fe(II), by ferrochelatase, into PPIX resulting in the formation of heme (Ryter & Tyrrell, 2000).

The mitochondrion not only assembles [Fe-S] clusters, for incorporation into mitochondrial [Fe-S] requiring proteins, but it is also integral to the biogenesis of [Fe-S] proteins located in the nucleus and cytosol (Lill *et al.,* 2012). Iron-sulfur cluster formation within the mitochondria occurs in three main steps. Step one involves the formation of persulfide on the scaffold protein, Isu1, via the removal of sulfur from cysteine by the cysteine desulfurase complex Nfs1-Isd11 (Lill *et al.,* 2012; Pandey *et al.,* 2015). The second step is the formation of [2Fe-2S] on the Isu1 scaffold protein, the mechanism of which has still not been fully elucidated and the final step is the incorporation of [2Fe-2S] into apoproteins (Pandey *et al.,* 2015).

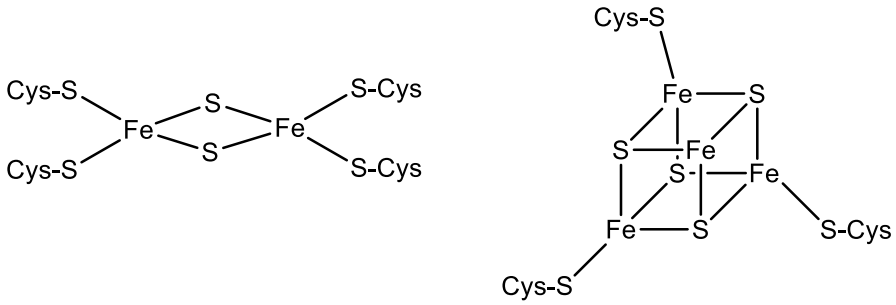

Figure 1-2. Structure of [2Fe-2S] and [4Fe-4S] clusters.

One of the major functions of [Fe-S] clusters is to facilitate the transport of electrons through the inner mitochondrial membrane during cellular respiration via mitochondrial complexes I, II and III, part of the electron transport chain (Devlin, 2002). The transfer of electrons between complexes occurs through the reduction and oxidation of iron within each complex. This movement of electrons is coupled with the transfer of protons across the inner membrane into the intermembrane space, creating a proton gradient. The resulting gradient powers the synthesis of ATP, from ADP + P_i, via the influx of protons into the mitochondrial matrix, down the proton gradient, through ATP synthase (Devlin, 2002).

1.3.2 Cytosolic Iron

There are two major classes of cytosolic enzymes that require the binding of inorganic iron; namely non iron-sulfur cluster proteins and iron-sulfur cluster proteins With the non iron-sulfur cluster proteins, iron(II) is presented to the apo enzyme and bound through three to

six ligands whilst the apo iron-sulfur enzymes are presented with an iron-sulfur cluster for incorporation (Hider & Kong, 2013).

As previously mentioned DNA synthesis requires iron. Ribonucleotide reductase is a non-identical two subunit enzyme that converts ribonucleotides to deoxyribonucleotides with an iron-tyrosine free radial centre in the second subunit. The iron-tyrosine centre consists of two iron atoms that have a six ligand co-ordination via four carboxylates and two histidine ligands (Sjöberg *et al.,* 1978). Ribonucleotide reductase expression is closely associated with the cell cycle and the enzyme widely distributed (Eriksson *et al.,* 1984).

Lipoxygenases are the class of enzymes that facilitate the functionalisation of unsaturated lipids to cell signalling agents, via oxygen attack. Lipoxygenases contain an iron molecule bound via five ligands, 3-4 histidine residues and 1-2 oxo ligands, with the sixth ligand occupied either by water or the lipid substrate (Kuban, 1998).

Dioxygen (O_2) will incorporate into organic substances without the involvement of enzymes however as the reaction rate is slow, iron(II)-dependent dioxygenases are used to increase the rate of reaction (Martinez & Hausinger, 2015). A large class of these dixoygenases use iron(II) and 2-oxoglutarate to form the desired product, with succinate and CO_2 as by-products. Iron(II)-dependent dioxygenases are used to facilitate various oxidative transformations including, but not limited to; halogenation (Vaillancourt *et al.,* 2005), desaturation (Topf *et al.,* 2004), hydroxylation as well as ring closure and expansion. These oxidative transformations are required for many vital cellular mechanisms including; post-translational modifications to collagen, metabolism of fatty acids (Wanders *et al.*, 2011) and the repair of both DNA and RNA (Trewick *et al.,* 2002).

Iron-sulfur clusters have a wide range of biochemical functions including electron transfer (Lange *et al.,* 2000), redox reactions, stabilisation of proteins and regulatory sensors (Brunelle *et al.,* 2005). The most common forms of iron-sulfur clusters are [2Fe-2S], a rhombus shape, and [4Fe-4S], a cubic shape (Lill & Muhlenhoff, 2008) (Figure 1-2).

1.3.3 Inorganic Labile Iron Pool

Williams (1982) proposed that the cytosolic inorganic labile iron pool was dominated by ferrous iron (iron(II)) due to the reducing potential of the cytosol and that the concentration of it had to be between 10^{-7} and 10^{-6} M due to the affinity constants of many cytosolic enzymes requiring iron constants to be above 10^{-8} M. Egyed and Saltman (1984) were the first to show that over 90% of the inorganic labile iron pool in the cytosol of cells

was in the reduced, iron(II) state, and both Breuer *et al.* (1995) and Petrat *et al.* (1999) confirmed this finding subsequently in different cell types. The kinetic lability of iron(II) in aqueous solutions is $3x10^4$ higher than that of iron(III), allowing for faster cellular responses from iron dependent pathways and enzymes, than if iron(III) was utilised (Helm & Merbach 2005). Furthermore the solubility of iron(II) in aqueous solutions is much higher than that of iron(III) and is less likely to form oligomeric and polymeric structures. Typical cytosolic iron concentrations fall between 1×10^{-7} and 1×10^{-6} M (Hider & Kong, 2013). Therefore, the chemistry of iron(II) supports the research findings of Egyed, Breuer and Petrat that the inorganic labile iron pool is predominantly in the ferrous state. The concentration of the inorganic labile iron pool has been shown, through the use of fluorescent probes, to be between 2×10^{-7} and 5×10^{-6} M (Breuer *et al.,* 1995; Petrat *et al.,* 1999; Zhong *et al.,* 2004) as predicted in 1982 by Williams.

1.4 Inorganic Iron Transport

1.4.1 Inorganic Iron Absorption

Primates do not have an iron excretion pathway and therefore iron homeostasis must be tightly regulated through the absorption of iron in the GI tract from the diet.

Inorganic iron is found in plant based foods, (cereal, fruit and vegetables) and makes up the majority of iron consumed; however, as inorganic iron absorption is only 5 -10% efficient it constitutes only a third of dietary iron intake, particularly In Western societies (Han, 2011). Inorganic iron, once liberated from other components of ingested food in the GI tract is predominantly in the ferric state, which is relatively insoluble, therefore, unavailable for absorption. Dietary components, such as ascorbic acid and cysteine reduce ferric iron, to the more soluble ferrous iron state (Han *et al.,* 1995; Glahn and Campen, 1997), whilst citric acid chelates ferric inorganic iron keeping it in solution (Salovaara *et al.,* 2002). Both the reduction and weak chelation of ferric inorganic iron increase the bioavailability of ingested inorganic iron by maintaining the iron in solution. Whilst numerous dietary components increase inorganic iron absorption strong inorganic iron chelators, such as tannic acid and phytate (Hallberg *et al.,* 1989; Petry *et al.,* 2014), decrease absorption through binding inorganic iron with a high affinity, rendering the iron unavailable for import via divalent metal transport 1 (DMT1) into the enterocytes. If ingested iron is not reduced to ferrous iron by dietary components, before reaching enterocytes, the brush

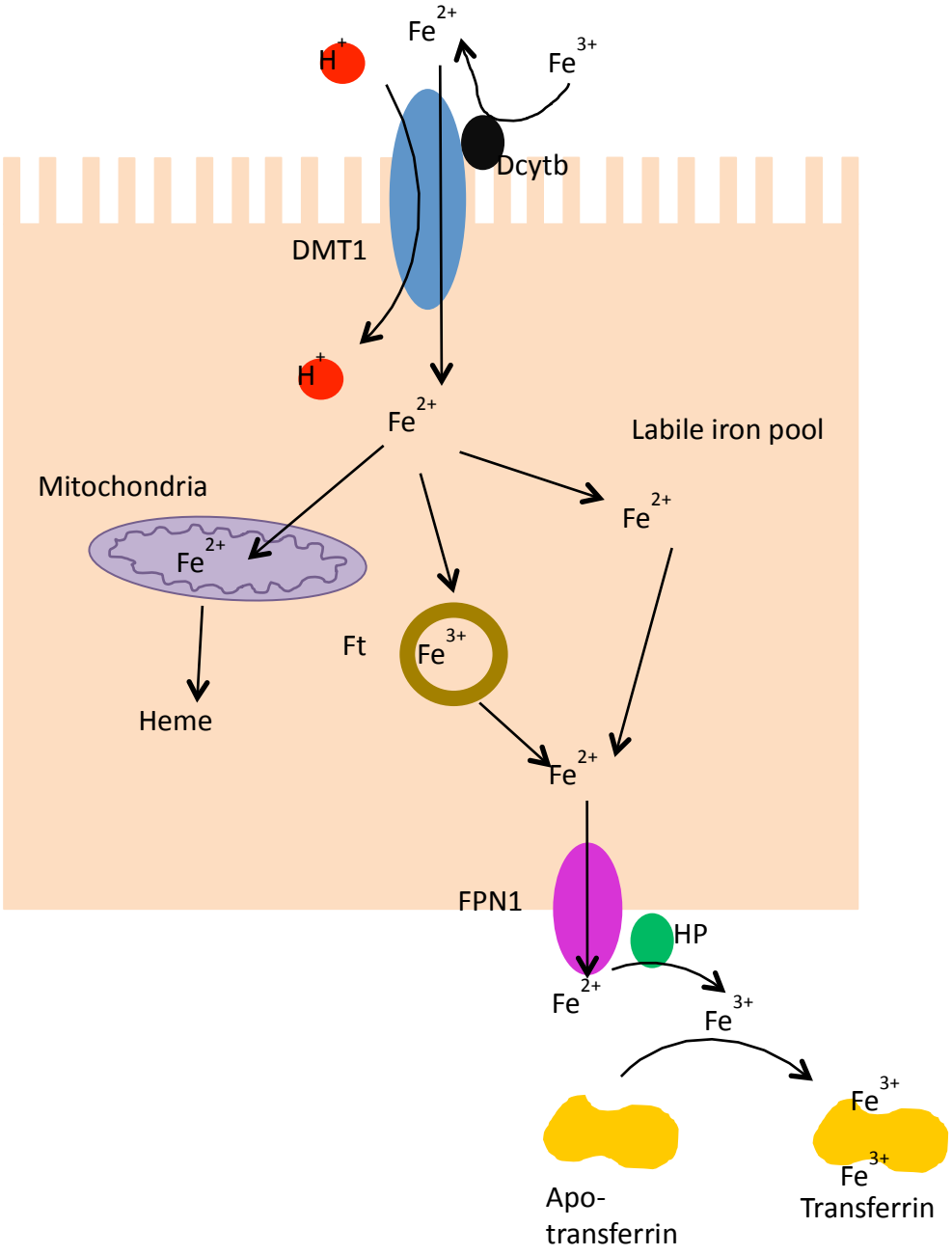

Figure 1-3. Iron absorption through duodenum enterocytes. Fe(III) is reduced by duodenal cytochrome b (Dcytb), a ferroreductase. The reduced Fe(II) is transported into the cytosol of the cell via the proton-dependant divalent metal transporter 1 (DMT1), from where it either enters the labile iron pool as Fe(II), ferritin (Ft) where it is oxidised to form Fe(III)-O-Fe(III), or the mitochondria where it is used for electron transport and heme synthesis. Fe(II) is exported out of the cell through ferroportin (Fpn1), and is oxidised to Fe(III) by hephaestin(Hp) a ferroxidase which in non-enterocytes is ceruloplasmin. Two Fe(II) ions bind to apo-transferrin and transported via the blood to cells requiring iron or to hepatocytes for storage.

border membrane ferrireductase, duodenal cytochrome b (Dcytb), a heme containing b-type cytochrome will do so by using ascorbate to reduce the ferric iron (Pountney *et al.,* 1999; McKie *et al.,* 2000; Han, 2011). The ferrous iron is then co-transported, with a proton, across the brush border membrane via DMT1 into the enterocyte (Gunshin *et al.,* 1997) where it is either sequestered by ferritin, transported to the mitochondria, for organic iron and [Fe-S] cluster synthesis or enters the inorganic labile iron pool (Figure 1-3).

1.4.2 Distribution of Inorganic Iron

Once iron is absorbed into enterocytes, predominantly in the duodenum or accumulated in reticuloendothelial macrophages, through the degradation of senescent erythrocytes, the iron must be transported to the bone marrow for utilisation or the liver for storage. Ferroportin 1 (Fpn1) exports Fe(II) from the basolateral membrane (McKie *et al.,* 2000), however, iron can only be released from Fpn1 once it has been oxidised to Fe(III) by a ferroxidase, hephaestin (Hp) in enterocytes and ceruloplasmin in the serum (Vulpe *et al.*, 1999; Chen *et al.,* 2004). Once oxidised, Fe(III) binds to apo-transferrin found in the blood and extracellular space (Figure 1-4). Transferrin is a glycoprotein which binds two Fe(III) ions, one each at the carboxyl and amino terminus of the protein and is the major protein for iron transport within the body (Zhao & Enns, 2012). It is predominantly produced in the liver from where it is secreted into the blood for circulation (Zhao & Enns, 2012).

Transferrin transports the two Fe(III) bound ions predominantly to hepatocytes for storage or the bone marrow for erythropoiesis where transferrin binds to transferrin receptor (TfR1) on the plasma membrane and the complex is internalised through clathrin-mediated endocytosis (Yamashiro *et al.,* 1984). Once internalised the vesicles are acidified by proton pumps promoting the dissociation of Fe(III) from transferrin whilst leaving transferrin bound to TfR1 (Dautry-Vasrsat *et al.,* 1983; Yamashiro *et al.*, 1984). The iron is reduced to Fe(II) by a ferrireductase (Steap 3) and transported out of the vesicle into the cytosol through DMT1 (Ohgami *et al.,* 2005). The vesicle fuses with the plasma membrane; in polarised cells it fuses with the basolateral membrane, to recycle TfR1 and apo-transferrin (Pan & Johnstone, 1983; Snider & Rogers, 1985). The increase in pH due to the dispersion of the vesicle causes the apo-transferrin to dissociate from TfR1 as apo-transferrin has a significantly lower affinity for TfR1 than transferrin at pH 7.4 (Dautry-Vasrsat *et al.,* 1983) (Figure 1-4).

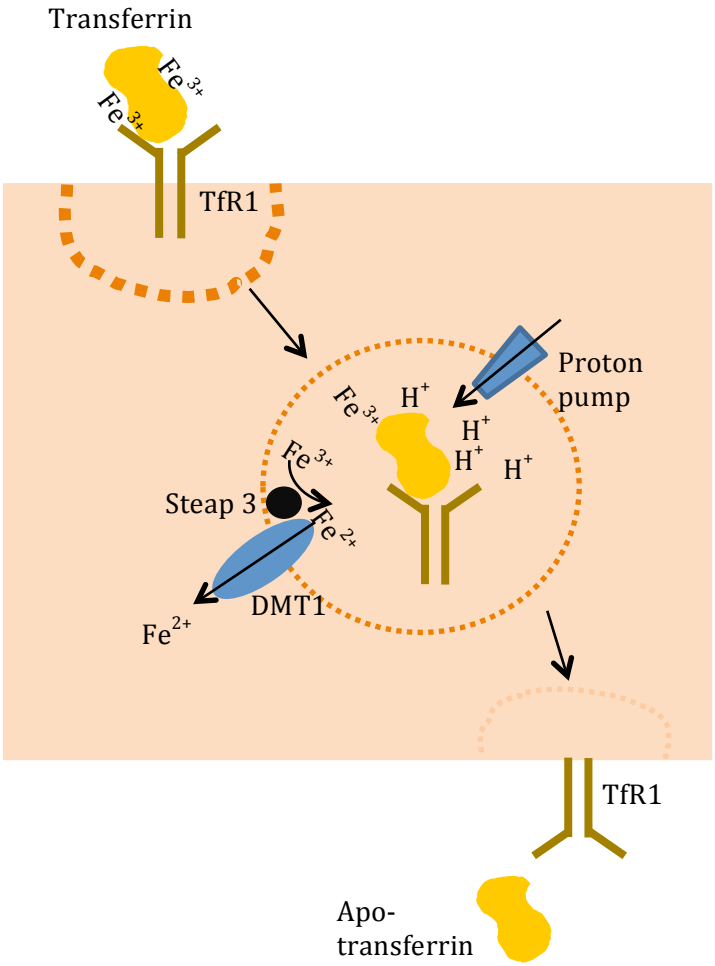

Figure 1-4. Transferrin-TfR1 transport through cells. Transferrin binds to the membrane bound receptor transferrin receptor 1 (TfR1) and the complex is internalised by clathrin-mediated endocytosis. Proton pumps acidify the vesicle resulting in the release of Fe(III) from transferrin. Fe(III) is reduced to Fe(II) by a ferrireductase (Steap 3), allowing Fe(II) to be transported out of the vesicle into the cytosol by divalent metal transporter 1 (DMT1). The apo-transferrin-TfR1 complex is recycled to the plasma membrane where the increase in pH, due to the vesicle dissipating, causes the apo-transferrin to dissociate from the receptor back into the blood stream.

An increase in liver iron concentration results in the upregulation and secretion of hepcidin, a hormone synthesised in hepatocytes (Pigeon *et al.,* 2001). Hepcidin, once secreted into the blood, binds to Fpn1, on the surface of cells, inducing the ubiquitination, internalisation and degradation of Fpn1 (Nemeth *et al.,* 2004; Qiao *et al.,* 2012). Both enterocytes of the GI tract, specifically in the duodenum, and reticuloendothelial macrophages have high expression levels Fpn1 due to their roles in iron absorption and iron recycling (McKie *et al.,* 2000; Knutson *et al.,* 2003), therefore these cell types are the main target for hepcidin. Hepcidin, upon binding to Fpn1, causes the ubiquitination of the iron transporter. The ubiquitinated Fpn1 is internalised, via endocytosis, and degraded (Ross *et al.,* 2012; Qiao *et*

al., 2012). The resulting decrease in Fpn1 on the membrane of enterocytes and reticuloendothelial macrophages leads to a decrease in Fe(II) export from the cells into circulation. Instead the iron is stored within the cells via ferritin and is released once liver iron concentrations decrease resulting in the subsequent decrease in secreted hepcidin.

1.5 Organic Iron

Organic iron can be in the reduced state, heme, or the oxidised state, hematin or hemin (depending on the bound ligand), within the body (Figure 1-1). The iron atom within heme contains two free coordination bonds, one on either side of the porphyrin ring (Bowman & Rand, 1980). Oxidised organic iron has only has one free coordination bond as the second is occupied by either a hydroxyl (hematin) or chloride (hemin) ligand resulting in a more stable form of organic iron under physiological conditions.

Organic iron is incorporated into hemeproteins through the coordination of side chains of amino acid residues within the protein to the free coordination sites of heme. For example in haemoglobin the imidazole side group of histidine, residue 87 (α chain) and 92 (β chain), tightly bind to one coordination bond on heme. The second coordination bond of iron in heme is loosely coordinated with a second histidine residue in globin. This loose coordination is displaced by molecular oxygen resulting in the oxygenation of the heme and the transport of oxygen, rather than the oxidation of heme (Bowman & Rand, 1980). Around 2% of haemoglobin in the blood is auto-oxidised, by oxygen or oxidizing metabolites in the blood, to methaemoglobin. Methaemoglobin has a hydroxyl ligand bound, rather than the weak interaction with the imidazole of histidine residue 58 (α chain) or 63 (β chain) (Bowman & Rand, 1980). Unlike the imidazole group of histidine, molecular oxygen cannot displace the hydroxyl ligand resulting in the inability of methaemoglobin to bind and transport oxygen. Methaemoglobin is reduced back to haemoglobin by glutathione (Simoni *et al*., 2009)

Hemeproteins have a wide range of functions including; oxygen transport and storage via haemoglobin and myoglobin; electron transfer, via cytochromes; gaseous sensing, for example soluble guanylyl cyclase senses nitric oxide (NO) and the catalysis of biological reactions, for example the degradation of H_2O_2 by catalase. Heme also regulates the expression of several proteins and enzymes, such as heme oxygenase 1 and regulates the differentiation and proliferation of various cells types (Kumar & Bandyopadhyay, 2005).

1.6 Organic Iron Absorption

In Western societies organic iron constitutes up to two thirds of the total daily iron absorbed but accounts for only 10% of daily dietary iron ingested (Han, 2011). The discrepancy between ingestion and absorption of organic iron compared to inorganic iron is due to the increased bioavailability of organic iron.

Walsh *et al.* (1955) were the first to show that organic iron, in the form of digested haemoglobin, was absorbed by human subjects. In the intervening 60 years many groups have explored the mechanism by which heme is absorbed into enterocytes, however the exact details are still not forthcoming. Noyer *et al.* (1998), Worthington *et al.* (2001) and Arredondo *et al.* (2008) showed that heme uptake was saturable, temperature and ATP dependant and indicated that it was receptor mediated both in enterocytes (Caco-2 cell line) and hepatocytes (rat hepatocytes and HepG2 cell line).

Currently there are two mechanisms proposed for heme absorption. The first is that heme is absorbed into enterocytes through a transporter, the folate importer, proton-coupled folate transporter (PCFT), also known as the heme carrier protein (HCP1) (Shayeghi *et al.* 2005; Laftah *et al.* 2009; Le Blanc *et al.* 2012). An alternative concept dates back to 1979 (Grasbeck *et al.* 1979) and proposes that heme is transported into enterocytes via receptor mediated endocytosis.

1.6.1 Organic Iron absorption by PCFT/HCP1

Within a year two groups discovered the same nutritional transporter but proposed different roles, Shayeghi *et al.* (2005) proposed that it was involved in heme transport, whilst Qiu *et al.* (2006) proposed that it was a folate transporter. In humans the transporter contains 2,097 bp encoding a 459 amino acid protein, 50 kDa, with nine predicted transmembrane domains (Shayeghi *et al.,* 2005; Qiu *et al.,* 2006). Shayeghi *et al.* (2005) published first suggesting the transporter was involved in heme transport into enterocytes, therefore naming the protein HCP1 (Figure 1-5). Subtractive hybridization between the ileum and duodenum of hypotransferrinaemic ($tfr^{hpx/hpx}$) mice was used to isolate cDNA specific to the duodenum, where the majority of heme is absorbed. The resulting cDNA was analysed and named HCP1. *Xenopus* oocytes and HeLa cells transfected with HCP1 demonstrated a significant increase in heme absorption compared to control cells. The inhibition of HCP1 through the use of a HCP1 antibody showed that in mouse everted duodenal sacs there was a 30-40% decrease in absorbed heme compared to control sacs. These results led to the conclusion that the identified protein, HCP1, was the

long sort after heme transporter (Shayeghi *et al.,* 2005). Shayeghi *et al.* (2005) did not elucidate the mechanism by which HCP1 transported heme into cells; however due to the homology between HCP1 and bacterial tetracycline transporters, that function as a proton antiporter (Yamaguchi *et al.,* 1992), it was suggested that HCP1 could also be a proton driven transporter.

A year later Qiu *et al.* (2006) published data that the same protein was a proton-coupled folate transporter (PCFT). They showed that the transporter had a high affinity for folate (K_i = 0.6 µM) and that Caco-2 cells incubated with PCFT/HCP1 interfering RNA downregulated folate absorption by 80%. This information and subsequent work (Inoue *et al.,* 2008; Le Blanc *et al.,* 2012) has led to the conclusion that the protein is a folate transporter with low affinity for heme.

1.6.2 Organic Iron absorption by Endocytosis

The discovery of heme binding to a, triton soluble, protein within the brush border surface of both porcine and human duodenum was first discovered in 1979 (Grasbeck *et al., 1*979). Further work elucidated the heme-binder complex had a dissociation constant of 10^{-6} – 10^{-9} mol/L suggesting that the complex was a protein receptor for heme (Tenhunen *et al.,* 1980; Grasbeck *et al.,* 1982). Using the immunohistochemical stain diaminobenzidine (DAB), the path heme took into and through canine duodenum closed loops was assessed (Parmley *et al*., 1981). The DAB-stained cells showed that vesicles formed in the apical intracellular space engulfing heme, and that vesicle formation increased over time, (15 minutes to 2 hours). The mitochondria were heavily stained for heme whilst the vesicles were not detected in the lateral intracellular space of the basal extracellular space. Although heme-containing vesicles were not detected in the lateral intracellular space of the enterocytes inorganic iron was detected both in the lateral intracelluar space and the basal extracellular space (Parmley *et al*., 1981). This clear division of organic and inorganic iron within the cell suggested that heme was absorbed via endocytosis, was translocated either to the mitochondria or to a more central area of the cell. There it was degraded by heme oxygenase-1 (HO-1) and inorganic iron released. This inorganic iron was then translocated to the lateral side of the cell and exported out into the basal extracellular space via the inorganic iron exporter Fpn1 to apotransferrin (Figure 1-4).

A similar experiment, again using DAB, demonstrated vesicle formation, translocation and eventual disappearance, coinciding with the appearance of inorganic heme in rat duodenum (Wyllie & Kaufman, 1982). Fifteen to 60 minutes after the administration of

organic iron (in the form of haemoglobin or hemin), heme was visualised on the surface of the enterocytes. Heme was visualised in apical pits and vesicles located in the apical cytoplasm encased by a trilaminar membrane, corresponding to the structure of the apical plasma membrane and apical pits (Wyllie & Kaufman, 1982). This strongly indicated that the vesicles containing heme originated from the apical membrane of the cells and therefore heme was absorbed via endocytosis. One to two hours after the administration of heme, the heme-containing vesicles took on the appearance of secondary lysosomes. These lysosome-like vesicles were still encased by a trilaminar membrane however they were concentrated in the centre of the cytosol rather than the apical side (Wyllie & Kaufman, 1982). Three hours after organic iron administration no heme was seen in the secondary lysosomes implying that heme had been degraded within these lysosomal structures. Neither vesicles nor secondary lysosome-like vesicles containing heme were observed in the lateral side of the cell or on the basolateral membrane (Wyllie & Kaufman, 1982).

From these experiments, knowledge of heme degradation by HO-1 (discussed in Section 1.4.1.2) and the knowledge of inorganic iron movement through enterocytes (see Section 1.2.4) the path of organic iron through enterocytes can be deduced. First heme binds to a heme-receptor on the apical membrane of the enterocytes (Tenhunen *et al.,* 1980; Grasbeck *et al.,* 1982). The heme is then internalised through endocytosis and the vesicle is translocated to the supranuclear region of the cell (Parmley *et al*., 1981; Wyllie & Kaufman, 1982). Once in a more central position within the cell the vesicle fuses with a lysosome (Wyllie & Kaufman, 1982) where HO-1 HO-1 catabolises heme releasing inorganic iron. It is suggested that DMT1 transports the liberated inorganic iron out of the lysosome (Soe-Lin *et al.,* 2010) (Figure 1-5). The inorganic iron translocates to the lateral part of the cytosol and is exported from the cell, via Fpn1, into the basal extracellular space or bloodstream where it is bound to apotransferrin (Parmley *et al*., 1981).

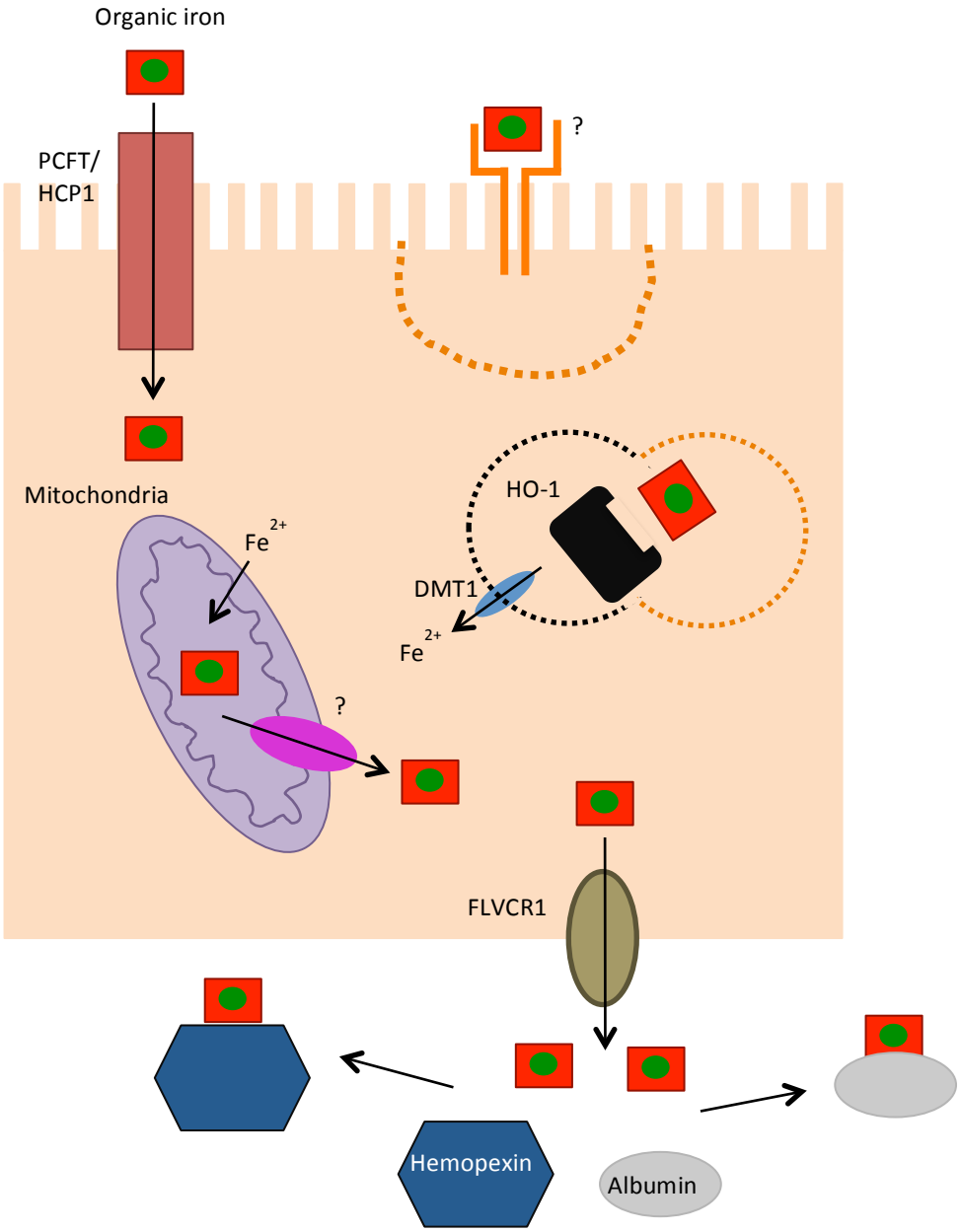

Figure 1-5. Organic iron absorption and efflux from enterocytes. Organic iron is transported into the cell via the folate-heme transporter PCFT/HCP1 after which the fate of the organic iron is unknown. Or the organic iron is transported into the cell via receptor mediated endocytosis, however the receptor remains unknown. The resulting heme containing endosome combines with an HO-1 containing lysosome. This results in the catabolism of organic ion and the release of inorganic iron from the secondary lysosome through DMT1. Heme synthesised in the mitochondria is exported by as an as yet unknown process into the cytoplasm of the cell. Organic iron is exported out of the cell via FLVCR1. Once in the extracellular space heme is tightly bound by hemopexin or albumin.

Current information and experimental data suggests that heme absorption into enterocytes occurs through both mechanisms described. A small amount is transported

into the cell through PCFR/HCP1; however once inside the cell the path of the heme is unclear. However, the majority of the iron flux would appear to be absorbed through endocytosis as the inhibition of HCP1 only downregulated heme absorption by 30 – 40% (Shayeghi *et al.,* 2005).

1.7 Cellular Damage Resulting from Free Organic Iron

Organic iron not ligated or incorporated into proteins, redox cycles between oxidation states. This results in the production of free radicals through the Fenton reaction (Equation 1-1). These free radicals and reactive oxygen species (ROS) initiate a cascade of reactions resulting in cellular damage including lipid peroxidation, degradation of proteins and DNA damage.

$Fe^{2+} + H_2O_2 \rightarrow Fe^{3+} + OH^- + HO\bullet$ Equation 1-1.1

$Fe^{3+} + H_2O_2 \rightarrow Fe^{2+} + H^+ + HOO\bullet$ Equation 1-1.2

1.7.1 Lipid Peroxidation

Free radicals are highly reactive and often proceed in chain reactions where one radical begets another. Free heme catalyses the peroxidation of unsaturated lipids, in the presence of H_2O_2, through the formation of hydroxyl radicals or hydroperoxyl radicals (Vincent, 1989). Organic iron, being a hydrophobic planar molecule, partitions into membranes where it catalyses the formation of free radicals. These free radicals attack the closest electron donor, which is often a lipid thereby starting a lipid peroxidation chain reaction.

$L\text{-}H + HO\bullet \rightarrow H_2O + L\bullet$ Equation 1-2

The free radical attacks the fatty acid or fatty acyl side chain at a methylene carbon and abstracts hydrogen (Equation 1-2, Figure 1-6). This causes the carbon to have an unpaired electron, resulting in a carbon-centred lipid radical. The lipid radical will either abstract hydrogen from a neighbouring lipid, propagating the lipid radial or form a peroxyl radical (R-O-O•) through interaction with molecular oxygen (Figure 1-6) (Halliwell & Chirico, 1993). The peroxyl radical will either abstract hydrogen from another lipid, combine with another peroxyl radical or with a membrane protein. The interaction of peroxyl radicals with lipids propagates lipid peroxide synthesis whilst the interaction between two peroxyl radicals terminates the process (Figure 1-6).

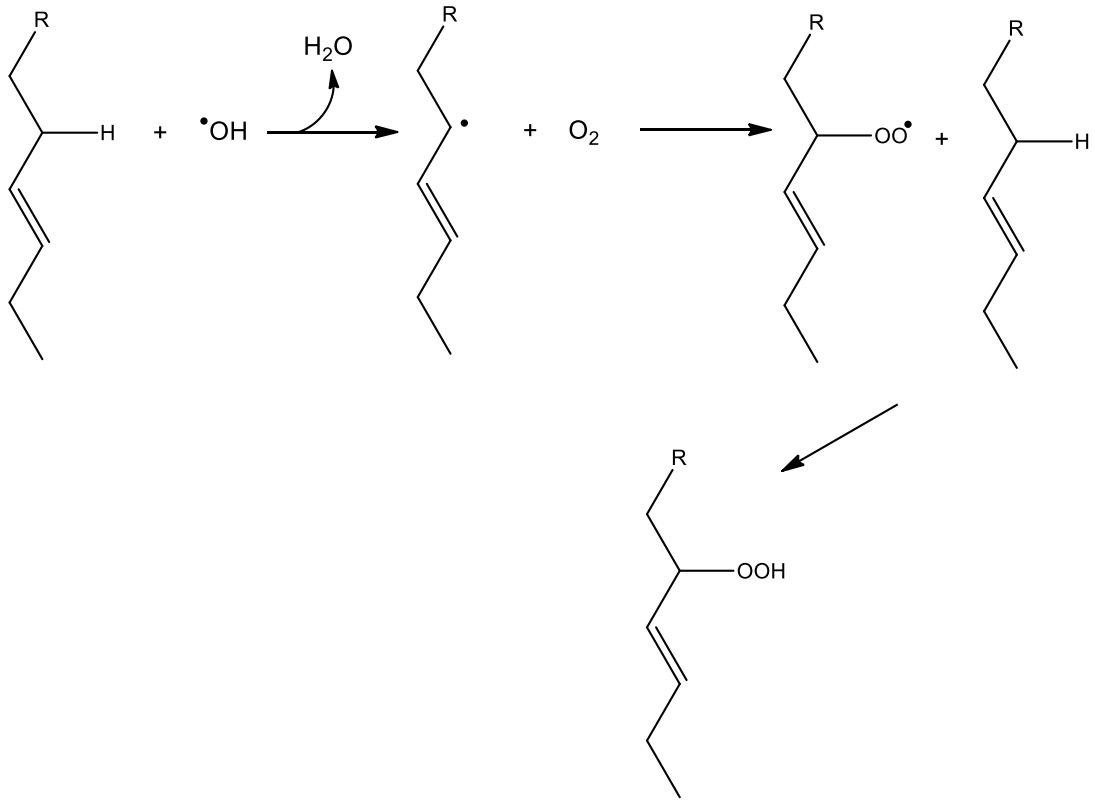

Figure 1-6. Mechanism of lipid peroxidation. Hydroxyl radical abstracts hydrogen from the side chain of a lipid, forming water. The resulting lipid peroxide radical reacts with molecular oxygen resulting in a hydroperoxyl lipid radical. The hydroperoxyl lipid radical abstracts hydrogen from a neighbouring lipid resulting in the propagation of further lipid peroxide radicals and formation of a peroxide group on the original lipid.

The lipid peroxidation cascade not only occurs in the plasma membrane but also the membrane of cellular organelles such as the mitochondria.

1.7.2 Protein Degradation

Free radicals produced during Fenton reactions can also interact with proteins causing oxidation, aggregate formation, covalent cross-linking and degradation to smaller peptides.

The indole ring of tryptophan is a main target for oxidation by reactive oxygen species produced through the Fenton reactions (Stadtman, 1993). The oxidation of tryptophan leads to the formation of formylkynurenine (Figure 1-7). Whilst the oxidation of the side chain of methionine leads to the formation of methionine sulfoxide which can be further oxidized to methionine sulfone (Figure 1-7). The side chains of cysteine, phenylalanine, tyrosine and histidine are also easily oxidised when in the presence of reactive oxygen species (Stadtman, 1992).

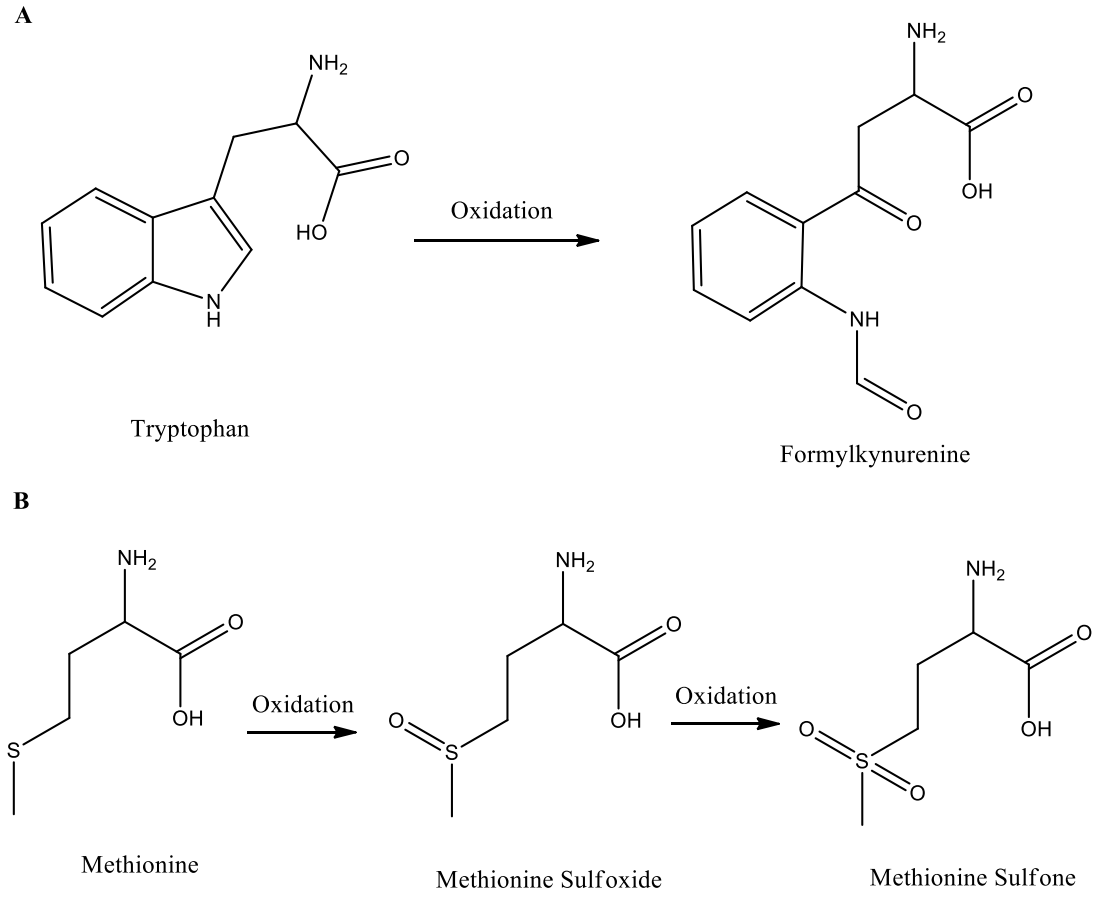

Figure 1-7. Oxidation of amino acids. The amino acids most prone to oxidation are tryptophan and methionine. **A** - The five membered ring on the side chain of tryptophan is opened and oxidation occurs both on the –NH and on the carbon. **B** - Methionine is sequentially oxidised on the sulfur residue resulting in the formation of methionine sulfone.

The oxidation of the amino acid side chains, especially the very hydrophobic tryptophan, leads to a decrease in the hydrophobicity of the protein chain. Which in turn is detrimental to protein structure.

1.7.3 Cellular Defences against Organic Iron

To inhibit the toxic side effects of heme the cell must decrease the labile organic iron concentration. To do this the cell can either export the heme or catabolise it.

1.7.3.1 Cellular Heme Export

Feline leukemia virus subgroup C receptor (FLVCR1) is a transmembrane protein consisting of 555 amino acid residues with 12 predicted transmembrane domains (Tailor *et al.,* 1999). By homology, FLVCR1 is a member of the major facilitator superfamily of secondary permeases. This group of cell surface proteins transport small solutes, such as glucose,

amino acids and ions, across membranes in response to chemico-osmotic gradients (Tailor *et al.,* 1999).

FLVCR1 is expressed in numerous cell types however those involved with the absorption (Caco-2 cell line) and storage (HepG2 cell line) of heme or synthesised high levels of heme (peripheral blood $CD34^+$ progenitor cells and K562 cell line) have high expression levels of FLVCR1 (Quigley *et al.,* 2004). However, erythrocytes themselves (HEL-R cell line) have low expression levels of FLVCR1 (Quigley *et al.,* 2004). Normal rat kidney cells (NRK cell line) transduced with human *FLVCR* and incubated with either zinc mesoporphyrin (ZnMP), a fluorescent homolog of heme, or radioactive heme, showed an increase of 50% heme export, compared to wild type NRK cells (Quigley *et al.,* 2004). Keel *et al.* (2008) showed that FLVCR1 was not only instrumental for erythrocyte maturation but FLVCR1-null mice had severe limb and cranial deformities and died midgestation. Combined, these experiments demonstrate that FLVCR1 is an organic iron transporter.

1.7.3.2 Heme Binding Serum Proteins

The export of heme from cells not only requires the presence of FLVCR1 on the cell surface but also a heme protein carrier in the extracellular space/plasma (Yang *et al.,* 2010) (Figure 1-5). The previous experiments that showed the function of FLVCR1 were either carried out *in vivo* (Keel *et al.,* 2008), or in cell lines cultured in fetal bovine serum (FBS) (Quigley *et al.,* 2004). *In vitro* experiments, that contained FBS in the cell medium, and *in vivo* experiments, both contain proteins normally found within plasma, these include albumin and hemopexin.

Yang *et al.* (2008) demonstrated that NRK/FLVCR did not export ZnMP when no hemopexin or albumin was present in the cell medium. In contrast when 1.5 μM of hemopexin was present in the medium NRK/FLVCR cells exported 49% of internalised ZnMP. However for a similar amount of ZnMP (56%) to be exported, in the presence of albumin, the concentration had to be 100x that of hemopexin, 151 μM. Similar results have also been demonstrated in human peripheral macrophages containing radioactive heme (Yang *et al.* 2008).

These experiments demonstrate that not only does FLVCR export heme from erythrocyte precursory cells but also from macrophages that engulf and degrade senescent erythrocytes. They also demonstrate that for heme export to occur hemopexin, or large concentrations of albumin, must be present in the extracellular space.

Hemopexin is one of the most abundant proteins in serum, ~1mg/mL, (Muller-Eberhard & Fraig, 1993) that has the highest dissociation constant, K_d 10^{-13} M, (Vincent, 1989) for heme of any known heme-protein. Hemopexin binds one molecule of heme and transports it to the hepatic parenchymal cells where it can be degraded by the reticuloendothelial system, liberating inorganic iron which can be recycled back into the circulating iron within the body. Albumin is an abundant serum protein with a dissociation constant for heme of K_d $5x10^{-6}$ M (Beaven *et al.*, 1974). Unlike hemopexin, albumin does not transfer bound heme to hepatocytes for recycling, instead albumin is used as a heme depository within blood plasma to minimise the toxic effects of extracellular organic iron.

1.7.3.3 Catalytic Degradation of Organic Iron

Cells not only export heme to protect themselves from cellular damage by organic iron but they also have mechanisms to degrade organic iron. The main way organic iron is degraded is via catabolism by heme oxygenase-1 (HO-1), a microsomal enzyme (Tenhunen *et al.,* 1968) with a half-life of ~20 hours (Ibrahim *et al.,* 1982). In the presence of NADPH, HO-1 catalyses the conversion of organic iron to; ferrous inorganic iron, CO and biliverdin (Tenhunen *et al.,* 1968; Reed *et al.*, 2010). The biliverdin is quickly reduced to bilirubin by biliverdin reductase (Reed *et al.,* 2010). Whilst the newly liberated inorganic iron is exported out of the cell to bind to apo-transferrin, stored in ferritin or enters the inorganic labile iron pool (Soe-Lin *et al.,* 2010).

HO-1 is the inducible isoform of HO, upregulated as a result of cellular stress, such as oxidative stress or hypoxia, whilst HO-2 is the constitutively expressed isoform. HO-1 expression is regulated by hematin concentration through Bach1, a heme-dependent transcription regulator protein. Bach1 forms a heterodimer with multiple small Maf proteins; this heterodimer binds to multiple Maf recognition elements (MAREs) on *ho-1*, repressing transcription, (Ogawa *et al.,* 2001; Sun *et al.*, 2002). When the concentration of hematin within the cell increases the amount of hematin bound to Bach1 increases, when hematin is bound to Bach1, Bach1 cannot form a heterodimer with Maf proteins leading to a decrease in *ho-1* repression, resulting in an upregulation of HO-1 expression, (Ogawa *et al.,* 2001; Sun *et al.,* 2002). The upregulation of HO-1 expression causes an increase in hematin catabolism, the resulting decrease in cellular hematin concentration leads to a decrease in hematin bound to Bach1, with more Bach1 available to form the transcription repressing heterodimer with Maf proteins *ho-1* transcription is once again repressed (Figure 1-8).

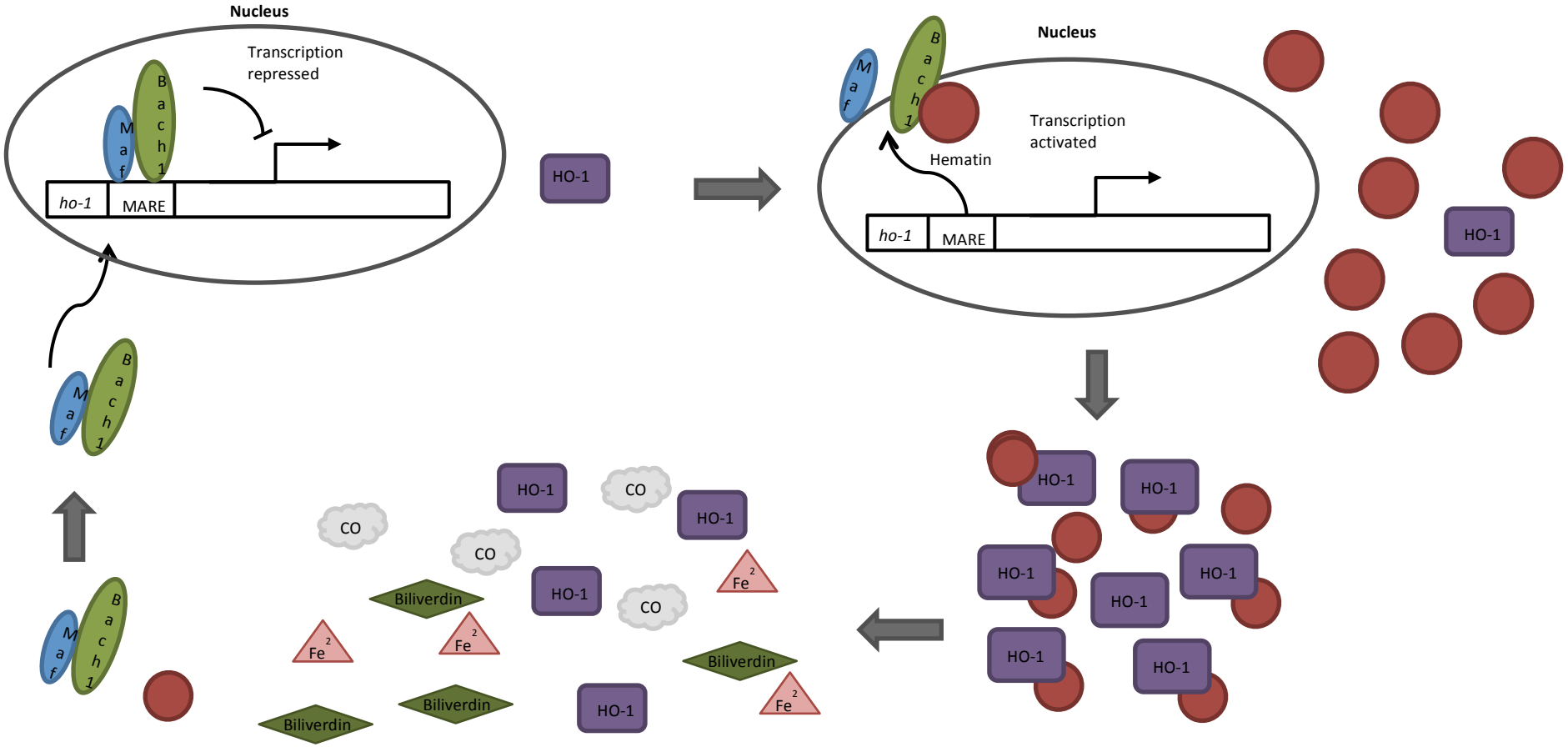

Figure 1-8. Schematic of the negative feedback repression of *ho-1* transcription via hematin. The heterodimer of Maf-Bach1 binds to the MARE region of *ho-1* when there is low/no labile organic iron. When the concentration of organic iron in the cell increases the free hematin binds to Bach1 resulting in the Maf-Bach1 heterodimer to dissociate from the MARE region of the *ho-1* gene thereby stopping the repression of transcription. The increase in HO-1 expression results in the metabolism of the labile hematin therefore there is less/no hematin to bind to Bach1 resulting in the Maf-Bach1 heterodimer binding to the MARE region of the gene thereby repression transcription once again.

1.8 The Chemical Nature of the Cytosolic Labile Iron Pool

Due to the redox nature of iron, labile iron, must be ligated or chelated to inhibit the production of free radicals and other toxic effects of both inorganic and organic iron.

1.8.1 Inorganic Iron

Several chelators of ferric iron have been identified for example, amino acids, inositol phosphates, ATP/AMP and 2,5-dihydroxybenzoic acid (Hider & Kong, 2011). However over 80% of the inorganic labile iron pool is ferrous iron (Petrat *et al.,* 2002) therefore these iron chelators would not be strong chelators of the inorganic labile iron pool. Citrate has been shown to chelate ferrous inorganic iron (Morey & Bezkorovainy, 1983). Whilst speciation plots at physiologically relevant conditions show Fe(II) would bind to citrate the Fe(II)-citrate complex would be prone to autoxidation at pH 7 therefore a second ligand capable of binding Fe(II) an immune to autoxidation must be present within the cytosol (Hider & Kong, 2011).

1.8.1.1 Chelation of Inorganic Iron by Thiol Groups

Cysteine contains a thiol group, is present in the cytosol of cells at concentrations ranging from 20 µM and 100 µM and has a log K_1 of 6.2 for ferrous iron (Martell & Hancock, 2013). At cellular conditions, pH 7, 1 µM ferrous iron less than 1% of ferrous iron would be chelated to cysteine (Hider & Kong, 2011). Therefore although cysteine contains a thiol group that can interact with ferrous iron at physiological conditions cysteine would not be a viable chelator.

Glutathione is present in the cytosol at a concentration between two and three orders of magnitude higher than the inorganic labile iron pool. This would suggest that even a weak affinity constant between glutathione and inorganic iron could lead to the ligation of inorganic iron without disrupting the glutathione pool within the cytosol. The glutathione pool within the cytosol is essential for maintaining the reduction potential of the cell. Hider and Kong (2011), through titration experiments with glutathione and ferrous sulphate, showed that at physiologically relevant conditions glutathione had a log K_1 value of 5.12 – 5.6. This equates to 85-95% of the labile iron pool being chelated to glutathione at concentrations of 1 µM Fe(II) and 2-8 mM glutathione at pH 7 (Figure 1-9). This observation fits with the fact that upwards of 80% of the inorganic labile iron pool is in the ferrous state. Ferrous iron within the cytosol slowly auto-oxidises however the ferric iron is quickly reduced back to the ferrous state by glutathione, which acts as a buffer for the inorganic labile iron pool (Hamed *et al.,* 1982).

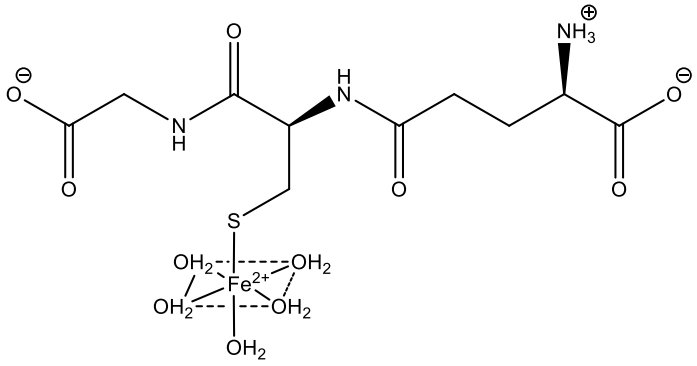

Figure 1-9. Ferrous iron chelated to glutathione. Inorganic ferrous iron chelated to glutathione through the thiol group.

Glutathione has also been shown to chelate [2Fe-2S] clusters (Fidai *et al.,* 2016) under physiological conditions, stabilising them in a [2Fe-2S](GS_4) complex. This complex can exchange the Fe-S clusters to Fe-S cluster proteins, therefore not only does glutathione stabilise iron it also has a chaperone role for inserting Fe-S clusters into Fe-S cluster proteins.

1.8.1.2 Glutathione

Glutathione (γ-L-Glutamyl-L-cysteinyl-glycine) is a tripeptide formed of glutamic acid, cysteine and glycine (Figure 1-9). Within the body reduced glutathione concentrations range from 2 mM (Kondo *et al.,* 1995) to 8 mM and up to 11 mM within the mitochondria (Soboll *et al.,* 1995). Glutathione synthesis is a two step process regulated by the negative feedback control of glutathione on γ-glytamylcysteine synthase. The availability of L-cysteine is also rate limiting for the synthesis of glutathione. The first step is the synthesis of the γ peptide bond between the γ carboxyl group on glutamic acid and the amine group of cysteine. This is catalysed by γ-glytamylcysteine synthase and requires energy from the hydrolysis of ATP (Equation 1-3). The second step is catalysed by glutathione synthetase, which also requires energy released from the hydrolysis of ATP, to form the peptide bond between the dipeptide γ-glytamylcysteine and glycine (Equation 1-4).

$$\text{γ-L-Glutamate + L-Cysteine + ATP} \xrightarrow{\text{γ-glytamylcysteine synthase}} \text{γ-L-Glutamyl-L-cysteine + ADP + } P_i$$

Equation 1-3

$$\text{γ-L-Glutamyl-L-cysteine + glycine + ATP} \xrightarrow{\text{Glutathione synthetase}} \text{γ-L-Glutamyl-L-cysteinylglycine + ADP + } P_i$$

Equation 1-4

The peptide bond between glutamic acid and cysteine is a γ-peptide linkage between the side chain carboxyl group (γ) of glutamic acid and the amine group of cysteine (Figure 1-10). This unusual γ-peptide linkage helps stabilise glutathione in intracellular conditions because most peptidases can only cleave α-peptide bonds (Lushchak, 2012).

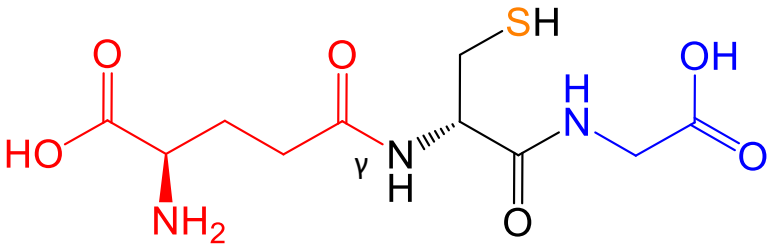

Figure 1-10. Glutathione structure. The structure of the tripeptide, glutathione; glutamic acid residue in red, cysteine residue in black and glycine in blue. γ-peptide linkage between carboxyl side group of glutamic acid and amine of cysteine denoted.

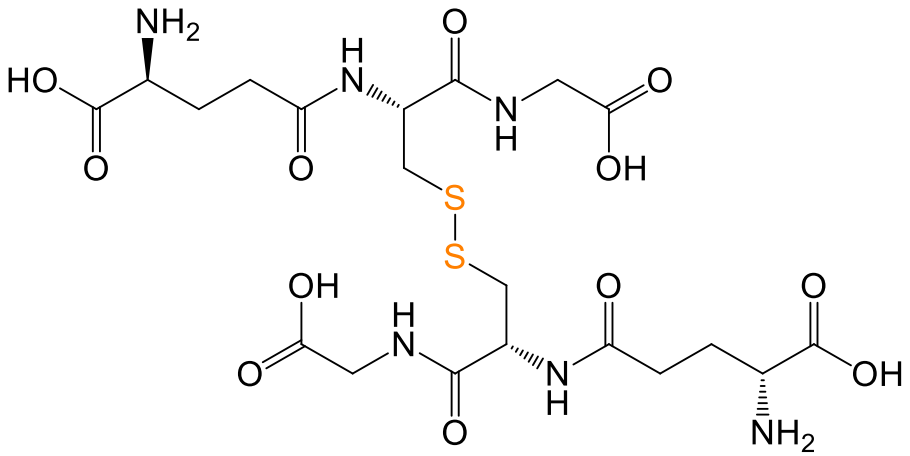

Figure 1-11. Glutathione disulphide structure. In oxidised glutathione a disulphide bond forms between the thiol groups (orange) of two glutathione molecules. This bond must be reduced to recycle the glutathione back to reduced glutathione, which can act as a reducing agent.

$$GSSG + NADPH^{+} + H^{+} \xrightarrow{\text{Glutathione reductase}} 2GSH + NADP^{+}$$

Equation 1-5

Glutathione is a strong reducing agent due to the thiol group on the cysteine residue, consequently it reduces disulphide bonds, stabilises thiol groups within proteins by acting as an electron donor and can be oxidised by free radicals. In doing so glutathione disulphide is produced (Figure 1-11). Glutathione disulphide is reduced back to glutathione through the enzyme glutathione reductase and NADPH (Equation 1-5).

1.8.2 Organic Iron

Investigations into the organic labile iron pool have resulted in the concentration being reported to be between 20 nM and 10 µM, in the liver and rat reticulocytes (Granick *et al.,* 1975; Garrick *et al.,* 1999; Hanna *et al*., 2016). The functions of organic iron are wide ranging and encompass both intracellular compartments and the cytosol. For example heme is required within the nucleus for gene expression via Bach1 and in the mitochondria where it is incorporated into cytochromes for electron transport (Ogawa *et al.,* 2001; Sun *et al.,* 2002). Within the cytosol organic iron is essential for gaseous sensing (Khan & Quigley, 2011) and as the prosthetic group in numerous enzymes. The required cellular distribution of organic iron for the large range of processes requiring heme would argue for the requirement of an organic labile iron pool (Khan & Quigley, 2011). However the toxic side effects of non-ligated organic iron would argue against this concept, leading to the conclusion that organic iron within the cell must be tightly regulated and possibly chaperoned when in the cytosol.

The chemical character of the organic labile iron pool is currently unknown.

1.9 Aims and Objectives

The overall aim of this project is to characterise the interaction between hematin and glutathione within mammalian cells. As discussed in the introduction organic iron is essential for aerobic life forms, however non-ligated iron has toxic side effects which can ultimately lead to cell death.

The first experimental chapter aims to determine if glutathione is a viable ligand for the organic labile iron pool within the mammalian cells. These aims will be met by:

- determining the affinity constant of glutathione for hematin under physiologically relevant conditions;
- determining the nature of the glutathione-hematin (GS.hematin) complex;
- developing an HPLC system to detect the GS.hematin complex within samples containing organic iron.

The second experimental chapter aims to investigate the influence glutathione has on the absorption of hematin into mammalian cells. This will be achieved through the use of [^{59}Fe]hematin and Caco-2 cells to determine:

- the effect of glutathione on hematin uptake;
- the effect of the constituent amino acids of glutathione on hematin uptake;
- the effect of amino acids known to interact with heme on hematin absorption.

The final experimental chapter aims to determine the biochemical nature of the interaction between hematin and glutathione. These aims will be met by:

- investigating the stability of the GS.hematin complex in the presence of hydrogen peroxide and ascorbic acid;
- investigating the influence of glutathione ligation has on the partitioning of hematin into lipid bilayers;
- investigating the presence of GS.hematin within mammalian cells;
- investigating the effect of glutathione on hematin catabolism by HO-1.

2. The Nature of the Chemical Interaction between Hematin and Glutathione

2.1 Introduction

It is well documented that there is a labile iron pool within the cytosol of cells (Greenberg & Wintrobe, 1946; Jacobs, 1977, and reviewed in Kakhlon & Cabantchik, 2002; Kruszewski, 2003; Breuer *et al,.* 2008). This labile iron pool can be further divided into inorganic, which has been shown to be predominantly iron(II) in erythrocytes, (Breuer *et al.,* 1995), with a typical concentration up to 1 μM, (Ma *et al.,* 2015), and organic (iron bound to PPIX), which has been shown to reach up to 10 μM in rat reticulocytes, (Garrick *et al.,* 1999). Both inorganic and organic iron is capable of redox cycling between oxidation states producing free radicals and reactive oxygen species, both of which are damaging to cells and cause oxidative stress. This redox process has to be carefully controlled. Organic iron is highly toxic within cells if not chelated or embedded in proteins. The production of free radicals from the redox cycling of organic iron results in DNA, lipid and protein damage, (Kumar & Bandyopadhyay, 2005). Organic iron, in the form of both; heme (Fe(II)) and hematin (Fe(III)), is essentially a planar hydrophobic molecule, meaning it can easily partition into lipid bilayers, such as the plasma membrane. If organic iron was to become more hydrophilic and less planar the ability for it to partition into lipid bilayers should be greatly reduced, this could be achieved by the ligation of organic iron to a chelator or ligand. This ligand should be hydrophilic, to keep organic iron in the cytosol, and be a strong reducing agent, to iron cycling between the ferrous and ferric oxidation state.

Glutathione has a concentration which ranges from 2 mM to 8 mM in the cytosol of mammalian cells, (Kondo *et al.,* 1995; Soboll *et al.,* 1995). Glutathione has been shown as a key component of the cytosolic and mitochondrial inorganic iron pool (Hider & Kong, 2011; Hider & Kong, 2013), whilst Shivro & Shaklai (1987) were the first scientists to postulate that glutathione could be a ligand for hemin in 1987. If glutathione bound to hematin, forming a GS.hematin complex, the resulting compound should contain a stable iron at its core and be less planar and hydrophobic then non-ligated organic iron. These new properties would mean organic iron would no longer redox cycle which would lead to a decrease the oxidative stress within the cell. All this, and the fact that glutathione is in excess of organic iron in the cytosol, by at least two orders of magnitude, and glutathione is a proven ligand of inorganic iron (Hider & Kong, 2013), indicates that glutathione is a likely candidate for the organic labile iron pool.

The aim of the studies described in this chapter are to determine if glutathione is a viable ligand for the organic labile iron pool (hematin), within the cytosol of mammalian cells, and the coordination of glutathione to hematin.

2.2 Materials and Methods

2.2.1 Reagents

Reagents were from Sigma Aldrich and reagent grade unless stated otherwise in Table 2-1

Table 2-1 Details on Reagents Used for Biochemical Experiments

Compound	**Specifications**	**Supplier**
Compounds		
Reduced glutathione	N/A	Santa Cruz Biotechnology
Oxidised glutathione	N/A	Santa Cruz Biotechnology
PPIX dimethyl ester	N/A	Santa Cruz Biotechnology
Ferrous Sulphate	$7H_2O$	Scientific Laboratory Suppliers
Potassium Chloride	≥ 99%	BDH laboratory supplies
Di-Sodium hydrogen phosphate anhydrous	> 98%	Fluka Chemika
Sodium Hydroxide	Laboratory reagent grade	Fisher Scientific
L-Ascorbic Acid sodium salt	99%	Acros Organics

Table 2-1 Continued

Compound	Specifications	Supplier
Solvents		
Triethylamine (TEA)	Laboratory reagent grade	Fisher Scientific
Water	HPLC grade	Fisher Scientific
Acetic Acid	Glacial	Fisher Scientific
Chloroform	Analytical reagent grade	Fisher Scientific
Ethyl Acetate	Analytical reagent grade	Fisher Scientific
Hydrochloric Acid	37 % in water	Acros Organics
Methanol	HPLC grade	Fisher Scientific
DMSO	≥ 99.7 %	Fisher Scientific
Acetone	Analytical reagent grade	Fisher Scientific
Radioactive material		
Iron-59 radionuclide	In 0.5 M HCl	PerkinElmer

2.2.2 Hemin

Due to the small quantity (< 0.5 mg) of hemin required to make micromolar solutions of hemin/hematin for the experiments, hemin had to be aliquoted into small known amounts. Larger known quantities (mg) of hemin were in methanol and triethylamine, (9:1 ratio) and aliquots, containing the correct quantity of hemin, for the desired final concentration of hemin for the experiment, were measured into glass vials. These aliquots were dried under a stream of nitrogen, in a warm water bath, and placed in a vacuum desiccator for 24 hours to ensure complete solvent evaporation. All work involving hemin/hematin was conducted under aluminium foil and aliquots were kept at 4^{o}C until required.

2.2.3 Phosphate Buffer Conditions for Dissolving Hemin

Hemin was dissolved, to a final concentration of 50 μM, in 10 mM phosphate buffer, 20 mM KCl at various pHs to find the best condition for hemin to be dissolved in for

experiments. The solution was centrifuged at 4,000 rpm for 10 minutes and the supernatant transferred to quartz cuvette with a path length of 10 mm. The hematin pellet left after centrifugation was dissolved in 10 mM phosphate buffer, 20 mM KCl, pH 9, vortexed for 5 minutes, centrifuged for 10 minutes at 4,000 rpm and transferred to a quartz cuvette with a path length of 10 mm.

2.2.3.1 Spectroscopy of Hematin in Various Phosphate Buffer Solutions

The absorbance of the hematin solutions was measured at 1 nm intervals between 550 and 750 nm using PerkinElmer UV/Vis spectrophotometer Lambda 2 coupled with Lambda25 software. Absorbance was plotted against wavelength in Microsoft Excel.

2.2.4 Determination of the Affinity Constant of Hematin – Glutathione Interaction

2.2.4.1 Glutathione Solutions

Reduced glutathione was dissolved in 10 mM phosphate buffer, 20 mM KCl, pH 8 at varying concentrations up to 5 mM and pH adjusted to 8 using 0.1 N NaOH. Hemin was dissolved in varying concentrations of glutathione phosphate buffer, (from 0 to 5 mM glutathione) to a final concentration of 10 µM, and vortexed for 10 minutes. The solution was centrifuged at 4,000 rpm for 10 minutes and the supernatant transferred to Spectrosil® quartz cuvette with a path length of 100 mm. This was repeated three times for each concentration of glutathione.

2.2.4.2 Spectroscopy of Hematin – Glutathione Solutions

The absorbance of the hematin-glutathione solutions was measured at 1 nm intervals between 500 and 700 nm using PerkinElmer UV/Vis spectrophotometer Lambda 2 coupled with Lambda25 software. Absorbance was plotted against wavelength in Graphpad Prism (GraphPad software, Inc). The wavelength at which peak absorption occurred for hematin solution and hematin in 5 mM glutathione solution was recorded. The delta absorption of each hematin-glutathione solution was calculated (hematin absorbance peak (618 nm) minus GS.hematin absorbance peak (655 nm)) and the average for each glutathione concentration was plotted against the log concentration of glutathione ± SEM.

2.2.4.3 Speciation Plot of GS.hematin Complex

HySS2009 programme, (http://www.hyperquad.co.uk/hyss.htm; Alderighi *et al.* 1999), was used to provide speciation plots of the formation of GS.hematin at pH 8.

2.2.5 Determination of the Affinity Constant of Hematin – Cysteine Interaction

2.2.5.1 Cysteine Solutions

Cysteine was dissolved in 10 mM phosphate buffer, 20 mM KCl , pH 8 at varying concentrations to 10 mM and pH adjusted to 8 using 0.1 N NaOH. Hemin was dissolved in varying concentrations of cysteine phosphate buffer, (from 0 to 10 mM cysteine) to a final concentration of 10 μM, and vortexed for 10 minutes. The solution was centrifuged at 4,000 rpm for 10 minutes and the supernatant transferred to Spectrosil® quartz cuvette with a path length of 100 mm. This was repeated three times for each concentration of cysteine.

2.2.5.2 Spectroscopy of Hematin – Cysteine Solutions

The absorbance of the hematin-cysteine solutions was measured at 1 nm intervals between 500 and 700 nm using PerkinElmer UV/Vis spectrophotometer Lambda 2 coupled with Lambda25 software. Absorbance was plotted against wavelength in Microsoft Excel and GraphPad Prism for each sample. The wavelength at which peak absorption occurred for both the hematin solution and hematin in 10 mM cysteine solution was recorded. The delta absorption of each hematin-cysteine solution was calculated (hematin absorbance peak (618 nm) minus Cys.hematin absorbance peak (655 nm)) and the average for each cysteine concentration was plotted against the log concentration of cysteine ± SEM.

2.2.5.3 Speciation Plot of Cys.hematin Complex

HySS2009 programme was used to provide speciation plots of the formation of Cys.hematin at pH 8.

2.2.6 [^{59}Fe]Hematin Synthesis

The protocol was adapted from Follett *et al.* (2002). 20 mL Glacial acetic acid was heated in a water bath to 50^{o}C under a continuous stream of nitrogen. 16.25 mg Protoporphyrin IX dimethyl ester dissolved in 2.75 mL chloroform and 1 mL pyridine was added over five minutes to the stirred glacial acetic acid. 14.8 MBq $^{59}FeCl_2$ in 0.1 N HCl dissolved in 100 uL 17 mM ascorbic acid was added to the acetic acid/protoporphyrin IX dimethyl ester solution and incubated at 50^{o}C under a stream of nitrogen for 90 minutes. 1.5 mg ferrous sulphate dissolved in 500 μL methanol and 50 μL acetic acid was added to the solution and incubated for two hours at 50^{o}C under nitrogen. The solution was cooled to room temperature, 50 ml chloroform added and solution washed in a separating funnel three times with 15 mL water. The chloroform fraction was evaporated under reduced pressure

to 2.5 mL, diluted with 12.5 mL ethyl acetate and stored at 4°C overnight. 12.5 mL ethyl acetate and 12.5 mL chloroform were added to the overnight solution, the organic fraction was washed in a separating funnel three times with 10 mL 4 N HCl and twice with 15 mL water. The solution was evaporated to dryness under reduced pressure and the residue was dispersed in 2.5 mL tetrahydrofuran. The dispersed residue was stirred under a continuous stream of nitrogen with 0.5 mL 3 N NaOH until the solution evaporated to dryness. 2.5 mL tetrahyrofuran and 0.5 mL water was added to the flask, the flask was sealed under nitrogen and incubated at room temperature, with stirring, for 20 hours. The solution was diluted with 1 mL water and transferred to four 1.5 mL Eppendorf tubes. The [^{59}Fe]hematin was precipitated by the addition of 0.5 mL 10 N HCl to each Eppendorf and centrifuged for five minutes at 14,000 rpm. The pellet was washed twice with 1 mL water and centrifuged at 14,000 rpm for five minutes. Supernatant was thoroughly aspirated and the pellets dried overnight in a desiccator. Each pellet was dissolved in 1 mL DMSO and stored at 4°C.

Subsequent synthesis of [^{59}Fe]hematin incorporated additional modifications including the addition of 17.16 MBq [^{59}Fe to the protoporphyrin IX dimethyl ester mix instead of 14.8 MBq. On day two 25 mL chloroform was added to the ethyl acetate mix instead of 12.5 mL chloroform and 12.5 mL ethyl acetate. This facilitated the separation of the two phases. The diluted [^{59}Fe]hematin solution was transferred to 12, 1.5 mL Eppendorf tubes instead of four and 1 mL of 10 N HCl added to each Eppendorf tube to precipitate the [^{59}Fe]hematin instead of 0.5 mL. Each pellet was dissolved in 200 μL DMSO instead of 1 mL DMSO and stored at 4°C.

2.2.6.1 Spectroscopic Analysis of Synthesised [^{59}Fe]hematin

30 μL of each batch of synthesised [^{59}Fe]hematin was diluted into 2 mL (dilution factor of 67) 10 mM phosphate buffer, 20 mM KCl, pH 8. Hemin dissolved in DMSO was diluted into 10 mM phosphate buffer, 20 mM KCl, pH 8 to a final concentration of 16.55 μM and 95.88 μM. The absorbance of the four solutions was measured at 1 nm intervals between 450 nm and 750 nm using a PerkinElmer UV/Vis spectrophotometer Lambda 2 coupled with Lambda 25 software in a quartz cuvette with a path length of 10 mm (Figure 2-1). The concentration of [^{59}Fe]hematin was calculated from the spectroscopy data using equation 2-1. The quantity, in mg and μmol, of [^{59}Fe]hematin synthesised was calculated using equations 2-2 & 2-3. The radioactivity of 2 μL of [^{59}Fe]hematin in DMSO was measured using 1282 Compugamma CS universal gamma counter (LKB Wallac) and the yield

calculated with equation 2-4. The specific activity of [^{59}Fe]hematin was calculated from the moles synthesised and radioactivity, knowing that the gamma counter had an efficiency of 28.5 %, using equations 2-5, 2-6 & 2-7.

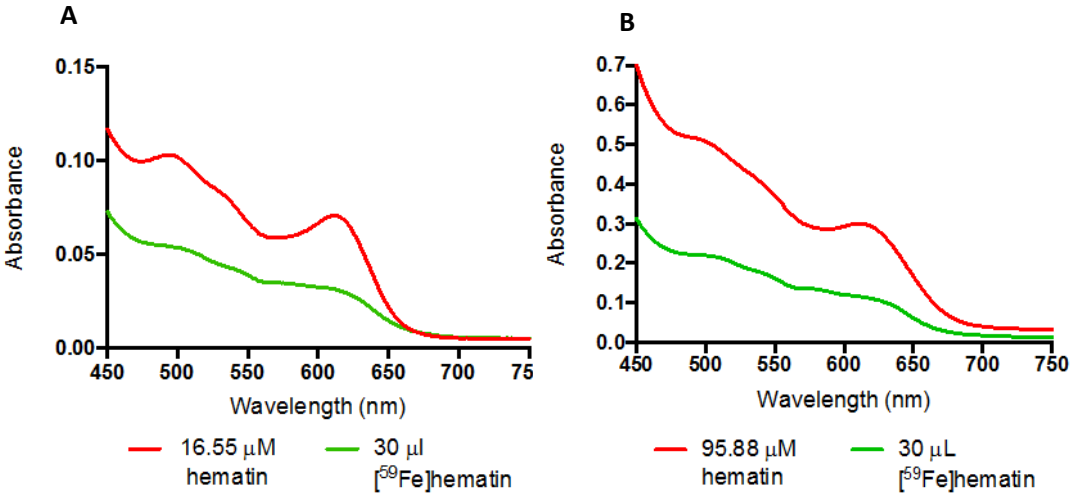

Figure 2-1. Spectroscopy of synthesised [^{59}Fe]hematin. Absorbance spectroscopy between 450 nm and 750 nm of synthesised [^{59}Fe]hematin and reference hematin dissolved in DMSO and diluted into a buffer consisting of 10 mM phosphate buffer, 20 mM KCl, pH 8. **A** – Spectroscopy of [^{59}Fe]hematin from first synthesis, red line [^{59}Fe]hematin, green line reference sample of hematin at a final concentration of 16.55 μM. **B** – Spectroscopy of [^{59}Fe]hematin in DMSO from the second synthesis of [^{59}Fe]hematin, red line [^{59}Fe]hematin, green line reference sample of hematin at a final concentration of 95.88 μM. All solutions had an absorbance peak at 612 nm.

$$[^{59}\text{Fe}]\text{hematin (mM)} = \left\{\left[\frac{(\text{HAbs}_{612}-\text{HAbs}_{700})}{(\text{RAAbs}_{612}-\text{RAAbs}_{700})}\right] \text{X concentration of H (mM)}\right\} \text{X } 67$$

Equation 2-1

$$[^{59}\text{Fe}]\text{hematin (mg)} = \left\{\left[\frac{[^{59}\text{Fe}]\text{hematin (M)}}{1/\text{Mw}}\right] \text{X volume (L)}\right\} \text{X } 1{,}000$$

Equation 2-2

$$[^{59}\text{Fe}]\text{hematin (μmoles)} = \left[\frac{\text{mass (g)}}{\text{Mw}}\right] \text{X } 1{,}000{,}000$$

Equation 2-3

$$[^{59}\text{Fe}]\text{hematin yield (\%)} = \left[\frac{\text{CPM of 2 μL X (total volume-2 μL)}}{\text{CPM of starting material}}\right] \text{X } 100$$

Equation 2-4

$$\text{Radioactivity of } [^{59}\text{Fe}]\text{hematin (Bq)} = \frac{\left[\left(\frac{\text{Total CPM}}{28.5}\right) \text{X } 100\right]}{60}$$

Equation 2-5

$$\text{Radioactivity of } [^{59}\text{Fe}]\text{hematin (µCi)} = \left(\frac{\text{Radioactivity of } [^{59}\text{Fe}]\text{hematin (Bq)}}{3.7\text{x}10^{10}}\right) \text{X } 1{,}000{,}000$$

Equation 2-6

$$[^{59}\text{Fe}]\text{hematin specific activity (µCi/µmol)} = \left(\frac{\text{Radioactivity of } [^{59}\text{Fe}]\text{hematin (µCi)}}{\text{Quantity } [^{59}\text{Fe}]\text{hematin synthesised (µmol)}}\right)$$

Equation 2-7

Table 2-2 Yield, Quantity and Specific Activity of [^{59}Fe]hematin Synthesised		
	First Synthesis	**Second Synthesis**
Starting amount of ^{59}Fe (µL)	102	167
Radioactivity of ^{59}Fe (CPM) 0.008 µL (1st), 0.1 µL (2nd)	17,311	156,362
Radioactivity of total starting material (CPM)	220,715,250	261,124,540
Volume of [^{59}Fe]hematin synthesised (µL)	4,000	2,400
Radioactivity of 2 µL of [^{59}Fe]hematin (CPM)	34,387	83,229
Radioactivity of total [^{59}Fe]hematin synthesised (CPM)	68,777,400	99,874,800
Yield of [^{59}Fe]hematin (%)	31.2	38.2
Molecular weight of [^{59}Fe]hematin	636.3	636.3
Concentration of [^{59}Fe]hematin (mM)	0.81	2.85
Total quantity [^{59}Fe]hematin synthesised (mg)	2.06	4.35
Total quantity [^{59}Fe]hematin synthesised (µmol)	3.24	6.84
Radioactivity of [^{59}Fe]hematin synthesised (Bq)	4.02x10^{6}	5.84x10^{6}
Radioactivity of [^{59}Fe]hematin synthesised (µCi)	108.7	157.9
Specific activity of [^{59}Fe]hematin (µCi/µmol)	**33.6**	**36.3**

2.2.7 Separation of Hematin and GS.hematin by HPLC

2.2.7.1 Protocol Development

Sato *et al.* (1994) and Tangerås (1984) both used HPLC to separate metal porphyrins in samples. Tangerås (1984) used a reverse phase LC-C18 column with a mobile phase of methanol and water. An Agilent PLRP-S polymeric revers phase column was tried for the separation of hematin from GS.hematin however no separation occurred and glutathione

does not dissolve in methanol. Sato *et al.* (1994) used a porous polymer gel, (type HP-125 from Showa Denko, Tokyo, Japan), which is no longer produced, functioning as a size exclusion column with a mobile phase of water and methanol. From this method size exclusion columns were tried (Agilent PL aquagel-OH 40 and Agilent PL aquagel-OH 30) with varying mobile phases, all consisting of phosphate buffer and glutathione. An aqueous mobile phase was desirable because both hematin and glutathione dissolve in phosphate buffer. These columns produced slight separation of GS.hematin from GSSG and GSH however further resolution was desired, hematin bound to both columns and only eluted in pure water. Although pure water eluted hematin from the column there was no interaction between the column and any compound therefore all compounds of interest eluted at the same time. Agilent PL aquagel-OH 20 is a column in the same class however it has optimal separation for compounds with a molecular weight up to 20,000 g/mol instead of between 10,000 and 200,000 g/mol (PL aquagel-OH 40) or between 100 and 60,000 g/mol (PL aquagel-OH 30).

2.2.7.2 Size Exclusion HPLC Controls

A Waters 626 HPLC system (comprising of; Waters 717 plus auto sampler, Waters 600S controller and Waters 626 pump) coupled with a Waters 2996 photodiode array detector and Milennium[32] computer software attached to an Agilent PL aquagel-OH 20 5 µM 300 x 7.5 mm column (Agilent, Stockport, UK) was used at room temperature with a mobile phase of 20 mM phosphate buffer, 2 mM glutathione, pH 8 at 0.4 mL/min. Samples were dissolved in 200 mM phosphate buffer, 20 mM KCl, pH 8 before injection, (injection buffer).

The buffer which samples were dissolved in, 200 mM phosphate buffer, 20 mM KCl, pH 8 (injection buffer) was injected to get a baseline of background absorbance, (Figures 2-2 & 2-3).

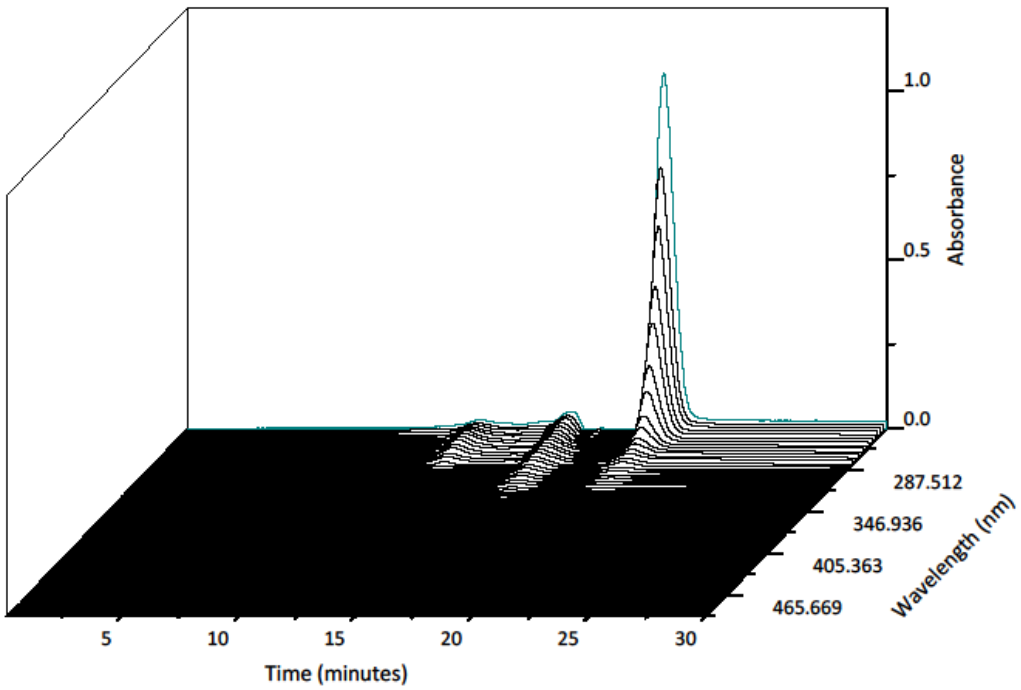

Figure 2-2. 3D chromatogram of injection buffer. Chromatogram of injection buffer (200 mM phosphate buffer, 20 mM KCl, pH 8), eluted on an Agilent PL aquagel-OH 20 column with a mobile phase of 20 mM phosphate buffer, 2 mM glutathione, pH 8 at 0.4 mL/min. Absorbance was detected over 30 minutes between 230 nm and 500 nm. The turquoise line denotes absorption spectrum of injection buffer at 230 nm over time, with peak absorption occurring at 20.5 minutes.

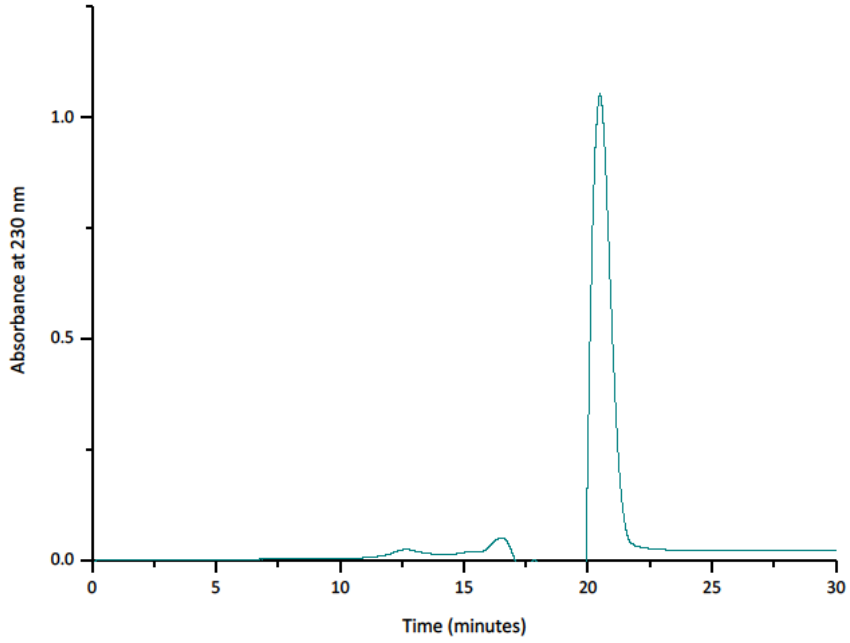

Figure 2-3. Chromatogram at 230 nm of injection buffer. Chromatogram of injection buffer (200 mM phosphate buffer, 20 mM KCl, pH 8), eluted on an Agilent PL aquagel-OH 20 column with a mobile phase of 20 mM phosphate buffer, 2 mM glutathione, pH 8 at 0.4 mL/min. Absorbance was detected at 230 nm over 30 minutes and showed the retention time of the injection buffer was 20.5 minutes.

The absorbance spectrum of the injection buffer, which is the solution used to dissolve samples for chromatography, 10 mM phosphate buffer, 20 mM KCl solution has a absorption peak at 20.5 minutes between 230 nm and 300 nm (Figure 2-2 & 2-3).

15 mM glutathione dissolved in 200 mM phosphate buffer, 20 mM KCl, had an elution time of 20.4 minutes (Figure 2-4). The injection buffer alone has an absorption peak at 20.4 minutes however with glutathione in the solution, this peak increases in absorption from 1 abs to 1.5 abs showing that glutathione elutes at 20.4 minutes along with the injection buffer (Figure 2-3 and 2-4).

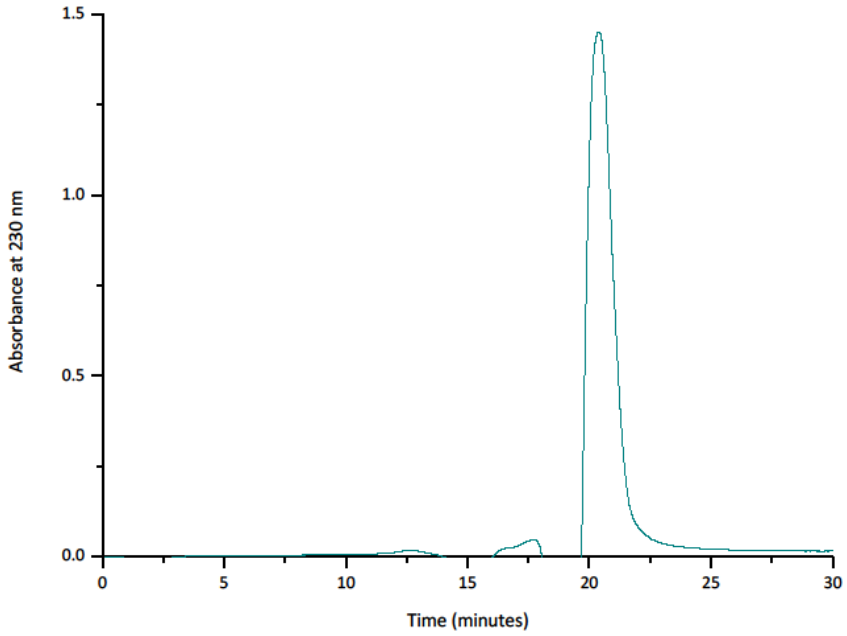

Figure 2-4. Chromatogram at 230 nm of 15 mM glutathione. Chromatogram of glutathione dissolved in injection buffer eluted on an Agilent PL aquagel-OH 20 column with a mobile phase of 20 mM phosphate buffer, 2 mM glutathione, pH 8 at 0.4 mL/min. Absorbance was detected at 230 nm over 30 minutes and showed glutathione had a retention time of 20.4 minutes.

Reduced glutathione, over time in the presence of oxygen, oxidises forming the glutathione dimer, glutathione disulphide (GSSG), with a molecular weight of 612.63. GSSG dissolved in 200 mM phosphate buffer, 20 mM KCl had an elution time of 17.6 minutes (Figure 2-5).

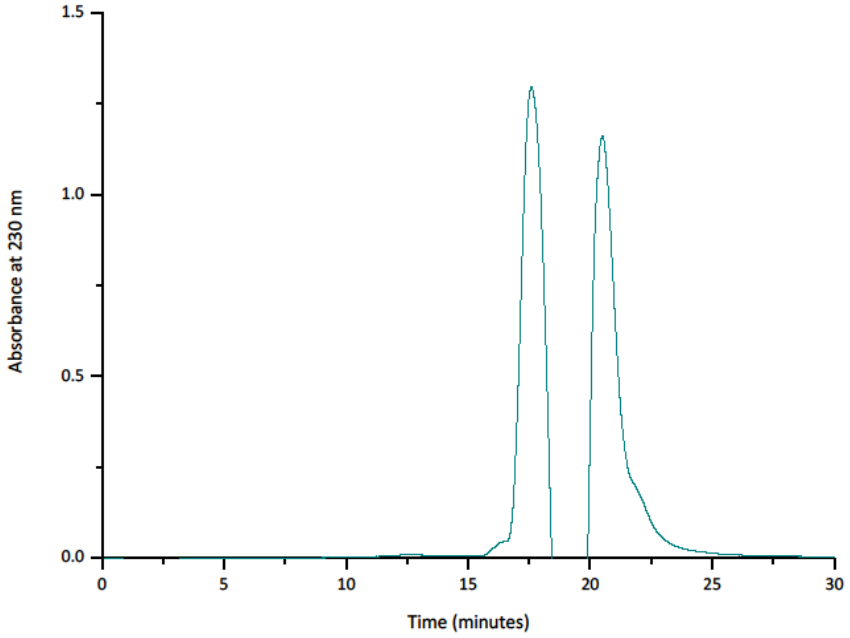

Figure 2-5. Chromatogram at 230 nm of 15 mM glutathione disulphide. Chromatogram of glutathione disulphide dissolved in injection buffer eluted on an Agilent PL aquagel-OH 20 column with a mobile phase of 20 mM phosphate buffer, 2 mM glutathione, pH 8 at 0.4 mL/min. Absorbance was detected at 230 nm over 30 minutes and showed two absorbance peaks, at 17.6 minutes and 20.4 minutes.

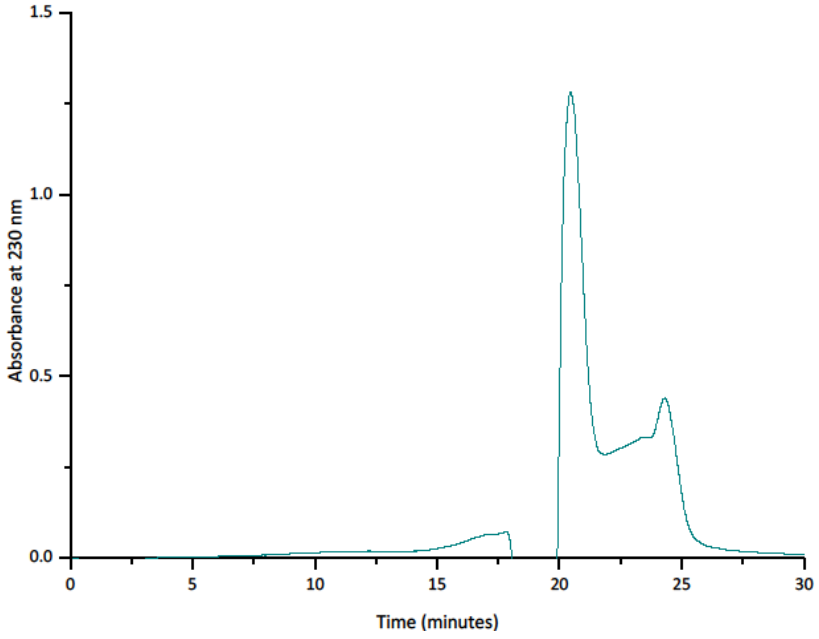

Figure 2-6. Chromatogram at 230 nm of DMSO. DMSO diluted 1/100 into injection buffer eluted on an Agilent PL aquagel-OH 20 column with a mobile phase of 20 mM phosphate buffer, 2 mM glutathione, pH 8 at 0.4 mL/min. Absorbance was detected at 230 nm over 30 minutes and showed DMSO had a retention time of 24.3 minutes.

Hematin dissolved in DMSO then diluted into 200 mM phosphate buffer, 20 mM KCl, pH 8 for injection into the HPLC system. As a control DMSO was diluted into 200 mM phosphate

buffer, 20 mM KCl, pH 8 and injected into the HPLC system. DMSO had an elution time of 24.3 minutes (Figure 2-6).

2.2.8 Mass spectroscopy of GS-hematin Complex

Aliquots of 20 μM GS.hematin complex in 10 mM phosphate buffer, 20 mM KCl, pH 8; 20 μM hematin in 10 mM phosphate buffer, 20 mM KCl, pH 8; 4 mM glutathione in 10 mM phosphate buffer, 20 mM KCl, pH 8 and 10 mM phosphate buffer 20 mM KCl, pH 8 were lyophilized (Lyotrap freeze dryer) overnight.

The samples were dissolved in 50% (v/v) methanol, 0.1% (v/v) formic acid in water (2 mg/mL). Direct injection for orbitrap exactive mass spectroscopy (Exactive plus orbitrap mass spectrometer, Thermo Fisher Scientific, Leicestershire) both positive and negative ion mode, was conducted on all samples. The results were analysed, and theoretical isotope models created using Xcalibur software (Thermo Fisher Scientific, Leicestershire).

Orbitrap exactive mass spectroscopy, in positive and negative ion mode, of samples dissolved in 50% (v/v) methanol in water was tried and LTQ XL mass spectroscopy (Thermo Fisher Scientific, Leicestershire) of samples in 50% (v/v) methanol, 0.1% (v/v) formic acid in water (1 mg/mL) in ion mode were investigated.

2.2.9 Interaction Between Gallium Protoporphyrin IX and Glutathione

2.2.9.1 Gallium Protoporphyrin IX Synthesis

The protocol for GaPPIX synthesis was adapted from Azad *et al.* (2012). PPIX and $GaCl_3$ were dissolved in 130 mM HCl in acetone in a 1:1 molar ratio in a sealed glass reaction vessel. The vessel was heated in an oil bath to 130^{o}C and incubated for 90 minutes. The vessel was cooled down in the oil bath to 45^{o}C. The solution was evaporated under reduced pressure, the liquid remaining, (containing PPIX not converted to GaPPIX), was decanted and evaporated with a stream of nitrogen, the fraction evaporated under reduced pressure was placed in a vacuum desiccator overnight. The GaPPIX compound, the PPIX starting material and hemin, were analysed with PerkinElmer FT-IR spectrophotometer Frontier coupled to PerkinElmer Universal ATR sampling accessary and PerkinElmer Spectrum computer software.

2.2.9.1 Interaction of GaPPIX with Glutathione

GaPPIX was dissolved in 200 mM phosphate buffer, 20 mM KCl, pH 8 to a final concentration of 10 μM, vortexed for 10 minutes, centrifuged at 4,000 rpm for 10 minutes

and supernatant decanted. GaPPIX was dissolved in 200 mM phosphate buffer, 20 mM KCl, 2 mM glutathione, pH 8 to a final concentration of 10 µM, vortexed for 10 minutes, centrifuged at 4,000 rpm for 10 minutes and supernatant decanted. PPIX, was dissolved in 200 mM phosphate buffer, 20 mM KCl, 2 mM glutathione, pH 8 to a final concentration of 10 µM, vortexed for 10 minutes, centrifuged at 4,000 rpm for 10 minutes and supernatant decanted. The absorbance of the three solutions was measured at 1 nm intervals between 300 nm and 800 nm using a PerkinElmer UV/Vis spectrophotometer Lambda 2 coupled with Lambda25 software. Solutions were measured in a quartz cuvette with a path length of 10 mm between 300 nm and 500 nm and in a Spectrosil® quartz cuvette with a path length of 100 mm between 500 nm and 800 nm. Absorbance was plotted against wavelength for each of the solutions in GraphPad Prism.

2.3 Results and Discussion

2.3.1 Phosphate Buffer Conditions for Dissolving Hematin

Previous experiments trying to mimic physiological conditions of hemin have followed Kirschner-Zilber's (1982) protocol to dissolve hemin, which calls hemin to be dissolved in NaOH, forming a stock solution that is diluted into phosphate buffers. Although the buffers used were in the proximity of being physiologically relevant the stock solution of hemin/hematin was not (Kirschner-Zilber's 1982; Silver *et al.* 1985; Shviro & Shaklai 1987; Sahini *et al.* 1996).

To more accurately mimic physiological conditions for hematin absorption several different solutions, all based around 10 mM phosphate buffer were tried. Only trace amounts of hematin dissolved in phosphate buffer alone, or in phosphate buffer containing arginine, which has previously been used to help keep organic iron in solution (Sievers *et al.* 1987). When KCl was added to the phosphate buffer, hematin dissolved. Therefore both pH and KCl concentration were further investigated to determine the best solution to dissolve hematin whilst keeping the solution as physiologically relevant as possible.

There was a slight increase in the amount of hematin dissolved in phosphate buffer at pH 8, containing 20 mM KCl compared 100 mM KCl, (Figure 2-7).

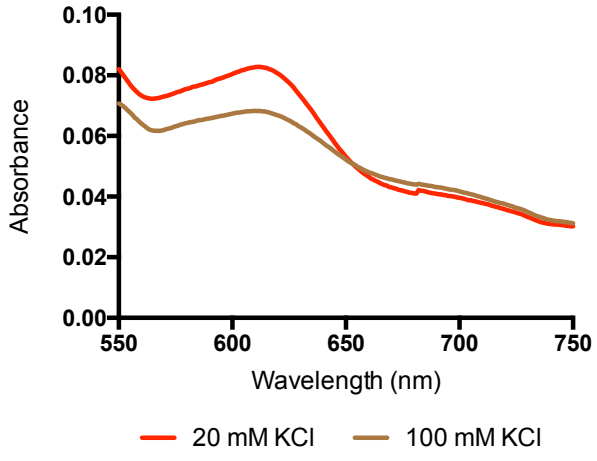

Figure 2-7. Effect of KCl concentration on hematin solubility. Absorbance spectrum of hematin (50 μM) dissolved in 10 mM phosphate buffer, pH 8 with either 20 mM KCl (red line) or 100 mM KCl (brown line) present. Both samples had peak absorption at 618 nm.

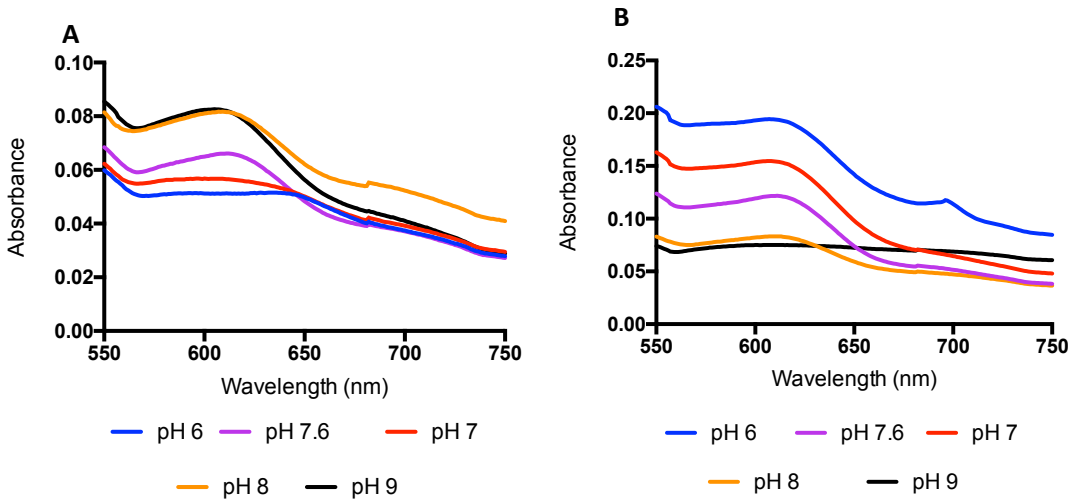

Figure 2-8. Effect of pH on hematin solubility. Hematin (50 μM) was dissolved in solutions of 10 mM phosphate buffer, 20 mM KCl at varying pH's (pH 6-9). The samples were centrifuged and supernatant aspirated for spectroscopy. The pellet of undissolved hematin was dissolved in a solution of 10 mM phosphate buffer, 20 mM KCl at pH 9 and absorption was read between 550 nm and 750 nm. **A** – Absorption spectrum of hematin supernatant from hematin (50 μM) dissolved in varying pH solutions**;** pH 6 (blue), pH 7.6 (purple), pH 7 (red), pH 8 (orange), pH 9 (black). All solutions had an absorption peak at 618 nm with hematin dissolved in a buffer at pH 8 or 9 having the highest absorption at 618 nm, indicating the highest amount of hematin dissolved. **B** – Absorption spectrum of the hematin pellets from hematin dissolved in phosphate buffer with varying pH, dissolved in 10 mM phosphate buffer, 20 mM KCl at pH 9. pH of original solution hematin was dissolved in; pH 6 (blue), pH 7.6 (purple), pH 7 (red), pH 8 (orange), pH 9 (black). The pellet from hematin dissolved in the phosphate buffer at pH 8 (orange) or pH 9 (black), dissolved in phosphate buffer at pH 9, had no absorption peak at 618 nm, meaning all hematin was dissolved in the original buffer.

The absorption of 50 μM hematin in 10 mM phosphate buffer, 20 mM KCl at different pH conditions showed that below pH 8 less than 98% of the hematin dissolved (Figure 2-8). This was confirmed when the hematin pellet was dissolved in phosphate buffer at pH 9 (Figure 2-8).

Hematin was dissolved in phosphate buffer at pH 8 with the addition of 20 mM KCl for any experiments where hematin was required to be in physiologically relevant conditions. The concentration of the phosphate buffer was increased for experiments where the solution required a larger buffering capacity to maintain pH 8.

2.3.2 Determination of the Affinity Constant of Hematin – Glutathione Interaction

There is a shift in peak absorbance to the blue (from 618 nm to 655 nm), when glutathione binds to hematin, forming the GS.heamtin complex, (Figure 2-9). This is in agreement with the report of Shviro & Shaklai (1987), who documented an absorption peak shift to the blue

with the addition of 8.7 mM glutathione to a solution of 20 µM hemin in phosphate buffer at pH 8.

The change in absorption between the hematin peak, at 618 nm, and the GS.hematin peak, at 655 nm, was plotted against the log concentration of glutathione (mM) to determine the affinity constant of hematin and glutathione, (Figure 2-10). The affinity constant was calculated to be K_a = 5.0 x 10^4 M^{-1}, at pH 8 using equation 2-8. This affinity constant is comparable to the affinity constant of (Shviro & Shaklai, 1987), who calculated it to be K_a = 3.1 x 10^4 M^{-1} from 17.1 µM hemin in phosphate buffer at pH 8 and a range of glutathione concentrations. (Sahini *et al.,* 1996) calculated the affinity constant of hemin and glutathione using spectroscopy as 2.8 x 10^3 M^{-1}, which is an order of magnitude lower then both Shviro & Shaklai and ours. Sahini calculated the affinity constant using 1 – 20 mM hemin and 1 – 5 mM glutathione. The concentration of hemin Sahini used is an order of magnitude higher than that used by Shviro & Shaklai and ourselves, however Sahini used the same range concentration of glutathione as in this study, which means that the ratio of hematin to glutathione was an order of magnitude different than ours. This could possibly lead to the discrepancy between the affinity constants calculated in this work and Sahini.

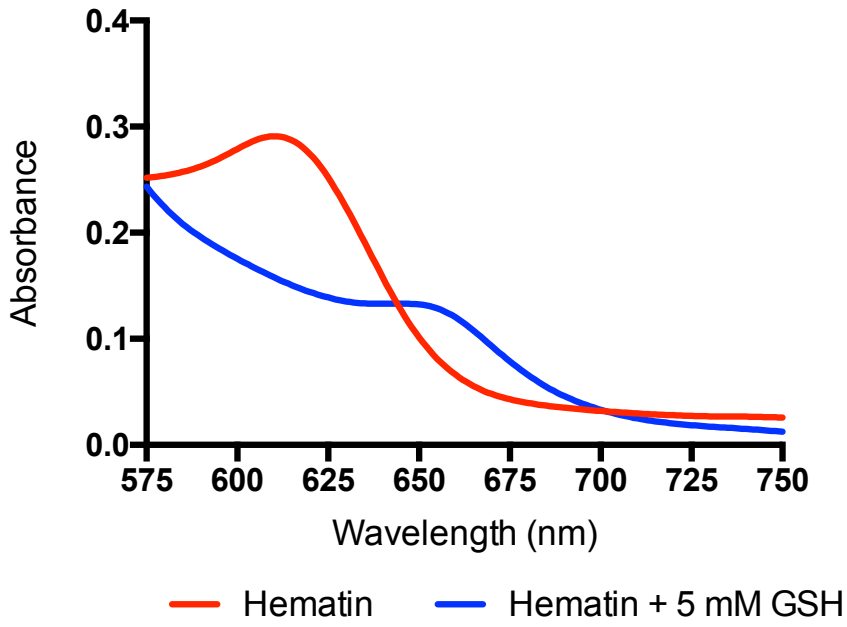

Figure 2-9. Absorption spectrum of hematin ± glutathione. Hematin was dissolved to a final concentration of 10 µM in 10 mM phosphate buffer, 20 mM KCl, pH 8 (red line) or 10 mM phosphate buffer, 20 mM KCl, 5 mM glutathione, pH 8 (blue line) and absorbance of solutions recorded between 575 nm and 750 nm. Hematin in phosphate buffer had an absorption peak at 618 nm whilst hematin in phosphate buffer in the presence of 5 mM glutathione had an absorption peak at 655 nm.

Both Shviro & Shaklai and Sahini used a stock solution of hemin dissolved in 10 mM NaOH which was diluted into the phosphate buffer to give a final concentration of 5 mM NaOH, although the phosphate buffer and pH conditions they used were in the philological range the use of NaOH is not ideal. We however dissolved the hemin straight into the phosphate buffer, with potassium chloride, and therefore we consider that our method of dissolving hemin is more relevant to the *in vivo* situation.

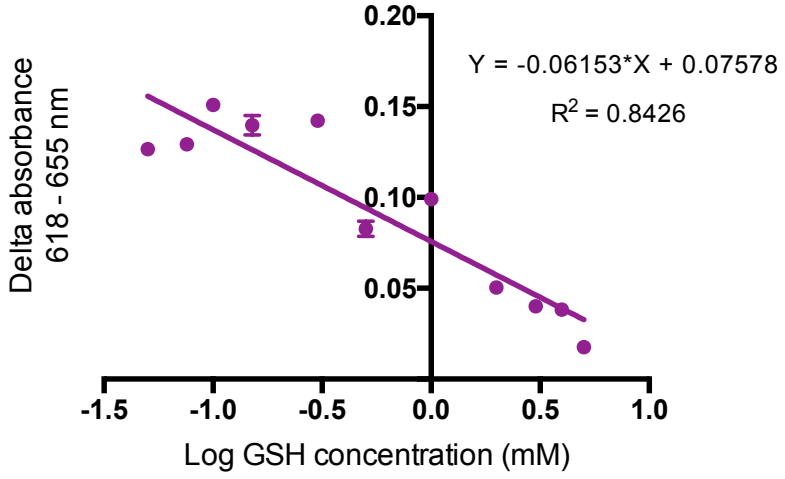

Figure 2-10. Effect of glutathione concentration on GS.hematin formation. Hematin was dissolved in 10 mM phosphate buffer, 20 mM KCl, pH 8 with varying concentrations of glutathione (0-5 mM) and absorption detected at 618 nm and 655nm. The log concentration of glutathione was plotted against the difference in absorption between the hematin (618 nm) and hematin in the presence of glutathione (655 nm). Values are means ± SEM (n = 3). Where error bars are not visible they are smaller than the point. A line with lineal regression was fitted to the graph with a slope of Y = -0.06153*X + 0.07578.

$$K_a = \frac{[GS.hematin][H^+]}{[Hematin][GSH]}$$

Equation 2-8

2.3.2.1 Speciation Plot of Hematin and Glutathione

The affinity constant of hematin and glutathione, k_a = 5.0 x 10^4 M^{-1}, was used to produce a speciation plot of hematin and glutathione at pH 8. The speciation plot shows that at physiologically relevant conditions, (< 10 µM hematin, 2 mM glutathione), 99 % of hematin in the cytosol would be complexed with glutathione, in the form of the GS.hematin complex (Figure 2-11 & 2-12).

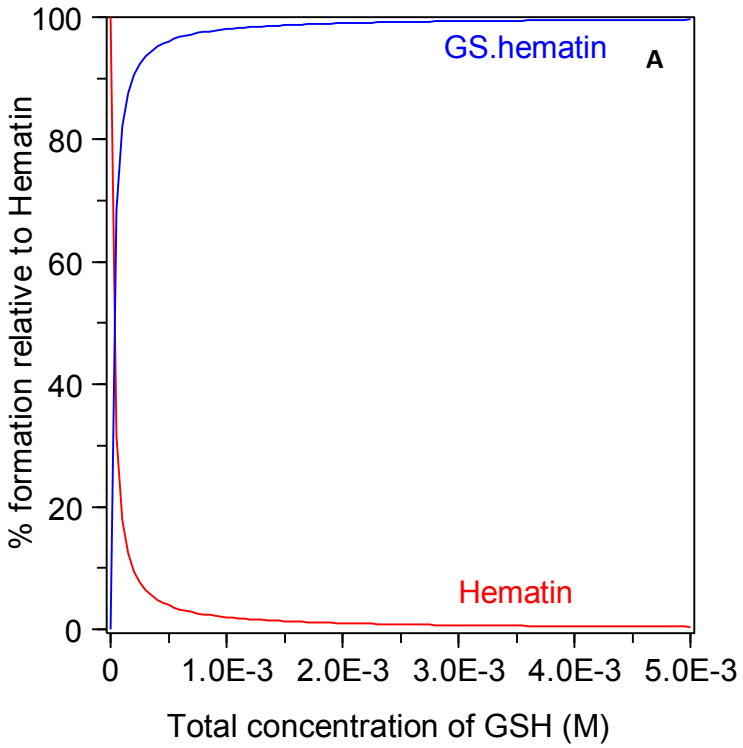

Figure 2-11. Speciation plots of the formation of GS.hematin. Speciation plots with parameters K_a = 5.0 x 10^4 M^{-1}, pH 8, total hematin concentration of 10 µM and total glutathione concentration 0-5 mM. The red line indicates the percentage of total hematin that would be free in solution; the blue line indicates the calculated amount of hematin in the solution that would bind to glutathione to form GS.hematin.

The concentration of 'free' glutathione within the cell, that which is not routinely required to maintain cell homeostasis or the redox potential of the cytosol, is unknown. Experiments designed to deplete cells of glutathione cannot deplete the cells completely of glutathione without causing cell death, therefore even glutathione-depleted cells contain

Table 2-3 Formation of GS.hematin at differing glutathione concentrations

Hematin concentration (µM)	GSH concentration (mM)	Formation of GS.hematin relative to hematin (%)
10	1	98.0
10	0.2	90.5
10	0.1	82.1
10	0.05	68.4

no less then 200 µM of glutathione. Table 2-3 shows that a reduced concentration of glutathione, 200 µM, over 90 % of labile hematin within cells (10 µM) would be ligated to glutathione. Even if glutathione reached as low as 50 µM, 68 % of hematin would still be bound to glutathione forming GS.hematin.

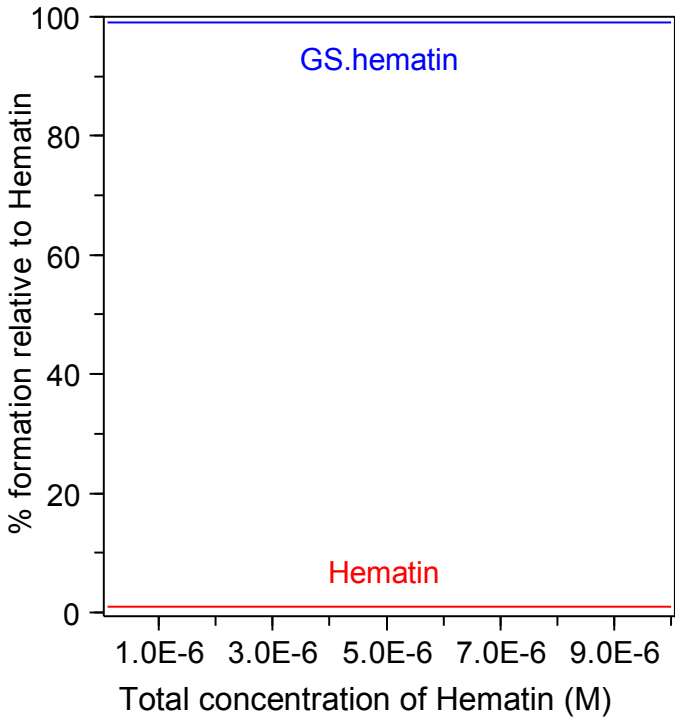

Figure 2-12. Speciation plot of the formation of GS.hematin. Speciation plot with parameters K_a = 5.0 x 10^4 M^{-1}, pH 8, total glutathione concentration of 2 mM, and total hematin concentration of 0.1 – 10 µM. The red line indicates the percentage of total hematin that would be free in solution; the blue line indicates the calculated amount of hematin in the solution that would bind to glutathione to form GS.hematin.

2.3.3 Determination of the Affinity Constant of Hematin – Cysteine Interaction

The shift in peak absorbance to the blue (from 618 nm to 655 nm) when cysteine binds to hematin, forming Cys.hematin complex, is the same as the shift when glutathione binds to hematin forming the GS.hematin complex, (Figure 2-13).

The change in absorption between the hematin peak, at 618 nm, and the Cys.hematin peak, at 655 nm, was plotted against the log concentration of cysteine (mM) to determine the affinity constant of hematin and cysteine, (Figure 2-14). The affinity constant was calculated to be K_a = 1.6 x 10^2 M^{-1}, at pH 8 using equation 2-8. This affinity constant is two orders of magnitude lower than that of glutathione to hematin (5.0 x 10^4 M^{-1}) under the same conditions. Previous studies have proved that the hematin – glutathione interaction is through the thiol group, on the cysteine residue in glutathione (Shiviro & Shaklai, 1987). If only the thiol group was involved in the interaction of hematin to glutathione the affinity constants of hematin – glutathione and hematin – cysteine would be similar however this is not the case.

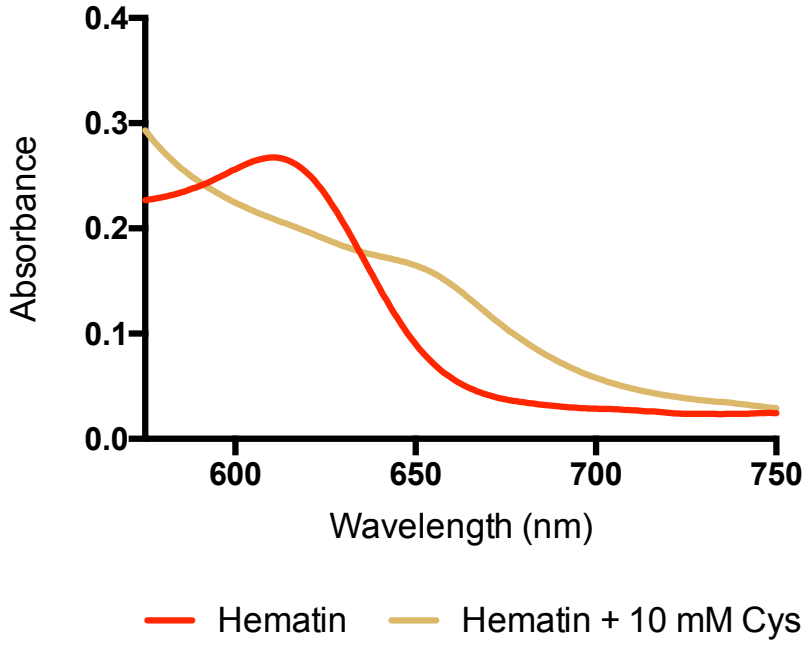

Figure 2-13. Absorption spectrum of hematin ± cysteine. Hematin was dissolved to a final concentration of 10 µM in 10 mM phosphate buffer, 20 mM KCl, pH 8 (red line) or 10 mM phosphate buffer, 20 mM KCl, 10 mM cysteine, pH 8 (gold line) and absorbance of solutions recorded between 575 nm and 750 nm. Hematin in phosphate buffer had an absorption peak at 618 nm whilst hematin in phosphate buffer in the presence of 10 mM cysteine had an absorption peak at 655 nm.

The difference in affinity constants indicates that other factors are involved in the interaction of hematin to glutathione; this is likely to be appreciable hydrophobic interaction between the planar and hydrophobic hematin compound and the peptide backbone in glutathione. Glutathione is a tripeptide consisting of a glutamic acid, cysteine and glycine residue whilst cysteine is a single amino acid, (Figure 2-15). Glutathione has more hydrophobic $-CH_2$ groups available for integration with hematin, therefore more Van der Waal interactions can take place between the PPIX ring of hematin and glutathione compared to cysteine. This indicates that hydrophobic interactions between glutathione and hematin are crucial for the formation of the relatively stable GS.hematin complex.

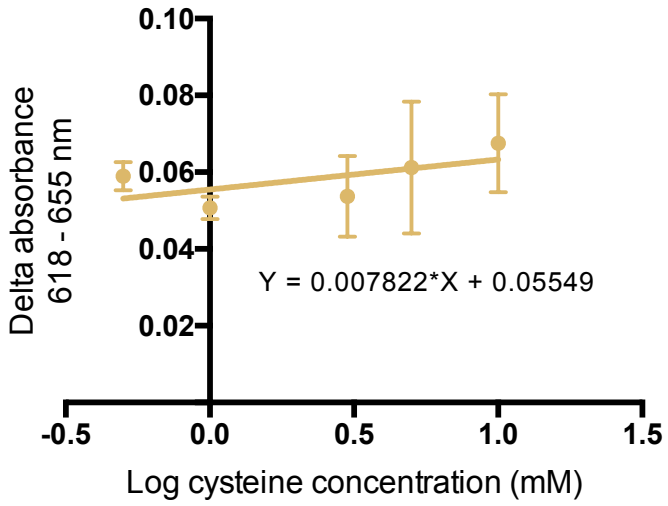

Figure 2-14. Effect of cysteine concentration of Cys.hematin formation. Hematin was dissolved in 10 mM phosphate buffer, 20 mM KCl, pH 8 with varying concentrations of cysteine (0-10 mM) and absorption detected at 618 nm and 655nm. The log concentration of cysteine was plotted against the difference in absorption between the hematin (618 nm) and hematin in the presence of cysteine (655 nm). Values are means ± SEM (n = 3). Where error bars are not visible they are smaller than the point. A line with lineal regression was fitted to the graph with a slope of Y = 0.007822*X + 0.05549.

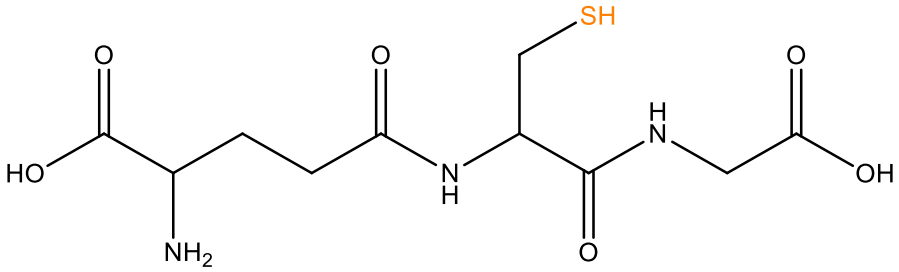

Figure 2-15. Structure of glutathione. Skeletal structure of glutathione, thiol group is in orange. (Drawn in Chem3D Ultra 12.0 software, PerkinElmer Ltd).

2.3.3.1 Speciation Plot of Hematin and Cysteine

The affinity constant of hematin and cysteine, k_a = 1.6 x 10^2 M^{-1}, was used to produce a speciation plot of hematin and cysteine at pH 8. The speciation plot shows that at physiologically relevant conditions, (10 µM hematin, 20 µM glutathione), less than 1 % of hematin in the cytosol would be complexed with cysteine (Figure 2-16).

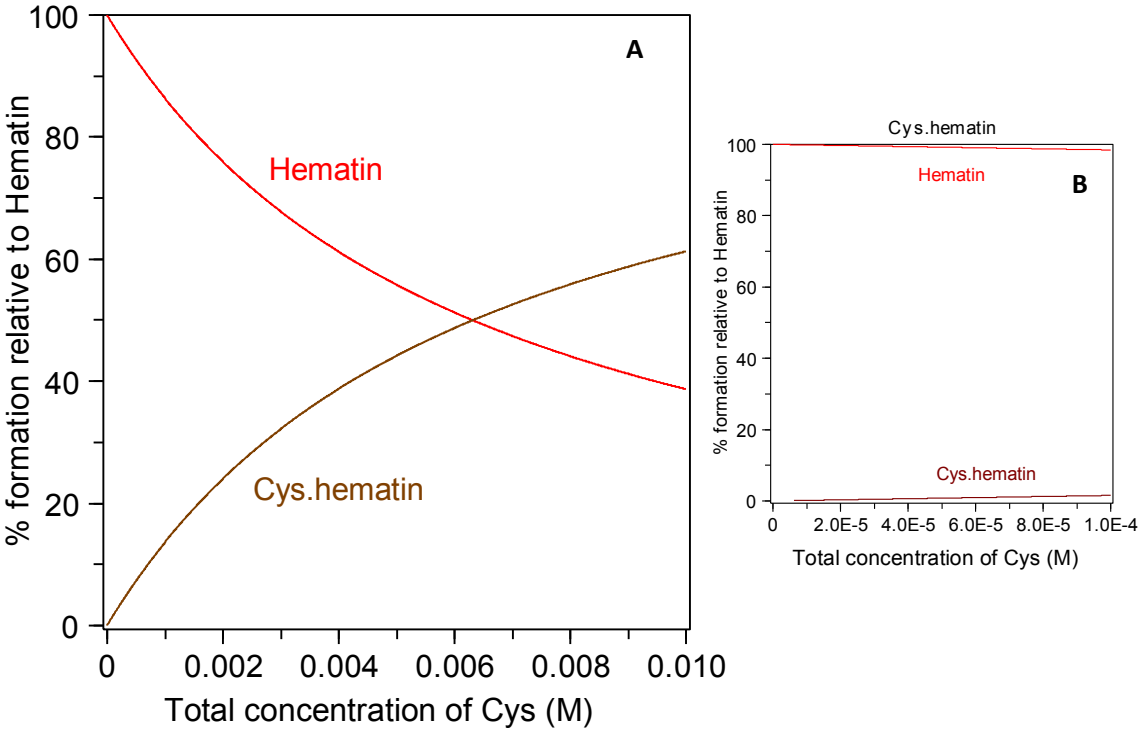

Figure 2-16. Speciation plot of the formation of Cys.hematin. Speciation plot with parameters K_a = 1.6 x 10^2 M^{-1}, pH 8, total hematin concentration of 10 µM and total cysteine concentration of **A** – 0 to 10 mM or **B** – 0 mM to 0.1 mM. The red line indicates the percentage of total hematin that would be free in solution; the gold line indicates the calculated amount of hematin in the solution that would bind to cysteine to form Cys.hematin.

2.3.4 [^{59}Fe]Hematin Synthesis

The first synthesis of [^{59}Fe]hematin resulted in a yield of 31.2%, a total quantity of 3.24 µmol [^{59}Fe]hematin synthesised, with a specific activity of 33.6 µCi/µmol (Table 2-2). The second synthesis resulted in a yield of 38.2%, a total quantity of 6.84 µmol [^{59}Fe]hematin synthesised with a specific activity of 36.3 µCi/µmol (Table 2-2). The yield of [^{59}Fe]hematin increased by 7%, the total quantity of [^{59}Fe]hematin synthesised increased by 3.6 µmol and the specific activity increased by 2.7 µCi/µmol between the first and second batch. The specific activity of the synthesised [^{59}Fe]hematin was 5.0 to 5.4 fold higher than the [^{59}Fe]hematin synthesised by Follett *et al.* 2002, (6.7 Ci/mol).

The addition of 25 mL chloroform on day two of the second synthesis, instead of 12.5 mL chloroform and 12.5 mL ethyl acetate, resulted in better separation between the aqueous and organic layers, due to chloroform being denser then ethyl acetate. The increased

volume of HCl used to precipitate the [^{59}Fe]hematin in the final step, from 0.5 mL per Eppendorf to 1 mL per Eppendorf, could also have contributed to the increase in [^{59}Fe]hematin yield by increasing the amount precipitated. These two slight modifications to the protocol resulted in an 7 % increase in yield that equated to a 112 % increase in amount [^{59}Fe]hematin synthesised, from 2.05 mg to 4.36 mg.

2.3.5 Separation of Hematin and GS.hematin by Size Exclusion HPLC

Hematin, dissolved in DMSO and diluted into 200 mM phosphate buffer, 20 mM KCl, pH 8 to a final concentration of 610 µM, failed to elute (Figure 2-17). The resulting chromatogram contained two peaks; corresponding to the injection artefact, at 20.4 minutes, and DMSO at 24.3 minutes (Figure 2-17). Thus hematin bound to the column.

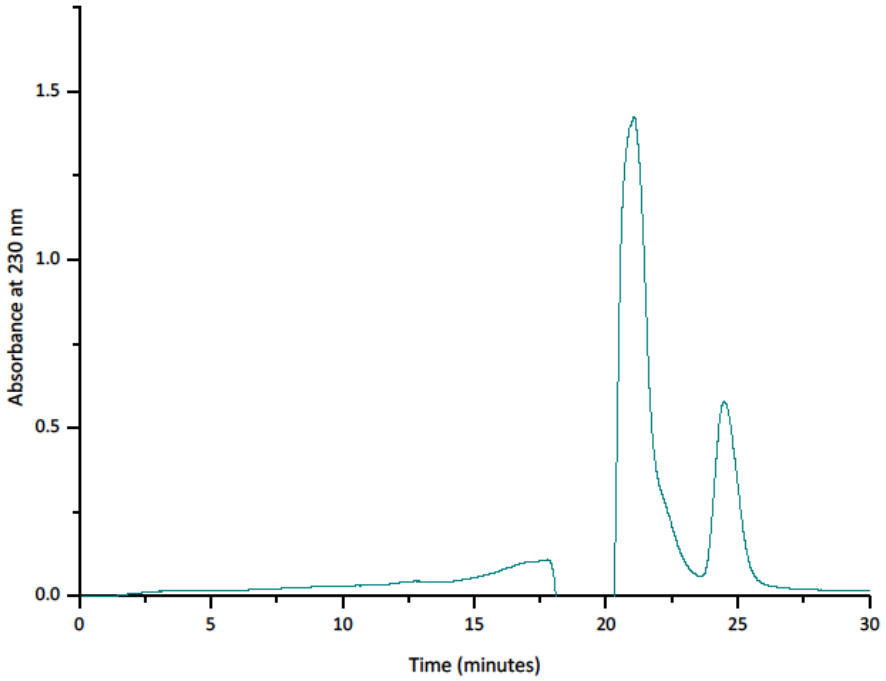

Figure 2-17. Chromatogram at 230 nm of hematin. Hematin (610 µM) in injection buffer eluted on an Agilent PL aquagel-OH 20 column with a mobile phase of 20 mM phosphate buffer, 2 mM glutathione, pH 8 at 0.4 mL/min. Absorbance was detected at 230 nm over 30 minutes and showed two elution peaks, at 20.4 minutes and 24.3 minutes, corresponding to the injection buffer artefact and DMSO respectively.

To confirm hematin bound to the column, and that the synthesised [^{59}Fe]hematin behaved in the fashion as non-radioactive hematin a sample of hematin was spiked with [^{59}Fe]hematin and injected into the HPLC system. One minute fractions were collected between 10 minutes and 30 minutes and counted for [^{59}Fe]hematin.

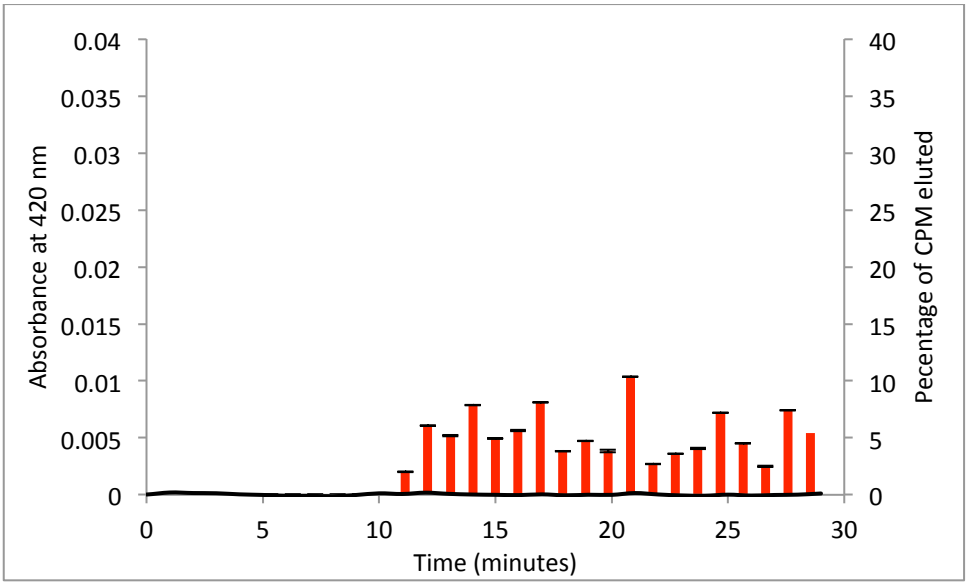

Figure 2-18. Chromatogram of [^{59}Fe]hematin at 420 nm and distribution of radioactivity eluted from hematin sample. Hematin (610 µM + [^{59}Fe]hematin) in injection buffer was eluted on an Agilent PL aquagel-OH 20 column with a mobile phase of 20 mM phosphate buffer, 2 mM glutathione, pH 8 at 0.4 mL/min. Absorbance was detected at 420 nm over 30 minutes (black line) and one minute fractions were collected between 10 and 30 minutes and counted for [^{59}Fe]hematin eluted (red bars). There was no absorption at 420 nm over 30 minutes (black line) and no peak in radioactivity (percentage of CPM eluted) eluted between 10 and 30 minutes (red bars).

The elution of hematin with [^{59}Fe]hematin present confirmed that hematin bound to the column and was essentially not eluted (Figure 2-18).

GS.hematin complex was formed by diluting a stock solution of hematin in DMSO into 200 mM phosphate buffer, 20 mM KCl, 15 mM glutathione, pH 8 to a final concentration of 610 µM. The GS.hematin solution was injected onto the column and the 2D chromatogram between 230 nm and 500 nm and 0 and 30 minutes was recorded (Figure 2-19).

The elution spectrum of GS.hematin showed several peaks at 230 nm; 20.4 minutes (glutathione and injection buffer), 24.3 minutes (DMSO), 17.7 minutes (GSSG) and an unidentified peak at 16.1 minutes, (Figures 2-19 & 2-20). This indicates that the peak at 16.1 minutes is the elution of GS.hematin (Figure 2-17).

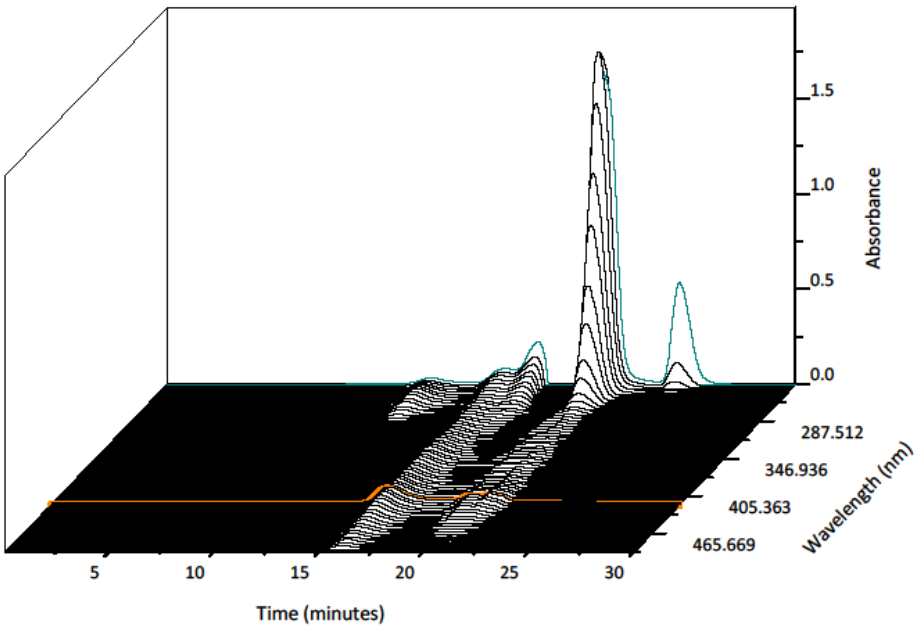

Figure 2-19. 3D chromatogram of GS.hematin. GS.hematin in injection buffer was eluted eluted on an Agilent PL aquagel-OH 20 column with a mobile phase of 20 mM phosphate buffer, 2 mM glutathione, pH 8 at 0.4 mL/min. Absorbance was detected between 230 nm and 500 nm, with absorbance at 230 nm denoted by the turquoise line and 420 nm by the orange line, over 30 minutes. Several absorption peaks were detected between 230 nm and 500 nm.

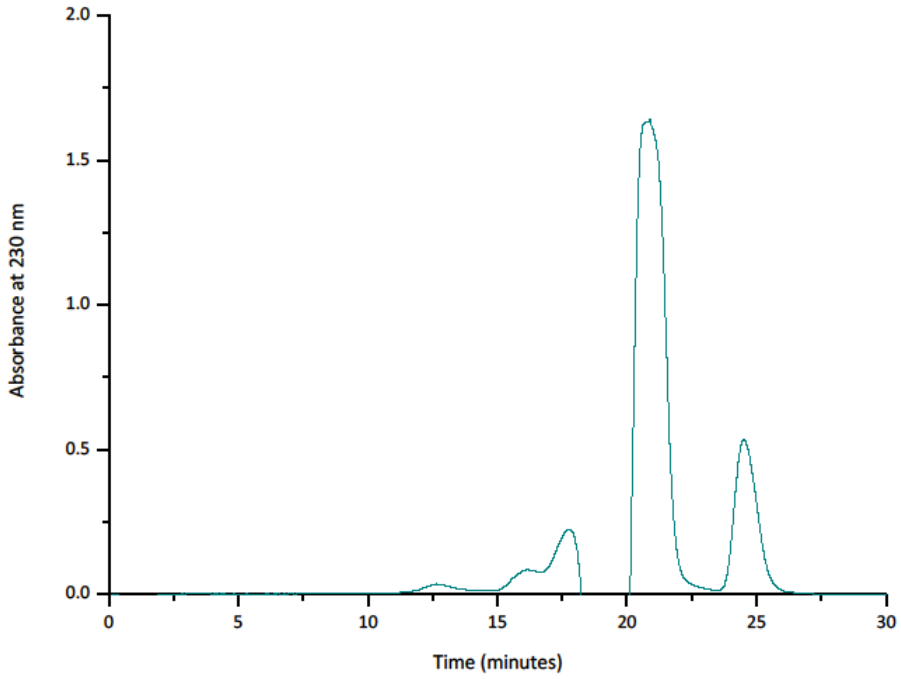

Figure 2-20. Chromatogram at 230 nm of GS.hematin. GS.hematin complex dissolved in injection buffer eluted on an Agilent PL aquagel-OH 20 column with a mobile phase of 20 mM phosphate buffer, 2 mM glutathione, pH 8 at 0.4 mL/min. Absorbance was detected at 230 nm over 30 minutes and showed four elution peaks at 16.1, 17.7, 20.4 and 24.3 minutes corresponding to GS.hematin, GSSG, injection buffer artefact and DMSO respectively.

DMSO, the injection buffer, glutathione and glutathione disulphide all absorb at wavelengths below 300 nm whilst GS.hematin absorbs at wavelengths up to 500 nm. The absorption spectrum between 300 and 500 nm at 16.1 minutes showed peak absorption occurred at 420 nm, corresponding to GS.hematin (Figure 2-21).

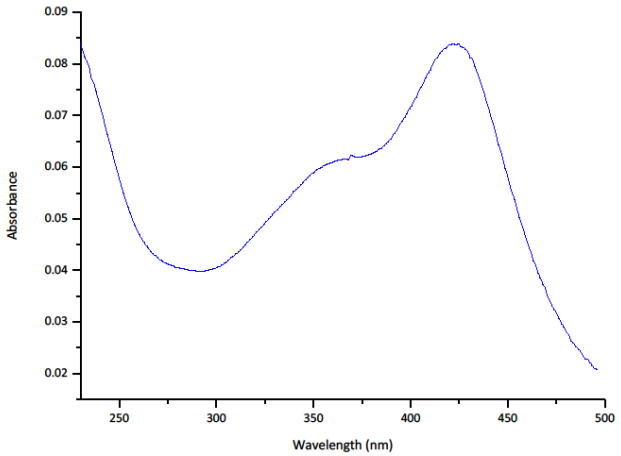

Figure 2-21. Absorption spectrum at 16.1 minutes of GS.hematin. GS.hematin dissolved in injection buffer eluted on an Agilent PL aquagel-OH 20 column with a mobile phase of 20 mM phosphate buffer, 2 mM glutathione, pH 8 at 0.4 mL/min. Absorbance detected at 420 nm at 16.1 minutes, showing peak absorption occurs at 420 nm, corresponding to GS.hematin.

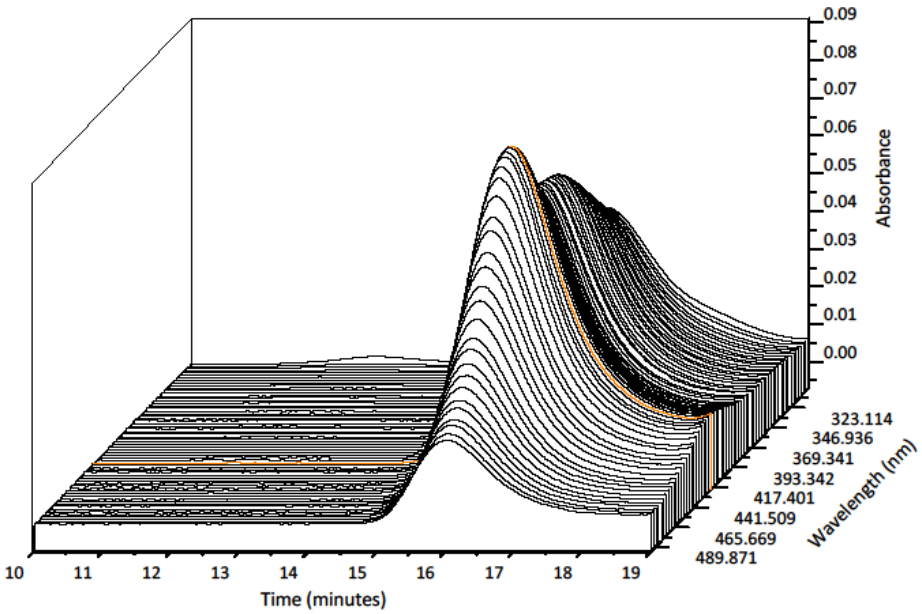

Figure 2-22. Magnified 3D chromatogram of GS.hematin. GS.hematin in injection buffer was eluted on an Agilent PL aquagel-OH 20 column with a mobile phase of 20 mM phosphate buffer, 2 mM glutathione, pH 8 at 0.4 mL/min. The chromatogram depicts the absorbance spectrum of the GS.hematin solution between 320 nm and 490 nm 10 to 20 minutes after injection onto the column. The orange line represents the absorption spectrum at 420 nm, indicating an absorption peak at 20.4 minutes.

The expanded 3D chromatogram (300 nm to 500 nm, 10 to 18 minutes) of GS.hematin elution verified that GS.hematin eluted at 16.1 minute as maximum absorption occurred at 420 nm (Figure 2-22).

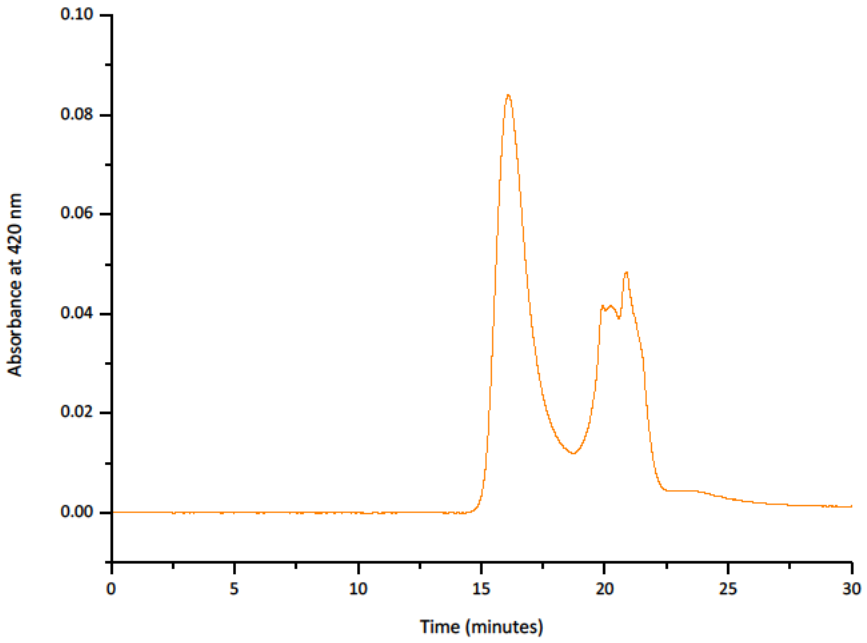

Figure 2-23. Chromatogram at 420 nm of GS.hematin. GS.hematin dissolved in injection buffer eluted on an Agilent PL aquagel-OH 20 column with a mobile phase of 20 mM phosphate buffer, 2 mM glutathione, pH 8 at 0.4 mL/min. Absorbance was detected at 420 nm over 30 minutes and showed two elution peaks, at 16.1 minutes, corresponding to GS.hematin and 20.4 minutes corresponding to the injection buffer artefact.

The absorbance at 420 nm (maximum absorbance for the compound eluting at 16.1 minutes) showed two peaks, one at 16.1 minutes with absorbance of 0.09 which has been deduced to be GS.hematin and a second, less prominent peak (absorbance at 0.05) at 20.4 minutes which is GSH and the injection buffer (Figure 2-23).

To confirm GS.hematin eluted at 16.1 minutes, and that the synthesised [^{59}Fe]hematin bound to glutathione and behaving in the same fashion as non-radioactive GS.hematin a sample of hematin was spiked with [^{59}Fe]hematin, dissolved in buffer containing glutathione, and injected into the HPLC system. One minute fractions were collected between 10 minutes and 30 minutes and counted for GS.[^{59}Fe]hematin.

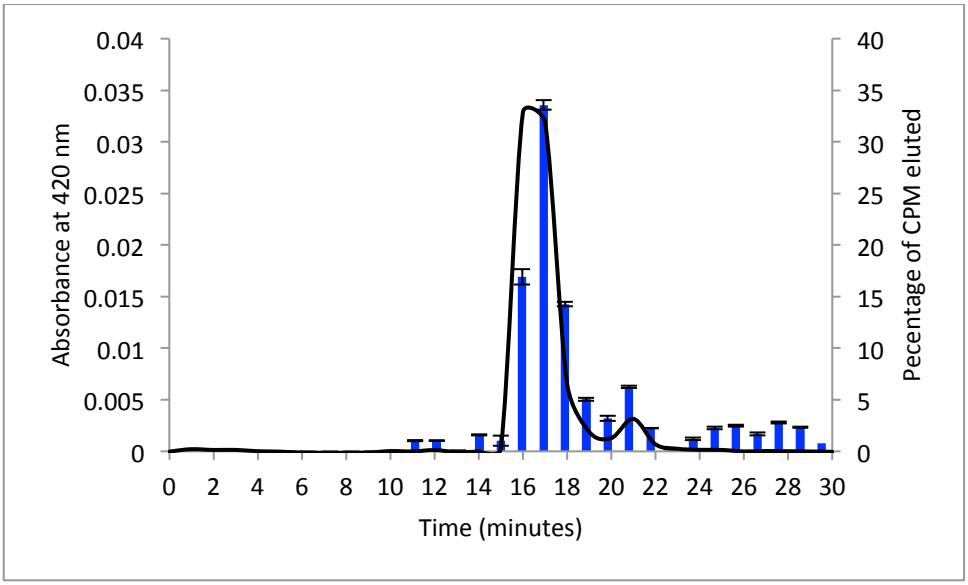

Figure 2-24. Chromatogram of GS.[^{59}Fe]hematin at 420 nm and distribution of radioactivity eluted from GS.hematin sample. GS.hematin (including [^{59}Fe]hematin) in injection buffer was eluted on an Agilent PL aquagel-OH 20 column with a mobile phase of 20 mM phosphate buffer, 2 mM glutathione, pH 8 at 0.4 mL/min. Absorbance was detected at 420 nm over 30 minutes (black line) and one minute fractions were collected between 10 and 30 minutes and counted for [^{59}Fe]hematin eluted (blue bars). The majority of the radioactivity (CPM) was eluted between 16 and 18 minutes (blue bars), corresponding to the absorption peak at 16.1 minutes at 420 nm (black line). This indicates that GS.hematin was eluted from the column at 16.1 minutes.

The elution of GS.hematin with [^{59}Fe]hematin present confirmed that GS.hematin eluted at 16.1 minutes (Figure 2-24). The majority of radioactive material eluted between 16 and 17 minutes which corresponds to the peak in absorbance at 420 nm at 16.1 minutes (Figure 2-24).

The elution time and peak absorbance of all compounds is summarised in Table 2-4. The data showed that GS.hematin could be separated and detected in samples when dissolved in 200 mM phosphate buffer with 20 mM KCl at pH 8, injected onto PL aquagel-OH 20 column and eluted at 0.4 mL/min with 20 mM phosphate buffer, 2 mM GSH at pH 8 whilst hematin stayed bound to the column.

Table 2-4 Summary of Elution Times for Compounds from PL aquagel-OH 20 column

Compound	**Molecular weight**	**Elution time (minutes)**	**Peak absorbance at 230 nm**	**Peak absorbance at 420 nm**
Injection buffer (200 mM phosphate buffer, 20 mM KCl)	94.97, 74.55	20.5	1.05	7.83×10^{-4}
glutathione	307.32	20.4	1.45	3.06×10^{-4}
glutathione disulphide	612.63	17.6	1.30	3.8×10^{-5}
DMSO	78.13	24.3	0.44	-1.3×10^{-3}
Hematin	633.2	/	/	/
GS.hematin complex	922.8	16.1	0.08	0.08

2.3.6 Mass Spectroscopy of GS-Hematin Complex

Glutathione has a molecular weight of 307.32 and is neutrally charged therefore must either be protonated or deprotonated to be detected by mass spectroscopy. Glutathione dissolved in 50% (v/v) methanol had a strong negative ion peak of m/z 306.08, which corresponds to $[M-H]^-$ (Figure 2-25).

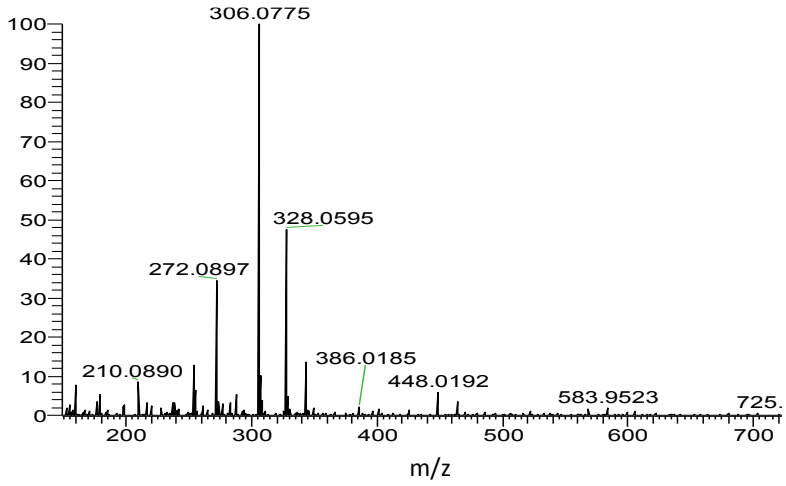

Figure 2-25. Negative ion mass spectroscopy of glutathione. Direct injection negative ion exactive mass spectroscopy of glutathione in 50% (v/v) methanol showing a m/z peak at 306.08 corresponding to $[M-H]^-$.

Hematin, without the hydroxyl ligand (ferriheme) has a molecular weight of 616.18 and an overall charge of +1. Ferriheme does not have to be protonated for it to be detected by mass spectroscopy. Hematin dissolved in 50% (v/v) methanol had a positive ion peak of m/z 616.18, which corresponds to $[M]^+$ where M is ferriheme (Figure 2-26).

If the organic iron within the sample were in the ferrous state it would have an overall charge of 0, requiring it to be protonated for detection by mass spectroscopy. The protonation of ferrous heme $[M+H]^+$ would result in an ion with a molecular mass of 617.18. This indicates that if the organic iron within the sample was in the ferrous state the m/z peak would be at 617.18 $[M+H]^+$ instead of 616.18 $[M]^+$. As the only peak of interest present is at m/z 616.18 it can be deduced that the iron with the sample is in the ferric state.

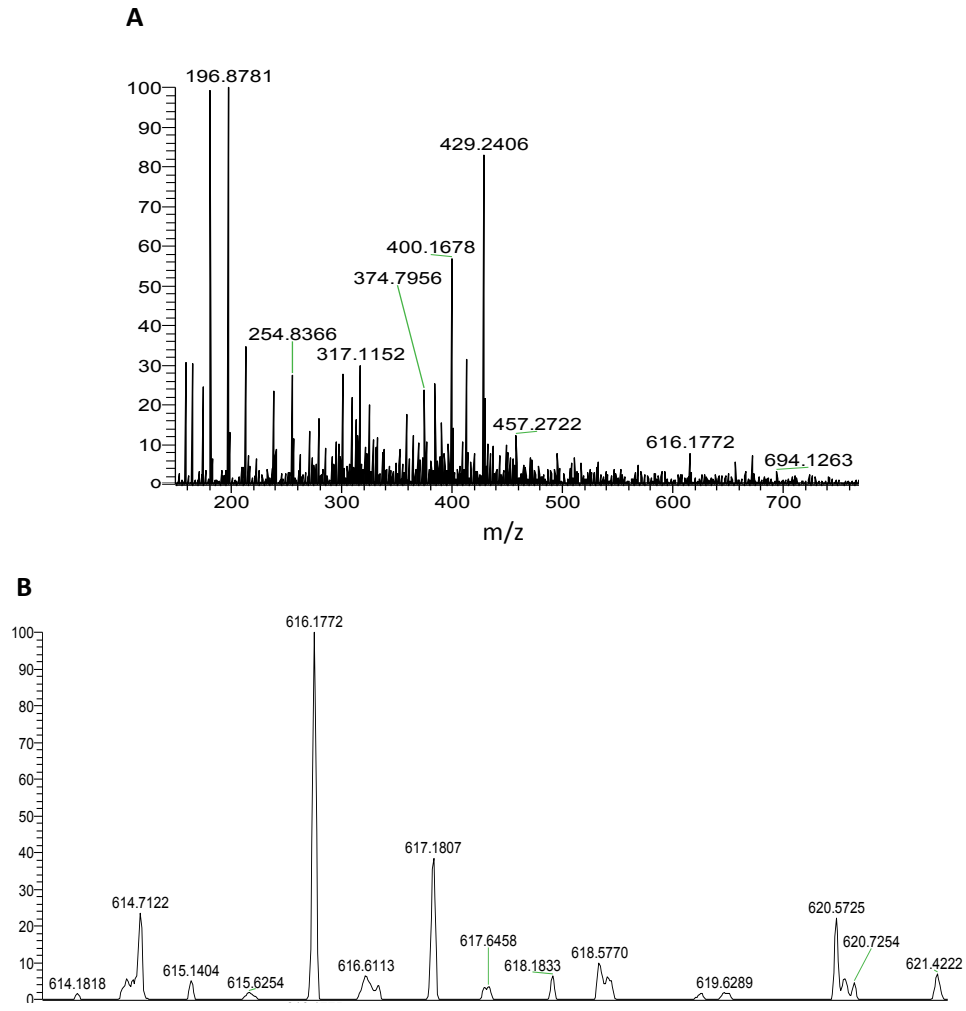

Figure 2-26. Positive ion mass spectroscopy of hematin. Direct injection positive ion exactive mass spectroscopy of hemain in 50 % (v/v) methanol showing a m/z peak at 616.18 corresponding to $[M]^+$. **A –** Spectrum of m/z 150 to 750, **B –** enhanced spectrum of m/z between 600 and 630.

The GS.hematin complex in a 1:1 ratio has a predictive molecular weight of 922.25 and an overall charge of 0. For GS.hematin to be detected by positive ion mass spectroscopy it would have to be protonated $[M+H]^+$ resulting in a predictive m/z peak of 923.26. The positive ion sample of GS.hematin in 50% (v/v) methanol had a weak peak at m/z 923.75 which could correspond to the protonated GS.hematin complex (Figure 2-27). No other peak was detected in the m/z range of interest. No positive ion m/z peak was detected corresponding to a 2[GS].hematin complex (2:1 ratio of glutathione to hematin).

LTQ XL mass spectroscopy and exactive mass spectroscopy with samples dissolved in 50% (v/v) methanol with 0.1% (v/v) formic acid in water did not produce any different data. UV/vis spectroscopy showed that the addition of formic acid resulted in the GS.hematin

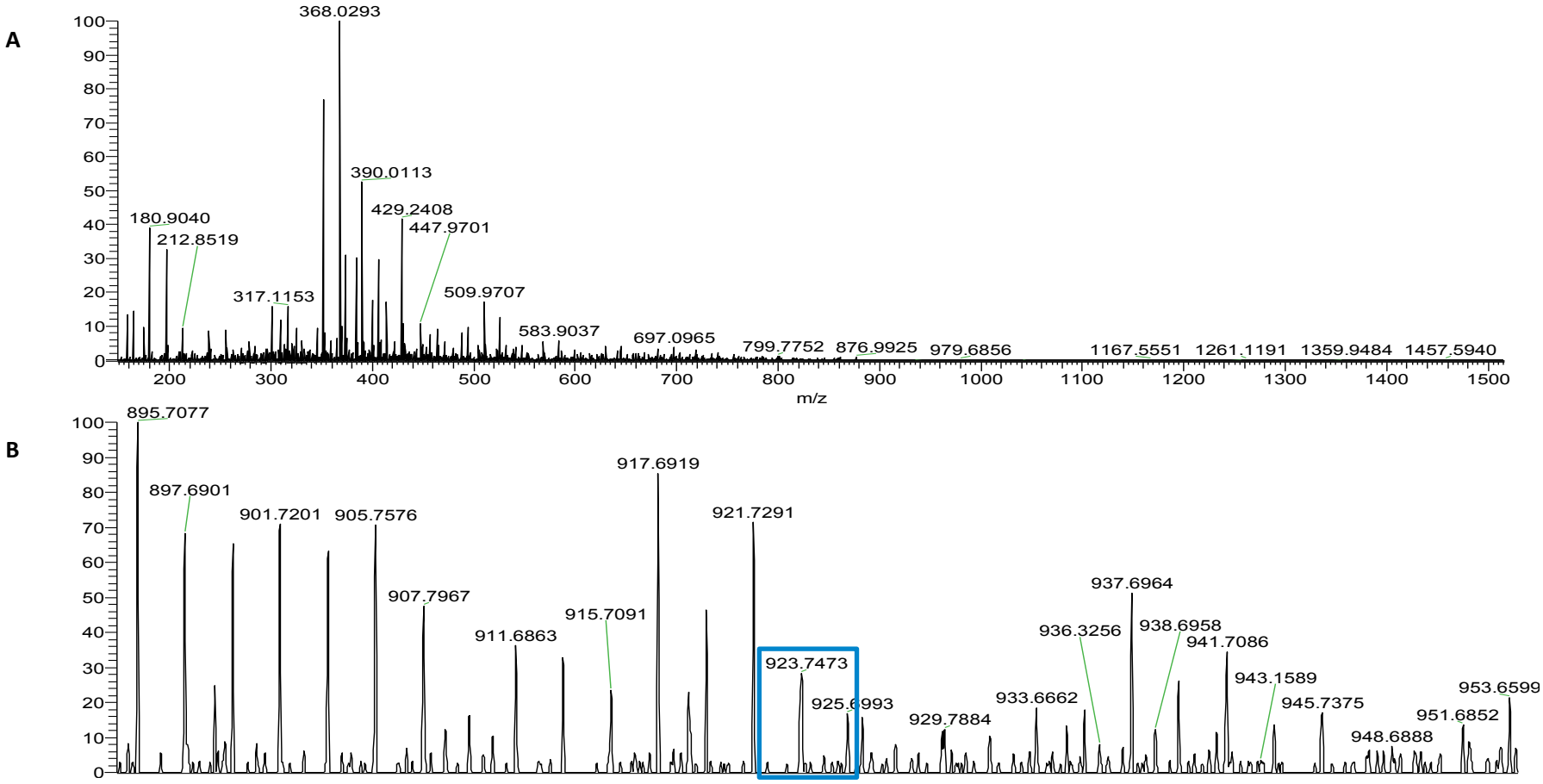

Figure 2-27. Positive ion mass spectroscopy of GS.hematin complex. **A** – There were no significant peaks corresponding to GS.hematin detected from direct injection positive ion mass spectroscopy of GS.hematin in 50 % (v/v) methanol with 0.1 % (v/v) formic acid. **B** – Enhanced view, 890 m/z to 960 m/z, of positive ion spectrum of GS.hematin in 50 % (v/v) methanol with 0.1 % (v/v) formic acid. A small peak at m/z 923.75 (blue box) could correspond to the GS.hematin complex that has a molecular weight of 923.26 for $[M+H]^+$.

complex not forming (data not shown) which possibly explains why no complex was seen in solutions containing formic acid.

Glutathione binds to hematin through the thiol group (Shiviro & Shaklai 1987) resulting in hydrogen being displaced by hematin. This causes glutathione within the GS.hematin complex to have a charge of -1 whilst hematin within the complex has a charge of +1. Thus GS.hematin has an overall neutral charge requiring the amine group of glutathione to be protonated, forming $[M+H]^+$, in order for the complex to be detected by mass spectroscopy. The amine group of glutathione in 50% (v/v) methanol with no formic acid present was not protonated, as no peak of m/z 308.32 was detected. Therefore the likelihood of the amine group of glutathione, in the GS.hematin complex, being protonated is low. It is conceivable that the complex is not sufficiently stable to survive in the mass spectroscopy instrument subsequent to being subjected to ionisation conditions. This has been observed for other iron complexes (Silva *et al.* 2009).

Whatever the reason, we could not gain conclusive mass spectroscopy evidence for the existence of the GS.hematin complex.

2.3.7 Interaction between Gallium Protoporphyrin IX and Glutathione

Paramagnetic atoms, such as iron, produce weak and diminished NMR signals. This means that the structure of the GS.hematin complex could not be deduced through 3D NMR as the GS.hematin complex contains iron. Gallium(III) is a metal ion with an oxidation state of +3, like iron in hematin. Unlike iron, gallium(III) is a diamagnetic atom and therefore any compound containing gallium, such as GaPPIX, can in principle have the structure deduced by 3D NMR. Gallium has a similar ionic radii to iron, 0.65 Å compared to 0.62 Å, Shannon (1976), and has the same oxidation state as iron(III), +3, meaning GaPPIX has a very similar charge density to hematin. Due to the similarities of hematin and GaPPIX IX it would be conceivable that glutathione would bind to GaPPIX producing a GS.GaPPIX complex. This complex could undergo 3D NMR from which the structure of GS.hematin could be deduced.

2.3.7.1 Gallium Protoporphyrin IX Synthesis

The structure of PPIX, hematin, hemin and GaPPIX are similar (Figure 2-28). PPIX has two secondary and two tertiary amines. The two secondary amines in PPIX undergo nucleophillic attraction to the metal ions, bonding the metal ion to the centre of the PPIX compound through the conversion of two secondary amines into two tertiary amines.

In an infrared spectrum a single absorption peak between 3,300 and 3,500 cm^{-1} is characteristic of a secondary amine whilst a tertiary amine does not produce a peak. The infrared spectrum of PPIX shows a peak at 3,300 cm^{-1} confirming that PPIX contains at least one secondary amine (Figure 2-29). Hemin should not contain a peak between 3,300 cm^{-1} and 3,500 cm^{-1} because the iron atom in the centre of the PPIX ring is bound to the ring through two nitrogen atoms, converting them to tertiary amines, (Figure 2-28). The infrared spectrum of hemin confirms there are no secondary amines in the structure as there is no peak between 3,300 and 3,500 cm^{-1} (Figure 2-29). If gallium were successfully incorporated into the PPIX ring, forming GaPPIX, there would be no peak between 3,300 and 3,500 cm^{-1} due to gallium binding to the nitrogen atoms (Figure 2-28). The infrared spectrum of the synthesised compound does not contain a peak between 3,300 and 3,500 cm^{-1} suggesting that GaPPIX was successfully synthesised (Figure 2-29).

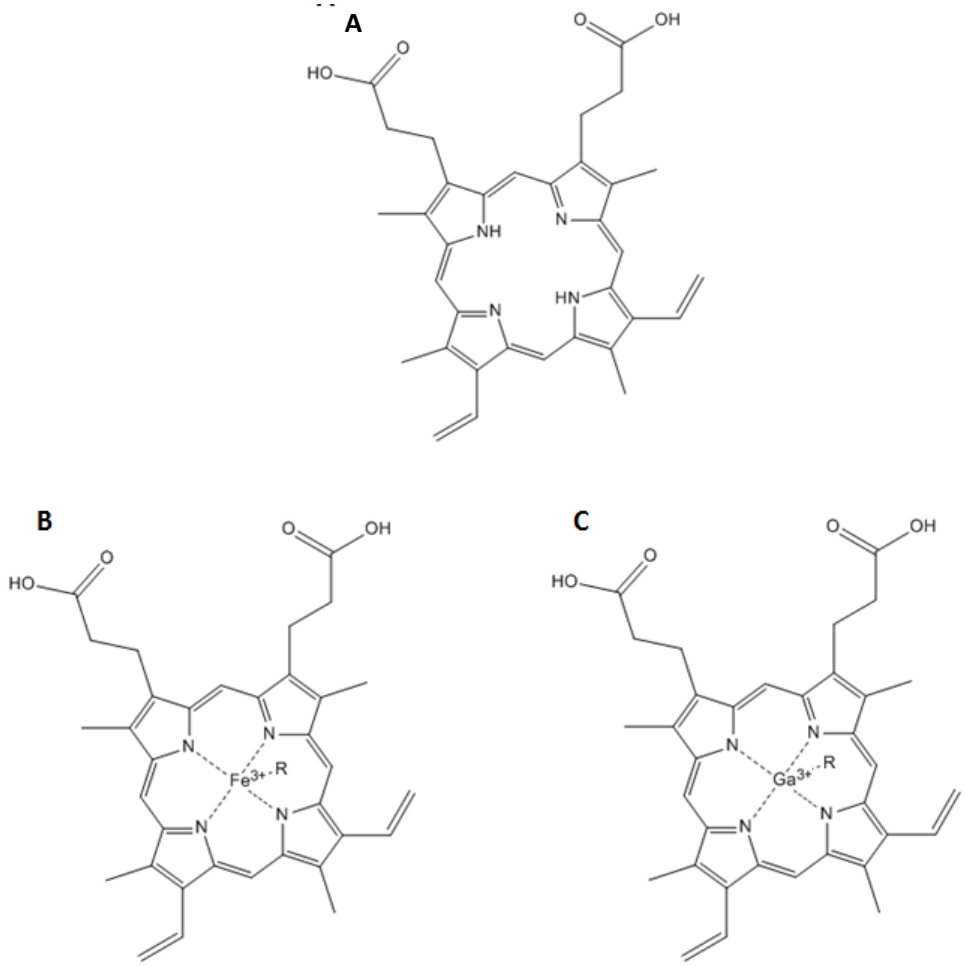

Figure 2-28. Metal protoporphyrin structures. **A** – PPIX, **B** – hematin (R = OH), hemin (R = Cl) and **C** – GaPPIX (R = OH or Cl). Note the two secondary amines present in PPIX that are not present in hematin, hemin or GaPPIX due to the incorporation of the metal ion into the PPIX. (Drawn in Chem3D Utlra 12.0 software).

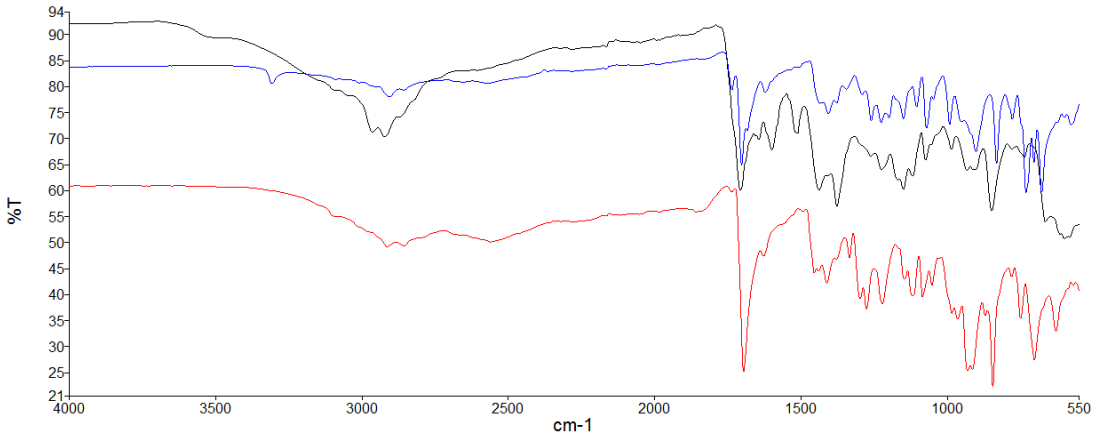

Figure 2-29. Infrared spectra of metal protoporphyrins. The infrared spectrum of PPIX (blue) has a peak at 3,300 cm^{-1}, corresponding to a secondary amine bond, whilst hemin (red) and synthesised GaPPIX (black) do not contain a peak at 3,300 cm^{-1}.

UV/vis spectroscopy of the final product contained absorption peaks at 536 nm and 582 nm confirming the successful synthesis of GaPPIX (Pinter *et al.*, 2012) (Figure 2-31).

2.2.7.2 Interaction of GaPPIX with Glutathione

The spectrum of GaPPIX in a solution containing glutathione was compared to the spectra of GaPPIX in solution, without glutathione present, and PPIX in solution, to deduce if glutathione bound to GaPPIX.

PPIX did not dissolve in 200 mM phosphate buffer, 20 mM KCl at pH 8, which explains the PPIX absorbance trace (black line in Figure 2-30 & 2-31). The absorption spectrum of GaPPIX is the same when dissolved in a solution containing glutathione as when glutathione is not present in the solution; they both have four absorption peaks at 375 nm, 536 nm, 582 nm and 640 nm (Figure 2-30 & 2-31). This indicates that glutathione does not bind to GaPPIX and therefore GaPPIX is not a suitable substitute, for hematin, in determining the structure of the GS.hematin complex through NMR. The lack of interaction between the two compounds could be due to the electron configuration in the 3d orbitals of gallium. Gallium is not a transition metal and in gallium(III) has a full 3d orbitals (five pairs of electrons), whilst iron(III) has five unpaired electrons in the 3d orbitals. This means gallium is less reactive then iron, leading to GaPPIX not interacting and binding to glutathione, unlike hematin.

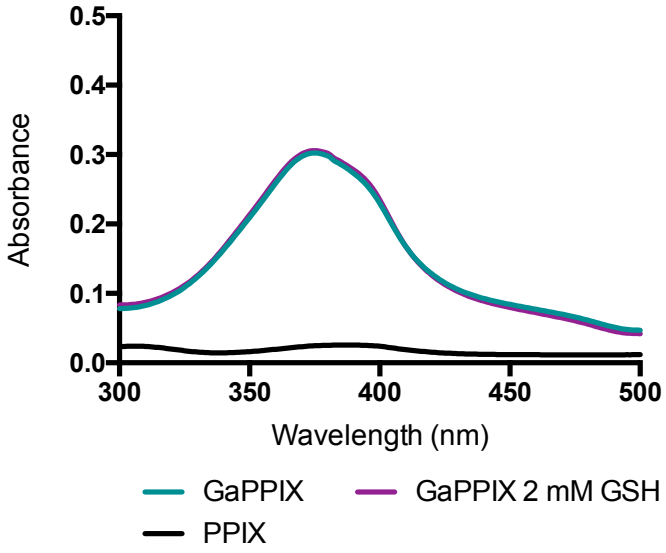

Figure 2-30. Absorption spectrum (300-500 nm) of gallium protoporphyrin ± glutathione. Absorption spectrum of GaPPIX (10 µM) in 200 mM phosphate buffer, 20 mM KCl, pH 8 (green), GaPPIX (10 µM) in 200 mM phosphate buffer, 20 mM KCl, 2 mM glutathione, pH 8 (purple, same trace as GaPPIX alone), and PPIX (10 µM) in 200 mM phosphate buffer, 20 mM KCl, pH 8 (black) between 300 nm and 500 nm in a 10 mm path length cuvette. GaPPIX in phosphate buffer in the presence (purple) and absence (green) of glutathione had peak absorption at 375 nm whilst there was no absorption peak for the solution containing PPIX (black).

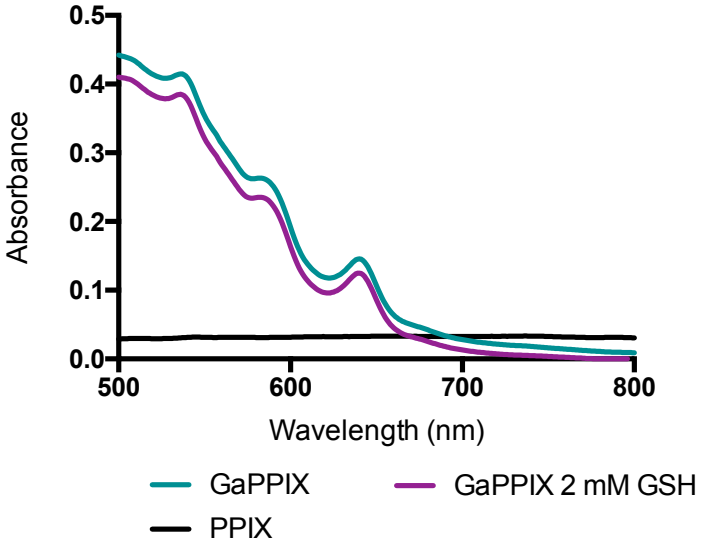

Figure 2-31. Absorption spectrum (500-800 nm) of gallium protoporphyrin ± glutathione. Absorption spectrum of GaPPIX (10 µM) in 200 mM phosphate buffer, 20 mM KCl, pH 8 (green), GaPPIX (10 µM) in 200 mM phosphate buffer, 20 mM KCl, 2 mM glutathione, pH 8 (purple), and PPIX (10 µM) in 200 mM phosphate buffer, 20 mM KCl, pH 8 (black) between 500 nm and 800 nm in a 100 mm path length cuvette. GaPPIX in phosphate buffer in the presence (purple) and absence (green) of glutathione had absorption peaks at 536 nm, 582 nm and 640 nm whilst there was no absorption peak for the solution containing PPIX (black).

2.3 General Discussion

We established that micromolar concentrations of hematin could be dissolved by using a phosphate buffer at pH 8 with the addition of potassium chloride (20 mM). This way of dissolving hematin is closer to physiological conditions and therefore is a more relevant way of handling hematin in experiments investigating physiologically relevant properties.

Several methods of mass spectroscopy were employed to analyse the GS.hematin complex, unfortunately none of them provided a definitive spectrum of the GS.hematin complex. The inability of glutathione to bind to GaPPIX meant the structure of GS.hematin could not be deduced from NMR spectra of GS.GaPPIX, a structural analogue of GS.hematin.

Shviro & Shaklai (1987) and Sahini *et al.* (1996) showed that the interaction between hematin and glutathione is readily followed with UV/vis spectroscopy due to the blue shift that occurs when glutathione is present. The difference in absorption at 618 nm and 655 nm of hematin in varying concentrations of glutathione was used to calculate the affinity constant of glutathione and hematin, K_a = 5.0 x 10^4 M^{-1}. Using this affinity constant a speciation plot was constructed, which showed at physiologically relevant concentrations up to 99% of hematin in the cytosol could be complexed to glutathione, forming GS.hematin. This however does not hold true for cysteine binding to hematin. The affinity constant for cysteine and hematin was significantly lower, 1.6 x 10^2 M^{-1} and the speciation plot showed at physiologically relevant concentrations (20-100 μM and 10 μM respectively) less than 3% of hematin is predicted to be complexed to cysteine. The large difference in affinity constants between glutathione and cysteine binding to hematin demonstrates that hydrophobic interactions between glutathione and hematin are essential for the enhanced stability of the GS.hematin complex.

'Cold' hematin is difficult to detect at physiologically relevant conditions (below 100 μM, in low experimental volumes), whereas [^{59}Fe]hematin can be readily detected at micromolar concentrations and below, in much smaller volumes, with a gamma counter. Therefore [^{59}Fe]hematin proved ideal for *in vitro* experiments conducted under physiological concentrations. We established that the synthesised organic [^{59}Fe] was [^{59}Fe]hematin, using UV-vis spectroscopy, and confirmed that the formation of GS.[^{59}Fe]hematin occurs under physiological conditions using HPLC.

2.4 Conclusions

These experiments have demonstrated that glutathione binds to hematin under physiologically relevant conditions. Silver & Lukas (1985) showed through Mössbauer spectroscopy that hematin was not reduced to heme in the presence of 100 fold excess of glutathione. Therefore we can conclude that in the GS.hematin complex iron is in the ferric form, a finding further confirmed by UV-vis spectroscopy.

Overall the results of this chapter provide strong evidence that hematin under conditions found in the cytosol forms a 1:1 complex with glutathione and this GS.hematin complex is likely to dominate the organic cytosolic labile iron pool.

3. Hematin Uptake into Caco-2 Cells

3.1 Introduction

Iron homeostasis is unique in the fact that it is maintained exclusively by regulating iron absorption, in the proximal small intestine, as the human body does not contain an iron excretory pathway (Alvarez-Hernandez *et al*., 1991). Iron absorption is regulated by the iron requirement of erythropoiesis and the hormone hepcidin (Johnson, 1978; Leong & Lonnerdal, 2004; Ross *et al.,* 2012), and is predominantly carried out in the enterocytes of the duodenum of the GI tract. The cell line derived from heterogeneous human epithelial colorectal adenocarcinoma cells (Caco-2 cells) spontaneously differentiate into bipolar enterocytes (Garcia *et al.,* 1996). Caco-2 cells exhibit microvilli on the apical membrane, tight gap junctions, excretion of brush border associated enzymes and the exportation of nutrients from the basolateral membrane (Grasset *et al.*, 1984; Garcia *et al.,* 1996). These criteria make Caco-2 cells an excellent model for nutritional absorption by the intestine and they have been used as such for decades (Grasset *et al.*, 1984; Sandberg, 2010).

There are various ways to measure the iron absorbed and exported from Caco-2 cells including; the change in ferritin levels and the detection of iron via the ferrozine assay and radioactive iron. The ferrozine assay relies on the chelation of inorganic ferrous iron within a given sample by three molecules of ferrozine (3-(2-Pyridyl)-5,6-diphenyl-1,2,4-triazine-*p,p*'-disulfonic acid) (Stookey, 1970). The chelation of ferrozine to ferrous iron results in a change in electron configuration causing an increase in absorption at 562 nm (Stookey, 1970). Therefore the amount of ferrous inorganic iron within a sample can be calculated from a standard curve of ferrous iron concentration and the absorbance of the sample at 562 nm. There are some drawbacks to using ferrozine for the detection of organic iron. Ferrozine molecules will only bind inorganic iron in the ferrous state therefore inorganic iron must be liberated from the porphyrin ring of organic iron. This requires strong acidic conditions whilst the ferrozine assay only works in a pH range of 4-9 (Anastácio *et al.,* 2008). Inorganic iron constitutes only 9% of the molecular weight of hematin, therefore a 50 µM sample of hematin would equate to only a 4.5 µM sample inorganic iron for detection by ferrozine. In addition as the detection is by spectrophotometric absorption low concentrations are liable to inaccurate measurements.

The use of radioactive organic iron for absorption studies dates back to 1955 (Walsh *et al.* 1955) and is a direct way of measuring organic iron absorption, based on the radioactivity

of the final sample. The main drawback to this method of organic iron absorption studies is that the radioactively labelled organic iron source must first be synthesised. This can be undertaken either in the laboratory, from protoporphyrin IX dimethyl ester and $^{59}FeCl_3$ (Follett *et al.,* 2002) or by injecting laboratory animals with radioactive iron and harvesting their blood for haemoglobin (Walsh *et al.,* 1955; Parmley *et al.,* 1981). Radiolabelled haemoglobin is a more representative source of the organic iron available within the diet. However haemoglobin is heme bound to globulin and therefore contains protein as well as organic iron. This protein could influence organic iron absorption therefore the absorption and effect of organic iron alone cannot fully be examined using this iron source. Laboratory synthesised radioactive hematin has the advantage of being a pure organic iron source which allows for the flexibility of adding known quantities of compounds of interest in order to understand their role in organic iron absorption.

Iron absorption is known to differ depending on the iron source and other nutrients present in the diet or uptake medium (Layrisse *et al.,* 1984; Glahn & Van Campen, 1997, Au & Reddy, 2000). Protein has been shown to affect organic iron absorption (Follet *et al.,* 2002) however; the effect of single amino acids and organic acids on organic iron absorption is less well understood. The ability for the GS.hematin complex to form under physiological conditions has been presented in Chapter 2. Through enzymatic activity and the acidic environment of the stomach, ingested proteins are degraded into small peptides and amino acids. Glutathione is a tripeptide with a γ-peptide linkage which the majority of peptidases cannot cleave (Lushchak, 2012). This could result in the enterocytes of the GI tract being presented with GS.hematin in the presence of the constituent amino acids of glutathione, from ingested food sources. Therefore the effect of glutathione on organic iron absorption is of dietary interest.

The aim of this chapter is to understand the effect of glutathione on organic iron (hematin) absorption into cells using the established iron absorption cell line, Caco-2 cells. Work involving the identification of the organic iron form within cells and the effect of glutathione on hematin catabolism (reported in Chapter 4); requires a cell line routinely associated with iron absorption and catabolism research. Caco-2 cells are polarised and known to catabolise absorbed organic iron by HO-1 (Uc *et al.,* 2004), exporting the resulting inorganic iron from the basolateral membrane. These qualities render Caco-2 cells a good choice of cell line for these organic iron studies.

3.2 Materials and Methods

3.2.1 Reagents

Reagents were purchased from Sigma Aldrich unless stated otherwise in Table 3-1.

Table 3-1 Details of Reagents used for Biological Experiments

Compound	Specifications	Supplier
Compounds		
Reduced glutathione	N/A	Santa Cruz Biotechnology
Oxidised glutathione	N/A	Santa Cruz Biotechnology
Ferrous sulphate	$7H_2O$	Scientific Laboratory Suppliers
Potassium chloride	≥ 99%	BDH laboratory supplies
di-Sodium hydrogen phosphate anhydrous	> 98%	Fluka Chemika
Sodium hydroxide	Laboratory reagent grade	Fisher Scientific
L-ascorbic acid sodium salt	99%	Acros Organics
Solvents		
Water	HPLC grade	Fisher Scientific
Chloroform	Analytical reagent grade	Fisher Scientific
Ethyl Acetate	Analytical reagent grade	Fisher Scientific
Hydrochloric Acid	37% in water	Acros Organics
Methanol	HPLC grade	Fisher Scientific
DMSO	≥ 99.7%	Fisher Scientific

Table 3-1 Continued

Compound	Specifications	Supplier
Cell Culture		
Caco-2 cells	Passage 15	American Type Culture Collection (ATCC)
Fetal bovine serum (Gibco)	Qualified	Fisher Scientific

3.2.2 Caco-2 Cell Culture, Plating and Growth

Caco-2 cells used in experiments were at passages 40-50. Stock cell cultures were maintained at pH 7.4 in Dulbecco's Modified Eagle Medium (DMEM) with high glucose (4,500 mg/L), supplemented with 10% (v/v) fetal bovine serum (FBS), 1% (v/v) penicillin-streptomycin solution, 1% (v/v) non-essential amino acid solution and 1% (v/v) L-glutamine solution. The cells were cultured at 37^{o}C in an incubator with 5% CO_2 and 95% air atmosphere.

Cells were seeded in 6-well plates (6-well cell culture cluster plates, Corning, New York, USA), 12-well plates (12-well cell culture cluster plates, Corning, New York, USA) 6-well transwell plates (6-well transwell, clear polyester membrane, 24 mm, 0.4 mm, Corning, New York, USA) or 96-well plates (96-well cell culture cluster plates, Corning New York, USA).

Cells were plated into the plates specified in each section. Microscopic examination of cultures revealed that confluence was reached 3-4 days post seeding. Cell medium was changed every 2-3 days and experiments were conducted 14-18 days after seeding. At 14-18 days post seeding, except for cell viability assays which were used three days post seeding, medium was removed from cells and the monolayers were washed once with Minimum Essential Medium Eagle (MEM). Cells were cultured in MEM for 16 hours at 37^{o}C, 5% CO_2, 95% air atmosphere, to deplete iron stores within the cells.

It was noted that stock solutions of hematin in 0.1 N NaOH precipitated out of solution when MEM was used as the uptake medium. After further investigation it was deduced that the phenol indicator within the medium was causing the precipitation and hematin

could be kept in solution if the MEM did not contain phenol and potassium phosphate buffer. Therefore Minimum Essential Medium Eagle Modified (phenol free MEM) was used supplemented with potassium phosphate buffer as the uptake solution.

Phenol free MEM was made up as directed in sterile Milli-Q water, supplemented with 3.7 g/L sodium bicarbonate, adjusted to pH 7.4 with 1 N NaOH and 1 N HCl and filter-sterilised through a 0.22-µm filter.

3.2.3 Cell Viability using MTT Assay

Cells were seeded at $1x10^4$ cells per well in 96 well plates (96 well cell culture cluster plates, Corning New York, USA). Each experiment was conducted in triplicate and experimental treatment performed in triplicate for each replication of the experiment. The triplicates were averaged and the mean values were used for statistical analysis.

The experimental conditions were as described in sections 3.2.4, 3.2.5 and 3.2.6 except that no radioactive hematin or iron was added to the treatments and cells were used 3 days post seeding. Once the incubations were complete instead of lysing the cells, cells were washed with PBS and incubated in 110 µL MTT solution and a further incubation at 37 ^{o}C, 5% CO_2, 95% air atmosphere was conducted for 3 hours in the dark. MTT solution consisted of, 3-(4,5-dimethylthiazol-2-yl)-2,5-diphenyltetrazolium bromide dissolved in PBS, to a concentration of 5 mg/mL, diluted 1 in 11 into MEM. After 3 hours culture medium was removed, DMSO (100 µL) added to cells, and cells were further incubated at room temperature in the dark, at 30 rpm for 15 minutes. The absorbance was read at 490 nm and 650 nm using a spectrophotometric plate reader. Absorbance at 650 nm was subtracted from absorbance at 490 nm. The absorbance of the negative control was taken as 100% cell metabolism and the percentage of each condition from this was calculated. The results were exported to GraphPad Prism where the mean value with standard error of the mean (SEM) of cell metabolism (as a percentage of the negative control) was plotted against each condition.

3.2.4 Influence of Amino Acids, Ascorbic Acid and Glutathione on Hematin Absorption Analysed by Radioactive Hematin

Cells were seeded in 12 well plates (12 well cell culture cluster plates, Corning, New York, USA). The experiment with additional compounds at 4.5 mM was repeated in triplicate and at concentrations of 0.9 mM in duplicate. Each experimental treatment was performed in

triplicate for each replication of the experiment. The triplicates were averaged and mean values were used for statistical analysis.

3.2.4.1 Formulation of Uptake Solutions

Stock solutions of hematin (5 mM) in 0.1 N NaOH and iron(II) chloride (5 mM) in ddH_2O were prepared immediately prior to use. Stock solutions of glutathione (45.5 mM), cysteine (45.5 mM), ascorbic acid (9 mM), arginine (45.5 mM), histidine (45.5 mM) and glycine (45.5 mM) were made in 200 mM potassium phosphate buffer (pH 8) and adjusted to pH 8 with 0.1 N NaOH.

Hematin uptake solutions in phenol free MEM supplemented with a final concentration of 66.7 mM potassium phosphate buffer contained 50 µM hematin, and either 4.55 mM or 0.91 mM of glutathione, cysteine, arginine, histidine and glycine, 0.4 mM or 0.08 mM ascorbic acid or no additive. Approximately 0.58 KBq [^{59}Fe]hematin was used per 0.5 mL of uptake solution.

Iron(II) chloride uptake solution in phenol free MEM supplemented with a final concentration of 66.7 mM potassium phosphate buffer contained 50 µM $FeCl_2$, $^{59}FeCl_3$ in 0.1 N HCl diluted 1 in 100 in DMSO and 900 uM ascorbic acid. Approximately 0.58 KBq of $^{59}FeCl_3$ was used per 0.5 mL uptake solution.

All solutions were prepared immediately prior to use and filter-sterilised through 0.22-µm filters.

3.2.4.2 Incubation with Hematin or $FeCl_2$

Minimum Essential Medium was aspirated from each well after 16 hours and monolayers were washed once with phenol free MEM. Hematin uptake solution (0.5 mL) was added to each well and monolayers incubated for 1 hour at 37^{o}C, 5% CO_2, 95% air atmosphere. Medium was aspirated from monolayers and transferred to 1.5 mL Eppendorf tubes. Cell monolayers were washed twice with PBS (150 µL), the wash added to aspirated medium and the solution counted for [^{59}Fe]hematin or $^{59}FeCl_3$ with a 1282 Compugamma CS universal gamma counter (LKB Wallac). Cells were collected with 0.1 N NaOH (160 µL) and counted for [^{59}Fe]hematin or $^{59}FeCl_3$.

3.2.4.3 Protein Assay

The protein content of the disrupted cells was determined using BioRad DC Protein Assay Kit. Solution S (40 µL) was added to 2 mL of solution A, forming solution X. Disrupted cells were diluted one in four in ddH_2O, and 40 µL added to 40 µL of solution X, solution B (320

µL) was then added to the c-solution X mix and left to incubate at room temperature for 10 minutes. The protein assay solution (100 µL) was plated in triplicate in a 96-well plate and absorbance read at 750 nm on a spectrophotometric plate reader. Standards using BSA dissolved in water were run and a standard curve drawn with lineal regression in GraphPad Prism. The mean absorbance for each sample and the protein standard curve was used to determine the amount of protein in each sample.

3.2.4.4 Statistical Analysis of Iron Absorption

The amount of hematin or $FeCl_2$ absorbed into cells (nmol) per µg protein was calculated from the mean of each experimental repeat. The mean value with standard error of the mean (SEM) plotted for each condition in GraphPad Prism. A 1-way ANOVA in GraphPad Prism, with alpha set at 0.05, was conducted on the mean repeat values to determine if there was a significant difference in hematin (or $FeCl_2$) absorbed from each condition compared to cells incubated with only hematin.

3.2.5 [^{59}Fe]Hematin and $^{59}FeCl_3$ Uptake into Caco-2 Cells

Cells were seeded in 12 well plates (12 well cell culture cluster plates, Corning, New York, USA). Each experimental treatment was performed in triplicate for each replication of the experiment. The triplicates were averaged and mean values were used for statistical analysis.

3.2.5.1 Formulation of Uptake Solutions

Stock solutions of hematin (5 mM) in 0.1 N NaOH and iron(II) chloride (5 mM) in ddH_2O were prepared immediately prior to use. Stock solutions of glutathione (20 mM), cysteine (6.7 mM) and ascorbic acid (9 mM) were made in 200 mM potassium phosphate buffer (pH 8) and adjusted to pH 8 with 0.1 N NaOH.

Pre-incubation solutions in MEM contained either 2 mM glutathione, 670 µM cysteine or no additional compound.

Hematin uptake solutions in phenol free MEM supplemented with a final concentration of 66.7 mM potassium phosphate buffer contained 50 µM hematin, [^{59}Fe]hematin in DMSO and either 2 mM glutathione or no added ligand. Approximately 0.58 KBq [^{59}Fe]hematin was used per 0.5 mL of uptake solution.

Iron(II) chloride uptake solution in phenol free MEM supplemented with a final concentration of 66.7 mM potassium phosphate buffer contained 50 µM $FeCl_2$, $^{59}FeCl_3$ in

0.1 N HCl diluted 1 in 100 in DMSO and 900 µM ascorbic acid. Approximately 0.58 KBq of $^{59}FeCl_3$ was used per 0.5 mL uptake solution.

All solutions were prepared immediately prior to use and filter-sterilised through 0.22-µm filters.

3.2.5.2 Incubation with [^{59}Fe]Hematin or $^{59}FeCl_3$

Minimum Essential Medium was aspirated from each well after 16 hour depletion incubation and the monolayers had pre-incubation solution (0.5 mL) containing, glutathione, cysteine or medium alone added to each well (Figure 3-1). Cells were cultured for 1 hour at 37^{o}C in 5% CO_2, 95% air atmosphere.

After 1 hour pre-incubation culture medium was removed from monolayers and the monolayers were washed twice with phenol free MEM. Wells that were pre-incubated with glutathione or cysteine were incubated with hematin uptake solution (0.5 mL) for one or 4 hours at 37^{o}C, 5% CO_2, 95% air atmosphere, (Figure 3-1). Wells that were pre-incubated with medium alone were incubated with either hematin uptake solution (0.5 mL), hematin-glutathione uptake solution (0.5 mL) or $FeCl_2$ uptake solution (0.5 mL) for one or 4 hours at 37^{o}C, 5% CO_2, 95% air atmosphere. Medium was aspirated after one or 4 hours and cell monolayers washed twice with ice cold PBS (150 µL), the wash was added to the aspirated medium and the solution counted for [^{59}Fe]hematin or $^{59}FeCl_3$. Cells were collected in 0.1 N NaOH (160 µL) and counted for [^{59}Fe]hematin or $^{59}FeCl_3$. The protein content of the collected cells was determined using the BioRad DC Protein Assay Kit and the protocol described in section 3.2.4.3. The amount of hematin or $FeCl_2$ absorbed into cells (pmol) per µg protein was calculated from the mean of each experimental repeat and analysis conducted as described in section 3.2.4.4.

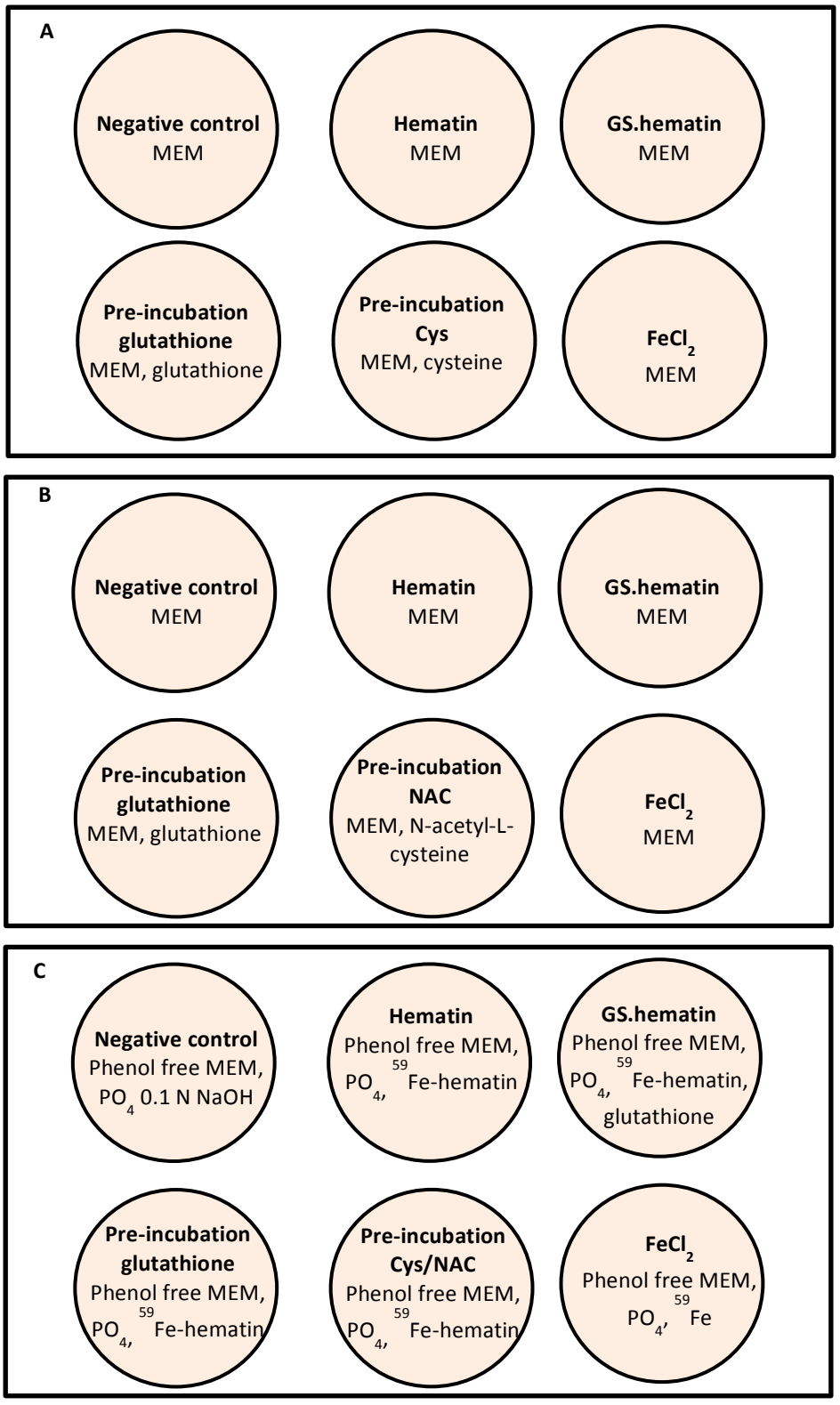

Figure 3-1. Schematic of supplementations for experiments where pre-incubations occurred. **A** – Plate layout of solutions used to pre-incubate Caco-2 cell monolayers in unicameral experiments, **B** – Plate layout of solutions used to pre-incubate Caco-2 cell monolayers in bicameral experiments, **C** – Plate layout of solutions used for hematin absorption after pre-incubation into Caco-2 cell monolayers for both unicameral and bicameral experiments.

4.2.6 [^{59}Fe]Hematin and $^{59}FeCl_3$ Uptake into and Export from Caco-2 Cells in Bicameral Chambers

Cells were seeded in 6 well transwell plates (6 well transwell, clear polyester membrane, 24 mm, 0.4 mm, Corning, New York, USA). The 1 hour incubation experiment was repeated in triplicate and the 24 hour incubation in duplicate. Each experimental treatment was performed in triplicate for each replication of the experiment. The triplicates were averaged and mean values were used for statistical analysis.

4.2.6.1 Transepithelial Electrical Resistance

Once cells had been seeded for 14 days the transepithelial electrical resistance (TEER) of each monolayer was measured with Millicell®-ers (Millipore) every two days until it reached a minimum of 250 Ωcm^2. TEER measurements were used to determine when tight gap junctions had formed, once TEER had reached 250 Ωcm^2 the monolayers were used for experiments.

4.2.6.2 Formulation of Solutions

Stock solutions of hematin (5 mM) in 0.1 N NaOH and iron(II) chloride (5 mM) in ddH_2O were prepared immediately prior to use. Stock solutions of glutathione (20 mM), cysteine (6.7 mM) and ascorbic acid (9 mM) were made in 200 mM potassium phosphate buffer (pH 8) and adjusted to pH 8 with 0.1 N NaOH.

Pre-incubation solutions in MEM contained either 2 mM glutathione, 670 µM N-acetyl-L-cysteine or no additional solution (MEM only).

Hematin uptake solutions in DMEM supplemented with a final concentration of 66.7 mM potassium phosphate buffer contained 50 µM hematin, [^{59}Fe]hematin in DMSO and either 2 mM glutathione or no added compound. Approximately 0.58 KBq [^{59}Fe]hematin was used per 1 mL of uptake solution.

Iron(II) chloride uptake solution in phenol free MEM supplemented with a final concentration of 66.7 mM potassium phosphate buffer contained 50 µM $FeCl_2$, $^{59}FeCl_3$ in 0.1 N HCl diluted 1 in 100 in DMSO and 900 uM ascorbic acid. Approximately 0.58 KBq of $^{59}FeCl_3$ was used per 1 mL uptake solution.

Human apo-transferrin was dissolved in phenol free MEM to a final concentration of 12.5 µM for the basal medium.

All solutions and basal medium were prepared immediately prior to use and filter-sterilised through 0.22-µm filters.

4.2.6.3 Incubation with [^{59}Fe]Hematin or $^{59}FeCl_3$

Minimum Essential Medium was aspirated from cell monolayers within each well after 16 hours. Pre-incubation solution (0.5 mL) containing either 2 mM glutathione, 670 µM N-acetyl-L-cysteine or medium alone, was added to each monolayer and MEM (2 mL) was added to the basal chamber of each well (Figure 3-1). Cells were cultured for 1 hour at 37°C, 5% CO_2, 95% air atmosphere.

After 1 hour all medium was removed from apical and basal chambers and both were washed twice with phenol free MEM. Basal medium (1.6 mL) was added to each basal chamber. Apical chambers pre-incubated with glutathione or cysteine had hematin uptake solution (1 mL) added. Apical chambers pre-incubated with medium alone had either hematin uptake solution (1 mL), hematin-glutathione uptake solution (1 mL) or $FeCl_2$ uptake solution (1 mL) added (Figure 3-1). Cells were cultured for 1 hour or 24 hours at 37°C, 5% CO_2, 95% air atmosphere. Apical medium was aspirated and transferred to 1.5 mL Eppendorf tubes. Basal medium was aspirated and transferred to 1.5 mL Eppendorf tubes for [^{59}Fe]hematin or $^{59}FeCl_3$ counting. Cell monolayers were washed twice with ice cold PBS (150 µL), the wash added to the aspirated apical medium and the solution counted for [^{59}Fe]hematin or $^{59}FeCl_3$. Cells were collected in 0.1 N NaOH (160 µL) and counted for [^{59}Fe]hematin or $^{59}FeCl_3$. The protein content of the collected cells was determined using BioRad DC Protein Assay Kit and according to the protocol described in section 3.2.4.3. The CPM for the negative control was deducted from the samples to take into account any background radioactivity from the gamma counter.

The amount of hematin and $FeCl_2$ absorbed by, and accumulated in, the cells and iron exported to the basal medium was calculated using equations 3-1 – 3-5.

$$\text{Total CPM} = \text{CPM of supernatant} + (\text{CPM of cells}) \times 4 + \text{CPM of basal medium}$$

Equation 3-1

$$\text{Hematin in Caco-2 cell monolayer (M)} = \left[\frac{(50 / 1{,}000{,}000)}{\text{Total CPM}}\right] \text{X } (\text{CPM of supernatant}) \text{ x } 4$$

Equation 3-2

$$\text{Hematin exported from Caco-2 monolayer (M)} = \left[\frac{(50 / 1{,}000{,}000)}{\text{Total CPM}}\right] \text{ X (CPM of basal medium)}$$

Equation 3-3

$$\text{Total hematin absorbed (M)} = \text{hematin in cell monolayer + hematin in basal medium}$$

Equation 3-4

$$\text{Hematin (pmol)} = \left(\text{hematin (M)x volume (L)}\right) \text{ X } 1{,}000{,}000{,}000{,}000$$

Equation 3-5

The average amount of hematin in the cell monolayer, absorbed in total and iron exported to the basal medium, for each condition was standardised to the amount of protein present in each sample. The amount of hematin, $FeCl_2$ (pmol) or iron (fmol), once standardised to protein content (µg) was plotted against the condition using GraphPad Prism with error bars of standard error of the mean (SEM).

Statistical analysis was conducted as described in section 3.2.4.4 for the amount of hematin (or $FeCl_2$) in the collected cells, basal medium and total absorbed compared to cells incubated with hematin only.

A 1-way ANOVA in GraphPad Prism, with alpha set at 0.05, was conducted on the mean repeat values to determine if there was a significant difference in the total amount hematin (or $FeCl_2$) absorbed between the two experimental incubation times (1 hour and 24 hours).

3.3 Results and Discussion

3.3.1 Cell Viability Measured by MTT Tetrazolium Assay

The viability of 2 cell monolayers incubated with all experimental uptake solutions used in unicameral chamber experiments was measured. This was to ensure the parameters and concentrations used were not toxic. The viability of the cells was compared to the negative control of the experiments, the cell viability of which was set at 100%.

The MTT tetrazolium assay indirectly measures the viability of cells by measuring the metabolism of cells (Riss *et al.*, 2016). MTT is transported into the mitochondria where NAD(P)H-dependant oxidoreductase enzymes reduce MTT to insoluble formazan (Riss *et al.*, 2016), the more active the enzymes the more MTT reduced to formazan. This indirect method of measuring cell viability implies that in theory cells can have over 100% viability when compared to a standard or negative control. This would occur if the incubation solutions increased the metabolism of the cells, or if the negative control was detrimental to cell metabolism compared to the incubation solutions.

3.3.1.1 Cell Viability of Caco-2 Cell Monolayers Incubated with Iron and Additional Nutrients

The viability of cells incubated with: 1 mM $FeCl_2$, 1 mM hematin alone or in the presence of various amino acids or glutathione at a concentration of 91 mM, or ascorbic acid at a concentration of 8 mM was measured to determine if the uptake solutions used for the ferrozine assay experiments (Appendix A) was detrimental to the cell monolayers.

Cells incubated with: 1 mM $FeCl_2$, 1 mM hematin in the presence of 8 mM ascorbic acid or 91 mM cysteine had a slight increase in cellular metabolism compared to the control (negative control for experiments) (Figure 3-2). Cells incubated with 1 mM hematin alone or in the presence of 91 mM of glutathione, arginine, histidine or glycine had a slight reduction in cellular metabolism, between 7 and 25%, compared to control cells (Figure 3-2). The fluctuations in cell metabolism from the negative control were not significant; therefore the uptake solutions had no significant effect on cell viability.

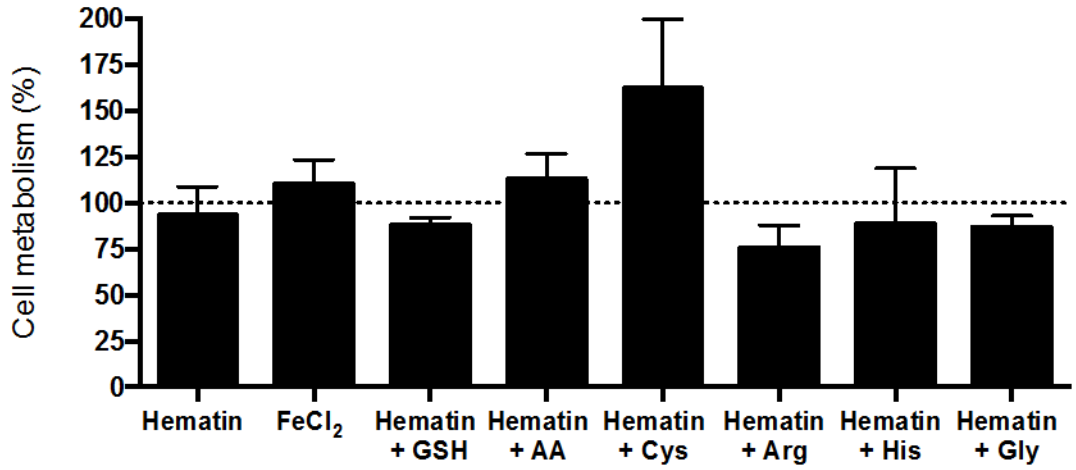

Figure 3-2. Viability of cells incubated with 1 mM iron source in the presence of amino acids or glutathione at 91 mM and ascorbic acid at 8 mM. Caco-2 cell monolayers were grown for 3 days in 96-well plates at 37 ^{o}C, 95 % air, 5 % CO_2, depleted of iron for 16 hours then incubated with either 1 mM $FeCl_2$, 1 mM hematin alone or 1 mM hematin supplemented with 91 mM of glutathione (GSH), cysteine (Cys), arginine (Arg), histidine (His) or glycine (Gly) or 8 mM ascorbic acid (AA) for 1 hour at 37 ^{o}C, 95 % air, 5 % CO_2. Monolayers were washed and incubated with MTT solution for 3 hours then the formazan crystals dissolved in DMSO and absorbance read at 490 nm and 650 nm. There was no significant change in cell viability, compared to cells incubated in only MEM (no iron) (dotted line), across any condition. Values are means ± SEM (n=3 experimental triplicates).

Cell viability of Caco-2 monolayers incubated for 1 hour with; 50 μM $FeCl_2$, 50 μM hematin alone or in the presence of various amino acids or glutathione at a concentration of 4.5 mM or 0.91 mM, or ascorbic acid at a concentration of 0.8 mM or 0.04 mM was monitored. This was conducted in order to determine if the uptake solutions used to investigate the affect amino acids and glutathione, at 4.5 mM, and ascorbic acid, at 0.8 mM, had on hematin uptake (Section 3.3.2) was detrimental to Caco-2 cell monolayers over a 1 hour incubation period.

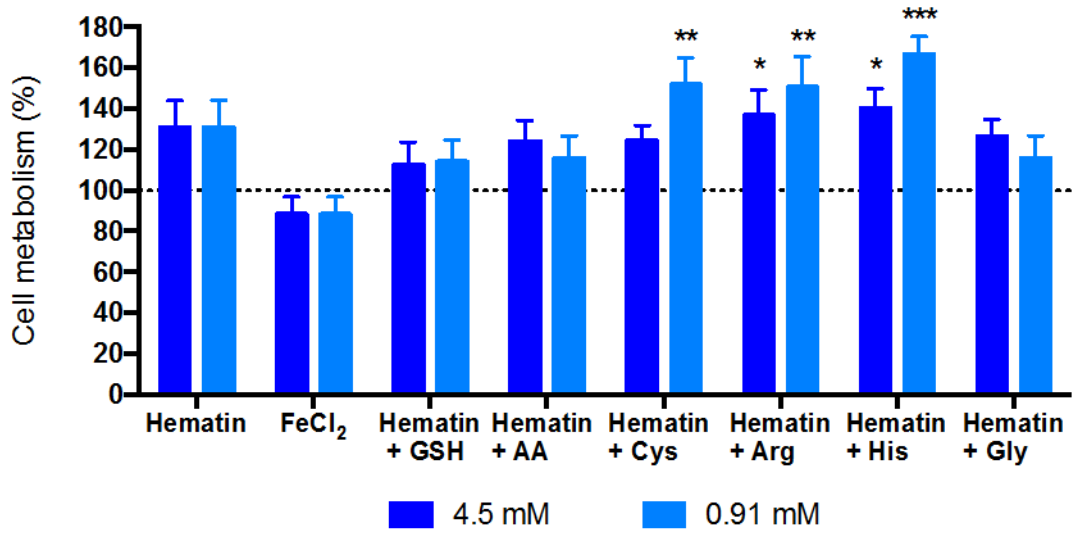

Figure 3-3. Viability of cells incubated with 50 μM iron source in the presence of amino acids, glutathione or ascorbic acid. Caco-2 cell monolayers were grown for 3 days in 96-well plates at 37 ^{o}C, 95 % air, 5 % CO_2, depleted of iron for 16 hours then incubated with either 50 μM $FeCl_2$ with 900 μM ascorbic acid or 50 μM hematin alone or supplemented with glutathione (GSH), cysteine (Cys), arginine (Arg), histidine (His) or glycine (Gly) at 4.5 mM (dark blue) or 0.91 mM (light blue) or ascorbic acid (AA) at 0.8 mM (dark blue) or 0.04 mM (light blue). Monolayers were washed and incubated with MTT solution for 3 hours then the formazan crystals dissolved in DMSO and absorbance read at 490 nm and 650 nm. Incubation with hematin + cys, hematin + arg or hematin + his, resulted in a significant increase in cell viability compared to cells incubated with only MEM (no iron) (dotted line). Values are means ± SEM (n=3 experimental triplicates). Asterisks indicate significant difference in cell metabolism (P < 0.05 *, < 0.01 **, < 0.001 ***), negative control (dotted line) vs. each condition.

Cells incubated with 50 μM hematin with either 4.5 mM arginine or 4.5 mM histidine had a significant (P < 0.05) increase in cellular metabolism compared to the negative control (Figure 3-3). Cells incubated with 50 μM hematin in the presence of 0.91 mM of cysteine, arginine or histidine had a significant (P < 0.01) increase in cellular metabolism compared to the negative control (100% cellular metabolism) (Figure 3-3). The fluctuations in cellular metabolism in monolayers incubated with the remaining 10 uptake solutions were not statistically significant (Figure 3-3).

The cellular metabolism, and therefore viability, of cells incubated with solutions to determine the effect of amino acids, glutathione and ascorbic acid on hematin uptake was either significantly higher than, or equal to, the negative control. This implies that none of the uptake solutions used in the experiments was toxic towards Caco-2 monolayers, over an incubation period of 1 hour. The significant increase in cellular metabolism of cells incubated with 50 μM hematin in the presence of cysteine, histidine and arginine, suggests

that under these conditions cells require more energy to absorb, metabolise and process the nutrients.

3.3.1.2 Cell Viability of Caco-2 Cell Monolayers Incubated with Various Iron Sources

Cell viability of Caco-2 monolayers incubated for 1 or 4 hours with; 50 μM $FeCl_2$, 50 μM hematin alone or in the presence of 2 mM glutathione or 50 μM hematin after a one hour incubation with 2 mM glutathione or 660 μM cysteine, was measured. This was to determine if the uptake solutions, used to investigate the effect of glutathione and incubation time on hematin absorption, (Section 3.3.3) were toxic to Caco-2 cell monolayers.

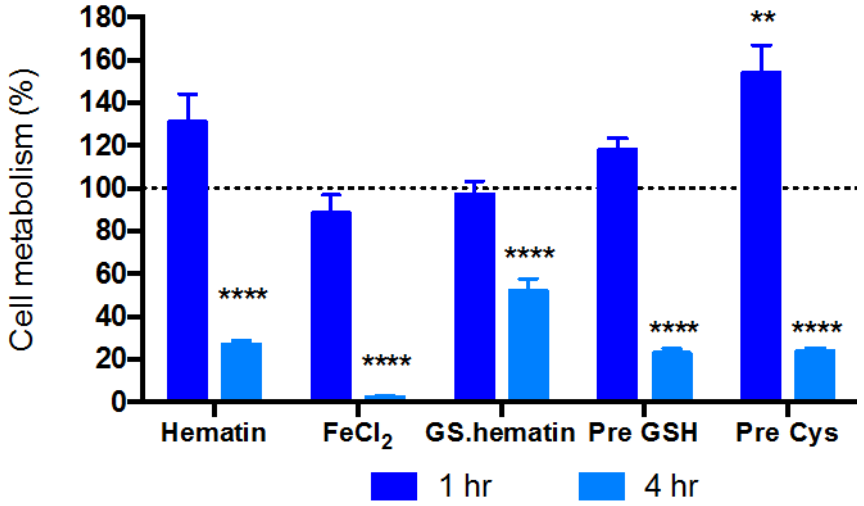

Figure 3-4. Viability of cells incubated with 50 μM iron source for 1 and 4 hours. Caco-2 cell monolayers were grown for 3 days in 96-well plates at 37 ^{o}C, 95 % air, 5 % CO_2, depleted of iron for 16 hours then pre-incubated with either MEM, then incubated with either 50 μM hematin (Hematin), 50 μM $FeCl_3$ with 900 μM ascorbic acid ($FeCl_2$), or 50 μM hematin, 2 mM glutathione (GS.hematin) or pre-incubated with 2 mM glutathione, then 50 μM hematin (Pre GSH) or pre-incubated with 660 μM cysteine, then 50 μM hematin (Pre Cys). Monolayers were washed and incubated with MTT solution for 3 hours then the formazan crystals dissolved in DMSO and absorbance read at 490 nm and 650 nm. There was a significant decrease in cell viability of monolayers incubated for 4 hours with all the iron uptake solutions compared to cells incubated with only MEM (no iron) (dotted line). Values are means ± SEM (n=3 experimental triplicates). Asterisks indicate significant difference in cell metabolism ($P < 0.01$ **, < 0.001 ***, < 0.0001 ****), negative control (dotted line) vs. each condition.

Cells pre-incubated with cysteine for an hour and thereafter incubated with 50 μM hematin for an hour induced a significant ($P < 0.01$) increase in cellular metabolism compared to the negative control (Figure 3-4). The remaining four uptake solutions had no effect on cell viability, when the incubation time was 1 hour, compared to the negative control (Figure 3-4).

When the incubation time was increased to 4 hours cellular metabolism, and therefore viability, of cells incubated with the five uptake solutions was significantly ($P < 0.0001$) reduced (Figure 3-4). This reduction in cellular metabolism indicates that the uptake solutions were toxic to the cells over a 4 hour incubation period.

The significant decrease in cell viability when incubated with iron sources for 4 hours is probably due to an increase in irreversible cellular damage, which ultimately led to cell death. The cellular damage may have been caused by oxidative stress, a toxic side effect of non-ligated iron, both organic and inorganic, within cells. The cell viability of monolayers incubated for only 1 hour with iron sources indicates that the cellular damage, probably resulting from an increase in cellular iron levels, did not reach critical levels after 1 hour.

3.3.2 Influence of Amino Acids, Glutathione and Ascorbic Acid on Hematin Absorption

The absorption of inorganic iron into Caco-2 cells is influenced by various organic and amino acids (Glahn & Campen, 1997; Salovaara *et al.,* 2002). The influence of amino acids and organic acids on organic iron absorption is less well understood and therefore, the effect of cysteine, arginine, histidine, glycine, glutathione and ascorbic acid on hematin absorption was explored using Caco-2 cells.

Arginine is used to keep organic iron from precipitating out of solutions (Sievers *et al.,* 1987). Cysteine and glycine are two of the constituent amino acids of glutathione. Histidine is a key co-ordination residue in many heme containing proteins (Bowman & Rand, 1980; Li *et al.,* 2011) therefore the presence and interaction of histidine with organic iron could influence absorption. The effect of glutathione on hematin absorption is of interest due to the ability of glutathione to bind hematin, forming the more hydrophilic GS.hematin complex, as shown in Chapter 2. This implies that within the GI tract hematin could bind glutathione and furthermore enterocytes would be presented with both GS.hematin and hematin.

Uptake experiments were conducted utilising the synthesised radioactive hematin ([^{59}Fe]hematin) from Chapter 2, allowing lower hematin concentrations to be used, 50 μM, as well as a quicker, more reliable protocol for collecting and analysing the cell associated hematin.

3.3.2.1 The use of [^{59}Fe]hematin to Detect Iron Absorbed into Caco-2 cells

Le Blanc *et al.* (2012) showed that increasing concentrations of organic iron, up to 50 µM, in the uptake medium increased the intracellular concentration of heme in Caco-2 cells. However, concentrations of heme higher than 50 µM in the uptake solution did not further increase intracellular heme concentrations. Consequently upon this finding hematin was used at a concentration of 50 µM for cellular experiments. Glahn & Van Campen (1997) showed that at a ratio of 90:1 amino acids could influence inorganic iron absorption, whereas a ratio of only 8:1 was required for ascorbic acid to influence ferric inorganic iron absorption (Salovaara *et al.,* 2002). Therefore amino acids and glutathione were used at a concentration of 4.5 mM, whilst ascorbic acid was used at a concentration of 0.4 mM.

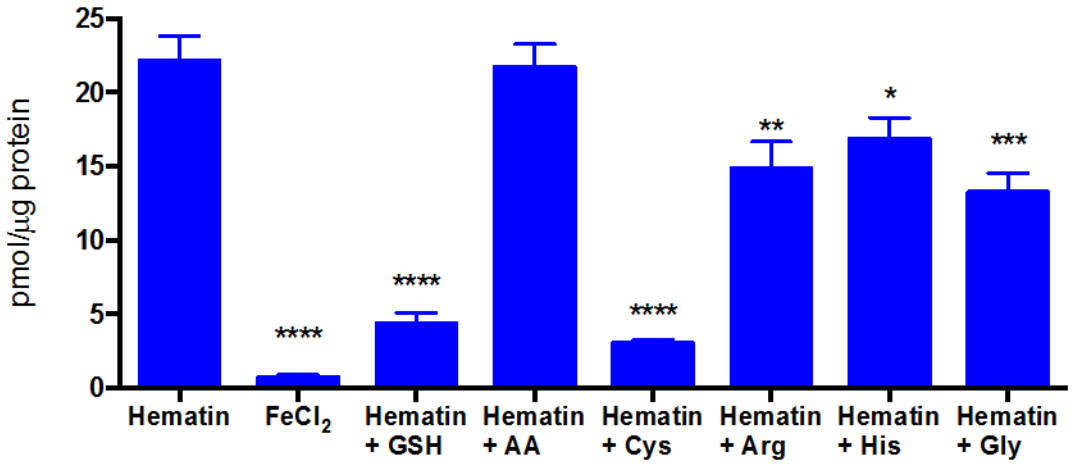

Figure 3-5. Influence of amino acids, glutathione and ascorbic acid in a 91:1 ratio on cell associated iron. Caco-2 cell monolayers were grown for 14 days in 12-well plates at 37 ^{o}C, 95 % air, 5 % CO_2, depleted of iron for 16 hours then incubated with either 50 µM $FeCl_2$ with 10,000 CPM of $^{59}FeCl_3$ and 900 µM ascorbic acid or 50 µM hematin with 10,000 CPM of [^{59}Fe]hematin alone or supplemented with glutathione (GSH), cysteine (Cys), arginine (Arg), histidine (His) or glycine (Gly) at 4.5 mM or ascorbic acid (AA) at 0.4 mM for 1 hour at 37 ^{o}C, 95 % air, 5 % CO_2. Monolayers were washed 3 times and cells collected for detection of [^{59}Fe]hematin or $^{59}FeCl_3$. Negative control contained no radioactive material or hematin and therefore had 0 pmol iron/µg protein. Values are means ± SEM (n=3 experimental triplicates). Asterisks indicate significant difference in hematin cell content (P < 0.05 *, < 0.01 **, < 0.001 ***, < 0.0001 ****) hematin vs. each condition.

After an incubation period of 1 hour, 22.1 pmol hematin/µg protein was associated with the Caco-2 cell monolayer compared 0.7 pmol $FeCl_2$/µg protein (Figure 3-5). The drastic difference in iron associated with the monolayers indicates that the results from the ferrozine assay (Appendix A) were misleading when it was used detect the amount of organic iron absorbed into Caco-2 cell monolayers.

Glutathione and cysteine had the greatest effect on the amount of hematin associated with the Caco-2 cells. In the presence of 4.5 mM glutathione and 4.5 mM cysteine the amount of hematin associated with the cells significantly ($P < 0.0001$) reduced, from 22.1 pmol/μg protein to 4.3 and 3.1 pmol/μg protein respectively (Figure 3-5). Ascorbic acid (0.4 mM) had no significant effect on hematin associated with the cell monolayer whilst arginine, histidine and glycine, at a concentration of 4.5 mM all significantly ($P < 0.05 > 0.0001$) decreased the amount of hematin associated with the Caco-2 cell monolayers (Figure 3-5). The amount of hematin associated with the cells decreased to 14.8, 16.9 and 13.3 pmol/μg protein in the presence of arginine, histidine and glycine respectively in this study (Figure 3-5).

Glahn & Van Campen (1997) showed that at the same ratio of amino acids or ascorbic acid to iron, cysteine and ascorbic acid significantly increased inorganic iron absorption, whilst glutathione and histidine had no effect. Salovaara *et al.* (2002) and Kalgaonkar & Lonnerdal (2008) showed that at ratios above 7:1, ascorbic acid to ferric inorganic iron, ascorbic acid significantly increased ferric inorganic iron absorption by reducing it to ferrous iron. These results demonstrate that amino acids, glutathione and ascorbic acid do not have the same effect on ferric organic iron (hematin) as they do on inorganic iron absorption. This is likely due the differences in the interaction between iron sources and small molecules and the different pathways involved in iron uptake into enterocytes, which depends on the iron source (Sharp & Srai, 2007).

To determine if the ratio of amino acid, glutathione or ascorbic acid to hematin had an effect on hematin uptake the experiment was repeated with the ratio of additives to hematin decreased fivefold.

When the amino acid and glutathione concentration was decreased to 0.91 mM the presence of glutathione and cysteine still significantly ($P < 0.01$) decreased hematin associated with the cells (Figure 3-6). The amount of hematin associated decreased from 9.2 pmol/μg protein to 2.0 and 2.7 pmol/μg protein respectively (Figure 3-6). The presence of; 0.08 mM ascorbic acid and 0.91 mM histidine, arginine and glycine had no significant effect on the amount of hematin associated with the Caco-2 cells over 1 hour (Figure 3-6). Whilst the amount of $FeCl_2$ associated with the monolayers, 0.3 pmol/μg protein, was significantly ($P < 0.001$) lower than that of the amount of hematin (Figure 3-7). This result indicates that arginine, histidine and glycine may have to be present in ratios higher then

18:1 to influence hematin association with Caco-2 cells, whilst glutathione and cysteine affect hematin at ratios as low as 18:1.

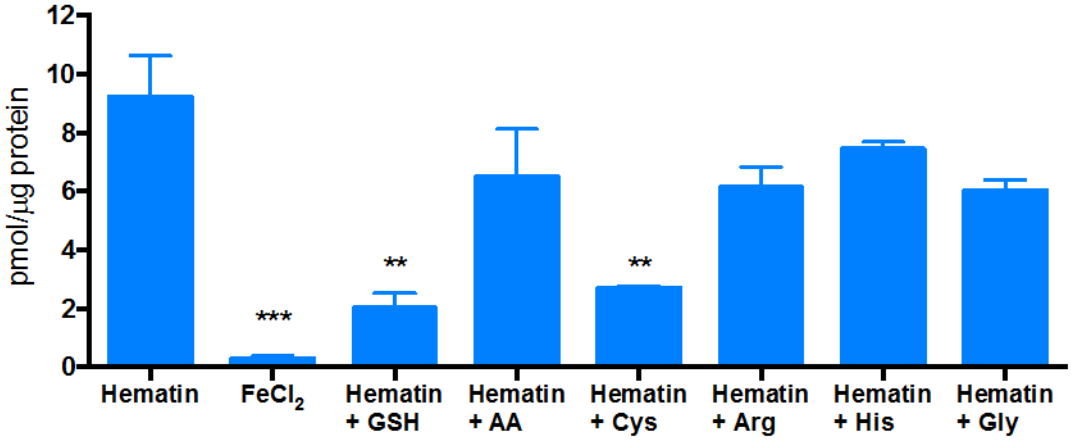

Figure 3-6. Influence of amino acids, glutathione and ascorbic acid in an 18:1 ratio on cell associated iron. Caco-2 cell monolayers were grown for 14 days in 12-well plates at 37 ^{o}C, 95 % air, 5 % CO_2, depleted of iron for 16 hours then incubated with either 50 µM $FeCl_2$ with 10,000 CPM of $^{59}FeCl_3$ and 900 µM ascorbic acid or 50 µM hematin with 10,000 CPM of [^{59}Fe]hematin alone or supplemented with glutathione (GSH), cysteine (Cys), arginine (Arg), histidine (His) or glycine (Gly) at 0.91 mM or ascorbic acid (AA) at 0.08 mM for 1 hour at 37 ^{o}C, 95 % air, 5 % CO_2. Monolayers were washed 3 times and cells collected for detection of [^{59}Fe]hematin or $^{59}FeCl_3$. Negative control contained no radioactive material or hematin and therefore had 0 pmol hematin/µg protein. Values are means ± SEM (n=2 experimental triplicates). Asterisks indicate significant difference in hematin cell content (P < 0.01 **, < 0.001 ***) hematin vs. each condition.

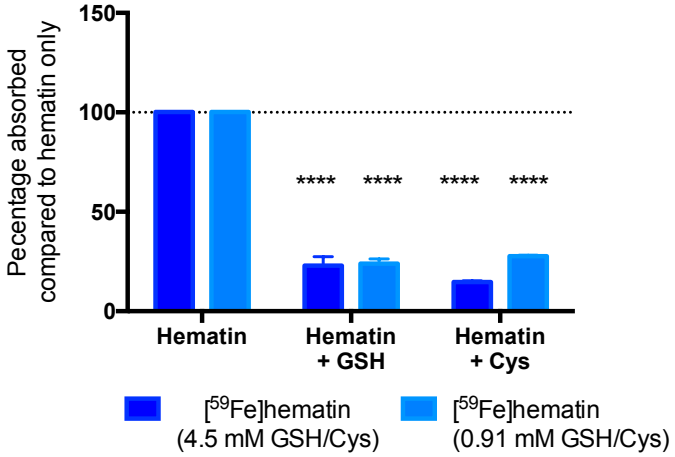

Figure 3-7. Effect of glutathione and cysteine concentration on cell associated [^{59}Fe]hematin. When the amount of hematin associated with Caco-2 cell monolayers over 1 hour was standardised to the amount of hematin in cells incubated with 50 µM hematin with 10,000 CPM of [^{59}Fe]hematin, there was a significant decrease in the amount of hematin associated with the cells when the uptake solutions included either 4.5 mM or 0.91 mM of glutathione or cysteine as well as 50 µM hematin. Values are means ± SEM (n=3 experimental triplicates for 4.5 mM and n=2 experimental triplicates for 0.91 mM experiments). Asterisks indicate significant difference in hematin cell content (P < 0.0001 ****) hematin vs. hematin + GSH and hematin vs. hematin + Cys.

There was a significant ($P < 0.0001$) decrease in hematin associated with the Caco-2 cell monolayers in the presence of glutathione (75% less) or cysteine (72-85% less) compared to cells incubated with hematin only (Figure 3-7).

Previous work, Sections 2.3.2 and 2.3.3, calculated the affinity constants for glutathione and cysteine to hematin and found that both glutathione and cysteine bound to hematin forming a GS.hematin and Cys.hematin complex respectively. The affinity constants and speciation plots are based on data from solutions containing phosphate buffer and potassium chloride at pH 8, rather than phenol free MEM supplemented with potassium phosphate buffer at pH 7.4-7.6. Nevertheless the differences between the two conditions are marginal and the speciation plot will provide a reasonable estimate of the amounts of GS.hematin and Cys.hematin formed in the uptake solutions.

In the presence of 0.91 mM glutathione up to 98% of 50 μM could be in the form of GS.hematin, which rises to 100% in the presence of 4.5 mM glutathione (Figure 3-8). In the presence of 0.91 mM cysteine up to 13% of hematin could be in the form of Cys.hematin, this rises to 42% when the concentration of cysteine is increased to 4.5 mM (Figure 3-8).

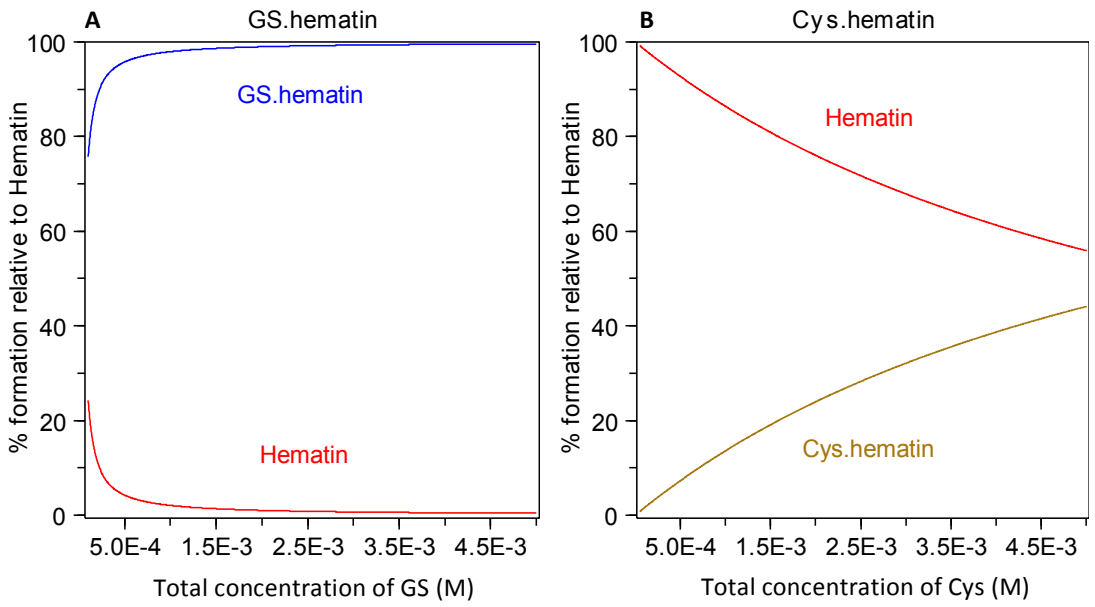

Figure 3-8. Speciation plots of GS.hematin and Cys.hematin. Speciation plots with parameters 50 μM hematin, pH 8 **A –** 0.5 mM to 5 mM glutathione and K_a = 5.0 x 10^4 M^{-1}, **B –** 0.5 mM to 5 mM cysteine and K_a = 5.0 x 10^4 M^{-1}. Red line indicates the percentage of total hematin that would be free in solution; the blue line indicates the calculated amount of hematin in the solution that would bind to glutathione to form GS.hematin and the gold line indicates the calculated amount of hematin in the solution that would bind to cysteine to form Cys.hematin.

This data strongly suggests the decrease in the cell associated hematin, in samples containing glutathione and cysteine, is due to the formation of the GS.hematin and Cys.hematin complex. The decrease in hematin association with cells, in the presence of arginine and histidine, which weakly interact with organic iron within proteins (Li *et al.,* 2011), gives further weight to the hypothesis that ligated hematin, is not absorbed as effectively as non-ligated hematin.

3.3.3 Hematin and Inorganic Iron Absorption into Caco-2 Cell Monolayers

The concentration of glutathione found in the cytosol of cells ranges from 2 mM to 8 mM (Kondo *et al.,* 1995, Soboll *et al.,* 1995). Reduced glutathione within the cell is either synthesised through the recycling of glutathione disulphide to reduced glutathione by glutathione reductase, or through the *de novo* synthesis of glutathione from its constituent amino acids. The rate of *de novo* synthesis is rate-limiting with respect to the first enzyme in glutathione synthesis namely, γ - glutamylcysteine synthetase and the availability of L-cysteine (Richman & Meister, 1974). To increase the probability of increasing the glutathione concentration in the cytosol of cells, Caco-2 cells were incubated for 1 hour with either glutathione or cysteine prior to incubation with hematin. This was to investigate if a potential increase in glutathione concentration within cells would influence hematin absorption.

3.3.3.1 1 hour Incubation

Significantly ($P < 0.0001$) less inorganic iron, 2.7 pmol /μg protein, was associated with Caco-2 cell monolayers compared to hematin, 30.6 pmol /μg protein over one hour (Figure 3-9). Whilst cells incubated with hematin in the presence of glutathione, therefore cells were presented with GS.hematin, had significantly ($P < 0.0001$) less hematin, 8.1 pmol/μg protein, associated with the cells compared to cells incubated with hematin only (Figure 3-9). There was no significant change in hematin associated with cells pre-incubated with glutathione or cysteine compared to cells incubated with hematin only (Figure 3-9).

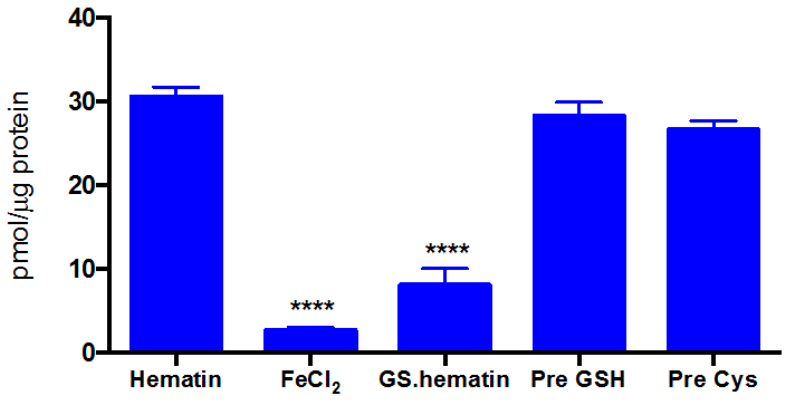

Figure 3-9. Iron associated with Caco-2 monolayers after 1 hour incubation. Caco-2 cell monolayers were grown for 14 days in 12-well plates at 37 ^{o}C, 95 % air, 5 % CO_2, depleted of iron for 16 hours then pre-incubated for 1 hour with either MEM, (Hematin, $FeCl_2$ and GS.hematin) or MEM supplemented with 2 mM glutathione (Pre GSH) or 660 µM cysteine (Pre Cys). Monolayers were washed twice and incubated for 1 hour with uptake solutions containing 50 µM hematin and 10,000 CPM of [^{59}Fe]hematin (Hematin, Pre GSH and Pre Cys), 50 µM $FeCl_3$ with 900 µM ascorbic acid and 10,000 CPM of $^{59}FeCl_3$ ($FeCl_2$), or 50 µM hematin with 2 mM glutathione and 10,000 CPM of [^{59}Fe]hematin (GS.hematin). Monolayers were washed 3 times and cells collected for detection of [^{59}Fe]hematin or $^{59}FeCl_3$. Negative control contained no radioactive material or hematin and therefore had 0 pmol hematin/µg protein. Values are means ± SEM (n=3 experimental triplicates). Asterisks indicate significant difference ($P < 0.0001$ ****), hematin vs. condition.

The significant decrease in hematin associated with cells incubated with hematin in the presence of glutathione is almost certainly due to the formation of the GS.hematin complex, which under the experimental conditions could constitute up to 99% of hematin in the uptake solution.

3.3.3.2 4 hour Incubation

Over an incubation period of 4 hours significantly ($P < 0.001$) less inorganic iron, 8.7 pmol/µg protein, was associated with Caco-2 cell monolayers compared to hematin, 35.4 pmol/µg protein (Figure 3-10). Unlike in a 1 hour incubation period, there was no significant difference in the amount of hematin associated with the cells incubated with hematin in the presence of glutathione, 30.8 pmol/µg protein, compared to cells incubated with hematin only (35.4 pmol/µg protein) (Figure 3-10). As with hematin association with Caco-2 cells over a 1 hour incubation period, there was no significant difference in the amount of hematin associated with the cells pre-incubated with glutathione or cysteine compared to cells incubation with hematin only (Figure 3-10).

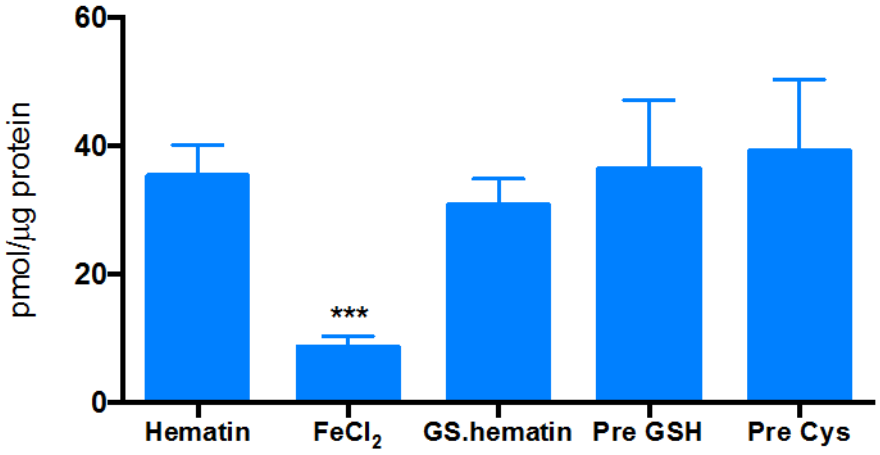

Figure 3-10. Iron associated with Caco-2 monolayers after 4 hours incubation. Caco-2 cell monolayers were grown for 14 days in 12-well plates at 37 °C, 95 % air, 5 % CO_2, depleted of iron for 16 hours then pre-incubated for 1 hour with either MEM (Hematin, $FeCl_2$ and GS.hematin) or MEM supplemented with 2 mM glutathione (Pre GSH) or 660 µM cysteine (Pre Cys). Monolayers were washed twice and incubated with uptake solutions containing 50 µM hematin and 10,000 CPM of [^{59}Fe]hematin (Hematin, Pre GSH and Pre Cys), 50 µM $FeCl_3$ with 900 µM ascorbic acid and 10,000 CPM of $^{59}FeCl_3$ ($FeCl_2$), or 50 µM hematin with 2 mM glutathione and 10,000 CPM of [^{59}Fe]hematin (GS.hematin) for 4 hours. Monolayers were washed 3 times and cells collected for detection of [^{59}Fe]hematin or $^{59}FeCl_3$. Negative control contained no radioactive material or hematin and therefore had 0 pmol hematin/µg protein. Values are means ± SEM (n=2 experimental triplicates). Asterisks indicate significant difference ($P < 0.001$ ***), hematin vs. condition.

The amount of hematin associated with the cells after a 4 hour incubation period was not significantly different from that after a 1 hour incubation period (Figure 3-11). This implies that Caco-2 cells can regulate the amount of hematin taken up, the majority of which occurs within the first hour of incubation. Hematin uptake subsequently ceased as further uptake could result in a higher than desired concentration of iron within the cell. This could lead to oxidative stress and ultimately lipid peroxidation and the production of free radicals via the Fenton reaction.

The amount of hematin associated with the Caco-2 cells pre-incubated with glutathione or cysteine did not change significantly when the incubation time was increased from 1 to 4 hours (Figure 3-11). The amount of hematin associated with Caco-2 cells incubated with hematin in the presence of glutathione (GS.hematin) significantly ($P < 0.01$) increased from 8.1 pmol/µg protein in 1 hour to 30.8 pmol/µg protein in 4 hours. The increase in inorganic iron associated with the cells, from 2.7 pmol/µg protein, to 8.7 pmol/µg protein was, however, not significant (Figure 3-11). This implies that uptake of inorganic iron is slower or less efficient than hematin absorption.

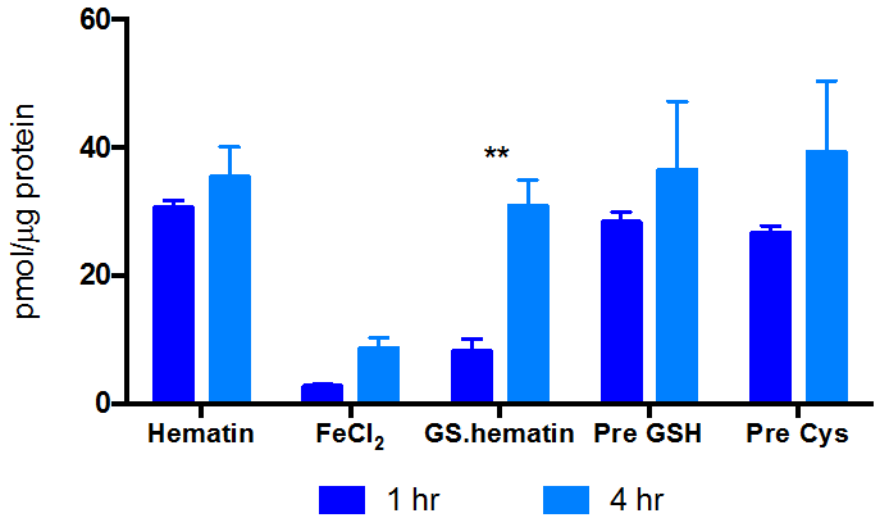

Figure 3-11. Iron retained over time in Caco-2 cell monolayers. Caco-2 cell monolayers were grown for 14 days in 12-well plates at 37 ^{o}C, 95 % air, 5 % CO_2, depleted of iron for 16 hours then pre-incubated for 1 hour with either MEM (Hematin, $FeCl_2$ and GS.hematin) or MEM supplemented with 2 mM glutathione (Pre GSH) or 660 µM cysteine (Pre Cys). Monolayers were incubated for 1 (dark blue) or 4 (light blue) hours with uptake solutions containing 50 µM hematin and 10,000 CPM of [^{59}Fe]hematin (Hematin, Pre GSH and Pre Cys), 50 µM $FeCl_3$ with 900 µM ascorbic acid and 10,000 CPM of $^{59}FeCl_3$ ($FeCl_2$), or 50 µM hematin with 2 mM glutathione and 10,000 CPM of [^{59}Fe]hematin (GS.hematin). Values are means ± SEM (n=3 experimental triplicates for 1 hour, n=2 experimental triplicates for 4 hours). Asterisks indicate significant difference ($P < 0.01$ **), 1 hr vs. 4hr for each condition.

The significant increase in GS.hematin associated with the cells between the 1 and 4 hour incubation suggests that, similar to inorganic iron, the uptake of GS.hematin is less efficient and therefore the uptake rate is slower than that of hematin alone. Therefore, for the cells to take up the same amount of hematin as cells incubated with hematin alone uptake of GS.hematin must continue after the first hour of incubation. This observation suggests that either GS.hematin is take up into cells by a different mechanism to that employed by non-ligated hematin, or that GS.hematin uses the same pathway but less effectively.

If the incubation of cells with glutathione or cysteine, prior to incubation with hematin, increased the cellular concentration of glutathione the subsequent increase in glutathione concentration did not affect the amount of hematin associated with the Caco-2 cells (Figure 3-11). This indicates that the concentration of glutathione within the cytosol had no effect on hematin association to Caco-2 cells.

3.3.4 Iron Uptake and Efflux into Caco-2 Cell Monolayers Cultured in Bicameral Chambers

Caco-2 cells are polarised with iron uptake occurring on the apical membrane and efflux on the basolateral membrane. To better simulate the uptake of hematin into the body, Caco-2 cells were grown on bicameral, instead of unicameral chambers, thereby allowing the efflux of cellular components, such as Fe(II), from the basolateral membrane. This approach also had the advantage of permitting the investigation of the uptake and efflux of iron concurrently in Caco-2 cell monolayers.

Under culture conditions, cysteine is quickly oxidised to cystine, which is imported into cells through the Na^+ cystine/glutamate antiporter (Murphy *et al.,* 1989). N-acetyl-L-cysteine is a cysteine prodrug, which has been shown to increase cellular concentrations of glutathione (Phelps *et al.,* 1992 and Atkuri *et al.,* 2007) and does not become oxidised in cell cultures. To increase the likelihood of cysteine entering the monolayer, prior to hematin incubation, acetylated cysteine (N-acetyl-L-cysteine) was employed instead of cysteine.

3.3.4.1 Uptake and Efflux of Iron into Caco-2 Cell Monolayers after 1 Hour Incubation

The association of and efflux of iron across Caco-2 cell monolayers grown in bicameral chambers were measured after 1 hour of incubation with either hematin or inorganic iron.

On average 15.4 pmol hematin/μg protein was associated with Caco-2 cells after 1 hour of incubation with hematin (Figure 3-12). Cells pre-incubated with either glutathione or acetylated cysteine accumulated 13.7 pmol hematin/μg protein associated with the cells over 1 hour (Figure 3-12). Cells incubated with hematin in the presence of glutathione (GS.hematin) had significantly ($P < 0.05$) less hematin, 4.3 pmol/μg protein, associated with the cells after 1 hour, compared to cells incubated with hematin only (Figure 3-12). Cells incubated with inorganic iron had significantly ($P < 0.01$) less iron, 1.8 pmol /μg protein, associated with the cells after 1 hour incubation compared to cells incubated with hematin alone (Figure 3-12).

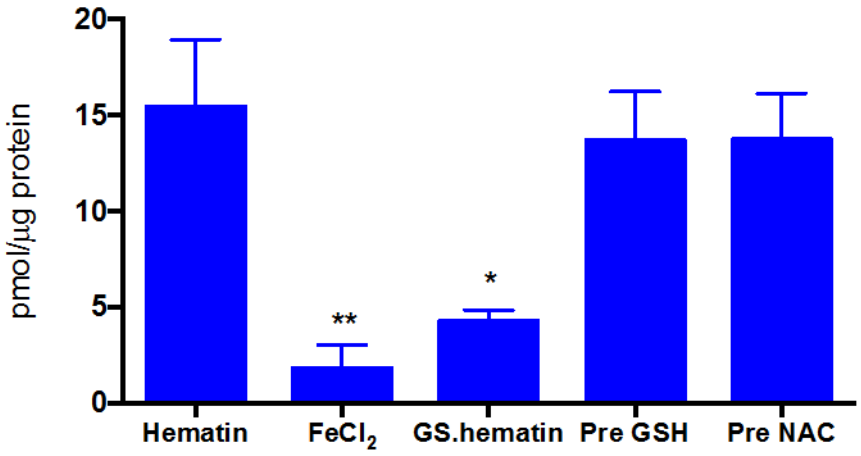

Figure 3-12. Iron associated with Caco-2 cell monolayers after 1 hour incubation. Caco-2 cell monolayers were grown in 6-well transwell plates at 37 ^{o}C, 95 % air, 5 % CO_2. Once TEER reached 250 Ωcm^2 they were depleted of iron for 16 hours then pre-incubated for 1 hour with either MEM (Hematin, $FeCl_2$ and GS.hematin) or MEM supplemented with 2 mM glutathione (Pre GSH) or 660 µM N-acteyl-L-cysteine (Pre NAC). Monolayers were washed twice and incubated for 1 hour with uptake solutions containing 50 µM hematin and 10,000 CPM of [^{59}Fe]hematin (Hematin, Pre GSH and Pre NAC), 50 µM $FeCl_3$ with 900 µM ascorbic acid and 10,000 CPM of $^{59}FeCl_3$ ($FeCl_2$), or 50 µM hematin with 2 mM glutathione and 10,000 CPM of [^{59}Fe]hematin (GS.hematin). The basal chamber contained 12.5 µM apo-transferrin in phenol free MEM. Monolayers were washed 3 times and cells collected for detection of [^{59}Fe]hematin or $^{59}FeCl_3$. Negative control contained no radioactive material or hematin 1and therefore had 0 pmol hematin/µg protein. Values are means ± SEM (n=3 experimental triplicates). Asterisks indicate significant difference (P < 0.05 *, < 0.01 **), hematin vs. condition.

The mean amount of iron (Fe(II)) exported into the basal medium, which contained human apo-transferrin, from cell monolayers incubated with $FeCl_2$ was 42 fmol/µg protein, whilst cells incubated with hematin only exported 2.2 fmol/µg protein (Figure 3-13). There was no significant difference in the amount of iron exported out of cells that were incubated with the different organic iron sources (Figure 3-13). Monolayers were not used until TEER measurements reached above 250 Ωcm^2 meaning tight gap junctions had formed (Follett *et al.,* 2002). The formation of tight gap junctions meant nutrients could not diffuse into the basal medium from the apical medium. Therefore any iron detected in the basal medium was due to exportation from the monolayer rather than diffusion from the apical uptake medium.

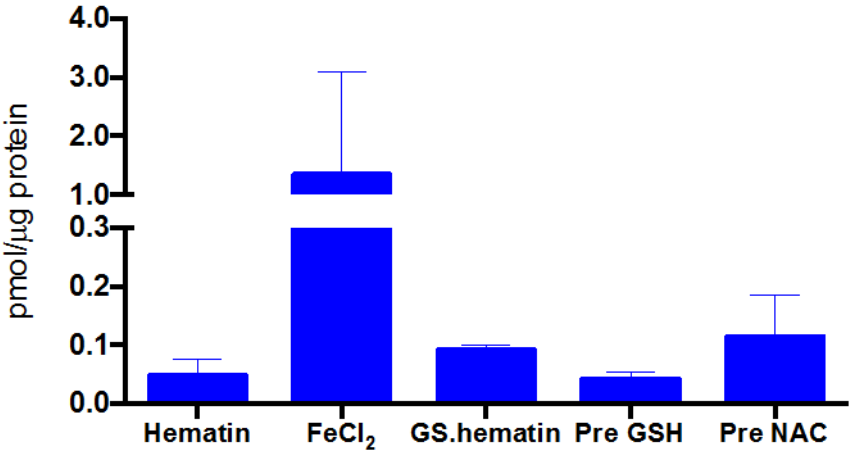

Figure 3-13. Iron exported from Caco-2 monolayers over 1 hour, grown in bicameral chambers. Caco-2 cell monolayers were grown in 6-well transwell plates at 37 ^{o}C, 95 % air, 5 % CO_2. Once TEER reached 250 Ωcm^2 they were depleted of iron for 16 hours then pre-incubated for 1 hour with either MEM (Hematin, $FeCl_2$ and GS.hematin) or MEM supplemented with 2 mM glutathione (Pre GSH) or 660 µM N-acetyl-L-cysteine (Pre NAC). Monolayers were washed twice and incubated for 1 hour with uptake solutions containing 50 µM hematin and 10,000 CPM of [^{59}Fe]hematin (Hematin, Pre GSH and Pre Cys), 50 µM $FeCl_3$ with 900 µM ascorbic aoucid and 10,000 CPM of $^{59}FeCl_3$ ($FeCl_2$), or 50 µM hematin with 2 mM glutathione and 10,000 CPM of [^{59}Fe]hematin (GS.hematin). The basal chamber contained 12.5 µM apo-transferrin in phenol free MEM which was collected for the detection of ^{59}Fe after 1 hour incubation. Negative control contained no radioactive material or hematin and therefore had 0 pmol hematin/µg protein. Values are means ± SEM (n=3 experimental triplicates).

The total amount of hematin or inorganic iron associated with the cell monolayers, cell associated iron added to iron in basal chamber, followed the same pattern as the amount associated with cell monolayers. Significantly ($P < 0.05$) less inorganic iron (2.7 pmol/µg protein) and GS.hematin (4.3 pmol /µg protein) were associated compared to 15.5 pmol/µg protein by cells incubated with hematin only, (Figure 3-14). Comparable amounts of hematin were associated, over 1 hour, by cells pre-incubated with glutathione, pre-incubated with acetylated cysteine or incubated with hematin alone (Figure 3-14).

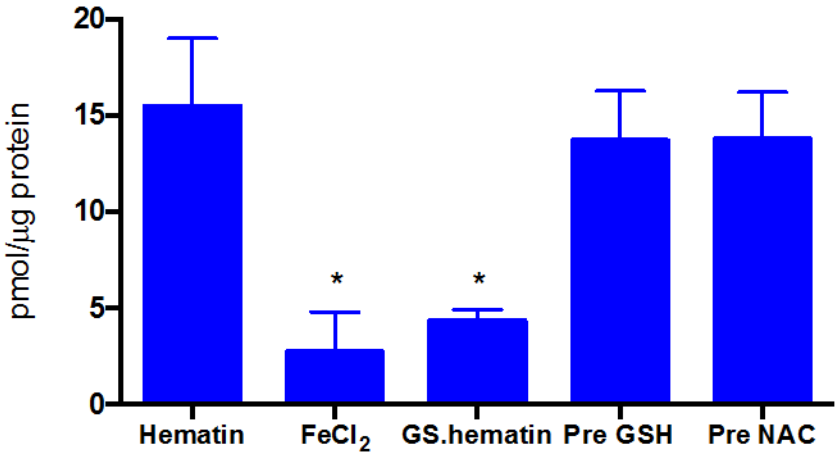

Figure 3-14. Total iron associated with Caco-2 monolayers and in basal medium after 1 hour incubation. Caco-2 cell monolayers were grown in 6-well transwell plates at 37 ^{o}C, 95 % air, 5 % CO_2. Once TEER reached 250 Ωcm^2 they were depleted of iron for 16 hours then pre-incubated for 1 hour with either MEM (Hematin, $FeCl_2$ and GS.hematin) or MEM supplemented with 2 mM glutathione (Pre GSH) or 660 µM N-actyl-L-cysteine (Pre NAC). Monolayers were washed twice and incubated for 1 hour with uptake solutions containing 50 µM hematin and 10,000 CPM of [^{59}Fe]hematin (Hematin, Pre GSH and Pre NAC), 50 µM $FeCl_3$ with 900 µM ascorbic acid and 10,000 CPM of $^{59}FeCl_3$ ($FeCl_2$), or 50 µM hematin with 2 mM glutathione and 10,000 CPM of [^{59}Fe]hematin (GS.hematin). Monolayers were washed 3 times and cells collected for detection of [^{59}Fe]hematin or $^{59}FeCl_3$, the basal medium, containing 12.5 µM apo-transferrin, was combined with collected cells and counted for effluxed ^{59}Fe. Negative control contained no radioactive material or hematin and therefore had 0 pmol hematin/µg protein. Values are means ± SEM (n=3 experimental triplicates). Values are means ± SEM (n=3 experimental triplicates). Asterisks indicate significant difference (P < 0.05 *), hematin vs. condition.

The data displayed the same absorption trend as found in Caco-2 cells incubated under similar conditions in unicameral chambers which is: inorganic iron < GS.hematin < pre-incubated with glutathione and cysteine ≤ hematin (Section 3.3.3.1). This outcome indicates that the potential increase in glutathione concentration within the cell had no significant effect upon hematin absorption into the cell whilst hematin ligated to glutathione, decreases hematin absorption into cells.

3.3.4.2 Uptake and Efflux of Iron into Caco-2 Cell Monolayers after 24 Hour Incubation

One hour is a relatively short incubation time, especially when the determination of the efflux of organic iron is of interest. The investigation was therefore repeated with the incubation time extended to 24 hours.

Over 24 hours, cells incubated with hematin had 38.8 pmol/µg protein of hematin associated with the monolayer whilst cells incubated with inorganic iron had significantly (P < 0.05) less at 4.6 pmol/µg protein (Figure 3-15). Cells pre-incubated with glutathione or

acetylated cysteine for 1 hour prior to the 24 hours incubation with hematin had 35.5 and 42.3 pmol /μg protein associated with the monolayer respectively (Figure 3-15). Unlike cells incubated for 1 hour with GS.hematin, there was no significant difference in the amount of hematin associated with the Caco-2 cell monolayer after 24 hours compared to cells incubated with hematin only (Figure 3-15).

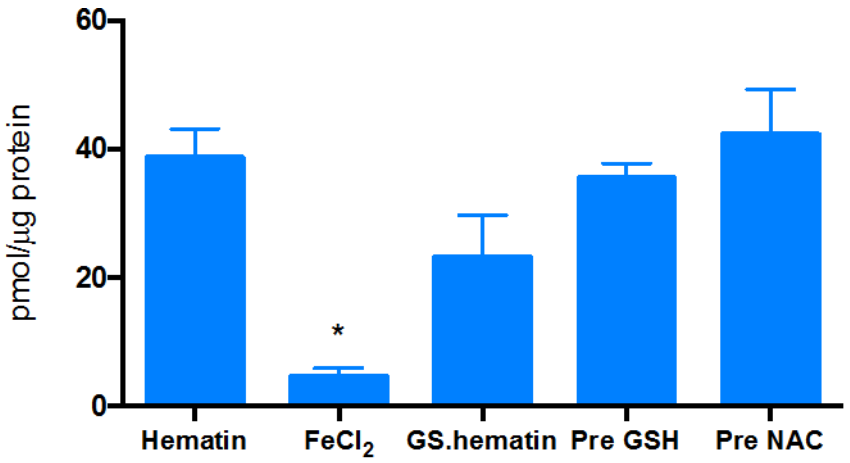

Figure 3-15. Iron associated with Caco-2 monolayers after 24 hour incubation. Caco-2 cell monolayers were grown in 6-well transwell plates at 37 ^{o}C, 95 % air, 5 % CO_2. Once TEER reached 250 Ωcm^2 they were depleted of iron for 16 hours then pre-incubated for 1 hour with either MEM (Hematin, $FeCl_2$ and GS.hematin) or MEM supplemented with 2 mM glutathione (Pre GSH) or 660 μM N-acetyl-L-cysteine (Pre NAC). Monolayers were washed twice and incubated for 24 hours with uptake solutions containing 50 μM hematin and 10,000 CPM[^{59}Fe]hematin (Hematin, Pre GSH and Pre NAC), 50 μM $FeCl_3$ with 900 μM ascorbic acid and 10,000 CPM $^{59}FeCl_3$ ($FeCl_2$), or 50 μM hematin with 2 mM glutathione and 10,000 CPM of [^{59}Fe]hematin (GS.hematin). The basal chamber contained 12.5 μM apo-transferrin in phenol free MEM. Monolayers were washed 3 times and cells collected for detection of [^{59}Fe]hematin or $^{59}FeCl_3$. Negative control contained no radioactive material or hematin and therefore had 0 pmol hematin/μg protein. Values are means ± SEM (n=2 experimental triplicates). Asterisks indicate significant difference ($P < 0.05$ *), hematin vs. condition.

The efflux of iron was higher, but not significantly so, from Caco-2 cell monolayers incubated with inorganic iron ($FeCl_2$), at 1,428 fmol/μg protein, compared with cells incubated organic iron (hematin), 184 fmol/μg protein (Figure 3-16). There was no significant difference in the amount of iron exported out of cell monolayers pre-incubated with glutathione or acetylated cysteine or GS.hematin when compared to cells incubated with hematin only for 24 hours (Figure 3-16). Due to the formation of tight gap junctions, hematin could not have diffused from the apical uptake solution to the basal medium, meaning iron detected in the basal medium had been exported from the monolayer.

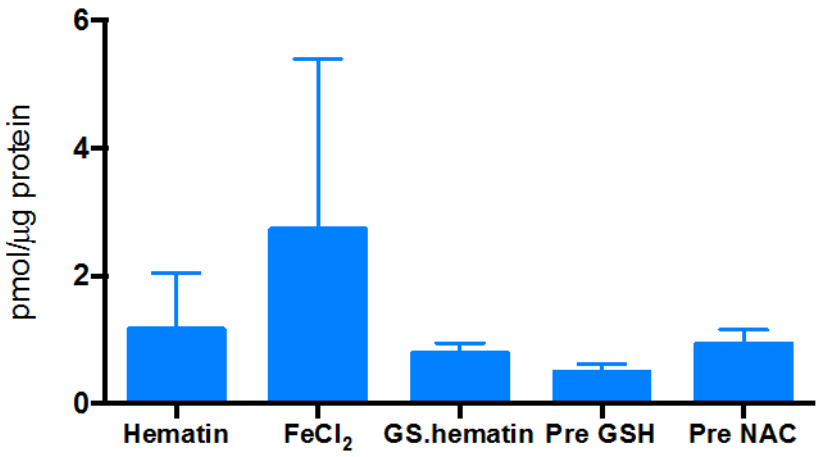

Figure 3-16. Iron exported out of Caco-2 monolayers over 24 hours, grown in bicameral chambers. Caco-2 cell monolayers were grown in 6-well transwell plates at 37 ^{o}C, 95 % air, 5 % CO_2. Once TEER reached 250 Ωcm^2 they were depleted of iron for 16 hours then pre-incubated for 1 hour with either MEM (Hematin, $FeCl_2$ and GS.hematin) or MEM supplemented with 2 mM glutathione (Pre GSH) or 660 µM N-acetyl-L-cysteine (Pre NAC). Monolayers were washed twice and incubated for 24 hours with uptake solutions containing 50 µM hematin and 10,000 CPM of [^{59}Fe]hematin (Hematin, Pre GSH and Pre NAC), 50 µM $FeCl_3$ with 900 µM ascorbic acid and 10,000 CPM of $^{59}FeCl_3$ ($FeCl_2$), or 50 µM hematin with 2 mM glutathione and 10,000 CPM of [^{59}Fe]hematin (GS.hematin). The basal chamber contained 12.5 µM apo-transferrin in phenol free MEM which was collected for the detection of ^{59}Fe after 24 hours incubation. Negative control contained no radioactive material or hematin and therefore had 0 pmol hematin/µg protein. Values are means ± SEM (n=2 experimental triplicates).

The general trend of iron export was that with an increase in incubation time resulted in increased amounts of iron exported from cells incubated with all iron sources.

There was a significant ($P < 0.05$) difference in the total amount (iron associated with monolayer plus iron in basal medium) of $FeCl_2$ associated (12.7 pmol/µg protein) with the monolayers over 24 hours compared to hematin (39.9 pmol/µg protein) (Figure 3-17). There was no significant difference in the amount of hematin associated with the monolayer when incubated with GS.hematin compared to cells incubated with hematin only (Figure 3-17). Similarly, no significant difference in hematin associated with the monolayer was found between cells pre-incubated with glutathione or acetylated cysteine for 1 hour prior to the 24 hour hematin incubation, compared to cells incubated with hematin only for 24 hour (Figure 3-17).

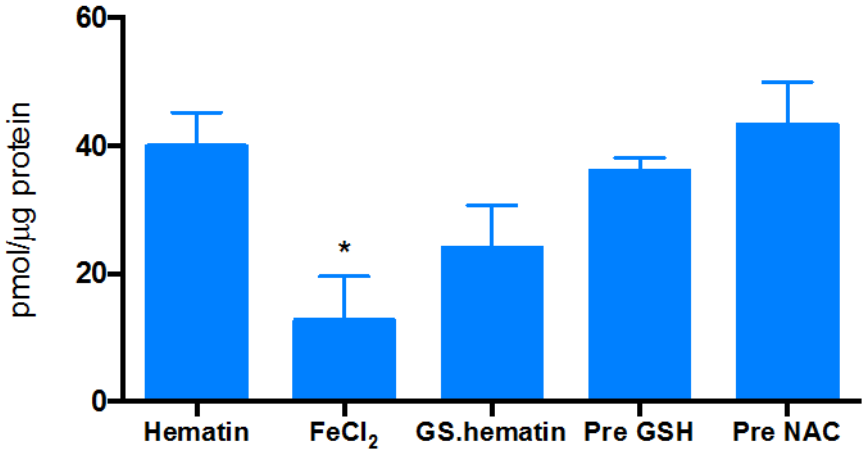

Figure 3-17. Total iron associated with Caco-2 monolayers after 24 hour incubation. Caco-2 cell monolayers were grown in 6-well transwell plates at 37 ^{o}C, 95 % air, 5 % CO_2. Once TEER reached 250 Ωcm^2 they were depleted of iron for 16 hours then pre-incubated for 1 hour with either MEM (Hematin, $FeCl_2$ and GS.hematin) or MEM supplemented with 2 mM glutathione (Pre GSH) or 660 µM N-actyl-L-cysteine (Pre NAC). Monolayers were washed twice and incubated for 24 hours with uptake solutions containing 50 µM hematin and 10,000 CPM of [^{59}Fe]hematin (Hematin, Pre GSH and Pre NAC), 50 µM $FeCl_3$ with 900 µM ascorbic acid and 10,000 CPM of $^{59}FeCl_3$ ($FeCl_2$), or 50 µM hematin with 2 mM glutathione and 10,000 CPM of [^{59}Fe]hematin (GS.hematin). Monolayers were washed 3 times and cells collected for detection of [^{59}Fe]hematin or $^{59}FeCl_3$, the basal medium, containing 12.5 µM apo-transferrin, was combined with collected cells and counted for effluxed ^{59}Fe. Negative control contained no radioactive material or hematin and therefore had 0 pmol hematin/µg protein. Values are means ± SEM (n=2 experimental triplicates). Values are means ± SEM (n=3 experimental triplicates). Asterisks indicate significant difference ($P < 0.05$ *), hematin vs. condition.

The mean amounts of total inorganic iron associated with Caco-2 cell monolayers did not significantly change with an increase in incubation time, even though the amount of $FeCl_2$ associated with the monolayers did increase slightly (Figure 3-18). However, cells incubated with hematin had a significant ($P < 0.01$) increase in hematin associated with the monolayer from 15.5 to 39.9 pmol/µg protein, with an increase in incubation time (Figure 3-18). There was a significant ($P < 0.05$) difference in hematin associated with the monolayer, from 4.3 pmol/µg protein to 24 pmol/µg protein, when cells were incubated for 24 hours with GS.hematin instead of 1 hour (Figure 3-18). The amount of hematin associated with the cells significantly ($P < 0.01$) increased when the hematin incubation time of cells pre-incubated with glutathione, or acetylated cysteine, was increased from 1 to 24 hours (Figure 3-18).

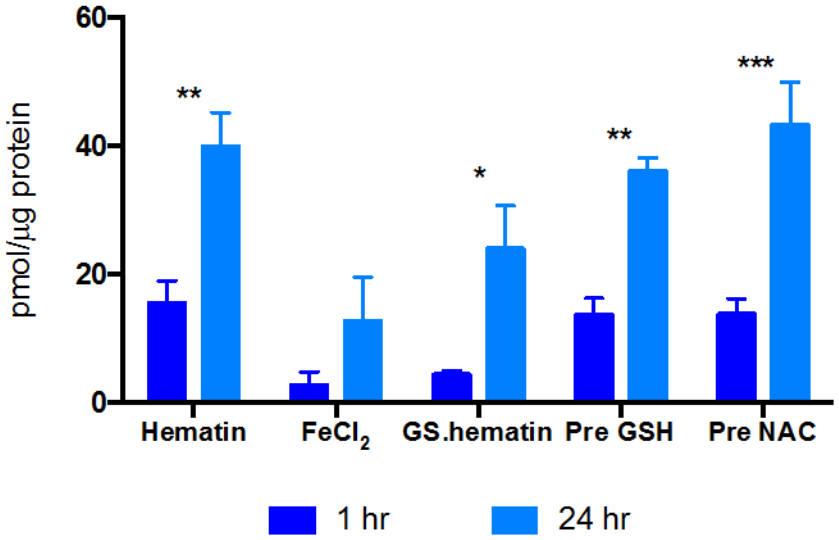

Figure 3-18. Comparison of total iron associated with Caco-2 monolayers after 1 and 24 hour incubation. Caco-2 cell monolayers were grown in 6-well transwell plates at 37 ^{o}C, 95 % air, 5 % CO_2. Once TEER reached 250 Ωcm^2 they were depleted of iron for 16 hours then pre-incubated for 1 hour with either MEM (Hematin, $FeCl_2$ and GS.hematin) or MEM supplemented with 2 mM glutathione (Pre GSH) or 660 µM N-actyl-L-cysteine (Pre NAC). Monolayers were washed twice and incubated for 1 or 24 hours with uptake solutions containing 50 µM hematin and 10,000 CPM of [^{59}Fe]hematin (Hematin, Pre GSH and Pre NAC), 50 µM $FeCl_3$ with 900 µM ascorbic acid and 10,000 CPM of $^{59}FeCl_3$ ($FeCl_2$), or 50 µM hematin with 2 mM glutathione and 10,000 CPM of [^{59}Fe]hematin (GS.hematin). Monolayers were washed 3 times and cells collected for detection of [^{59}Fe]hematin or $^{59}FeCl_3$, the basal medium, containing 12.5 µM apo-transferrin, was combined with collected cells and counted for effluxed ^{59}Fe. Negative control contained no radioactive material or hematin and therefore had 0 pmol hematin/µg protein. Values are means ± SEM (n=3 experimental triplicates for 1 hour and n=2 experimental triplicates for 24 hours). Asterisks indicate significant difference (P < 0.05 *, 0.01 **, < 0.001 ***) between time points (1 hr vs. 24 hr) for each condition.

The significant increase in hematin associated with the cells, from all organic iron sources; with an increase in incubation time indicates that the monolayers continued to uptake organic iron beyond the first hour of incubation. This indicates further that the cellular demand for iron was not fully met in the first hour by hematin.

3.4 General Discussion

The low amount of iron (9% by weight) in hematin, the possible influence other molecules present in the solution and the indirect way ferrozine measures organic iron resulted in the decision to use [^{59}Fe]hematin to study hematin uptake into Caco-2 cells.

Maintaining inorganic iron in solution, in a form that is compatible for absorption into Caco-2 cells, is challenging (He *et al.*, 2008; Pereira *et al.*, 2015). The pH of the cell medium, other components within the medium and the presence of oxygen, all have an effect on the speciation of iron within the solution, and therefore the form of iron presented to the cells (Whitehead *et al.*, 1996; He *et al.,* 2008; Mergler *et al*., 2012; Pereira *et al.*, 2015).

The speciation of the iron within the uptake solution used in these experiments, iron(II) chloride (50 μM) dissolved in water, ascorbic acid (0.9 mM), phenol free MEM and potassium phosphate buffer (66.7 mM), was not determined. This means that the amount, and speciation, of the inorganic iron presented to the cells throughout these experiments cannot be definitively known. However, presence of phosphate in the uptake solution is highly likely to have caused iron phosphate, an insoluble complex, to form. This insoluble complex would have precipitated out of solution decreasing the amount of iron presented to the Caco-2 cell monolayers. Another factor to consider is the presence of ascorbic acid, in a molar ratio of 18:1 (ascorbic acid : $FeCl_2$) in the uptake solution. This should have ensured that the inorganic iron was kept in the ferrous oxidation state, helping to maintain the solubility of the iron, as ferric iron in near neutral pH solutions readily precipitates (Mergler *et al*., 2012). Ascorbic acid has also been shown to help reduce the formation of inorganic iron microparticulates and nanoparticulates, which remain suspended in the uptake medium (Merglyer *et al*., 2012; Pereira *et al*., 2015), however may not be available for uptake via DMT1 due to particle size. Therefore due to the presence of ascorbic acid and the relavilty low concentration of $FeCl_2$ (50 μM), the formation of micro- and nano-particulates, which would decrease the iron available for transport into the cell via DMT1, would remain low.

Overall it is highly likely that some insoluble iron phosphate would have formed in the uptake solution. However, the majority of the iron would be ferrous iron, due to the presence of ascorbic acid, with a small percentage being in the form of micro- and nano-particulates. This would result in a lower concentration of iron being available to the Caco-

2 cell monolayers for uptake via DMT1, than the actual amount of $FeCl_2$ (50 μM) in the uptake solution.

Both hematin and inorganic iron adhere strongly to surfaces, including the outer membrane of cells (Mergler *et al*., 2012). In the experiments in this chapter after incubation with the iron source the cells were washed with PBS, rather than PBS-EDTA. This means it is highly likely that not all of the iron adhering to the outer cell membrane of monolayers would have been dislodged and washed away. This would mean that some of the iron present in the collected samples could be from iron associated with the outer membrane of the cells rather then that taken up by the Caco-2 cells. The cell samples were also collected in NaOH solution and therefore the entire cell, rather then just cell lysate was collected. This meant that the amount of iron detected within the samples was total iron associated with the Caco-2 cell monolayers rather then iron from only the cell lysate, and therefore only iron that had been taken up by the monolayers.

With the iron in the collected samples being both iron taken up by the cells and iron associated with the outside of the cell monolayers, the results could give a misleading representation of the amount of iron taken up by the monolayers. Because of the adherence properties of iron, and the washing steps in these experiments the iron detected in the basal medium of the Caco-2 cell monolayers gives a more accurate indication of how much iron had been taken up by the Caco-2 monolayers. This is because only iron exported out of the cells could be present in the basal medium, due to the formation of tight junctions between the cells in the Caco-2 cell monolayers, and the lack of any iron being present in the basal medium. The iron exported from the cells, into the basal medium, showed that although monolayers incubated with inorganic iron exported more then cells incubated with hematin this increase was not significant. The iron exported into the basal medium indicates that, contrary to the data on iron associated with Caco-2 cells, iron source did not significantly influence iron uptake into the Caco-2 cell monolayers, as there was no significant difference in the amount of iron effluxed from the cells.

The addition of 0.91 mM and 4.5 mM of glutathione or cysteine to the hematin uptake solution meant that up to 98% of hematin was in the form of GS.hematin and up to 42% was in the form of Cys.hematin. This ligation of hematin could account for the significant decrease in hematin associated with Caco-2 cells over 1 hour. The significant decrease in hematin association with the addition of 4.5 mM of arginine, histidine and glycine further

indicates that the ligation of hematin decreased the amount of hematin associated with the Caco-2 cells. This is in disagreement with previously published data on heme ligation by arginine (Sievers *et al.,* 1987). However in the aforementioned studies arginine was used to maintain heme in solution and thereby resulted in increased heme bioavailability and absorption. In the experiments described in this chapter hematin was maintained in a soluble bioavailable form in a potassium phosphate buffered phenol free medium. Hence these experiments investigated the effect of arginine on hematin association with Caco-2 cells rather than heme arginate absorption. This possibly accounts for the discrepancy between organic iron association observed in this chapter compared to previously published data.

Amino acids and small molecules have previously been shown to both increase and decrease inorganic iron absorption (Hallberg *et al.*, 1989; Rao & Rao, 1992; Glahn *et al.,* 1997; Petry *et al.,* 2014). The dominant factor for the difference in inorganic iron absorption in the presence of these additional nutrients was the affinity constant. Nutrients with high affinity for inorganic iron increase the solubility of iron; however the iron-ligand is not bioaccessible; whilst nutrients with low affinity for iron increase both bioavalibility and bioaccessibility.

The amount of GS.hematin associated with Caco-2 monolayers was found to be significantly less than that of hematin when incubated for 1 hour, both in unicameral and bicameral plates. However, the difference in hematin associated with Caco-2 monolayers decreased with an increase in incubation time. This finding implies that the rate of GS.hematin association is slower than that of hematin; however, GS.hematin did still associated with and get taken up by Caco-2 cells in the current study. Even though a mechanism of uptake of GS.hematin cannot be clearly deduced as yet from these experiments three hypotheses may be proposed. The first, that two separate uptake pathways are present in the cell, one for hematin and the other for ligand-hematin. The second hypothesis proposes that GS.hematin is taken up using the same pathway as hematin but less efficiently, due, likely, to the transformation of the planar, hydrophobic hematin molecule to the more globular, less hydrophobic GS.hematin. The final hypothesis proposes that glutathione dissociates from hematin before hematin uptake into Caco-2 cells. This hypothesis implies that the hematin receptor has a higher affinity for hematin than glutathione. This latter concept is conceivable as glutathione has an affinity constant

of 5 x 10^4 M^{-1} for hematin whilst the possible heme receptor has an affinity constant of 10^6 – 10^9 M^{-1} (Tenhunen *et al.,* 1980; Grasbeck *et al.,* 1982).

Previous studies on inorganic iron ligation and absorption in the presence of amino acids (Hallberg *et al.,* 1989; Glahn *et al.,* 1997) revealed that hematin absorption into Caco-2 cells follows a similar trend to that of inorganic iron. In that when hematin is in the form of hematin-ligand, uptake into Caco-2 monolayers decreases due to competition between the hematin receptor or transporter on the apical membrane of the Caco-2 cells and the hematin ligand within the medium.

The potential increase in cellular concentrations of glutathione, through pre-incubation with glutathione or acetylated cysteine, had no effect on hematin uptake or association with Caco-2 cell monolayers. This observation suggests, that similar to inorganic iron absorption, intracellular levels of glutathione have no effect on iron absorption (Simpson *et al.,* 1998).

The basal medium in bicameral chambers contained 12.5 μM of human apo-transferrin but no added hemopexin or albumin and the cells were only used once tight gap junctions had formed. Therefore the iron detected within the basal medium is most likely to be inorganic iron from catabolised organic iron that had been absorbed from the apical medium. Although the increase, over time, of inorganic iron present in the basal medium was not significant there was an appreciable increase nonetheless. This increase correlated with a significant increase in the amount of hematin associated with the Caco-2 cell monolayer. This suggests that enhanced association led to high organic iron catabolism by HO-1 and a concomitant export of the subsequent inorganic iron out of the basal medium.

3.5 Conclusions

For the detection of hematin uptake into, and association with, Caco-2 cell monolayers, [^{59}Fe]hematin was found to be more sensitive than iron quantification using the ferrozine assay.

The ligation of hematin by glutathione and various amino acids decreased hematin uptake into, and association with, Caco-2 cells over a 1 hour incubation period. This implies ligated hematin is less efficiently taken up and associated with Caco-2 cell monolayers than non-ligated hematin.

4. The Biochemical Properties of the Hematin-Glutathione Complex

4.1 Introduction

In chapters 2 and 3 evidence is presented to suggest that the cytosolic form heme is GS.hematin. In this chapter the influence of hydrogen peroxide (H_2O_2) and ascorbic acid (vitamin C) on the stability of the GS.hematin complex, the influence of glutathione on the inducible form of heme oxygenase (HO-1) and the ability, or otherwise, of glutathione to inhibit hematin partitioning into membranes is reported. By answering these questions the advantages of the formation of GS.hematin to cell viability will hopefully be explained.

Hydrogen peroxide (H_2O_2) is a strong oxidising agent found in the cytosol of cells and has been shown to degrade haemoproteins and heme, reviewed by, (Winterbourn *et al.,* 1976; Winterbourn, 1995; Nagababu & Rifkind, 2005). Chapter 2 showed that under physiological conditions hematin binds to glutathione, forming the GS.hematin complex. The stability of the GS.hematin complex in the presence of H_2O_2 was investigated in order to determine whether GS.hematin is more stable in the cytosol than hematin alone.

Hematin is a planar, hydrophobic molecule that quickly partitions into lipid bilayers where it redox cycles resulting in lipid peroxidation. It is unknown what effect the composition of the membrane has on hematin partitioning, or what affect glutathione has on hematin partitioning into membranes.

Due to the toxic effects of free organic iron, and the cell requirement for inorganic iron, hematin is quickly catabolised to inorganic iron, CO and biliverdin by the inducible enzyme heme oxygenase-1 (HO-1) in the presence of oxygen and NAPH, (Tenhunen *et al.,* 1968). It is known that HO-1 expression is induced by an increase in cellular hematin concentrations, (Ogawa *et al.,* 2001; Sun *et al.,* 2002), however it is not known what affect, if any, organic iron conjugates have on HO-1 expression.

Ascorbic acid is found within our cells and although it's concentration can vary depending on diet, on average cells have a concentration of 300 μM, (Diem & Lentner, 1970). Ascorbic acid is an antioxidant and reducing agent. It is well documented that ascorbic acid reduces inorganic ferric iron (Fe^{3+}) to ferrous iron (Fe^{2+}) (Elmagirbi, 2012), however its

effect on organic iron is less well understood and its effect on the GS.hematin complex is unknown.

This chapter aims to detect the GS.hematin complex within mammalian cells and show that the formation of the bulkier, and less hydrophobic GS.hematin complex is more stable than the labile hematin and therefore is the preferential form of labile organic iron in mammalian cells.

3.2 Materials and Methods

4.2.1 Reagents

Reagents were from Sigma Aldrich and reagent grade unless stated otherwise in Table 4-1

Table 4-1 Details on Reagents Used for Biochemical Experiments

Compound	**Specifications**	**Supplier**
Compounds		
Reduced glutathione	N/A	Santa Cruz Biotechnology
Oxidised glutathione	N/A	Santa Cruz Biotechnology
Ferrous Sulphate	$7H_2O$	Scientific Laboratory Suppliers
Potassium Chloride	≥ 99%	BDH laboratory supplies
di-Sodium hydrogen phosphate anhydrous	> 98%	Fluka Chemika
Sodium Hydroxide	Laboratory reagent grade	Fisher Scientific
L-Ascorbic Acid sodium salt	99%	Acros Organics
Cell Culture		
Caco-2 cells	Passage 15	American Type Culture Collection (ATCC)
Fetal bovine serum (Gibco)	Qualified	Fisher Scientific

4-1 Continued

Compound	Specifications	Supplier
Solvents		
Water	HPLC grade	Fisher Scientific
Chloroform	Analytical reagent grade	Fisher Scientific
Ethyl Acetate	Analytical reagent grade	Fisher Scientific
Hydrochloric Acid	37% in water	Acros Organics
Methanol	HPLC grade	Fisher Scientific
DMSO	≥ 99.7%	Fisher Scientific
Western Blot Reagents		
Heme Oxygenase-1 primary antibody	CST-70081	New England Biolabs
anti-rabbit secondary antibody	AP132P	Merck Millipore
anti-mouse secondary antibody	AP124P	Merck Millipore
Luminata Crescendo & Classico western HRP substrate	N/A	Merck Millipore
10x TRIS/Glycine/SDS		
10x TRIS/Glycine		
Milk powder	Electrophoresis grade	National Diagnostics
	Ultra pure grade	National Diagnostics
	Food grade	Marvel

4.2.2 Hematin and GS.hematin Stability in the Presence of Hydrogen Peroxide

Hematin was either dissolved in 10 mM phosphate buffer, 20 mM KCl, pH 8 or 10 mM phosphate buffer, 20 mM KCl, 2.04 mM glutathione, pH 8 to a final concentration of 10.2 μM and pH adjusted to pH 8 using 0.1 N NaOH. The solutions were vortexed for 10 minutes, centrifuged at 4,000 rpm for 10 minutes and supernatant transferred to Spectrosil® quartz cuvette with path length of 100 mm. This was repeated three times for each concentration of H_2O_2. H_2O_2 (1 mL) was added to the solutions to a final concentration of, 0 μM, 2 μM, 5 μM, 10 μM or 25 μM of H_2O_2, giving a final concentration of 10 μM hematin (2 mM glutathione if present) after the absorbance of the solution had been recorded.

4.2.2.1 Analysis of Hematin and GS.hematin Stability in the Presence of Hydrogen Peroxide

The absorbance of the hematin or GS.hematin in solution was measured between 575 nm and 700 nm at 1 nm intervals using PerkinElmer UV/Vis spectrophotometer Lambda 2 coupled with Lambda25 software. H_2O_2 (1 mL) was added to the solutions to give a final concentration of, 0 μM 2 μM, 5 μM, 10 μM or 25 μM, giving a final concentration of 10 μM hematin and 2 mM glutathione if present, and absorbance read every 5 minutes for 50 minutes. The average change in absorbance at 618 nm for hematin solutions, and 655 nm for GS.hematin solutions was plotted against time in GraphPad Prism with error bars of standard error of the mean (SEM). When error bars are shown but not visible SEM is smaller than the point. 2-way ANOVA in GraphPad Prism, with alpha set at 0.05, was used to determine if the change in absorption, for hematin and GS.hematin, from time point 0 was significant for each H_2O_2 concentration. 2-way ANOVA in GraphPad Prism, with alpha set at 0.05, was used to determine when degradation of hematin and GS.hematin had stopped. The change in absorbance at each time point was compared with the change in absorbance at the previous time point for each condition. If there was no statistically significant difference between the two time points it was assumed that no significant hematin or GS.hematin degradation had occurred.

4.2.3 Liposome Preparation and Partitioning

4.2.3.1 Phosphatidylcholine Liposome Preparation

Phosphatidylcholine from egg yolk (200 mg) was dissolved in 40 mL chloroform in a 250 mL round bottom flask. The mixture was reduced to dryness by rotary evaporation. 10 mM phosphate buffer (pH 8) and 150 mM KCl (40 mL) was added. Liposomes were incubated overnight at room temperature with shaking (25 rpm). The resulting liposomes were

centrifuged at 3,000 rpm for 5 minutes, supernatant aspirated and the liposomes were gently resuspended in 10 mM phosphate buffer (pH 8) and 150 mM KCl (10 mL). The liposomes were washed twice and finally the liposomes were resuspended in 10 mM phosphate buffer (pH 8) and 150 mM KCl (8 mL) and split equally between eight pre-weighed tubes, the liposomes were centrifuged at 3,000 rpm for 5 minutes, supernatant aspirated and tubes weighed to calculate the amount of lipid in each tube.

4.2.3.2 Phosphatidylcholine – Cholesterol Liposome Preparation

Phosphatidylcholine and cholesterol were dissolved in chloroform (40 mL) in a 250 mL round bottom flask in 1:1 molar ratio (125.2 mg phosphatidylcholine, 74.8 mg cholesterol). The mixture was reduced to dryness by rotary evaporation. 10 mM phosphate buffer (pH 8) and 150 mM KCl (40 mL) was added. Liposomes were incubated overnight at room temperature with shaking (25 rpm). The resulting liposomes were centrifuged at 3,000 rpm for 5 minutes, supernatant aspirated and the liposomes were gently resuspended in 10 mM phosphate buffer (pH 8) and 150 mM KCl (10 mL). The liposomes were washed twice and finally the liposomes were resuspended in 10 mM phosphate buffer (pH 8) and 150 mM KCl (8 mL) and split equally between eight pre-weighed tubes, the liposomes were centrifuged at 3,000 rpm for 5 minutes, supernatant aspirated and tubes weighed to calculate the amount of lipid in each tube.

4.2.3.3 Phosphatidylcholine – Cholesterol – Dicetyl Phosphate Liposome Preparation

Phosphatidylcholine, cholesterol and dicetyl phosphate were dissolved in a mix of chloroform (40 mL) and ethanol (20 mL) in a 250 mL round bottom flask in 2:2:1 molar ratio (59.2 mg phosphatidylcholine, 59.2 mg cholesterol, 41.8 mg dicetyl phosphate). The mixture was reduced to dryness by rotary evaporation. 10 mM phosphate buffer (pH 8) and 150 mM KCl (40 mL) was added and liposomes were incubated overnight at room temperature with shaking (25 rpm). The resulting liposomes were centrifuged at 3,000 rpm for 5 minutes, supernatant aspirated and the liposomes were gently resuspended in 10 mM phosphate buffer (pH 8) and 150 mM KCl (10 mL). The liposomes were washed twice and finally the liposomes were resuspended in 10 mM phosphate buffer (pH 8) and 150 mM KCl (8 mL) and split equally between eight pre-weighed tubes, the liposomes were centrifuged at 3,000 rpm for 5 minutes, supernatant aspirated and tubes weighed to calculate the amount of lipids in each tube.

4.2.3.4 Hematin and GS.hematin Solutions

Hemin was dissolved to a final concentration of 10 μM in 10 mM phosphate buffer (pH 8), 150 mM KCl or 10 mM phosphate buffer, 150 mM KCl, 2 mM glutathione, pH 8. The mixture was vortexed for 10 minutes, centrifuged at 4,000 rpm for 5 minutes and supernatant decanted. The solutions were made in triplicate.

4.2.3.5 Hematin and GS.hematin Incubation with Liposomes

The triplicate solutions of 10 mM phosphate buffer (pH 8) and 150 mM KCl, 10 μM hemin (20 mL) or 10 mM phosphate buffer (pH 8) and 150 mM KCl, 2 mM glutathione, 10 μM hemin (20 mL) were added to; 3x 42-52 mg phosphatidylcholine liposomes, 3x 105-120 mg phosphatidylcholine-cholesterol liposome or 3x 22-38 mg phosphatidylcholine-cholesterol-dicetyl phosphate liposomes, and incubated in a water bath at 37 ^{o}C with shaking (225 rpm). Aliquots (4 mL) were taken after 15 minutes, 1 hour, 2 hours and 4 hours of incubation. The aliquots were centrifuged at 4,000 rpm for 10 minutes, and supernatant discarded. The pellets were dissolved in DMSO (1.5 mL) by shaking (70 rpm) overnight. The resulting solution was centrifuged at 4,000 rpm for 10 minutes, supernatant aspirated and kept for measurement. The absorbance of the supernatant was recorded at 416 nm using a 1 cm quartz cuvette.

4.2.3.6 Analysis of Hematin and GS.hematin Partitioned into Liposomes

Varying concentrations of hemin (0-12.5 μM) were dissolved in DMSO and absorbance at 416 nm recorded in 1 cm quartz cuvette on UV/Vis spectrometer Lambda 2 (Perkin Elmer). Absorbance at 416 nm was plotted against hemin concentration (μM) and linear best fit was calculated for hemin concentration against absorbance at 416 nm in GraphPad Prism. Hematin in the liposome pellet dissolved in DMSO was calculated using a standard curve. The average amount of hematin in the liposome pellet (μg hematin/mg liposome) was plotted against time using GraphPad Prism with error bars of standard error of the mean (SEM). Where error bars are shown but not visible SEM is smaller than the point. The 2-way ANOVA in GraphPad Prism, with alpha set at 0.05, was used to determine if there was a significant difference in the amount of hematin in each liposome at each time point between the two conditions (hematin vs. GS.hematin).

4.2.4 Hematin and GS.hematin Partitioning into Erythrocytes

4.2.4.1 Erythrocyte Extraction and Preparation

Whole blood, containing 10% (v/v) acid citrate dextrose was centrifuged at 4°C at 1,000 *xg* for 10 minutes. The plasma was aspirated and discarded. The packed erythrocytes were washed twice with two times their volume of washing buffer (Tris-HCl 20 mM, pH 7.4, NaCl 130 mM). Cells were diluted to a concentration of 2.34×10^9 cells/mL in washing buffer and kept at 4°C until required. Cells were used within three days of being harvested.

4.2.4.2 Hematin and GS.hematin Partitioning into Erythrocytes

The protocol was adapted from Hider *et al.* (1990). Reduced glutathione was dissolved in each buffering solution (Table 4-2) to a final concentration of 2.4 mM and adjusted to pH 8 with 0.1 N NaOH. [^{59}Fe]hematin in DMSO in buffer (5 mL) or buffer containing 2.4 mM glutathione (5 mL) (Table 4-2), was incubated in a water bath at 37 °C for 10 minutes. Packed erythrocytes were added to give a final concentration of 3.9×10^8 cells/mL, 2 mM glutathione and 1 μM [^{59}Fe]hematin. The solution was incubated in a shaking (180 rpm) water bath at 37 °C, and aliquots (0.5 mL) taken at 1, 3, 5, 10, 15 and 30 minutes. The aliquots were immediately centrifuged at 14,000 rpm for 1 minute and the supernatant transferred to a 1.5 mL Eppendorf tubes. The pellets were washed in buffering solution (0.5 mL) (Table 4-2) centrifuged at 14,000 rpm for 2 minutes; the supernatant was aspirated and added to the initial supernatant. The supernatant and pellets were kept at 4°C until counted with the gamma counter. Percentage of [^{59}Fe]hematin in erythrocyte pellet was calculated from CPM data of pellet and supernatant of each sample, (Equation 4-1). The average percentage of [^{59}Fe]hematin in the erythrocyte pellet, for each buffering solution, was plotted against time using GraphPad Prism with error bars of standard error of the mean (SEM). Where error bars are shown but not visible SEM is smaller than the point. The 2-way ANOVA in GraphPad Prism, with alpha set at 0.05, was used to determine if the percentage of [^{59}Fe]hematin in each erythrocyte sample, at each time point, was significantly different between the two conditions (hematin vs. GS.hematin).

$$\text{Percentage of } [^{59}\text{Fe}]\text{hematin in erythrocytes} = \left[\frac{\text{CPM in erythrocytes}}{\text{CPM in supernatant}}\right] \times 100$$

Equation 4-1

Table 4-2 Buffer Solutions for Erythrocyte Incubation				
Buffering Solution	Phosphate buffer (pH)	NaCl (mM)	KCl (mM)	Glutathione (mM)
1a	7.4	130	0	0
2	7.4	130	0	2
3	8	130	0	0
4	8	130	0	2
5	7.4	0	130	0
6	7.4	0	130	2
7	8	0	150	0
8	8	0	150	2

4.2.5 Hematin, GS.hematin Separation from Caco-2 Cell Lysate Using Size Exclusion HPLC

4.2.5.1 Preparation of Caco-2 Cells

The experiment was performed in triplicate, with each repeat carried out on separate days using cells from different passage numbers (passage number 40-50). Caco-2 cells were seeded in 6-well transwell plates (6-well transwell, clear polyester membrane, 24 mm, 0.4 mm, Corning, New York, USA), in Dulbecco's Modified Eagle Medium (DMEM) with high glucose (4,500 mg/L), supplemented with 10% (v/v) fetal bovine serum (FBS), 1% (v/v) penicillin-streptomycin solution, 1% (v/v) non-essential amino acid solution and 1% (v/v) L-glutamine solution. The medium (2 mL) was placed in both the basal and apical chamber. Cells were cultured at 37 ^{o}C in an incubator with 5% CO_2 and 95% air atmosphere. Microscopic examination of cultures revealed that confluence was reached 3-4 days post seeding. The medium in the apical and basal chamber was changed every 2-3 days and uptake experiments were conducted 14-21 days after seeding. Once cells had been seeded for 14 days the transepithelial electrical resistance (TEER) of each monolayer was measured with Millicell®-ers (Millipore) every two days until it reached a minimum of 250 Ωcm^2. Once the TEER resistance had reached 250 Ωcm^2, cells were used for experimentation. The

medium was removed from the apical and basal chambers and both chambers washed once with minimum essential medium Eagle (MEM). MEM was added to the apical and basal chamber and the cells were cultured for 16 hours at 37 ^{o}C, under a 5% CO_2, 95% air atmosphere, in order to deplete iron stores within the cells.

4.2.5.2 Formulation of Uptake Solutions

Cell culture medium, Minimum Essential Medium Eagle Modified (phenol-free MEM), was made up as directed in sterile Milli-Q water, supplemented with 3.7 g/L sodium bicarbonate, adjusted to pH 7.4 with 1 N NaOH and 1 N HCl and filter-sterilised through a 0.22-µM filter.

Stock solution of glutathione (20 mM), cysteine (6.7 mM) and ascorbic acid (9 mM) were prepared in 200 mM potassium phosphate buffer (pH 8) and adjusted to pH 8 with 0.1 N NaOH. Pre-incubation solutions in MEM contained 2 mM glutathione or 670 µM N-acetul-L-cysteine or no further component.

Hematin uptake solutions in phenol-free MEM supplemented with a final concentration of 66.7 mM potassium phosphate buffer contained 50 µM [^{59}Fe]hematin in DMSO and either 2 mM glutathione or no added ligand. Human apo-transferrin was dissolved in phenol-free MEM to a final concentration of 12.5 µM for the basal media. All stock, pre-incubation, uptake solutions and basal medium were prepared immediately prior to use and filter-sterilised through 0.22-µM filters.

4.2.5.3 [^{59}Fe] Hematin Incubation

Minimum Essential Medium was aspirated from each after 16 hours and monolayers were washed once with phenol-free MEM. Pre-incubation solution (0.5 mL) containing 2 mM glutathione or 670 µM N-acteyl-L-cysteine or medium alone, were added to each monolayer and MEM (2 mL) was added to the basal chamber of each well (Figure 4-1). Cells were cultured for 1 hour at 37 ^{o}C, under a 5% CO_2, 95% air atmosphere. After 1 hour all medium was removed from apical and basal chambers and both were rinsed twice with phenol-free MEM. Basal medium (1.6 mL) was added to each basal chamber. The apical chambers pre-incubated with glutathione or cysteine had hematin uptake solution (1 mL) added. The wells pre-incubated with medium alone either had hematin uptake solution (1 mL) or hematin-glutathione uptake solution (1 mL) added (Figure 4-1). Cells were cultured for 24 hours at 37 ^{o}C, under a 5% CO_2, 95% air atmosphere. Apical medium was aspirated and transferred to 1.5 mL Eppendorf tubes. Basal medium was aspirated and transferred

to 1.5 mL Eppendorf tubes for counting. Cell monolayers were washed twice with ice cold PBS (150 µL), the wash added to the aspirated apical medium and the solution counted for [^{59}Fe]hematin. Cells were lysed in lysis buffer (100 µL) (50 mM Tris base (pH 6.8), 10% (v/v) glycerol, 2% (v/v) SDS), diluted in HPLC grade water (300 µL) (1/4 lysis buffer) and an aliquot (100 µL) taken for counting of [^{59}Fe]hematin.

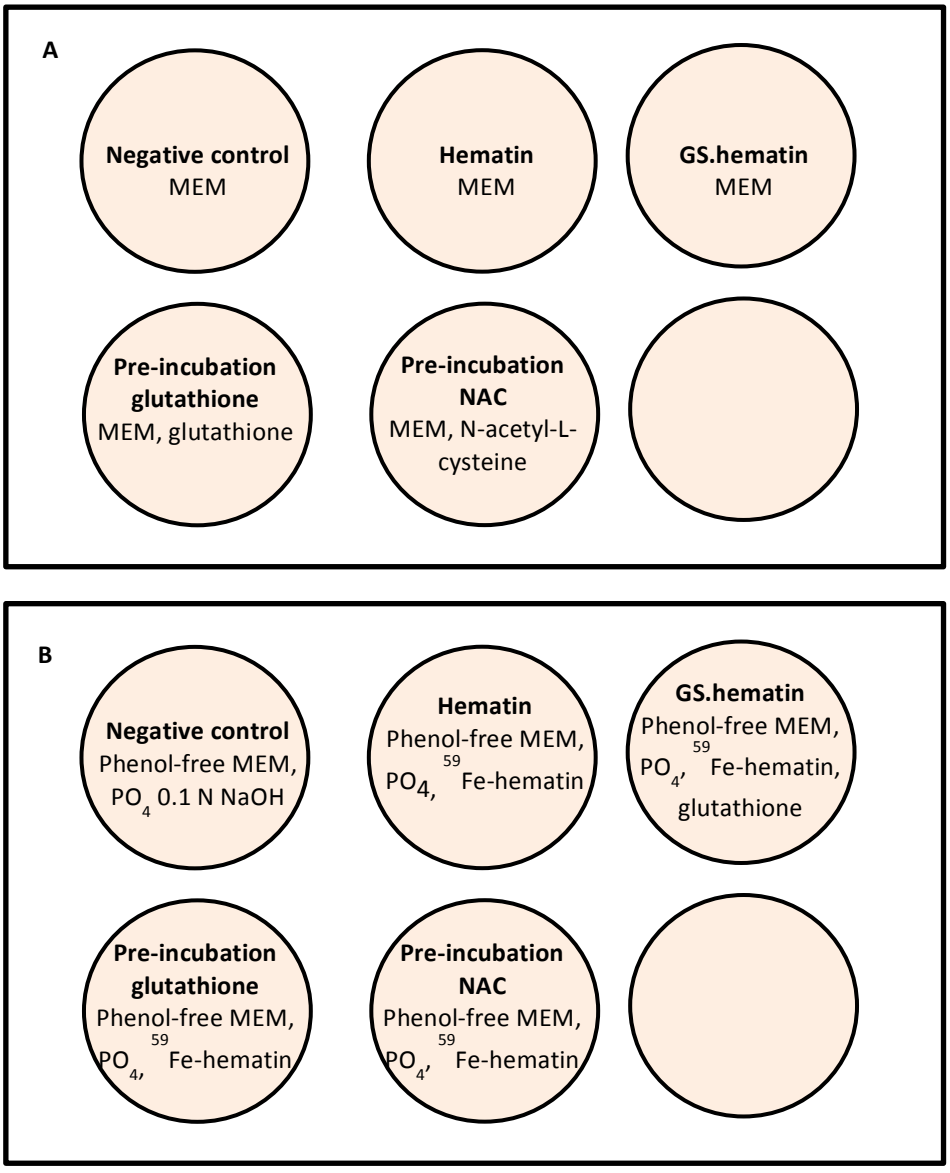

Figure 4-1. Schematic of supplementations for each Caco-2 cell absorption condition. **A** – Plate layout of solutions used to pre-incubate Caco-2 cell monolayers in unicameral experiments, **B** – Plate layout of solutions used for hematin absorption, after pre-incubation, into Caco-2 cell monolayers.

The protein concentration of the cell lysate was determined using BioRad DC Protein Assay Kit. Solution S (40 µL) was added to solution A (2 mL), forming solution X. Cell lysate was diluted one in four in ddH_2O, and added (40 µL) to solution X (40 µL), solution B (320 µL) was added to the lysate-solution X mix and left to incubate at room temperature for 10 minutes. The protein assay solution (100 µL) was plated in triplicate in a 96-well plate and absorbance read at 750 nm on a spectrophotometric plate reader (Bio-Tek ELx800 plate reader). Standards using BSA dissolved in water were run and a standard curve drawn with lineal regression drawn in GraphPad Prism. The average absorbance for each sample and the protein standard curve was used to determine the amount of protein in each sample.

4.2.5.3 Analysis of [^{59}Fe]hematin Absorption

The amount of hematin absorbed into the cells, exported into the basal medium and absorbed in total (lysate + basal media) was calculated using equations 4-2 – 4-6.

$$\text{Total CPM} = \text{CPM of supernatant} + (\text{CPM of lysate}) \times 4 + \text{CPM of basal medium}$$

Equation 4-2

$$\text{Hematin in Caco-2 cell monolayer (M)} = \left[\frac{(50 / 1{,}000{,}000)}{\text{Total CPM}}\right] \text{X } (\text{CPM of supernatant}) \text{ x } 4$$

Equation 4-3

$$\text{Hematin exported from Caco-2 monolayer (M)} = \left[\frac{(50 / 1{,}000{,}000)}{\text{Total CPM}}\right] \text{X } (\text{CPM of basal medium})$$

Equation 4-4

$$\text{Total hematin absorbed (M)} = \text{hematin in cell monolayer} + \text{hematin in basal medium}$$

Equation 4-5

$$\text{Hematin (pmol)} = (\text{hematin (M) X volume (L)}) \text{ X } 1{,}000{,}000{,}000{,}000$$

Equation 4-6

The average amount of hematin in the cell monolayer, the basal medium and absorbed in total, for each condition was standardised to the amount of protein present in each sample. The amount of hematin (pmol) absorbed standardised to protein content (µg) was plotted against the condition using GraphPad Prism with error bars of standard error of the mean (SEM). The CPM of the negative control was subtracted from the CPM of the samples to correct for the background of radioactivity of the gamma counter.

4.2.5.4 HPLC of Caco-2 Cell Lysate and Controls

A Waters 626 HPLC system (comprising of; Waters 717 plus auto sampler, Waters 600S controller and Waters 626 pump) coupled with a Waters 2996 photodiode array detector and Milennium[32] computer software. Photodiode array detector was set to scan between 230 nm and 500 nm.

Cell lysate (200 µL) (for all samples except cells incubated with $FeCl_2$) were centrifuged at 14,000 rpm for 10 minutes; supernatant decanted into HPLC insert vial and sonicated for 5 minutes. Cell lysate (100 µL) was injected into the HPLC system, eluted on Agilent PL-aquagel-OH 20 5 µM 300 x 7.5 mm column (Agilent, Stockport, UK) at room temperature with mobile phase of 20 mM phosphate buffer, 2 mM glutathione, pH 8 at a flow rate of 0.4 mL/min for 30 minutes. 1 minute fractions were collected between 10 minutes and 30 minutes and counted for [^{59}Fe]hematin.

Hematin (600 µM) spiked with [^{59}Fe]hematin was dissolved in 200 mM phosphate buffer and 20 mM KCl, pH 8 or 200 mM phosphate buffer, 20 mM KCl and 15 mM GSH, pH 8, was incubated at 37 ^{o}C, under a 5% CO_2, 95% air atmosphere for 24 hours. Hematin solution (100 µL) was diluted into 16.6 mM Tris-HCl, 3.3% (v/v) glycerol, 0.7% (v/v) SDS to a final concentration of 150 µM hematin, 50 mM phosphate buffer, 5 mM KCl, 12.5 mM Tris-HCl, 2.5% (v/v) glycerol, 0.5% (v/v) SDS. GS.hematin (100 µL) solution was diluted into 16.6 mM Tris-HCl, 3.3% (v/v) glycerol, 0.7% (v/v) SDS, 15 mM glutathione to a final concentration of 150 µM hematin, 50 mM phosphate buffer, 5 mM KCl, 12.5 mM Tris-HCl, 2.5% (v/v) glycerol, 0.5% (v/v) SDS and 15 mM glutathione. The samples were centrifuged at 14,000 rpm for 10 minutes, supernatant decanted into HPLC insert vial and sonicated for 5 minutes. The controls were injected (100 µL) into the HPLC system, eluted on Agilent PL-aquagel-OH 20 5 µM 300 x 7.5 mm column (Agilent, Stockport, UK) at room temperature with mobile phase of 20 mM phosphate buffer, 2 mM glutathione, pH 8 at a flow rate of 0.4 mL/min for 30 minutes. 1 minute fractions were collected between 10 minutes and 30 minutes and counted for [^{59}Fe]hematin.

The CPM for the negative control fractions were subtracted from the fractions of each sample to correct for background radioactivity of the gamma counter. The percentage of CPM eluted per minute for each sample was calculated from the total CPM eluted per sample. The average percentage of CPM eluted per minute for each condition was plotted against elution time using GraphPad Prism with error bars of standard error of the mean (SEM).

4.2.6 Western Blot for Heme Oxygenase-1 Protein

To determine if glutathione interfered with the rate of hematin catabolism by HO-1 a cell free experiment, based on the method developed by Reed *et al.* 2010, was tried. The results from these experiments were inconclusive and not reproducible therefore a Western Blot of HO-1 expression was done instead.

4.2.6.1 Preparation of Caco-2 Cells

Caco-2 cells were used in experiments at passages 40-50. Stock cell cultures were maintained at pH 7.4 in DMEM with high glucose (4,500 mg/L), supplemented with 10% (v/v) fetal bovine serum (FBS), 1% (v/v) penicillin-streptomycin solution, 1% (v/v) non-essential amino acid solution and 1% (v/v) L-glutamine solution. The cells were cultured at 37 ^{o}C, under a 5% CO_2 and 95% air atmosphere. For experiments cells were seeded in 6-well plates, microscopic examination of cultures revealed that confluence was reached 3-4 days post seeding onto plates. Medium was changed every 2-3 days and uptake experiments were conducted 15 days after seeding.

4.2.6.2 Formulation of Uptake Solutions

Cell culture medium, Minimum Essential Medium Eagle Modified (phenol-free MEM), was made up as directed in sterile Milli-Q water, supplemented with 3.7 g/L sodium bicarbonate, adjusted to pH 7.4 with 1 N NaOH and 1 N HCl and filter-sterilised through a 0.22-µM filter.

Stock solution of hemin (2.5 mM) was made in 0.1 N NaOH, immediately prior to use. Stock solutions of glutathione (20 mM) and N-acetyl-L-cysteine (6.7 mM) were made in 200 mM potassium phosphate buffer (pH 8) and adjusted to pH 8 with 0.1 N NaOH. Pre-incubation solutions in MEM contained glutathione (2 mM) or N-acetyl-L-cysteine (670 µM) or no further components. Hematin uptake solutions in phenol-free MEM supplemented with a final concentration of 66.7 mM potassium phosphate buffer contained 25 µM hemin, [^{59}Fe]hematin in DMSO and either glutathione (2 mM) or no further components. Approximately 0.58 KBq [^{59}Fe]hematin was used per mL of uptake solution. All stock, pre-incubation and uptake solutions were prepared immediately prior to use and filter-sterilised through 0.22-µM filters.

4.2.6.3 Hematin and $FeCl_2$ Incubation

Fifteen days after initial seeding growth medium was aspirated from each well and monolayers were washed twice with phenol-free MEM. Pre-incubation solution (1 mL)

either containing glutathione (2 mM) or N-acetyl-L-cysteine (670 µM) or medium alone was added to each well (Figure 4-1). Cells were cultured for 1 hour at 37 ^{o}C, under a 5% CO_2, 95% air atmosphere. After 1 hour pre-incubation medium was removed from wells and monolayers were rinsed twice with phenol-free MEM. Wells pre-cultured with glutathione or N-acetyl-L-cysteine had hematin uptake solution (1 mL) added (Figure 4-1). The wells pre-cultured with MEM alone either had hematin uptake solution (1 mL) or hematin-glutathione uptake solution (1 mL) added (Figure 4-1). Cells were cultured for 12 hours at 37 ^{o}C, under a 5% CO_2, 95% air atmosphere. Supernatant was aspirated and transferred to 1.5 mL Eppendorf tubes. Cell monolayers were washed twice with ice cold PBS (200 µL), the wash added to the aspirated medium and the solution counted for [^{59}Fe]hematin. Cells were lysed with lysis buffer (150 µL) (50 mM Tris-HCl, 10% glycerol, 2% SDS, 0.2% protein inhibitor cocktail), cultured on ice for 10 minutes and lysate collected. Lysate (50 µL) was transferred to a 1.5 mL Eppendorf tubes for [^{59}Fe]hematin counting. Hematin uptake was defined as hematin accumulated in cells (ng) standardised to protein content of sample (µg) over 12 hours.

Protein concentration of the cell lysate was determined using the BioRad DC Protein Assay Kit. Solution S (40 µL) was added to solution A (2 mL), forming solution X. Cell lysate was diluted one in eight in ddH_2O and added (40 µL) to solution X (40 µL). Solution B (320 µL) was added to the lysate-solution X mix and left to incubate at room temperature for 10 minutes. The protein assay solution (100 µL) was plated in triplicate in a 96-well plate and absorbance read at 750 nm on a spectrophotometric plate reader (Bio-Tek ELx800 plate reader). Standards using BSA dissolved in water were run and a standard curve drawn with lineal regression drawn in GraphPad Prism. The average absorbance for each sample and the protein standard curve was used to determine the amount of protein in each sample.

The amount of hematin absorbed per sample was calculated, expressed as amount of hematin (ng) standardised to protein content (µg) of each sample and the average plotted against experimental condition in GraphPad Prism with error bars of standard error of the mean (SEM).

4.2.6.3 Western Blot of Caco-2 Cell Lysate for HO-1 and β-actin

Cell lysate (40 µg) was heated at 95^{o}C for 5 minutes. 2-mercaptoethanol 10% (v/v) in bromophenol blue was added to samples to a final concentration of 2% (v/v) and the mix heated for 5 minutes at 95^{o}C. Denatured cell lysates were loaded onto a 12% SDS-PAGE gel and separated using electrophoresis at 150 V for 70 minutes, 1x electrophoresis buffer

(1/10 dilution of 10x TRIS/glycine/SDS in ddH_2O), 25 mM Tris (pH 8.3), 192 mM glycine, 0.1% (v/v) SDS in ddH_2O). The protein was electro-transferred onto polyvinylidene difluoride membranes using 1x transfer buffer (1/10 dilution of TRIS/glycine in ddH_2O), 25 mM Tris (pH 8.3), 192 mM glycine, 20% (v/v) methanol in ddH_2O) at 20 V for 2 hours. Membranes were blocked with 5% milk in PBS/0.1% Tween for 1 hour at room temperature at 75 rpm.

Membranes were washed 3x 5 minutes in PBS/0.1% Tween and incubated in anti-Heme Oxygenase-1 primary antibody, diluted 1:1,000 in 3% BSA (w/v) with sodium azide in PBS/0.1% (v/v) Tween, overnight at 4^{o}C, 75 rpm. Afterwards, membranes were washed 3x 5 minutes in PBS/0.1% (v/v) Tween and incubated in anti-rabbit secondary antibody, at 1:2,000 dilution in 3% milk, PBS/0.1% (v/v) Tween. Membranes were washed 3x 5 minutes in PBS/0.1% (v/v) Tween. Luminata Crescendo western HRP substrate was pipetted onto membrane and incubated for 1 minute. Membrane was exposed for 5 minutes and images captured for 20 minutes using G:Box Syngene in conjunction with GeneSnap computer software. Afterwards, HO-1 visualised membranes were washed 3x 5 minutes in PBS/0.1% (v/v) Tween and incubated in anti-β-actin primary antibody, diluted 1:15,000 in 3% BSA (w/v) with sodium azide in PBS/0.1% (v/v) Tween for 1 hour at room temperature, 75 rpm. Membranes were washed 3x 5 minutes in PBS/0.1% (v/v) Tween and incubated in anti-mouse secondary antibody, diluted 1:2,000 in 3% milk in PBS/0.1% (v/v) Tween at room temperature for 2 hours, 75 rpm. Membranes were washed 3x 5 minutes in PBS/0.1% (v/v) Tween. Luminata Classico western HPR substrate was pipetted onto the membrane, incubated for 20 seconds and exposed for 5 seconds with images captured for 25 seconds using G:Box Syngene in conjunction with GeneSnap computer software.

Immunoblot images were analysed using ImageJ, HO-1 protein expression, standardised to β -actin, in each sample was calculated. Expression of HO-1 protein standardised to β-actin and amount (ng) of hematin absorbed into 40 µg cell protein was calculated. The average expression of standardised HO-1 was plotted in GraphPad Prism with error bars of standard error of the mean (SEM).

4.2.6.4 Experimental Design

The experiment was performed in triplicate, with replicates using cells from different passage numbers and done on separate days. Each experimental treatment was performed in duplicate for each replication of the experiment. The duplicates of each

replicate were averaged and the resulting meane of each replicate was used for statistical analysis.

4.2.7 Hematin and GS.hematin Stability in the Presence of Ascorbic Acid

4.2.7.1 Hematin and GS.hematin in the Presence of Ascorbic Acid and Air

Hematin was either dissolved in 10 mM phosphate buffer and 20 mM KCl, pH 8 or 10 mM phosphate buffer, 20 mM KCl and 2.04 mM glutathione, pH 8 to a final concentration of 10.2 μM or 1.02 μM and pH adjusted to 8 using 0.1 N NaOH. The solution was vortexed for 10 minutes, centrifuged at 4,000 rpm for 10 minutes and supernatant transferred to Spectrosil® quartz cuvette with path length of 100 mm. This was repeated three times for each concentration of H_2O_2 and hematin. Ascorbic acid (1 mL) was added to a final concentration of, 0 μM, 100 μM (10 μM hematin only) or 300 μM once the absorbance of the solution had been recorded.

4.2.7.2 Hematin and GS.hematin in the Presence of Ascorbic Acid in 5% Oxygen

Hematin was dissolved in 50 mM phosphate buffer and 20 mM KCl, pH 8 or 50 mM phosphate buffer, 20 mM KCl and 2 mM glutathione, pH 8 to a final concentration of 10.2 μM and pH adjusted to 8 with 0.1 N NaOH. The solutions were vortexed for 10 minutes, centrifuged at 4,000 rpm for 10 minutes and supernatant decanted. 5% oxygen, 5% carbon dioxide, 90% nitrogen was bubbled through the mix for 15 minutes and the cuvette sealed. This was repeated in triplicate for each concentration of ascorbic acid. 5% oxygen, 5% carbon dioxide, 90% nitrogen was bubbled through the stock solution of ascorbic acid for 15 minutes and the Falcon tube sealed. Once absorbance of the solutions was recorded, ascorbic acid (1 mL), to a final concentration of 0 μM, 100 μM or 300 μM, was added to the solution and the cuvette resealed.

4.2.7.3 Hematin and GS.hematin in the Presence of Ascorbic Acid in 100% Nitrogen

Hematin was dissolved in buffer containing glutathione as described in section 3.2.3.1, nitrogen was bubbled through the solutions for 15 minutes and the cuvette sealed, repeated in triplicate. Nitrogen was bubbled through the stock solution of ascorbic acid for 15 minutes and the Falcon tube sealed. Once absorbance of the solutions was recorded, ascorbic acid (1 mL) to a final concentration of 300 μM was added to the solution and the cuvette resealed.

4.2.7.4 Analysis of Hematin and GS.hematin Solutions in the Presence of Ascorbic Acid

The absorbance of the hematin or GS.hematin in solutions, (containing air, 5% oxygen or 100% nitrogen), was measured between 575 nm and 700 nm at 1 nm intervals using PerkinElmer UV/Vis spectrophotometer Lambda 2 coupled with Lambda25 software. Ascorbic acid (1 mL) (either in air, 5% oxygen or 100% nitrogen) was added to the solutions, and the cuvette resealed, to give a final concentration of, 0 μM, 100 μM or 300 μM once the absorbance of the solution had been recorded. The absorbance of the solutions containing ascorbic acid was measured as previously stated every 5 minutes for 60 minutes. The concentration of hematin and glutathione were 10 μM and 2 mM respectively once ascorbic acid (1 mL) was added. The average change in absorbance at 618 nm for the hematin solutions, and 655 nm for the GS.hematin solutions was plotted against time in GraphPad Prism with error bars of standard error of the mean (SEM), for each condition. Where error bars are shown but not visible SEM is smaller than the point. 2-way ANOVA in GraphPad Prism, with alpha set at 0.05, was used to determine if the change in absorption from time point 0 was significant for each condition. 2-way ANOVA in GraphPad Prism, with alpha set at 0.05, was used to determine when degradation of hematin/GS.hematin had stopped. The change in absorbance at each time point was compared with the change in absorbance at the previous time point for each condition. If there was no statistically significant difference between the two time points no significant hematin or GS.hematin degradation had occurred.

4.3 Results and Discussion

4.3.1 GS.hematin Stability in the Presence of Hydrogen Peroxide

Hydrogen peroxide is the simplest peroxide and formed as a by-product of various cellular reactions. It is a strong oxidising agent, which reacts with labile iron producing reactive oxygen species (ROS) through Fenton reactions. Glutathione is known to reduce H_2O_2 to water within the cell, through the enzyme glutathione peroxidase, therefore decreasing H_2O_2 cytosolic concentrations however H_2O_2 is still present in trace amounts. The stability of the GS.hematin complex in the presence of trace amounts of H_2O_2 is currently unknown.

4.3.1.1 Absorption Spectrum of Hematin and GS.hematin in the Presence of Hydrogen Peroxide

The degradation of hematin and GS.hematin by H_2O_2 was followed through spectroscopy, with the change in absorption over time calculated by deducting the absorption of the solution at time point 0 minutes (before H_2O_2 was added) from the absorption of the solution at 5 minute intervals.

Hematin (10 μM) in solution has an absorbance peak at 618 nm that over time in the presence of H_2O_2 disappears, (Figure 4-2). 50 minutes after the addition of H_2O_2 (10 μM) to hematin there is a decrease in absorption between 500 nm and 550 nm and 580 nm and 640 nm, and an increase in absorption between 640 nm and 700 nm, resulting in the disappearance of the peak at 618 nm (Figure 4-2). The disappearance of the peak at 618 nm means the hematin is being degraded by H_2O_2. Hematin in the presence of glutathione has two absorption peaks; at 550 nm and 655 nm, that in the presence of H_2O_2 over time remain constant, meaning GS.hematin complex is not degraded or reduced by H_2O_2 (Figure 4-3). There is a slight change in absorption between 560 nm and 660 nm when H_2O_2 is added to a solution containing GS.hematin with the largest change in absorption occurring at 601 nm (Figure 4-3).

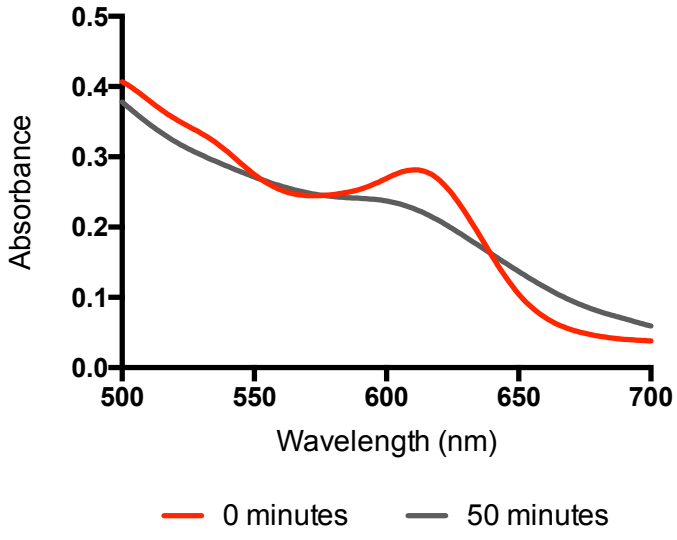

Figure 4-2. Absorption spectrum of 10 µM hematin in the presence of 10 µM H_2O_2, over 50 minutes. Hematin was dissolved, to a final concentration of 10 µM, in 10 mM phosphate buffer, 20 mM KCl, pH 8 and an initial absorption reading between 500 nm and 700 nm was taken (red line, 0 minutes), prior to the addition of 10 µM H_2O_2 after which absorption readings were taken every 5 minutes, (only 50 minute absorption reading shown, grey line). The initial solution had an absorption peak at 618 nm that diminished over time once H_2O_2 was added to the solution.

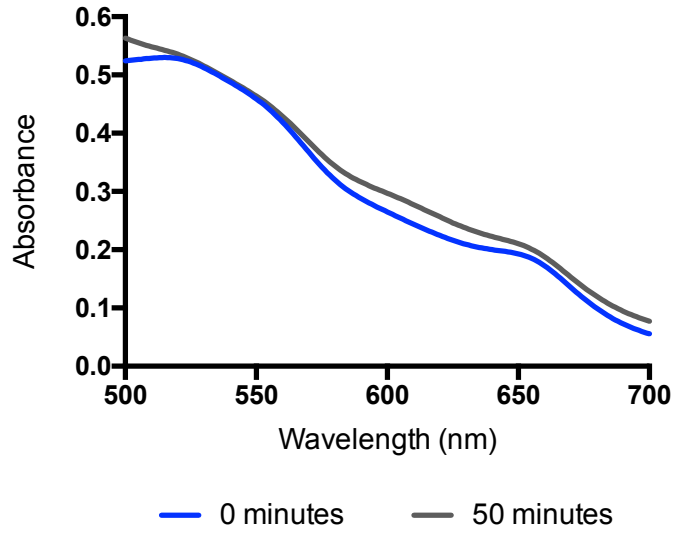

Figure 4-3. Absorption spectrum of 10 µM GS.hematin in the presence of 10 µM H_2O_2, over 50 minutes. Hematin was dissolved, to a final concentration of 10 µM, in 10 mM phosphate buffer, 20 mM KCl, 2 mM glutathione, pH 8 and an initial absorption reading between 500 nm and 700 nm was taken (blue line, 0 minutes), prior to the addition of 10 µM H_2O_2 after which absorption readings were taken every 5 minutes, (only 50 minute absorption reading shown, grey line). A slight change in the absorption spectrum occurs after the addition of 10 µM H_2O_2 with the greatest change occurring at 601 nm.

The solution of hematin (10 μM) and glutathione (2 mM) could contain up to 1% unbound hematin, due to the affinity constant of hematin and glutathione at pH 8, which could account for the slight increase seen in absorption at 655 nm, (Figure 4-3). The degradation of GS.hematin by H_2O_2 was followed at 601 nm, as this was the wavelength where the largest change of absorption occurred when 2 – 25 μM H_2O_2 was added to the solution, at concentrations of H_2O_2 higher than 25 μM the largest change in absorption occurred at 550 nm (data not shown). The degradation of hematin by H_2O_2 was followed at 618 nm, the wavelength where the largest change of absorption occurred.

4.3.1.2 Hematin and GS.hematin Degradation by Hydrogen Peroxide

The change in absorbance over time of hematin and GS.hematin in the presence of varying concentrations of H_2O_2 indicated that both hematin and GS.hematin were relatively stable in the presence of 2 μM H_2O_2, over 50 minutes, (Figure 4-4).

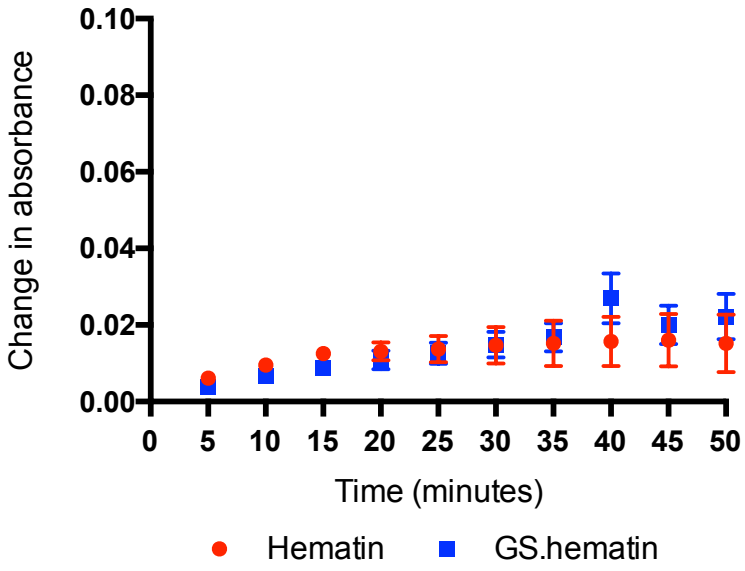

Figure 4-4. Degradation of hematin and GS.hematin over time by 2 μM H_2O_2. Hematin (10 μM) or GS.hematin (10 μM hematin, 2 mM glutathione) was dissolved in 10 mM phosphate buffer, 20 mM KCl, pH 8 and absorbance recorded at 601 nm (GS.hematin) and 618 nm (hematin), time point 0 minutes. H_2O_2 was added to a final concentration of 2 μM and absorbance at 601 nm (GS.hematin) and 618 nm (hematin) taken at 5 minute intervals, for 50 minutes. Change in absorbance from time point 0 was plotted against time. Red circles indicate change in absorbance at 618 nm, from time point 0, for hematin solution containing 2 μM H_2O_2; blue squares indicate change in absorbance at 601 nm, from time point 0, for GS.hematin solution containing 2 μM H_2O_2. There was no significant change in absorbance, therefore no significant degradation of either hematin or GS.hematin. Values are means ± SEM (n=3). Where error bars are not visible they are smaller than the point.

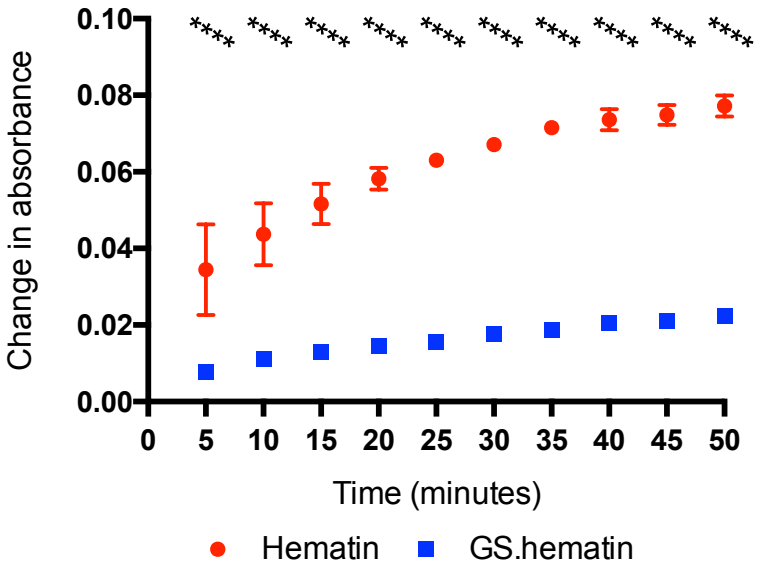

Figure 4-5. Degradation of hematin and GS.hematin over time by 5 μM H_2O_2. Hematin (10 μM) or GS.hematin (10 μM hematin, 2 mM glutathione) was dissolved in 10 mM phosphate buffer, 20 mM KCl, pH 8 and absorbance recorded at 601 nm (GS.hematin) and 618 nm (hematin), time point 0 minutes. H_2O_2 was added to a final concentration of 5 μM and absorbance at 601 nm (GS.hematin) and 618 nm (hematin) taken at 5 minute intervals, for 50 minutes. Change in absorbance from time point 0 was plotted against time. Red circles indicate change in absorbance at 618 nm, from time point 0, for hematin solution containing 5 μM H_2O_2; blue squares indicate change in absorbance at 601 nm, from time point 0, for GS.hematin solution containing 5 μM H_2O_2. Values are means ± SEM (n=3). Asterisks indicate significant difference ($P < 0.0001$ ****) in change in absorbance hematin vs. GS.hematin at individual time points. Where error bars are not visible they are smaller than the point.

In the presence of 5 μM H_2O_2, hematin was significantly degraded ($P < 0.0001$) within the first 5 minutes. Degradation of hematin continued throughout the 50 minutes incubation however after 25 minutes the rate of degradation decreased. There was significant ($P < 0.05$) degradation of GS.hematin after 20 minutes of incubation with 5 μM H_2O_2. Although both hematin and GS.hematin were significantly degraded over time by 5 μM H_2O_2 hematin degradation was significantly higher ($P < 0.0001$) then GS.hematin degradation at each time point over the 50 minute incubation period (Figure 4-5).

In the presence of 10 μM H_2O_2 significant degradation ($P < 0.05$) occurred to hematin within the first 5 minutes with degradation plateauing after 25 minutes, whilst the GS.hematin complex remained stable throughout the 50 minutes incubation (Figure 4-6). There was significant ($P < 0.01$) degradation of hematin compared to GS.hematin when incubated with 10 μM H_2O_2 throughout the 50 minute incubation (Figure 4-6).

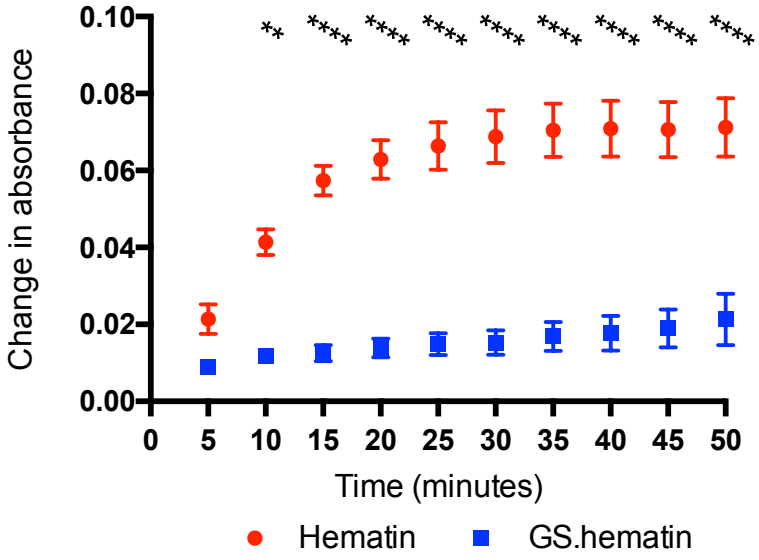

Figure 4-6. Degradation of hematin and GS.hematin over time by 10 μM H_2O_2. Hematin (10 μM) or GS.hematin (10 μM hematin, 2 mM glutathione) was dissolved in 10 mM phosphate buffer, 20 mM KCl, pH 8 and absorbance recorded at 601 nm (GS.hematin) and 618 nm (hematin), time point 0 minutes. H_2O_2 was added to a final concentration of 10 μM and absorbance at 601 nm (GS.hematin) and 618 nm (hematin) taken at 5 minute intervals, for 50 minutes. Change in absorbance from time point 0 was plotted against time. Red circles indicate change in absorbance at 618 nm, from time point 0, for hematin solution containing 10 μM H_2O_2; blue squares indicate change in absorbance at 601 nm, from time point 0, for GS.hematin solution containing 10 μM H_2O_2. Values are means ± SEM (n=3). Asterisks indicate significant difference ($P < 0.01$ **, < 0.0001 ****) in change in absorbance hematin vs. GS.hematin at individual time points. Where error bars are not visible they are smaller than the point.

Both hematin and GS.hematin were significantly ($P < 0.001$) degraded within the first 5 minutes of incubation with 25 μM H_2O_2 (Figure 4-7). However, after 15 minutes of incubation with 25 μM H_2O_2 hematin degradation was significantly higher then that of GS.hematin ($P < 0.05$) (Figure 4-7).

This data indicates that although glutathione does not fully protect or stabilise hematin from degradation by H_2O_2 (≤ 25 μM), the formation of the GS.hematin complex does offer significant protection for hematin from degradation by H_2O_2 (Figures 4-4 – 4-7).

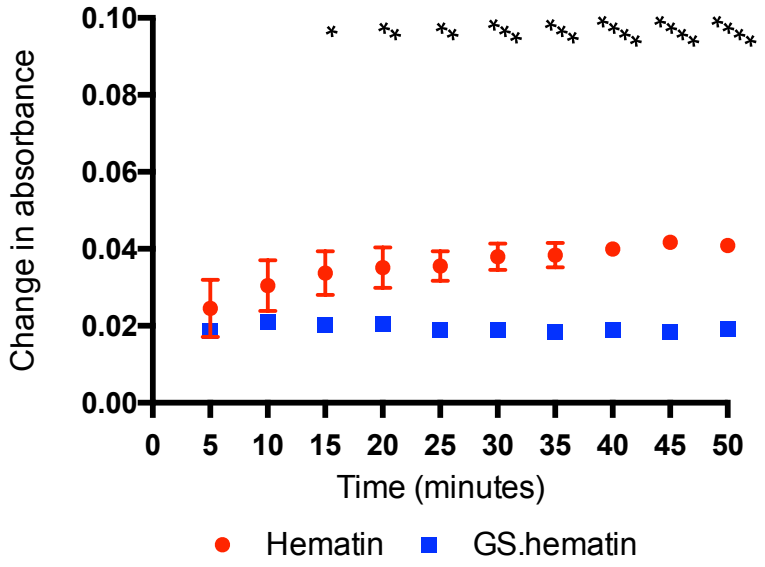

Figure 4-7. Degradation of hematin and GS.hematin over time by 25 µM H_2O_2. Hematin (10 µM) or GS.hematin (10 µM hematin, 2 mM glutathione) was dissolved in 10 mM phosphate buffer, 20 mM KCl, pH 8 and absorbance recorded at 601 nm (GS.hematin) and 618 nm (hematin), time point 0 minutes. H_2O_2 was added to a final concentration of 25 µM and absorbance at 601 nm (GS.hematin) and 618 nm (hematin) taken at 5 minute intervals, for 50 minutes. Change in absorbance from time point 0 was plotted against time. Red circles indicate change in absorbance at 618 nm, from time point 0, for hematin solution containing 25 µM H_2O_2; blue squares indicate change in absorbance at 601 nm, from time point 0, for GS.hematin solution containing 25 µM H_2O_2. Values are means ± SEM (n=3). Asterisks indicate significant difference (P < 0.05 *, 0.01 **, < 0.001 ***, < 0.0001 ****) in change of absorbance hematin vs. GS.hematin at individual time points. Where error bars are not visible they are smaller than the point.

The initial rate of hematin degradation was dependent on the concentration of H_2O_2 whilst the total amount of hematin degraded was independent of H_2O_2 concentration above 2 µM (Figure 4-8). When hematin was incubated with H_2O_2, at concentrations higher than 2 µM, there was no significant difference in the final amount of hematin degraded, indicating that although the rate of hematin degradation increased in relation to the concentration of H_2O_2, concentrations of H_2O_2 above 2 µM degraded the same amount of hematin when the reaction was given sufficient time (Figure 4-8).

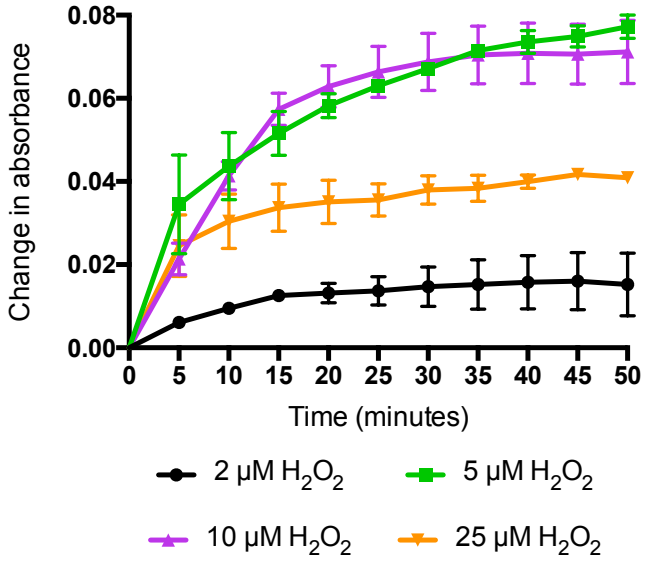

Figure 4-8. Degradation of hematin over time by H_2O_2. Hematin (10 μM) was dissolved in 10 mM phosphate buffer, 20 mM KCl, pH 8 and absorbance recorded 618 nm, time point 0 minutes. H_2O_2 was added to at various concentrations, 2 μM (black), 5 μM (green), 10 μM (purple) and 25 μM (orange) and absorbance at 618 nm taken at 5 minute intervals, for 50 minutes. Change in absorbance from time point 0 was plotted against time. Values are means ± SEM (n=3). Where error bars are not visible they are smaller than the point.

These results not only corroborate previously published data (Nagababu & Rifkind, 2000), that H_2O_2 degrades organic iron, but that this degradation can be significantly decreased by the formation of the GS.hematin complex.

4.3.2 Hematin and GS.hematin Partitioning into Liposomes

Hematin is known to partition into lipid bilayers where the iron can redox cycle resulting in lipid peroxidation (Vincent, 1989; Kumar & Bandyopadhyay, 2005). Lipid bilayers are composed of many different components however the most common phospholipid in all membranes is phosphatidylcholine. Cholesterol is found in mammalian lipid bilayers at varying concentrations. Cell membranes are asymmetric both in terms of protein orientation and phospholipid composition. The internal face of healthy cell membranes contains phosphatidylserine, a phospholipid containing a negatively charged head group, whilst the outside face does not. Dicetyl phosphate is a synthetic lipid that also carries a net negative charge (Figure 4-9). The incorporation of dicetyl phosphate into liposomes renders the liposome similar to the cytosolic face of cell membranes.

Phosphatidylcholine carries an overall neutral charge due to the positive charge on the nitrogen and the negative charge on the phosphate. The phosphatidylcholine used was from lyophilised egg yolks and was comprised of 66% palmitic acid (C_{16}) and 33% steric acid

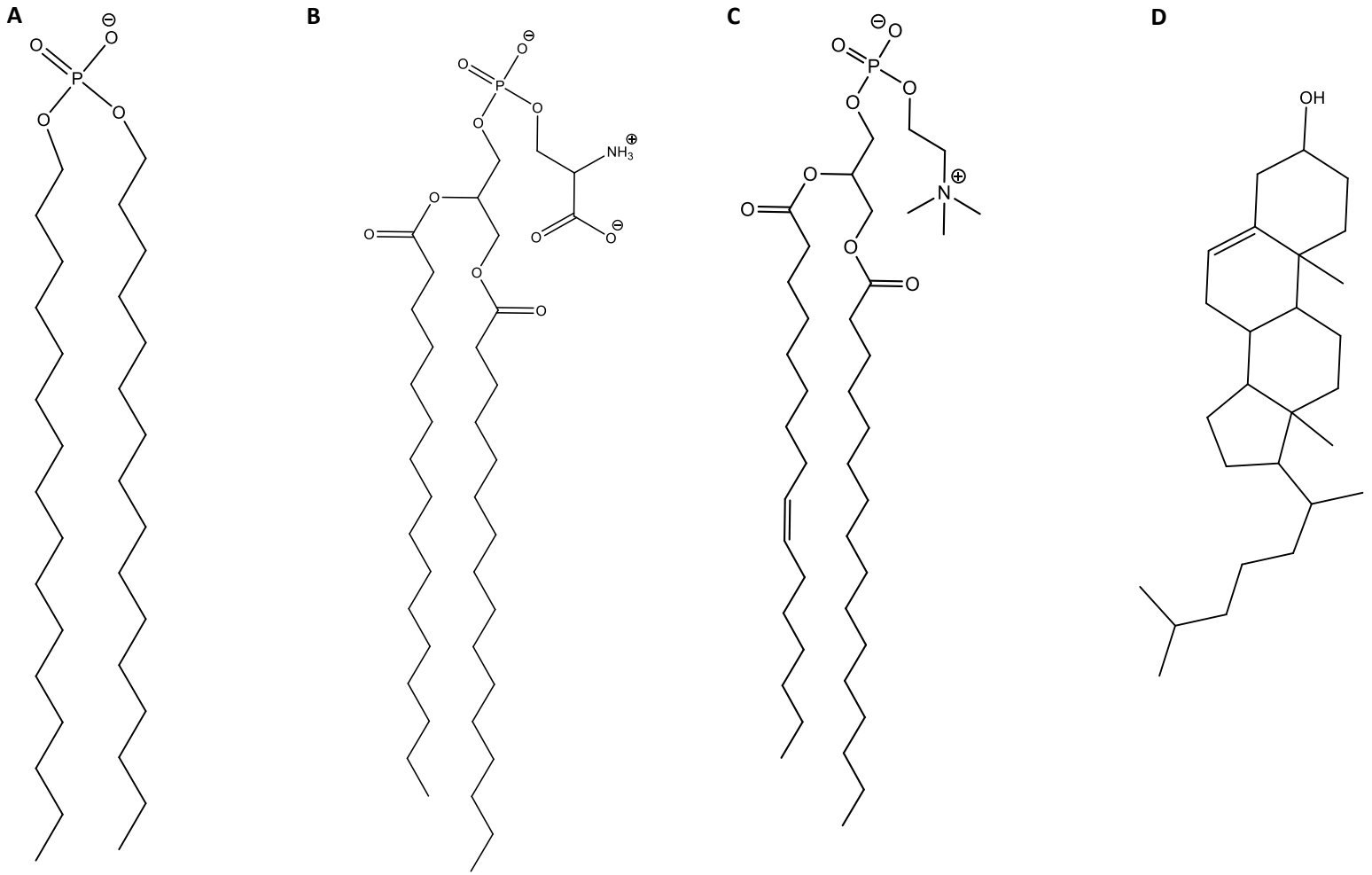

Figure 4-9. Structure of phospholipids. A) Dicetyl phosphate – overall negatively charged (C_{16}), **B)** phosphatidylserine – overall negatively charged, **C)** phosphatidylcholine – overall neutrally charged, phosphatidylcholine used was from egg yolk comprised of 66% palmitic acid (C_{16}) and 33% steric acid (C_{18}), **D)** cholesterol.

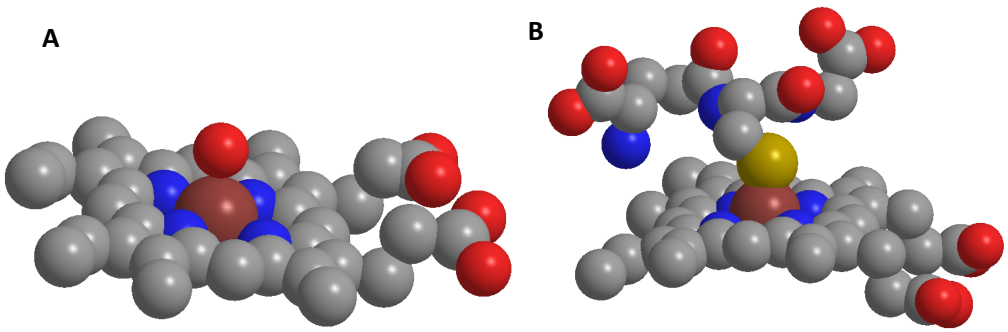

Figure 4-10. Structure of hematin and GS.hematin. Carbon is depicted in grey, oxygen in red, nitrogen in blue, iron in brown and sulfur in yellow. **A** – Hematin structure, the two hydrophilic carboxylate groups of the porphyrin ring are positioned at one end of the ring whilst the hydrophobic vinyl groups are at the opposite end of the planar molecule. **B** – GS.hematin structure, with the addition of two carboxylate groups and an amine group the complex is less hydrophobic and more bulky when compared to the planer hematin molecule.

Table 4-3 The Ratio of Hematin to Lipid for Each Liposome Composition

	Liposome composition		
	Phosphatidylcholine	Phosphatidylcholine and cholesterol	Phosphatidylcholine, cholesterol and dicetyl phosphate
Phosphatidylcholine (mg)	200.0	125.2	99.0
Cholesterol (mg)	0.0	74.8	59.2
Dicetyl phosphate (mg)	0.0	0.0	41.8
Average amount of lipid per experiment (mg)	46	115	24
Starting amount of hematin (mg)	0.1	0.1	0.1
μg hematin per mg lipid	2.27	0.91	4.35
Ratio of hematin to lipid	*1:460*	*1:1,150*	*1:240*

(C_{18}) (Figure 4-9). Phosphatidylserine carries an overall negative charge and two fatty acid chains whilst dicetyl phosphate carries a negative charge however its hydrocarbon chains (C_{16}) do not include the carboxylate group that phosphatidylserine does and is therefore a straighter molecule (Figure 4-9). This allows for tighter packing into the lipid bilayer compared to phosphatidylserine.

The GS.hematin complex is a larger, more bulky, less hydrophobic compound compared to hematin and therefore the ligation of hematin to glutathione could reduce hematin partitioning into lipid bilayers and cell membranes (Figure 4-10).

When comparing the amount of hematin partitioned into each type of liposome the quantity of each liposome type has to be taken into consideration. The three types of liposomes were prepared from the same quantity (200 mg) of lipid however the amount of liposome synthesised varied greatly (Table 4-3). Those prepared only from phosphatidylcholine on average had 46 mg of liposome present per experiment, totalling 327 mg of liposome prepared. Liposomes composed of phosphatidylcholine and cholesterol had on average 115 mg of liposome present per experiment (802 mg in total) whilst liposomes composed of phosphatidylcholine, cholesterol and dicetyl phosphate had

on average 24 mg per experiment (172 mg in total), (Table 4-3). The large variation in liposome mass is due to the liposomes structure, with liposomes containing larger lumens (phosphatidylcholine and cholesterol) containing more aqueous solution weighing more than those with smaller lumens (phosphatidylcholine, cholesterol and dicetyl phosphate). The difference in liposome structure is due to the phospholipids present within the liposome.

Within 15 minutes of incubation with hematin negatively charged liposomes, had significantly more ($P < 0.0001$) hematin partitioned into them when compared to the two neutrally charged liposome preparations, (0.53 μg/mg, compared to 0.1-0.25 μg/mg) (Figure 4-11). There was no significant difference between the amount of hematin partitioned into the different liposome preparations after one and two hours of incubation with hematin. After four hours of incubation the phosphatidylcholine and cholesterol liposome had significantly less ($P < 0.01$) hematin in, at 0.06 μg/mg, compared to the other two liposome preparations, which both had 0.26 μg/mg, (Figure 4-11).

The difference in the amount of hematin partitioned into the different liposome preparations within the first 15 minutes could be due to the different charge density

resulting from the head groups of the phospholipids. The decrease in hematin partitioning into the negatively charged liposomes after 15 minutes could be due to the liposomes becoming overloaded with hematin, causing the lipid bilayer to fracture, and reform into smaller liposomes. These smaller liposomes will not be pelleted during the centrifugation step resulting in a decrease in the amount of hematin in the lipid pellet and an increase in the amount of hematin in the supernatant. This could also account of the significant decrease in hematin partitioned in the cholesterol containing liposomes after 4 hours of incubation.

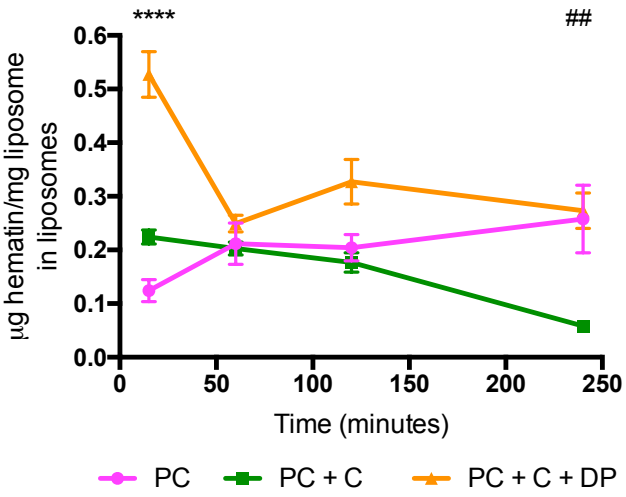

Figure 4-11. Hematin partitioning into liposomes over time. Hematin (10 μM) dissolved in 10 mM phosphate buffer, 150 mM KCl, pH 8 was incubated, shaking, at 37 ^{o}C with various liposomes for 4 hours. Aliquots were taken at various time points and amount of hematin (μg hematin per mg liposome) partitioned into the three different compositions of liposomes deduced through spectroscopic methods. Liposome compositions were; phosphatidylcholine (PC, pink), phosphatidylcholine with cholesterol (PC + C, green) and phosphatidylcholine, cholesterol with dicetyl phosphate (PC + C + DP, organe). Values are means ± SEM (n=3). Asterisks indicate significant difference (P < 0.0001 ****) between PC + C + DP liposomes and both PC and PC + C liposomes. Hashes indicate significant difference (P < 0.01 $^{\#\#}$) between PC + C liposomes and both PC and PC + C + DP. Where error bars are not visible they are smaller than the point.

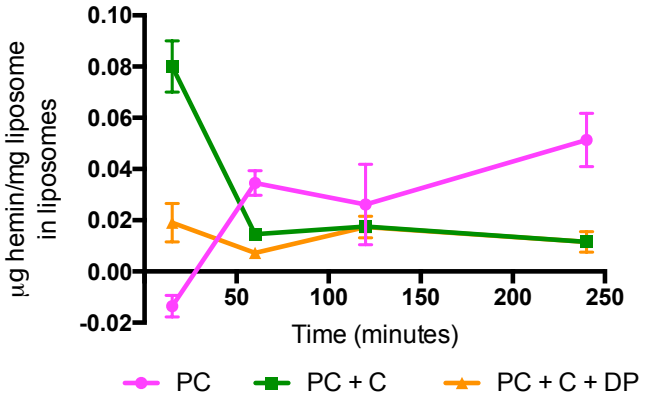

Figure 4-12. GS.hematin partitioning into liposomes. Hematin (10 μM) dissolved in 10 mM phosphate buffer, 150 mM KCl, 2 mM glutathione pH 8 was incubated, shaking, at 37 ^{o}C with various liposomes for 4 hours. Aliquots were taken at various time points and amount of hematin (μg hematin per mg liposome) partitioned into the three different compositions of liposomes deduced through spectroscopic methods. Liposome compositions were; phosphatidylcholine (PC, pink), phosphatidylcholine with cholesterol (PC + C, green) and phosphatidylcholine, cholesterol with dicetyl phosphate (PC + C + DP, organe). Values are means ± SEM (n=3). Asterisks indicate significant difference ($P < 0.0001$ ****) between PC + C + DP liposomes and both PC and PC + C liposomes. Hashes indicate significant difference ($P < 0.01$ $^{\#\#}$) between PC + C liposomes and both PC and PC + C + DP. Where error bars are not visible they are smaller than the point.

The data shows that glutathione prevents hematin from partitioning into all three types of liposomes. Our previous work showed that up to 99% of 10 μM hematin in a solution of 2 mM glutathione could be ligated to glutathione forming the GS.hematin complex. From this, and the data on liposome partitioning work, it can be deduced that glutathione inhibits hematin partitioning into liposomes through binding to hematin, causing the formation of GS.hematin, a less planar and lipophilic molecule than hematin.

4.3.2.2 Hematin and GS.hematin Partitioning into Phosphatidylcholine Liposomes

Within 15 minutes of hematin (10 μM) being incubated with liposomes, composed of phosphatidylcholine, 0.12 μg of hematin per mg lipid had partitioned into the liposome and after 4 hours this had doubled to 0.26 μg hematin per mg lipid, (Figure 4-13). When GS.hematin was incubated with phosphatidylcholine liposomes after 15 minutes none had partitioned into the liposome and after 4 hours as little as 0.05 μg of hematin per mg of lipid had partitioned into the liposomes, (Figure 4-13). Thus glutathione effectively inhibits hematin partitioning into liposomes composed of phosphatidylcholine.

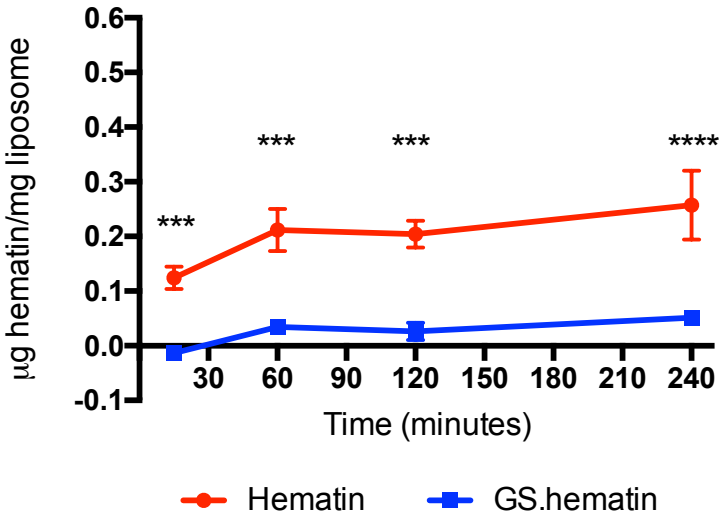

Figure 4-13. Effect of glutathione on hematin partitioning into phosphatidylcholine liposomes. Hematin (10 μM) dissolved in either; 10 mM phosphate buffer, 150 mM KCl, pH 8 or 10 mM phosphate buffer, 150 mM KCl, 2 mM glutathione, pH 8 and incubated, shaking, at 37 °C with phosphatidylcholine liposomes for 4 hours. Aliquots were taken at various time points and the amount of hematin (μg hematin per mg liposome) partitioned into the liposome in the presence (GS.hematin, blue square) or absence (hematin, red circle) of glutathione deduced through spectroscopic methods. Values are means ± SEM (n=3). Asterisks indicate significant difference ($P < 0.001$ ***, 0.0001 ****) hematin vs. GS.hematin at individual time points. Where error bars are not visible they are smaller than the point.

4.3.2.3 Hematin and GS.hematin Partitioning into Phosphatidylcholine-Cholesterol Liposomes

Hematin rapidly partitions into neutral liposomes containing cholesterol, after 15 minutes 0.22 μg of hematin per mg liposome had partitioned into the liposomes. However unlike neutral liposomes containing no cholesterol, over time the amount of hematin partitioning into the liposomes decreased to 0.07 μg hematin/mg liposome after 4 hours (Figure 4-14). With glutathione present, therefore hematin was in the form of GS.hematin complex, significantly less hematin partitioned into the liposomes in the first 15 minutes (0.08 μg hematin/mg liposome) ($P < 0.0001$) however this decreased to less than 0.01 μg hematin/mg liposome after 1 hour (Figure 4-14).

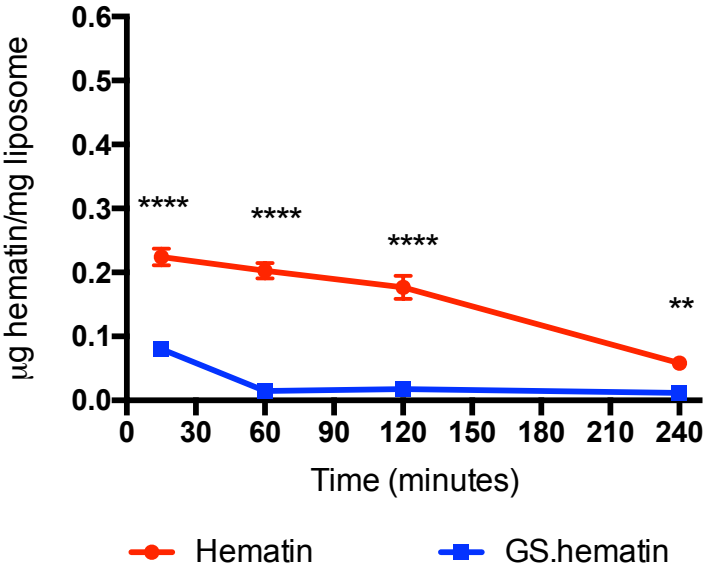

Figure 4-14. Effect of glutathione on hematin partitioning into phosphatidylcholine, cholesterol liposomes. Hematin (10 μM) dissolved in either; 10 mM phosphate buffer, 150 mM KCl, pH 8 or 10 mM phosphate buffer, 150 mM KCl, 2 mM glutathione, pH 8 and incubated, shaking, at 37 °C with phosphatidylcholine, cholesterol, liposomes for 4 hours. Aliquots were taken at various time points and the amount of hematin (μg hematin per mg liposome) partitioned into the liposome in the presence (GS.hematin, blue square) or absence (hematin, red circle) of glutathione deduced through spectroscopic methods. Values are means ± SEM (n=3). Asterisks indicate significant difference ($P < 0.01$ **, < 0.0001 ****) hematin vs. GS.hematin at individual time points. Where error bars are not visible they are smaller than the point.

The amount of hematin that partitioned into the liposomes decreased after the initial 15 minutes, following the same trend as GS.hematin partitioning, however the concentration of hematin in the liposomes was still significantly higher ($P < 0.01$) than the concentration of GS.hematin in the liposomes throughout the four hour incubation, (Figure 4-14). Thus, as with phosphatidylcholine liposomes, glutathione prevents hematin from partitioning into the lipid bilayer.

4.3.2.4 Hematin and GS.hematin Partitioning into Phosphatidylcholine – Cholesterol – Dicetyl Phosphate Liposomes

Within 15 minutes of hematin being incubated with negatively charged liposomes 0.53 μg hematin per mg lipid had partitioned into the liposomes whilst after 4 hours this decreases to 0.27 μg hematin/mg liposome (Figure 4-15). When negatively charged liposomes were incubated with the GS.hematin complex, less than 0.02 μg hematin per mg lipid had partitioned into the liposome throughout the four hour incubation period (Figure 4-15).

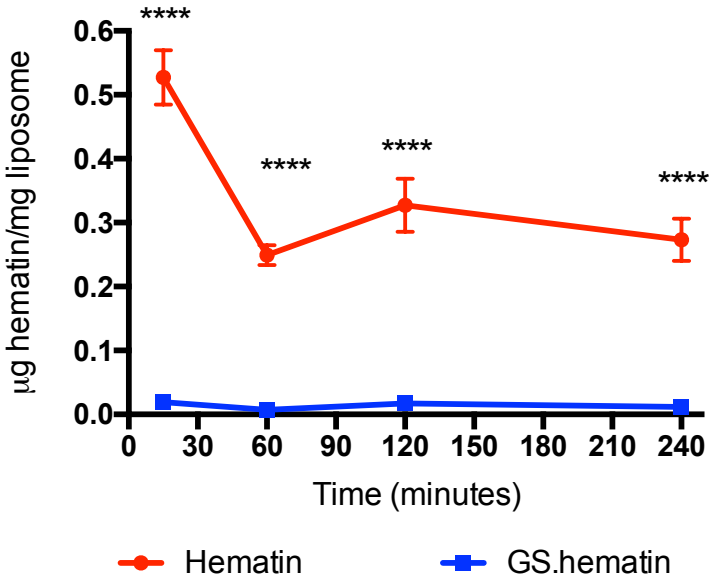

Figure 4-15. Effect of glutathione on hematin partitioning into phosphatidylcholine, cholesterol, dicetyl phosphate liposomes. Hematin (10 μM) dissolved in either; 10 mM phosphate buffer, 150 mM KCl, pH 8 or 10 mM phosphate buffer, 150 mM KCl, 2 mM glutathione, pH 8 and incubated, shaking, at 37 ^{o}C with phosphatidylcholine, cholesterol, dicetyl phosphate liposomes for 4 hours. Aliquots were taken at various time points and the amount of hematin (μg hematin per mg liposome) partitioned into the liposome in the presence (GS.hematin, blue square) or absence (hematin, red circle) of glutathione deduced through spectroscopic methods. Values are means ± SEM (n=3). Asterisks indicate significant difference ($P < 0.0001$ ****) hematin vs. GS.hematin at individual time points. Where error bars are not visible they are smaller than the point.

Hematin is an amphiphilic molecule and at pH 7 the two carboxylate functions at one end of the structure are fully deprotonated, whilst the two vinyl groups at the opposite end are highly hydrophobic, (Figure 4-16). This results in hematin being able to partition into the lipid bilayers vinyl group first, leaving the negatively charged carboxylate groups external to the lipid bilayer.

The increase in hematin partitioning into the negatively charged liposomes compared to the neutrally charged liposome could be associated with different phospholipid packing into the three preparations. The negative charge on the head group of dicetyl phosphate would repel the head group of another nearby dicetyl phosphate thereby causing the phospholipids within the liposome to be less densely packed. With larger time variable spaces between the liposome constituents there would be more space available for hematin to partition into the liposome. Thus more hematin can partition in the negatively charged liposomes when compared to the neutrally charged preparations.

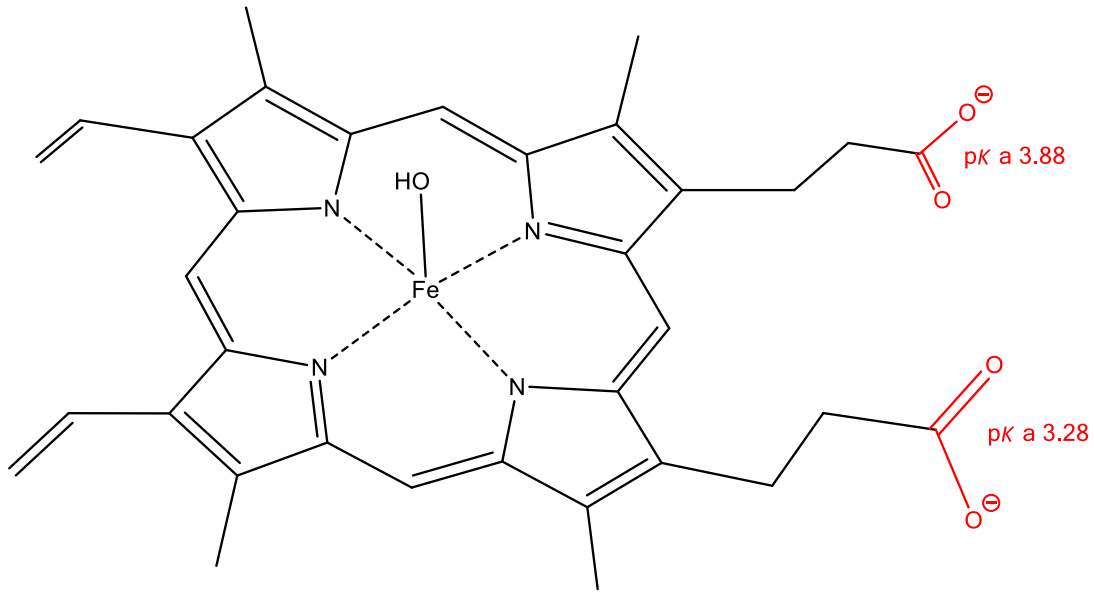

Figure 4-16. p*K*a of carboxylate groups of hematin. Structure of hematin showing the p*K*a of the two carboxylate groups (denoted in red), calculated using Marvin Sketch 5.4.0.1 software (ChemAxon, www.chemaxon.com/download/marvin-suite). At physiological pH, and pH 8, the carboxylates would be fully deprotonated resulting in a negative two charge at one end of hematin whilst the two vinyl groups at the opposite end of hematin would result in the molecule being amphiphilic.

The amount of hematin partitioned into liposomes that were incubated with GS.hematin was significantly less ($P < 0.01$) than when incubated with hematin only across all liposome types. The main reason for this is likely to be in increase in size and bulk of the GS.hematin complex compared to hematin.

The amount of GS.hematin partitioned into the negatively charged liposomes was the lowest throughout the four hour incubation when comparing all three liposome types. On average the amount of hematin partitioned into the neutral liposomes decreased by 0.17 μg hematin per mg lipid in the presence of glutathione, whilst hematin partitioning into negatively charged liposomes decreased by 0.39 μg hematin per mg lipid, in the presence of glutathione. Unlike hematin the GS.hematin complex has negative charges spread across it's surface due to the two additional carboxylate groups on the glutathione, both of which are be fully deprotonated at pH 8, (Figure 4-17).

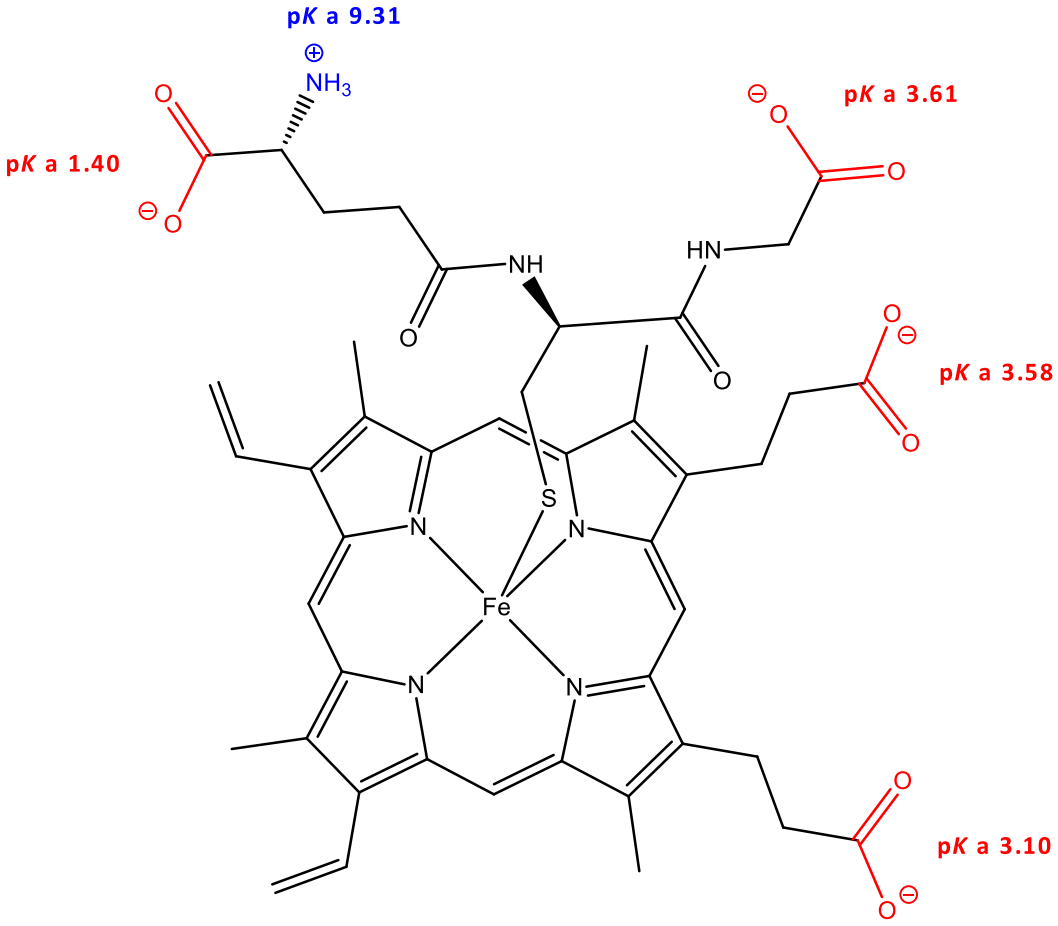

Figure 4-17. p*K*a of carboxylate and amine groups of GS.hematin. Structure of GS.hematin showing the p*K*a of the four carboxylate groups (denoted in red) and one amine group (denoted in blue), calculated using Marvin Sketch 5.4.0.1 software. At physiological pH, and pH 8, all carboxylates would be fully deprotonated, resulting in the GS.hematin complex having two negative charges across one face, one at either end, and two negative charges at one end of the GS.hematin complex via hematin.

The addition of the two negative charges associated with glutathione causes a more even spread of charge across the complex. This together with the increase in bulk (effective cross sectional radius) of the hematin renders the conjugate less likely to partition into the time variable spaces that are continuously created in the fluid mosaic structure of the membrane (Singer & Nicolson 1972; Mouritsen & Andersen 1998).

4.3.3 Hematin and GS.hematin Partitioning into Erythrocytes

Cell membranes are composed of various phospholipids as well as cholesterol and protein. The composition of lipid bilayers is asymmetric with different compositions on the extracellular and intracellular faces (Reichstein & Blostein, 1975). For instance, erythrocyte membranes are composed of protein, including glycoprotein that is only found on the extracellular face of the membrane, lipids and a small percentage of carbohydrates,

however these carbohydrates are associated either with glycoproteins or glycolipids; and the majority are located on the outer surface of the membrane (Ballas & Krasnow 1980). The lipid composition of membranes is also asymmetric with negatively charged phosphatidylserine only occurring in the intracellular face, phosphatidylcholine, occurring predominantly in the extracellular face and cholesterol found in equal measures in the intra and extracellular face, (Dodge & Phillips, 1967; Verkleij *et al.,* 1973) (Figure 4-18).

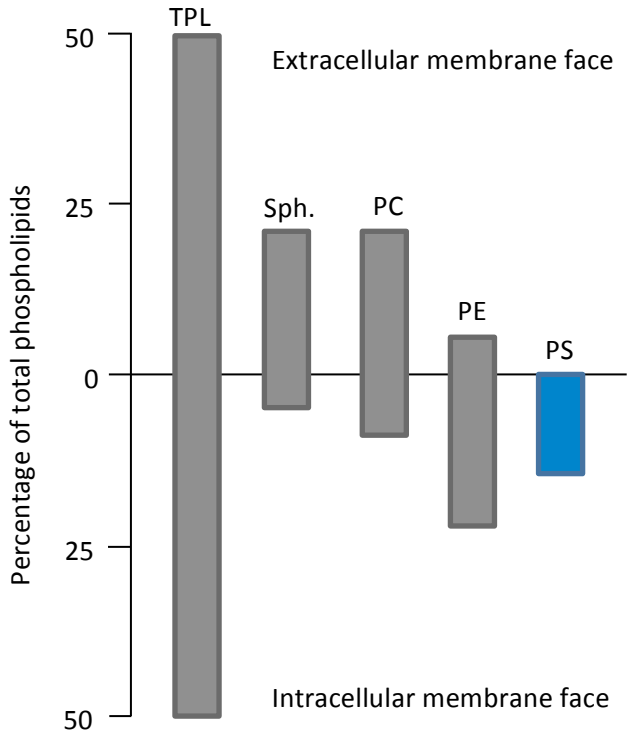

Figure 4-18. Distribution of phospholipids in human erythrocyte cell membrane. Distribution of phospholipids between the intra- and extra- cellular membrane faces. TPL = total phospholipid, Sph. = sphingomyelin, PC = phosphatidylcholine, PE = phosphatidylethanolamine, PS = phosphatidylserine, negatively charged phospholipid (blue). Adapted from Verkleij *et al.* 1973.

Hematin partitioning into liposomes was conducted at pH 8, the optimal pH for hematin dissolving in phosphate buffer, however the cytosol of mammalian cells and blood has a pH closer to pH 7.4. To deduce if the higher pH changed hematin partitioning into liposomes the erythrocyte experiments were conducted at both pH 7.4 and pH 8. This was possible due to the tenfold decrease in hematin concentration and the use of radioactive hematin ([^{59}Fe]hematin), which was dissolved in DMSO before being added to phosphate buffer.

4.3.3.1 Hematin and GS.hematin Partitioning into Erythrocytes in the Presence of NaCl

When hematin was incubated with erythrocytes at pH 8, 58% of the hematin had partitioned into the erythrocytes within the first minute, this decreased to 42% when glutathione was present, which was a significant decrease ($P < 0.0001$) (Figure 4-19). Over the course of the hour incubation a total of 62% of hematin, and 46% of GS.hematin, partitioned into the erythrocytes. Thus over 90% of the hematin or GS.hematin that partitioned into the erythrocytes did so within the first minute of incubation.

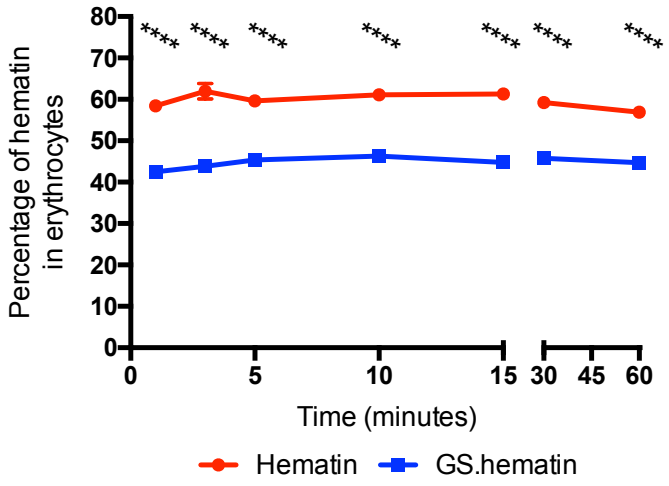

Figure 4-19. Effect of glutathione on hematin partitioning into erythrocytes with NaCl present at pH 8. [^{59}Fe]hematin was dissolved to a final concentration of 1 μM in either; 10 mM phosphate buffer, 130 mM NaCl, pH 8 or 10 mM phosphate buffer, 130 mM NaCl, 2 mM glutathione, pH 8 and incubated, shaking, with 2.34x10^{9} erythrocytes at 37 ^{o}C for 1 hour. Aliquots were taken at various time points and the percentage of hematin partitioned into the erythrocytes in the presence (GS.hematin, blue squares), or absence (hematin, red circles) of glutathione was calculated. Values are means ± SEM (n=3). Asterisks indicate significant difference ($P < 0.0001$ ****) hematin vs. GS.hematin at individual time points. Where error bars are not visible they are smaller than the point.

When the pH of the solution was decreased to pH 7.4 the amount of hematin that partitioned into erythrocytes in the first minute increased to 68% and the amount of GS.hematin that partitioned into the erythrocytes increased to 54%, (Figure 4-20). Over the hour incubation a maximum of 73% hematin, and 61% GS.hematin, partitioned into erythrocytes. Thus, similar to partitioning at pH 8, 90% of the hematin that partitioned into the erythrocytes did so within the first minute of incubation.

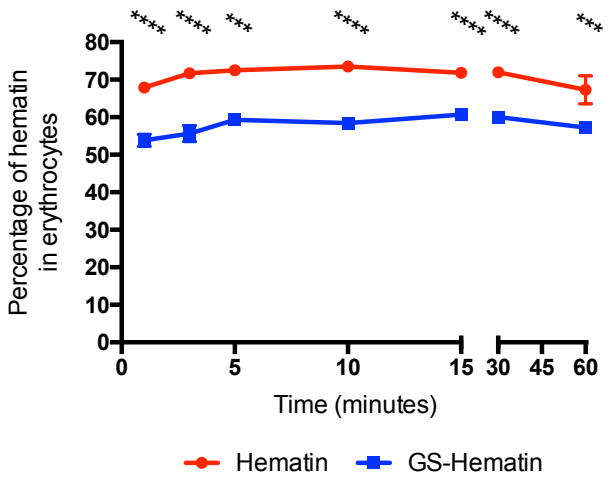

Figure 4-20. Effect of glutathione on hematin partitioning into erythrocytes with NaCl present at pH 7.4. [^{59}Fe]hematin was dissolved to a final concentration of 1 μM in either; 10 mM phosphate buffer, 130 mM NaCl, pH 7.4 or 10 mM phosphate buffer, 130 mM NaCl, 2 mM glutathione, pH 7.4 and incubated, shaking, with 2.34x10^{9} erythrocytes at 37 ^{o}C for 1 hour. Aliquots were taken at various time points and the percentage of hematin partitioned into the erythrocytes in the presence (GS.hematin, blue squares), or absence (hematin, red circles) of glutathione was calculated. Values are means ± SEM (n=3). Asterisks indicate significant difference (P < 0.001 ***, < 0.0001 ****) hematin vs. GS.hematin at individual time points. Where error bars are not visible they are smaller than the point.

The amount of hematin that partitioned into the erythrocytes over time was significantly lower (P < 0.001) when glutathione was present in the solution. Thus the formation of the GS.hematin complex decreases the amount of hematin that partitions into the cell membrane, both at pH 8 and 7.4.

There was a significant increase (P <0.001) in the amount of hematin, (average 11%) and GS.hematin, (average 13%) that partitioned into erythrocytes at pH 7.4 compared to pH 8, although the rate at which it partitioned was not affected by the change in pH, (Figure 4-21 & 4-22). Hematin partitioning into erythrocytes in buffers at pH 7.4 and pH 8 followed the same trend. Over 90% of the final amount of hematin that partitioned into the erythrocytes over 60 minutes did so within the first minute, and in both pH buffers there was a decrease of 5.5% hematin partitioned into the erythrocytes between 15 and 60 minutes (Figure 4-21).

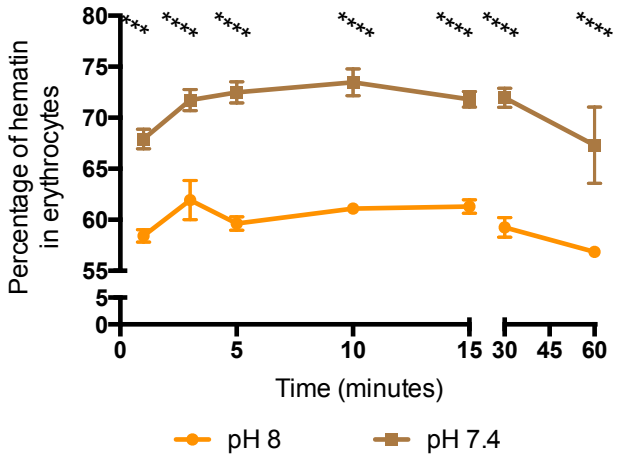

Figure 4-21. Effect of pH on hematin partitioning into erythrocytes in buffer containing NaCl. [^{59}Fe]hematin was dissolved to a final concentration of 1 μM in either; 10 mM phosphate buffer, 130 mM NaCl, pH 8 or 10 mM phosphate buffer, 130 mM NaCl, pH 7.4 and incubated, shaking, with 2.34x10^{9} erythrocytes at 37 ^{o}C for 1 hour. Aliquots were taken at various time points and the percentage of hematin partitioned into the erythrocytes in the pH 8 solution (orange circles) and the pH 7.4 solution (brown squares) was calculated. Values are means ± SEM (n=3). Asterisks indicate significant difference (P < 0.001 ***, < 0.0001 ****) pH 8 vs. pH 7.4 at individual time points. Where error bars are not visible they are smaller than the point.

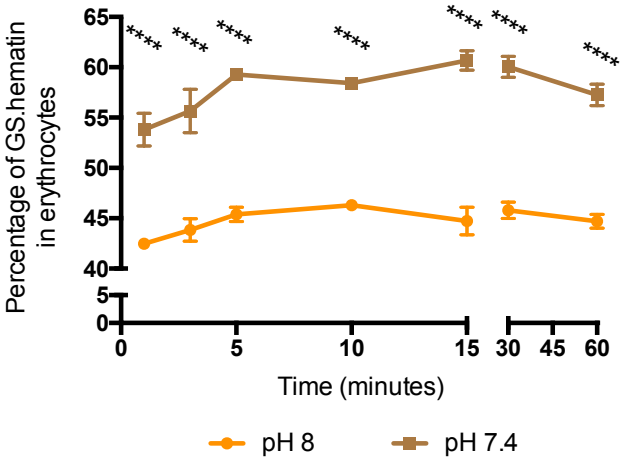

Figure 4-22. Effect of pH on GS.hematin partitioning into erythrocytes in buffer containing NaCl. [^{59}Fe]hematin was dissolved to a final concentration of 1 μM in either; 10 mM phosphate buffer, 130 mM NaCl, 2 mM glutathione, pH 8 or 10 mM phosphate buffer, 130 mM NaCl, 2 mM glutathione, pH 7.4 and incubated, shaking, with 2.34x10^{9} erythrocytes at 37 ^{o}C for 1 hour. Aliquots were taken at various time points and the percentage of hematin partitioned into the erythrocytes in the pH 8 solution (orange circles) and the pH 7.4 solution (brown squares) was calculated. Values are means ± SEM (n=3). Asterisks indicate significant difference (P < 0.0001 ****) pH 8 vs. pH 7.4 at individual time points. Where error bars are not visible they are smaller than the point.

GS.hematin partitioning into erythrocytes in buffers at pH 7.4 and pH 8 followed the same trend. 90% of the final amount of GS.hematin that partitioned into the erythrocytes over 60 minutes did so within the first minute, and 100% did so within 5 minutes.

In pH 7.4 there was a decrease of 4% of GS.hematin partitioned into erythrocytes between 15 and 60 minutes whilst at pH 8 this decreased to 1% (Figure 4-22).

The decrease in hematin and GS.hematin detected within the erythrocytes after 15 minutes is likely due to a small minority of erythrocytes lysing from the irreversible damage to the membrane by the hematin and GS.hematin partitioned into the membranes. There was no visible change in supernatant colour however if only a few erythrocytes lysed insufficient haemoglobin would be released to record a colour change. The decrease in hematin partitioning between 15 and 60 minutes was larger than that of GS.hematin indicating that the decrease in hematin partitioning into membranes when ligated to glutathione decreases cell lysis.

4.3.3.2 Hematin, GS.hematin Partitioning into Erythrocytes in the Presence of KCl

In an environment that is similar to the cytosol of cells, (150 mM KCl, pH 8) 70% of hematin partitioned into the erythrocytes within the first minute of incubation, this accounted for 100% of the hematin that partitioned into the erythrocytes over the 60 minute incubation (Figure 4-23). When glutathione was present only 46% of the GS.hematin complex partitioned into the erythrocytes in the first minute, this accounted for 90% of the total percentage of GS.hematin that partitioned into the erythrocytes over the 60 minute incubation (Figure 4-23).

When erythrocytes were incubated with hematin or GS.hematin at pH 7.4 in the presence of KCl 66% of hematin partitioned into the erythrocytes within the first minute, this significantly decreased ($P < 0.0001$) to 50% in the presence of glutathione, (Figure 4-24). Within the first minute 89% the total amount of hematin that partitioned into the membranes in 60 minutes had done so, this increased to 93% in the first minute for GS.hematin.

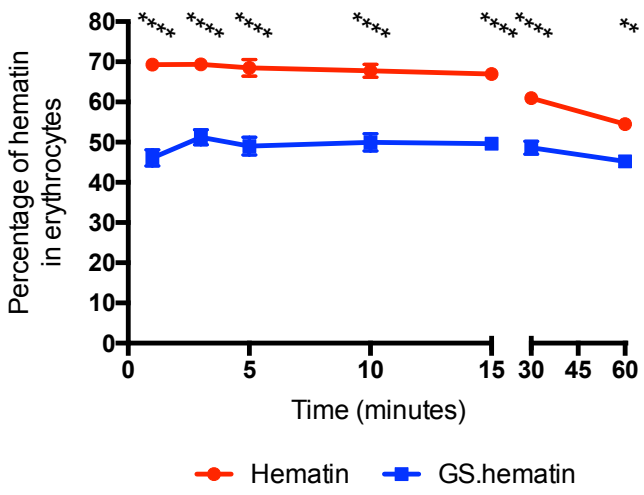

Figure 4-23. Effect of glutathione on hematin partitioning into erythrocytes in buffer containing KCl at pH 8. [^{59}Fe]hematin was dissolved to a final concentration of 1 μM in either; 10 mM phosphate buffer, 150 mM KCl, pH 8 or 10 mM phosphate buffer, 130 mM NaCl, 2 mM glutathione, pH 8 and incubated, shaking, with 2.34x10^{9} erythrocytes at 37 ^{o}C for 1 hour. Aliquots were taken at various time points and the percentage of hematin partitioned into the erythrocytes in the presence (GS.hematin, blue squares), or absence (hematin, red circles) of glutathione was calculated. Values are means ± SEM (n=3). Asterisks indicate significant difference (*P* < 0.01 **, < 0.001 ***, < 0.0001 ****) hematin vs. GS.hematin at individual time points. Where error bars are not visible they are smaller than the point.

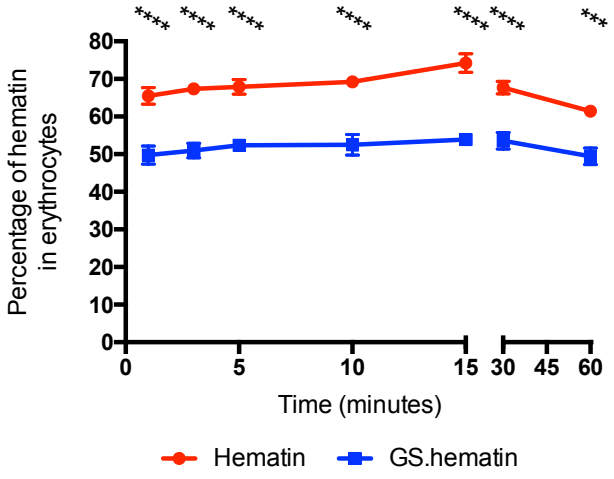

Figure 4-24. Effect of glutathione on hematin partitioning into erythrocytes in buffer containing KCl at pH 7.4. [^{59}Fe]hematin was dissolved to a final concentration of 1 μM in either; 10 mM phosphate buffer, 150 mM KCl, pH 8 or 10 mM phosphate buffer, 130 mM KCl, 2 mM glutathione, pH 7.4 and incubated, shaking, with 2.34x10^{9} erythrocytes at 37 ^{o}C for 1 hour. Aliquots were taken at various time points and the percentage of hematin partitioned into the erythrocytes in the presence (GS.hematin, blue squares), or absence (hematin, red circles) of glutathione was calculated. Values are means ± SEM (n=3). Asterisks indicate significant difference (*P* < 0.001 ***, < 0.0001 ****) hematin vs. GS.hematin at individual time points. Where error bars are not visible they are smaller than the point.

There was no significant difference in the amount of hematin or GS.hematin that partitioned into erythrocytes within the first 10 minutes of incubation when comparing cells incubated at pH 8 compared to pH 7.4 (Figure 4-25 & 4-26). 15 minutes after hematin was added to cells in solution at pH 7.4, there was an increase ($P < 0.01$) in the amount hematin partitioned into the membrane when compared to cells incubated at pH 8 (Figure 4-25).

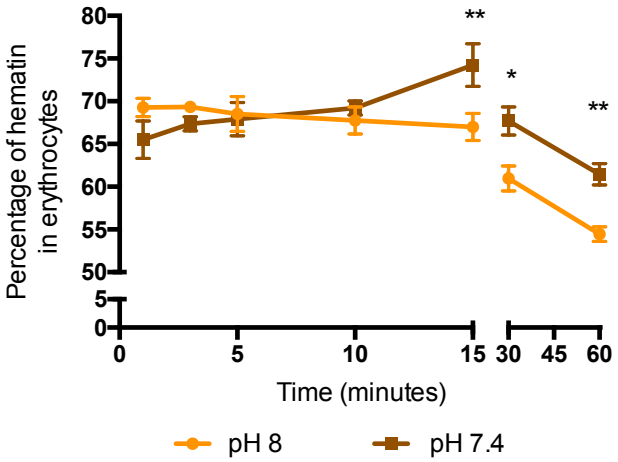

Figure 4-25. Effect of pH on hematin partitioning into erythrocytes in buffer containing KCl. [^{59}Fe]hematin was dissolved to a final concentration of 1 μM in either; 10 mM phosphate buffer, 150 mM KCl, pH 8 or 10 mM phosphate buffer, 130 mM KCl, pH 7.4 and incubated, shaking, with 2.34x10^{9} erythrocytes at 37 ^{o}C for 1 hour. Aliquots were taken at various time points and the percentage of hematin partitioned into the erythrocytes in the pH 8 solution (orange circles) and the pH 7.4 solution (brown squares) was calculated. Values are means ± SEM (n=3). Asterisks indicate significant difference ($P < 0.05$*, $P < 0.01$ **) pH 8 vs. pH 7.4 at individual time points. Where error bars are not visible they are smaller than the point.

Both hematin and GS.hematin partitioning into erythrocytes in buffers at pH 7.4 and pH 8 followed the same trend. At least 90% of the final amount of hematin or GS.hematin that partitioned into the erythrocytes over 60 minutes did so within the first minute, (Figure 4-25 & 4-26). Cells incubated with hematin had a decrease in hematin partitioned into the membranes between 15 and 60 minutes of between 12 and 14% whilst cells incubated with GS.hematin had a decrease of only 4%. This strongly suggests, as with cells incubated in solutions containing NaCl, by decreasing the amount of hematin partitioned into the membranes, through hematin's ligation with glutathione, the GS.hematin complex decreases cell lysis caused by irreversible damage to the cell membrane caused by hematin partitioning into the lipid bilayer.

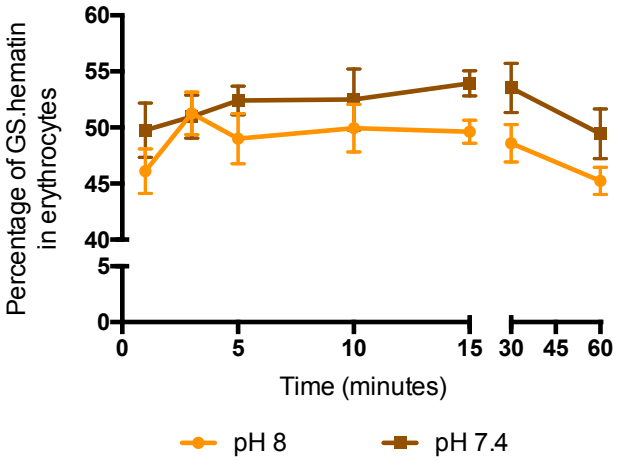

Figure 4-26. Effect of pH on GS.hematin partitioning into erythrocytes in buffer containing KCl. [^{59}Fe]hematin was dissolved to a final concentration of 1 μM in either; 10 mM phosphate buffer, 150 mM KCl, 2 mM glutathione, pH 8 or 10 mM phosphate buffer, 130 mM KCl, 2 mM glutathione, pH 7.4 and incubated, shaking, with 2.34x10^{9} erythrocytes at 37 ^{o}C for 1 hour. Aliquots were taken at various time points and the percentage of hematin partitioned into the erythrocytes in the pH 8 solution (orange circles) and the pH 7.4 solution (brown squares) was calculated. Values are means ± SEM (n=3).

The salt present, (NaCl or KCl), in the solution of cells incubated at pH 7.4 with either hematin or GS.hematin had no effect on the rate of hematin/GS.hematin partitioning, nor did the salts have a significant effect on the percentage of hematin or GS.hematin partitioned into the cell membranes over 15 minutes, (Figure 4-27). This data indicates that at pH 7.4 the rate, and amount, of GS.hematin and hematin that partitioned into the extracellular face of the erythrocyte membrane would be equal. However, although KCl was used to mimic the cytosol of erythrocytes the hematin and GS.hematin was still partitioning into the extracellular face of the membrane as the cells had not been inverted. As mentioned at the beginning of this section erythrocytes cell membranes are asymmetric both in the composition of phospholipids and proteins in them (Reichstein & Blostein 1975). In erythrocytes the extracellular face of the membrane is composed of a large percentage of glycoproteins which are not present in the intracellular face, whilst the intracellular face contains negatively charged phospholipids. Thus hematin partitioning into negatively charged liposomes is more representative of hematin partitioning from the cytosol into the intracellular face of the cell membrane due to the asymmetric nature of cell membranes.

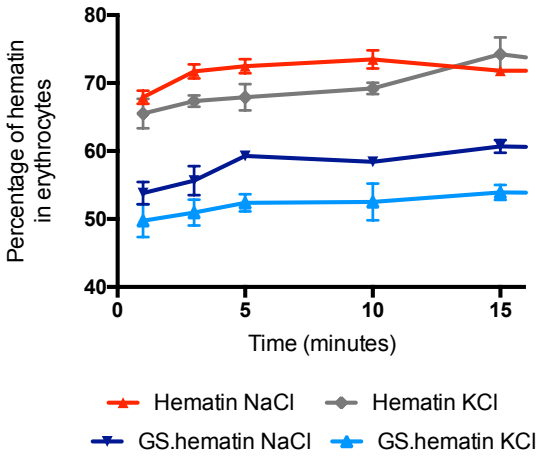

Figure 4-27. Effect of salt on hematin and GS.hematin partitioning into erythrocytes at pH 7.4. [^{59}Fe]hematin was dissolved to a final concentration of 1 μM in either; 10 mM phosphate buffer, 130 mM NaCl, pH 7.4 (red), 10 mM phosphate buffer, 139 mM NaCl, 2 mM glutathione, pH 7.4 (dark blue), 10 mM phosphate buffer, 130 mM KCl, pH 7.4 (grey) or 10 mM phosphate buffer, 130 mM KCl, 2 mM glutathione, pH 7.4 (light blue) and incubated shaking, with 2.34x10^9 erythrocytes at 37 ^{o}C for 1 hour. Aliquots were taken at various time points and the percentage of hematin partitioned into the erythrocytes was calculated and percentage of hematin partitioned into erythrocytes over the first 15 minutes was plotted. Values are means ± SEM (n=3). Where error bars are not visible they are smaller than the point.

Under all conditions, within both erythrocytes and liposomes, the presence of glutathione significantly decreased ($P < 0.01$) the percentage of hematin that partitioned into the lipid bilayers. It likely did this by forming the GS.hematin complex that is more bulky, less hydrophobic and less planar then hematin. These changes in the complex being less suited to partitioning into the hydrophobic environment of lipid bilayers.

4.3.4 HPLC of Caco-2 Cell Lysate

If the GS.hematin complex could be detected within mammalian cells incubated with the GS.hematin complex and hematin only it would provide further weight to the concept that glutathione is the main physiological ligand for the organic labile iron pool. HPLC based size exclusion chromatography was used to separate [^{59}Fe]hematin from GS.[^{59}Fe]hematin which had been isolated from cell lysates.

4.3.4.1 Elution Time of Standards

The column used for HPLC separation of the GS.hematin complex from hematin was a size exclusion column (Agilent PL-aquagel-OH 20), the compounds with large molecular weights elute more rapidly than compounds with smaller molecular weights. The elution time of compounds with known molecular weights; GS.hematin, oxidised glutathione, reduced

glutathione and DMSO, were plotted against the log molecular weight of the corresponding compound and a line with linear regression fitted (Figure 4-28).

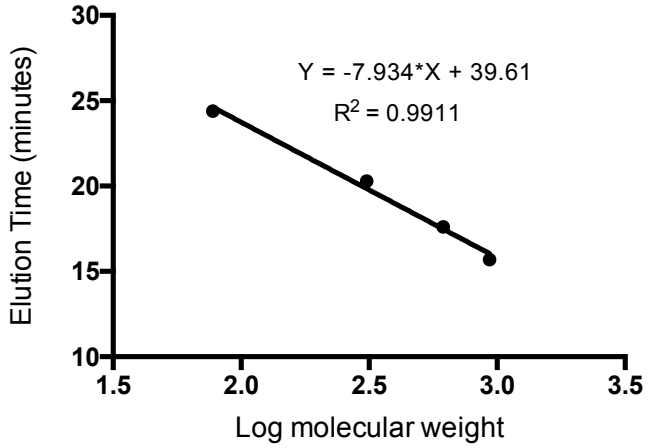

Figure 4-28. Elution time of compounds from Agilent PL-aquagel-OH 20 column. GS.hematin, oxidised glutathione, reduced glutathione and DMSO were dissolved in a solution of 50 mM phosphate buffer, 5 mM KCl, 12.5 mM Tris-HCl, 2.5 % (v/v) glycerol, 0.5 % (v/v) SDS. Samples were eluted from a Waters 626 HPLC system on a PL-aquagel-OH 20 column with a mobile phase of 20 mM phosphate buffer, 2 mM glutathione, pH 8 at 0.4 mL/min. The elution time of the compounds was plotted against the log molecular weight of the compounds and a line with lineal regression fitted. The equation for the line of best fit was calculated to be Y = -7.934*X + 39.61.

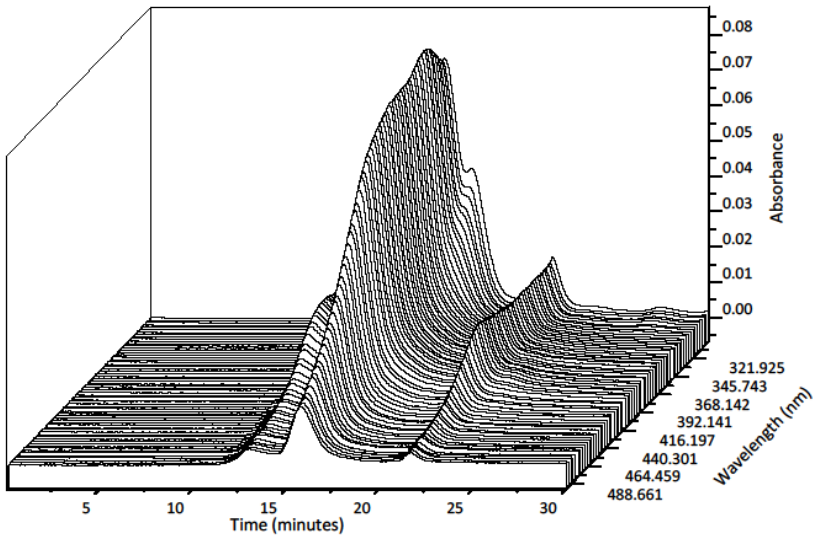

Figure 4-29. 3D HPLC spectrum of GS.hematin. GS.hematin (38 μM hematin, 10,000 CPM of [^{59}Fe]hematin, 15 mM glutathione) was dissolved in a solution of 50 mM phosphate buffer, 5 mM KCl, 12.5 mM Tris-HCl, 2.5 % (v/v) glycerol, 0.5 % (v/v) SDS and 100 μL injected onto an Agilent PL aquagel-OH 20 column. The sample was eluted with a mobile phase of 20 mM phosphate buffer, 2 mM glutathione, pH 8 at 0.4 mL/min over 30 minutes. The chromatogram depicts the absorbance spectrum of the eluted compounds between 300 nm and 500 nm across the entire run time (0-30 minutes). The largest elution peak, corresponding to GS.hematin, occurs 15.8 minutes after injection and with the highest absorption occurring at 420 nm.

GS.[^{59}Fe]hematin dissolved in ¼ lysis buffer, (12.5 mM Tris base (pH 6.8), 2.5% (v/v) glycerol, 0.5% (v/v) SDS), eluted at 15.8 minutes, with highest absorption at 420 nm between 230 nm and 500 nm (Figure 4-29). The percentage of radioactive counts (CPM) from the fractions collected between 10 and 30 minutes showed that a small amount of radioactive material eluted between 12.5 and 14.5 minutes, corresponding to a small amount of hematin unbound to glutathione, whilst the majority of the radioactive material eluted between 15.5 and 17.5 minutes, corresponding to the peak for GS.[^{59}Fe]hematin elution (Figure 4-30).

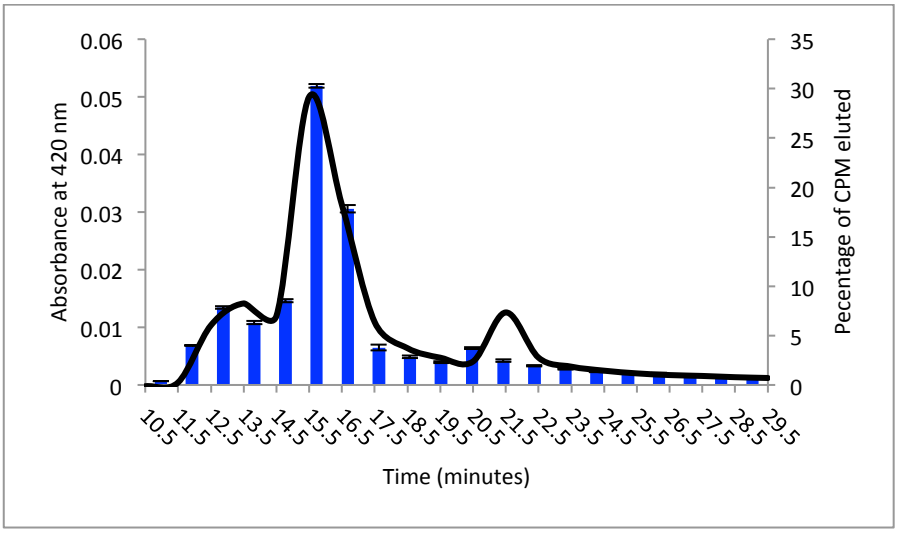

Figure 4-30. Chromatogram of GS.[^{59}Fe]hematin at 420 nm and distribution of radioactivity eluted from GS.hematin sample. GS.hematin (38 μM hematin, 10,000 CPM of [^{59}Fe]hematin, 15 mM glutathione) was dissolved in a solution of 50 mM phosphate buffer, 5 mM KCl, 12.5 mM Tris-HCl, 2.5 % (v/v) glycerol, 0.5 % (v/v) SDS and 100 μL injected onto an Agilent PL aquagel-OH 20 column. The sample was eluted with a mobile phase of 20 mM phosphate buffer, 2 mM glutathione, pH 8 at 0.4 mL/min over 30 minutes. Absorbance was detected at 420 nm over 30 minutes (black line) and 1 minute fractions were collected between 10 and 30 minutes and counted for eluted [^{59}Fe]hematin (blue bars). The largest absorption peak, corresponding to GS.hematin occurs at 15.8 minutes, the majority of the radioactive material eluted between 15 and 17 minutes (blue bars) aligning with the elution of GS.hematin.

When [^{59}Fe]hematin was injected onto the column the majority of [^{59}Fe]hematin bound to the stationary phase however a small absorbance peak at 420 nm occurred at 13.1 minutes (Figure 4-31).

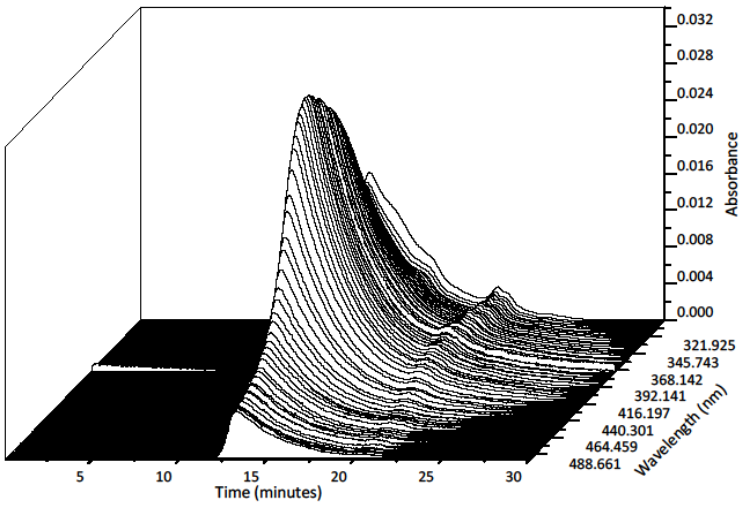

Figure 4-31. 3D HPLC spectrum of hematin. Hematin (38 μM hematin, 10,000 CPM of [^{59}Fe]hematin) was dissolved in a solution of 50 mM phosphate buffer, 5 mM KCl, 12.5 mM Tris-HCl, 2.5 % (v/v) glycerol, 0.5 % (v/v) SDS and 100 μL injected onto an Agilent PL aquagel-OH 20 column. The sample was eluted with a mobile phase of 20 mM phosphate buffer, 2 mM glutathione, pH 8 at 0.4 mL/min over 30 minutes. The chromatogram depicts the absorbance spectrum of the eluted compounds between 300 nm and 500 nm across the entire run time (0-30 minutes). There is a very small absorption peak at 13.1 minutes, with absorbance occurring at 420 nm.

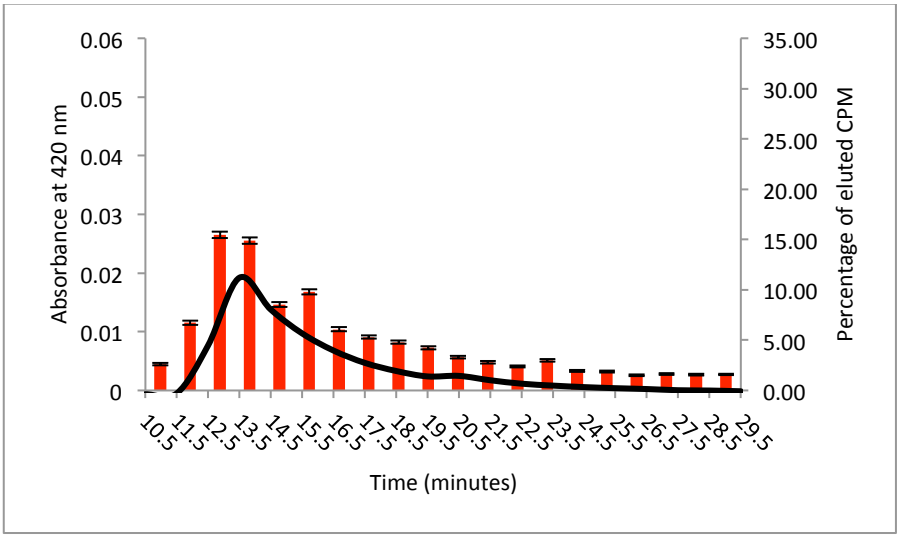

Figure 4-32. Chromatogram of [^{59}Fe]hematin at 420 nm and distribution of radioactivity eluted from hematin sample. Hematin (38 μM hematin, 10,000 CPM of [^{59}Fe]hematin) was dissolved in a solution of 50 mM phosphate buffer, 5 mM KCl, 12.5 mM Tris-HCl, 2.5 % (v/v) glycerol, 0.5 % (v/v) SDS and 100 μL injected onto an Agilent PL aquagel-OH 20 column. The sample was eluted with a mobile phase of 20 mM phosphate buffer, 2 mM glutathione, pH 8 at 0.4 mL/min over 30 minutes. Absorbance was detected at 420 nm over 30 minutes (black line) and 1 minute fractions were collected between 10 and 30 minutes and counted for eluted [^{59}Fe]hematin (red bars). Maximum absorption occurs at 13.1 minutes, whilst the majority of radioactive material elutes between 12 and 14 minutes (red bars) indicating that a small amount of hematin elutes at 13.1 minutes, however the majority remains bound to the column.

Table 4-4 Calculated Molecular Weight of Compounds from Elution Time

Compound	Molecular weight	Log(Mw)	Elution Time (minutes)	Log Mw calculated from graph	Mw calculated from graph	Difference in calculated & actual Mw	Percentage difference (%)
DMSO	78.1	1.89	24.4	1.92	82.6	4.5	6
GSH	307.3	2.49	20.3	2.43	271.5	35.8	12
GSSG	612.6	2.79	17.6	2.77	594.5	18.1	3
GS.hematin	922.8	2.97	15.7	3.01	1,031.8	109.0	12
hematin	633.2	2.80	13.1	3.34	2,194.4	1,561.2	247
ferriheme	616.5	2.79	13.1	3.34	2,194.4	1,577.9	256
ferriheme dimer	1,233.0	3.09	13.1	3.34	2,194.4	961.4	78
ferriheme trimer	1,849.5	3.27	13.1	3.34	2,194.4	344.9	19
ferriheme tetramer	**2,478.0**	**3.39**	**13.1**	**3.34**	**2,194.4**	**283.6**	**11**

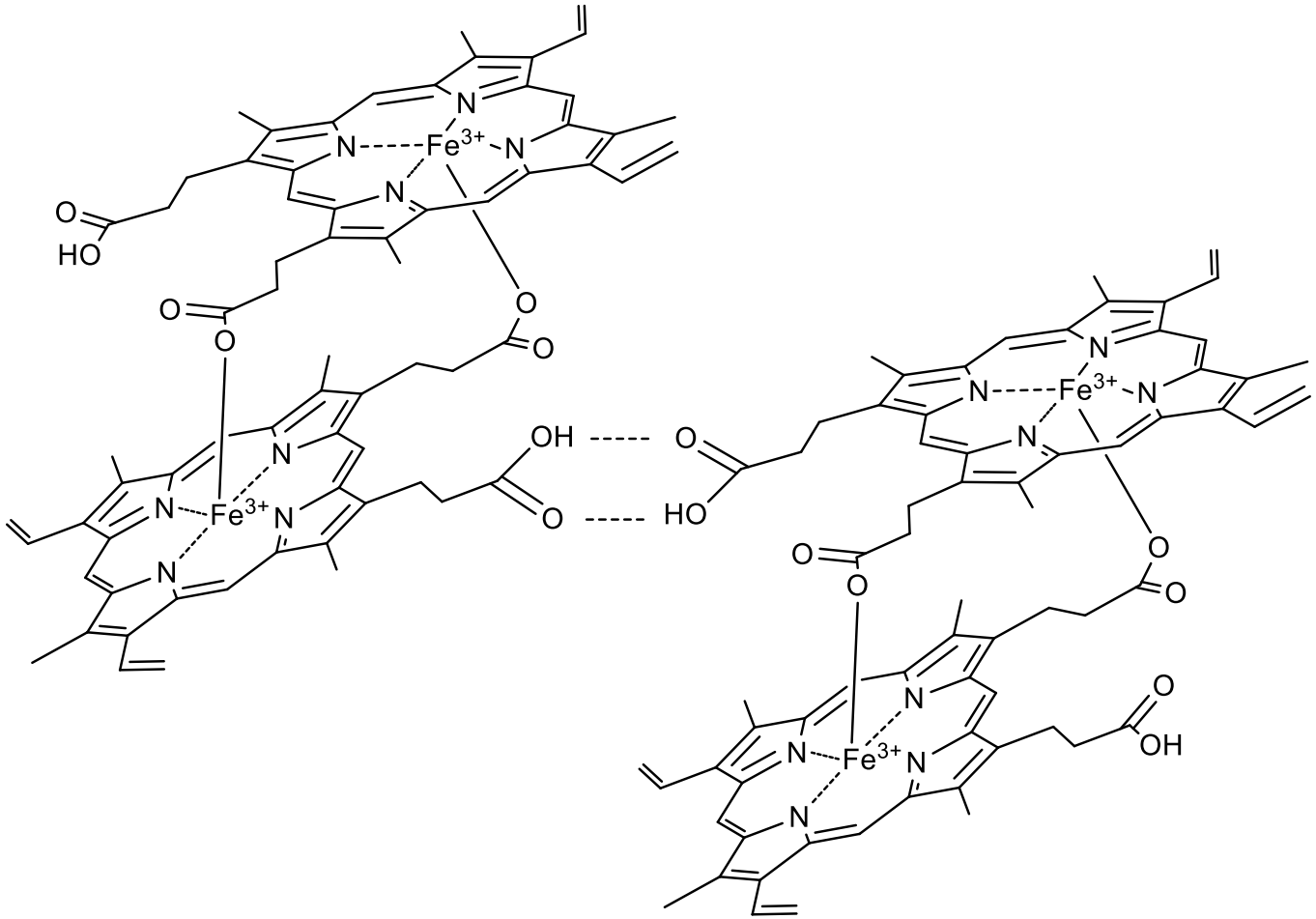

Figure 4-33. Schematic of ferriheme tetramer. Dative covalent bonds form between the oxygen atom in one carboxylic acid group with the Fe^{3+} ion in a second hematin molecule, and hydrogen bonds (- - -) between two carboxylic acid groups on separate dimers. The molecular weight of this ferriheme tetramer is 2,478.

The percentage of radioactive counts (CPM) from the fractions collected between 10 and 30 minutes showed that the majority of the radioactive material eluted between 12.5 and 14.5 minutes, corresponding to the absorbance peak at 13.1 minutes, (Figure 4-32).

The elution time of the radioactive material from the [^{59}Fe]hematin sample indicates the molecular weight of the eluted compound is higher than both hematin (633.2) and GS.hematin (922.8). The calculated molecular weight of the compound eluting at 13.1 minutes is 2,478 which corresponds to the molecular weight of a [^{59}Fe]ferriheme tetramer (Table 4-4, Figure 4-33). Oligomers of hematin, including ferriheme tetramer, are found within parasites, for example *Plasmodium*, therefore the formation of a ferriheme tetramer is plausible (Gorka *et al.,* 2013). The elution of the ferriheme tetramer indicates that single hematin molecules bind to the stationary phase whilst a small proportion form ferriheme tetramer that bind less tightly to the stationary phase and are eluted at 13.1 minutes.

4.3.4.2 HPLC of Caco-2 Cell Lysate for GS.hematin

Caco-2 cells were incubated with either [^{59}Fe]hematin or GS.[^{59}Fe]hematin for 24 hours and the lysed cells injected onto the size exclusion HPLC column. There was no significant difference in hematin absorption or iron effluxed from Caco-2 cell monolayers treated four different ways. The monolayers were either treated with 50 μM [^{59}Fe]hematin, 50 μM [^{59}Fe]hematin with 2 mM glutathione, 2 mM glutathione then 50 μM [^{59}Fe]hematin or 660 μM N-acetyl-L-cysteine then 50 μM [^{59}Fe]hematin. On average the monolayers absorbed in total 25.6 pmol hematin per μg protein and exported 1.8 pmol per μg protein, (Figure 4-34).

HPLC of cell lysate from cells incubated with [^{59}Fe]hematin had 43% of radioactivity eluted between 12.5 and 14.5 minutes, corresponding to ferriheme tetramer, and 27% eluted between 15.5 and 17.5 minutes, corresponding to the GS.hematin complex. This indicates that once absorbed into the cell a small amount of hematin binds to glutathione forming the GS.hematin complex (Figure 4-35).

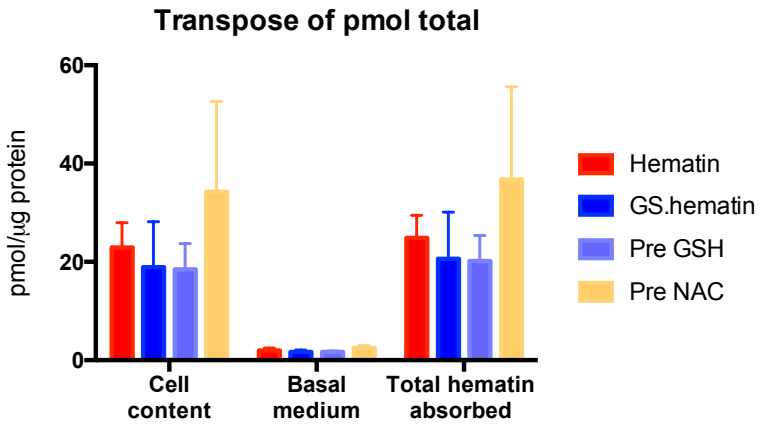

Figure 4-34. Total [^{59}Fe]hematin absorbed by Caco-2 monolayers over 24 hours. Caco-2 cell monolayers were grown in 6-well transwell plates at 37 ^{o}C, 95 % air, 5 % CO_2. Once TEER reached 250 Ωcm^2 they were depleted of iron for 16 hours then pre-incubated for 1 hour with either MEM (Hematin, $FeCl_2$ and GS.hematin) or MEM supplemented with 2 mM glutathione (Pre GSH) or 660 µM N-actyl-L-cysteine (Pre NAC). Monolayers were washed twice and incubated for 24 hours with uptake solutions containing 50 µM [^{59}Fe]hematin (Hematin, Pre GSH and Pre NAC), or 50 µM [^{59}Fe]hematin with 2 mM glutathione (GS.hematin). Monolayers were washed 3 times and cell content collected for detection of [^{59}Fe]hematin and separation by HPLC on PL-aquagel-OH 20 column. The basal medium, containing 12.5 µM apo-transferrin, was collected and counted for effluxed ^{59}Fe. Negative control contained no [^{59}Fe]hematin and therefore had 0 pmol hematin/µg protein. Values are means ± SEM (n=3). There was no significant difference in total amount of hematin absorbed or exported between the different conditions.

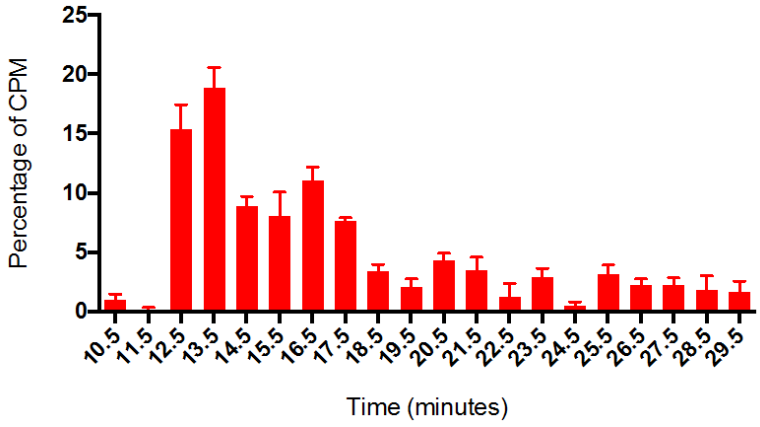

Figure 4-35. Distribution of radioactivity eluted by HPLC on PL-aquagel-OH 20 column from Caco-2 cell lysate incubated with [^{59}Fe]hematin for 24 hours. Cell lysate (100 µL), from Caco-2 cells incubated for 24 hours at 37 ^{o}C, 95 % air, 5 % CO_2 with 50 µM [^{59}Fe]hematin, in a solution of 50 mM phosphate buffer, 5 mM KCl, 12.5 mM Tris-HCl, 2.5 % (v/v) glycerol, 0.5 % (v/v) SDS was injected onto an Agilent PL aquagel-OH 20 column. The sample was eluted with a mobile phase of 20 mM phosphate buffer, 2 mM glutathione, pH 8 at 0.4 mL/min over 30 minutes. 1 minute fractions were collected between 10 and 30 minutes and counted for eluted [^{59}Fe]hematin. The percentage of radioactivity eluted each minute was calculated and plotted against time, showing the majority of the eluted radioactivity was between 12 and 14 minutes and at 16 and 17 minutes, corresponding to ferriheme and GS.hematin respectively. Values are means ± SEM (n=3).

Cells incubated with [^{59}Fe]hematin, 2 mM glutathione had radioactive material eluted between 12.5 and 14.5 minutes and 15.5 and 17.5 minutes, corresponding to ferriheme tetramer and GS.hematin respectively (Figure 4-36).

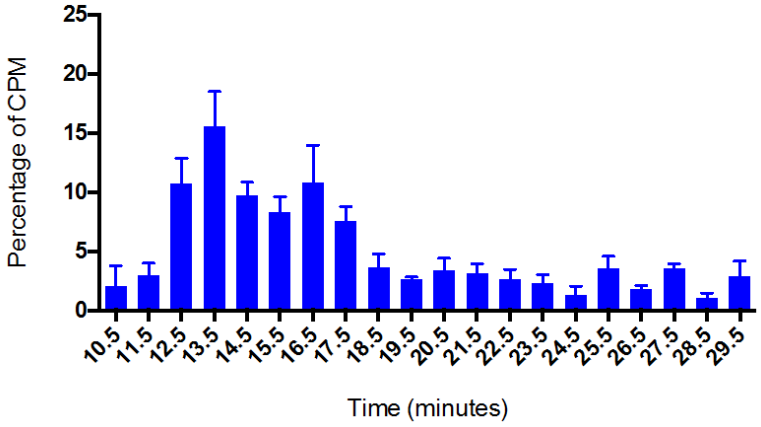

Figure 4-36. Distribution of radioactivity eluted by HPLC on PL-aquagel-OH 20 column from Caco-2 cell lysate incubated with GS.[^{59}Fe]hematin for 24 hours. Cell lysate (100 μL), from Caco-2 cells incubated for 24 hours at 37 ^{o}C, 95 % air, 5 % CO_2 with 50 μM GS.[^{59}Fe]hematin, in a solution of 50 mM phosphate buffer, 5 mM KCl, 12.5 mM Tris-HCl, 2.5 % (v/v) glycerol, 0.5 % (v/v) SDS was injected onto an Agilent PL aquagel-OH 20 column. The sample was eluted with a mobile phase of 20 mM phosphate buffer, 2 mM glutathione, pH 8 at 0.4 mL/min over 30 minutes. 1 minute fractions were collected between 10 and 30 minutes and counted for eluted [^{59}Fe]hematin. The percentage of radioactivity eluted each minute was calculated and plotted against time, showing the majority of the eluted radioactivity was between 12 and 14 minutes and 16 and 17 minutes, corresponding to ferriheme and GS.hematin respectively. Values are means ± SEM (n=3).

The control of [^{59}Fe]hematin incubated with 2 mM glutathione at 37 ^{o}C showed that the dominant form of hematin in the solution was GS.hematin after 24 hours (Figure 4-30), absorb the GS.hematin complex for any radioactivity to be detected within the cells. Once inside the cell a fraction of GS.hematin dissociated, into hematin and glutathione, because 37% of the radioactivity was eluted by HPLC between 12.5 and 14.5 minutes, corresponding to the elution time of tetra-ferriheme. 27% of the radioactivity eluted between 15.5 and 17.5 minutes showing that some of the GS.hematin complex was not degraded and remained as a complex within the cells (Figure 4-36).

Caco-2 cell lysate, from cells incubated for 1 hour with either 2 mM glutathione or 660 μM N-acetyl-L-cysteine, then 24 hours with 50 μM [^{59}Fe]hematin. Both had 43 – 44% of the samples radioactive material eluted between 12.5 and 14.5 minutes, corresponding to ferriheme tetramer, and 21- 24% of the samples radioactive material eluted between 15.5 and 17.5 minutes, corresponding to GS.hematin (Figures 4-37 & 4-38).

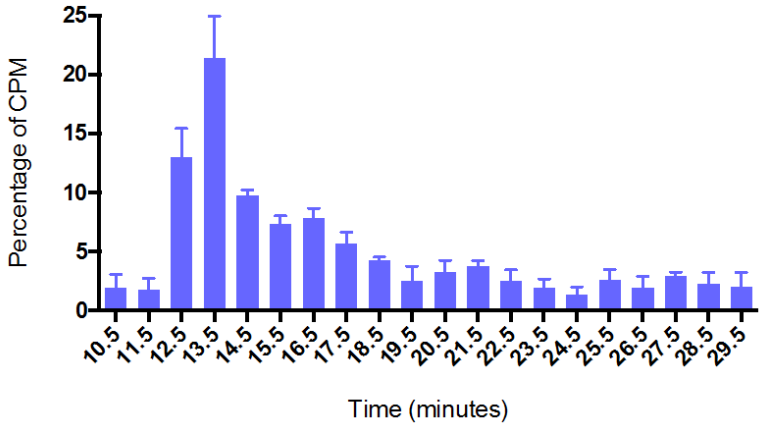

Figure 4-37. Distribution of radioactivity eluted by HPLC on PL-aquagel-OH 20 column from Caco-2 cells incubated with glutathione prior to incubation with [^{59}Fe]hematin for 24 hours. Cell lysate (100 μL), from Caco-2 cells incubated for 1 hour with 2 mM glutathione then 24 hours at 37 ^{o}C, 95 % air, 5 % CO_2 with 50 μM [^{59}Fe]hematin, in a solution of 50 mM phosphate buffer, 5 mM KCl, 12.5 mM Tris-HCl, 2.5 % (v/v) glycerol, 0.5 % (v/v) SDS was injected onto an Agilent PL aquagel-OH 20 column. The sample was eluted with a mobile phase of 20 mM phosphate buffer, 2 mM glutathione, pH 8 at 0.4 mL/min over 30 minutes. 1 minute fractions were collected between 10 and 30 minutes and counted for eluted [^{59}Fe]hematin. The percentage of radioactivity eluted each minute was calculated and plotted against elution time, showing the majority of the eluted radioactivity was between 12 and 14 minutes, corresponding to ferriheme. Values are means ± SEM (n=3).

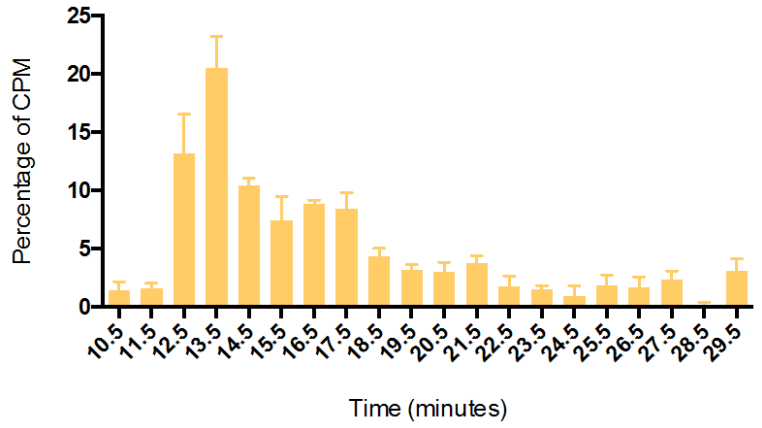

Figure 4-38. Distribution of radioactivity eluted by HPLC on PL-aquagel-OH 20 column from Caco-2 cells incubated with NAC prior to incubation with [^{59}Fe]hematin for 24 hours. Cell lysate (100 μL), from Caco-2 cells incubated for 1 hour with 660 μM N-acetyl-L-cysteine (NAC) then 24 hours at 37 ^{o}C, 95 % air, 5 % CO_2 with 50 μM [^{59}Fe]hematin, in a solution of 50 mM phosphate buffer, 5 mM KCl, 12.5 mM Tris-HCl, 2.5 % (v/v) glycerol, 0.5 % (v/v) SDS was injected onto an Agilent PL aquagel-OH 20 column. The sample was eluted with a mobile phase of 20 mM phosphate buffer, 2 mM glutathione, pH 8 at 0.4 mL/min over 30 minutes. 1 minute fractions were collected between 10 and 30 minutes and counted for eluted [^{59}Fe]hematin. The percentage of radioactivity eluted each minute was calculated and plotted against time, showing the majority of the eluted radioactivity was between 12 and 14 minutes, corresponding to ferriheme. Values are means ± SEM (n=3).

This suggests that once inside the cell, as with cells incubated with hematin alone, a percentage of the absorbed hematin became ligated to glutathione forming the GS.hematin complex.

Table 4-5 Percentage of Radioactive Material with Elution Time that Corresponds to Ferriheme Tetramer and GS.hematin

Treatment	Form of hematin	
	[^{59}Fe]ferriheme tetramer (12.5-14.5 minutes) (% of CPM)	GS.[^{59}Fe]hematin (15.5-17.5 minutes) (% of CPM)
[^{59}Fe]Hematin	43	27
[^{59}Fe]Hematin + glutathione	37	27
Glutathione then [^{59}Fe]hematin	44	21
N-acetyl-L-cysteine then [^{59}Fe]hematin	43	24

Pre-incubating the cells with glutathione, or N-acetyl-L-cysteine the availability of which is the limiting step in glutathione synthesis, did not influence the amount of hematin absorbed or the amount of hematin ligated to glutathione compared to cells incubated with hematin only (Table 4-5).

The percentage of hematin eluted as ferriheme tetramer or GS.hematin from the Caco-2 cell monolayers did not significantly change between the different treatments (Table 4-5).

Overall these results indicate that, not only does the cytoplasm of cells which absorbed GS.[^{59}Fe]hematin contain GS.[^{59}Fe]hematin, but also cells that absorbed [^{59}Fe]hematin alone. This indicates that once [^{59}Fe]hematin is absorbed it binds cytosolic glutathione to form the GS.[^{59}Fe]hematin complex.

4.3.5 Western Blot for Heme Oxygenase-1 Protein Expression

Cells incubated with glutathione or acetylated cysteine for 1 hour prior to incubation with 25 μM hematin for 12 hours absorbed significantly ($P < 0.5$) more hematin then cells which didn't, average 6 ng hematin per μg protein compared to 4.5 ng hematin per μg protein, (Figure 4-39). Thus under these conditions GS.hematin was absorbed at the same rate over 12 hours as hematin, indicating they have the same or similar uptake mechanisms into the cell. The potential increase in concentration of glutathione and cysteine within the cell, through incubating the cells with glutathione or acetylated cysteine prior to hematin incubation, increased hematin absorption by 2 ng/μg protein from cells incubated with only hematin (Figure 4-39).

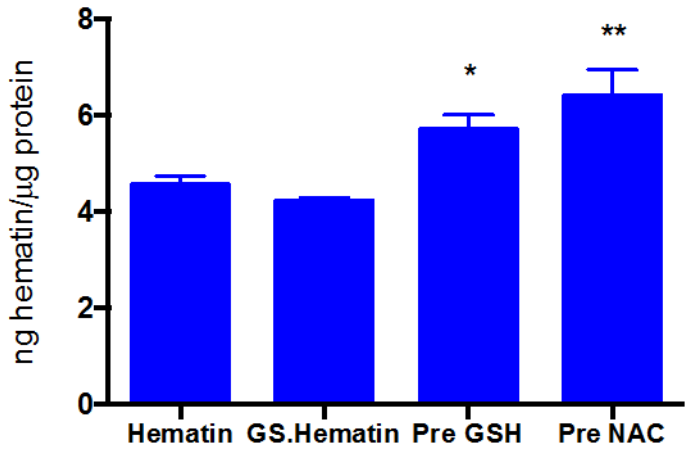

Figure 4-39. Hematin retained in Caco-2 monolayers over 12 hours. Caco-2 cell monolayers were grown for 14 days in 12-well plates at 37 ^{o}C, 95 % air, 5 % CO_2, depleted of iron for 16 hours then pre-incubated for 1 hour with either MEM, (Hematin and GS.hematin) or MEM supplemented with 2 mM glutathione (Pre GSH) or 660 μM N-acetyl-L-cysteine (Pre NAC). Monolayers were washed twice and incubated for 12 hours with uptake solutions containing 25 μM hematin and 10,000 CPM of [^{59}Fe]hematin (Hematin, Pre GSH and Pre Cys), or 25 μM hematin with 2 mM glutathione and 10,000 CPM of [^{59}Fe]hematin (GS.hematin). Monolayers were washed 3 times and cell content collected for detection of [^{59}Fe]hematin. Negative control contained no radioactive material or hematin and therefore had 0 pmol hematin/μg protein. Values are means ± SEM (n=3 experimental duplicates). Asterisks indicate significant difference ($P < 0.05$ *, 0.01 **) hematin vs. condition.

Caco-2 cells incubated with 25 μM hematin had a significantly higher ($P < 0.001$) expression level of HO-1 compared to cells incubated only with no hematin (negative control), (Figure 4-40). Cells pre-incubated with glutathione or acetylated cysteine, then incubated with 25 μM hematin, or cells incubated with 25 μM hematin and 2 mM glutathione had a significant decrease ($P < 0.05$) in HO-1 expression compared to cells incubated with only 25 μM hematin (Figure 4-40, 4-41 & 4-42).

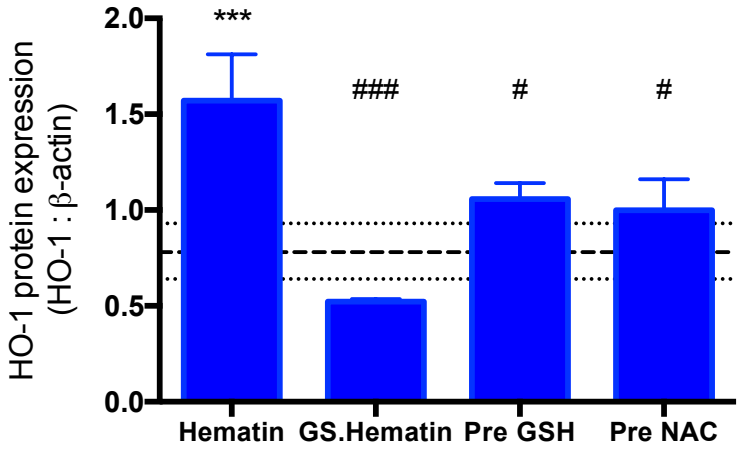

Figure 4-40. HO-1 expression levels in Caco-2 cells incubated with hematin for 12 hours. Expression levels of HO-1 protein as a ratio of β-actin protein in Caco-2 cells pre-incubated for 1 hour with either MEM, (Hematin and GS.hematin) or MEM supplemented with 2 mM glutathione (Pre GSH) or 660 μM N-acetyl-L-cysteine (Pre NAC) then incubated for 12 hours with uptake solutions containing 25 μM hematin and 10,000 CPM of [^{59}Fe]hematin (Hematin, Pre GSH and Pre Cys), or 25 μM hematin with 2 mM glutathione and 10,000 CPM of [^{59}Fe]hematin (GS.hematin) at 37^{o}C, 95 % air, 5 % CO_2. Negative control contained no hematin, and the mean (- - -) ± SEM (· · ·) is plotted on the graph. Values are means ± SEM (n=3 experimental duplicates). Asterisks indicate significant difference (P < 0.001 ***) negative control vs. condition. Hash tags indicate significant difference (P < 0.05 $^{\#}$, P < 0.001 $^{\#\#\#}$) hematin vs. condition.

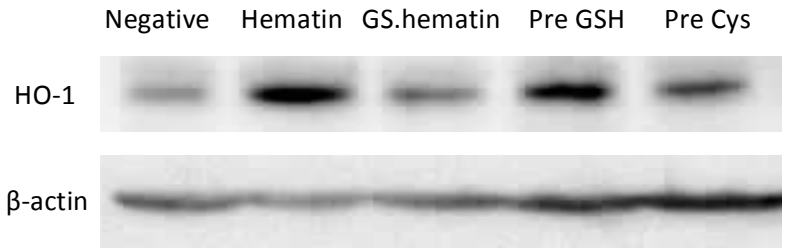

Figure 4-41. Representative Western Blot of HO-1 expression in Caco-2 monolayer incubated with hematin. Caco-2 cells pre-incubated for 1 hour with either MEM, (Hematin and GS.hematin) or MEM supplemented with 2 mM glutathione (Pre GSH) or 660 μM N-acetyl-L-cysteine (Pre NAC) then incubated for 12 hours with uptake solutions containing 25 μM hematin and 10,000 CPM of [^{59}Fe]hematin (Hematin, Pre GSH and Pre Cys), or 25 μM hematin with 2 mM glutathione and 10,000 CPM of [^{59}Fe]hematin (GS.hematin) at 37^{o}C, 95 % air, 5 % CO_2. Expression of HO-1 was assessed by immunoblotting and expressed as a ratio of β-actin. Cell protein was separated on 12 % SDS-PAGE gel by electrophoresis at 150 V for 70 minutes and HO-1 and β-actin protein was visualised through immunoblotting with HO-1 and β-actin primary antibodies, followed by anti-rabbit and anti-mouse secondary antibodies respectively and HPR substrate with images captured with G:Box Syngene.

The ratio of HO-1 expression to β-actin, when standardised to hematin, showed a significant increase (P < 0.01) in HO-1 expression in cells incubated with only hematin, compared to cells incubated with hematin in the presence of glutathione (GS.hematin) or

cells pre-incubated with glutathione (Pre GSH) or acetylated cysteine (Pre NAC) then hematin (Figure 4-42). Cells incubated with only hematin had 0.08 HO-1 protein expression standardised to β-actin and hematin absorbed, double the amount of HO-1 expressed compared to cells incubated with GS.hematin, pre-incubated with glutathione then hematin or cells pre-incubated with acetylated cysteine then hematin, which had an average of 0.04 HO-1 protein expression standardised to β-actin and hematin absorbed (Figure 4-42).

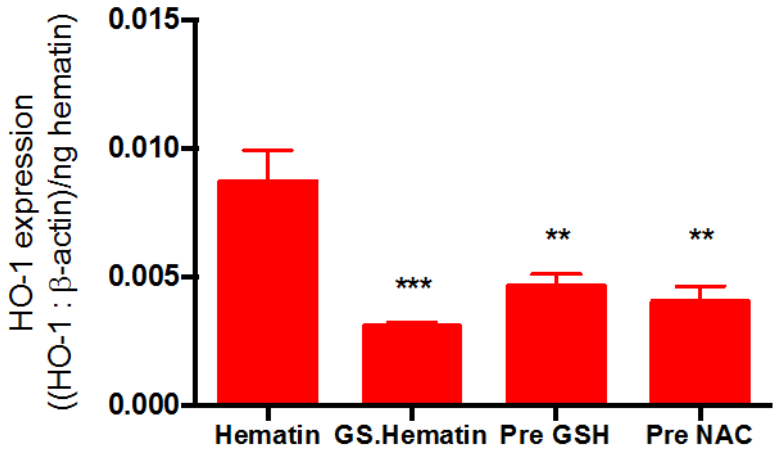

Figure 4-42. HO-1 expression levels standardised to hematin cell content in Caco-2 cells incubated with hematin for 12 hours. Expression of HO-1 as a ratio of β-actin expressed and hematin in Caco-2 cells pre-incubated for 1 hour with either MEM, (Hematin and GS.hematin) or MEM supplemented with 2 mM glutathione (Pre GSH) or 660 μM N-acetyl-L-cysteine (Pre NAC) then incubated for 12 hours with uptake solutions containing 25 μM hematin and 10,000 CPM of [^{59}Fe]hematin (Hematin, Pre GSH and Pre Cys), or 25 μM hematin with 2 mM glutathione and 10,000 CPM of [^{59}Fe]hematin (GS.hematin) at 37^{o}C, 95 % air, 5 % CO_2. Negative control was not incubated with hematin and therefore not present on the graph. Values are means ± SEM (n=3 experimental duplicates). Values are means ± SEM (n=3 experimental duplicates). Asterisks indicate significant difference (P < 0.05 *, 0.01 **, 0.001 ***) hematin vs. condition.

The significant increase (P < 0.001) in HO-1 expression in cells incubated with hematin, and the decrease in HO-1 expression in cells incubated with GS.hematin, compared to cells incubated with no hematin (negative control), indicates that whilst hematin and GS.hematin affect HO-1 expression in Caco-2 cells they do so in different ways (Figure 4-40). HO-1 is an enzyme that catabolises hematin, protecting the cell from the harmful affects of labile organic iron. Therefore, the increase in HO-1 expression in cells incubated with hematin is logical, whilst the decrease in HO-1 expression in cells incubated with GS.hematin suggests that HO-1 is not required to protect the cell from hematin when hematin is ligated to glutathione.

This data implies that glutathione decreases the expression of HO-1 by forming the GS.hematin complex with hematin. The resulting decrease in labile hematin means less hematin is able to bind to Bach1 resulting in the continued repression of *ho-1* transcription. HO-1 protects the cell from oxidative stress, which free hematin causes through the productions of free radicals. When hematin is bound to glutathione the redox state of iron is stable and therefore free radicals are not produced. This means that GS.hematin minimises oxidative stress caused from the redox cycling of free organic iron and therefore HO-1 is not required to catabolise hematin to prevent the oxidative stress.

4.3.6 GS.hematin Stability in the Presence of Ascorbic Acid

4.3.6.1 Absorption Spectrum of Hematin and GS.hematin in the Presence of Ascorbic Acid

There is minimal change in absorption between 500 nm and 700 nm when hematin is incubated with 300 µM ascorbic acid for an hour (Figure 4-44). However when GS.hematin was incubated with 300 µM ascorbic acid for an hour the absorbance spectrum changed, (Figure 4-45).

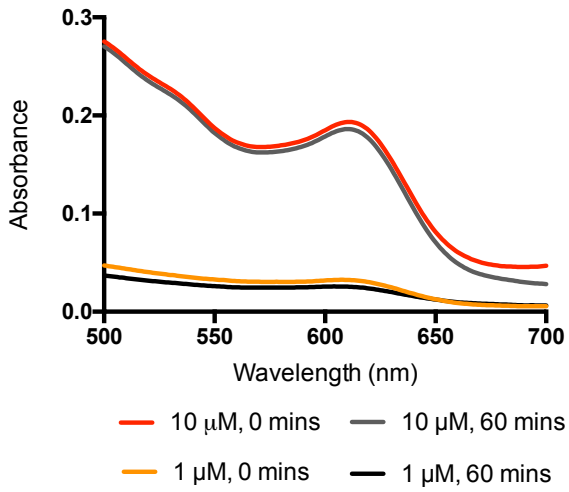

Figure 4-44. Absorption spectrum of hematin in the presence of 300 µM ascorbic acid, over 50 minutes. Hematin was dissolved, to a final concentration of 10 µM or 1 µM, in 10 mM phosphate buffer, 20 mM KCl, pH 8 and an initial absorption reading between 500 nm and 700 nm was taken (10 µM red line, 1 µM orange line), prior to the addition of 300 µM ascorbic acid after which absorption readings were taken every 5 minutes, (only 60 minute absorption reading shown, 10 µM hematin grey line, 1 µM hematin black line). The initial solutions of hematin had an absorption peak at 618 nm that remained after 60 minutes incubation with 300 µM ascorbic acid.

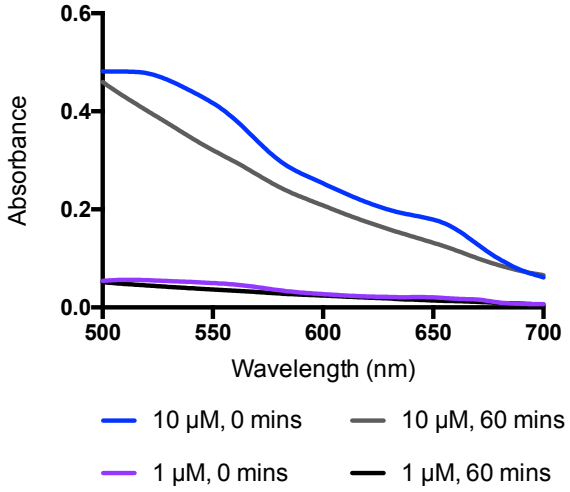

Figure 4-45. Absorption spectrum of GS.hematin in the presence of 300 µM ascorbic aicd, over 60 minutes. Hematin was dissolved, to a final concentration of 10 µM or 1 µM, in 10 mM phosphate buffer, 20 mM KCl, 2 mM glutathione, pH 8 and an initial absorption reading between 500 nm and 700 nm was taken (10 µM blue line, 1 µM purple line), prior to the addition of 300 µM ascorbic acid after which absorption readings were taken every 5 minutes, (only 60 minute absorption reading shown, 10 µM grey line, 1 µM black line). The initial solutions (blue and purple lines) had two absorption peaks, at 550 nm and 655 nm, which disappear with the addition of ascorbic acid (grey and black lines) indicating ascorbic acid degrades the GS.hematin complex.

The peaks at 550 nm and 655 nm, which correspond to GS.hematin, disappeared over 60 minutes resulting in a decreasing linear absorption spectrum from 500 nm to 700 nm. If ascorbic acid caused glutathione to dissociate from hematin the appearance of an absorption peak at 618 nm, corresponding to hematin, would be expected. Previous experiments in our lab, (not shown), showed that glutathione does not bind heme. Therefore if the hematin, within the GS.hematin complex, was reduced to heme by ascorbic acid it would cause glutathione to dissociate and an absorption peak to appear at 580 nm corresponding to heme (Shviro & Shaklai, 1987). No peak appeared at either 580 nm or 618 nm indicating that ascorbic acid degraded/interacted with the GS.hematin complex rather than causing glutathione to dissociate from hematin, or causing the reduction of hematin to heme (Figure 4-45).

The degradation of GS.hematin and hematin by ascorbic acid was followed by the change in absorbance at 550 nm and 618 nm respectively.

4.3.6.2 Hematin and GS.hematin Stability in the Presence of Ascorbic Acid in Air

In the presence of 100 µM ascorbic acid, GS.hematin was not degraded in the first 15 minutes however significant degradation ($P < 0.05$) of the GS.hematin complex had

occurred within 35 minutes whilst hematin was not degraded over the 60 minute experiment (Figure 4-46).

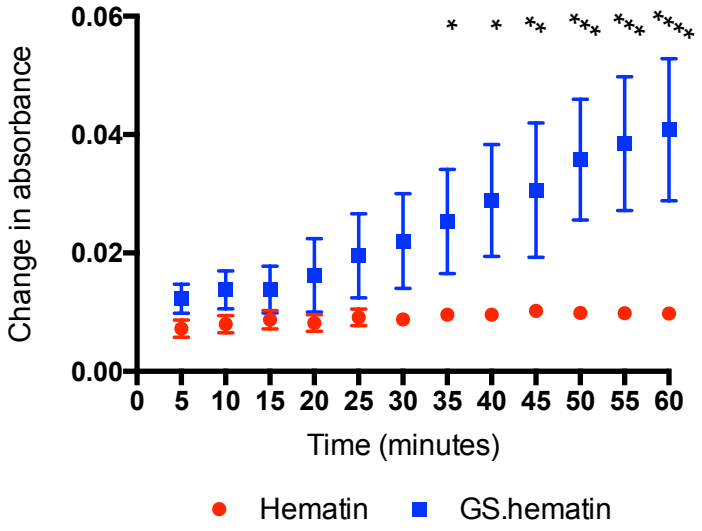

Figure 4-46. Degradation of hematin and GS.hematin over time by 100 µM ascorbic acid. Hematin (10 µM) or GS.hematin (10 µM hematin, 2 mM glutathione) was dissolved in 10 mM phosphate buffer, 20 mM KCl, pH 8 and absorbance recorded at 550 nm (GS.hematin) and 618 nm (hematin), time point 0 minutes. Ascorbic acid was added to a final concentration of 100 µM and absorbance at 550 nm (GS.hematin) and 618 nm (hematin) taken at 5 minute intervals, for 60 minutes. Change in absorbance from time point 0 was plotted against time. Red circles indicate change in absorbance at 618 nm, from time point 0, for hematin solution containing 100 µM ascorbic acid; blue squares indicate change in absorbance at 550 nm, from time point 0, for GS.hematin solution containing 100 µM ascorbic acid. Values are means ± SEM (n=3). Asterisks indicate significant difference (P < 0.05 *, < 0.01 **, < 0.001 ***, < 0.0001 ****) GS.hematin time point 0 vs. GS.hematin individual time points. Where error bars are not visible they are smaller than the point.

In the presence of 300 µM ascorbic acid, GS.hematin (10 µM) degradation occurred within the first 10 minutes and significant degradation (P < 0.05) occurred within 15 minutes, (Figure 4-47). There was no significant degradation of hematin when in the presence of 300 µM ascorbic acid throughout the 60 minute experiment (Figure 4-47). When the concentration of hematin was decreased to 1 µM there was no significant degradation of either hematin or GS.hematin in the presence of 300 µM ascorbic acid over 60 minute period (data not shown). The lack of GS.hematin degradation, when at 1 µM, suggests that ascorbic acid has a weak affinity for the degradation of GS.hematin. It indicates that GS.hematin has to be present in relatively high cellular concentrations for ascorbic acid to degrade the complex.

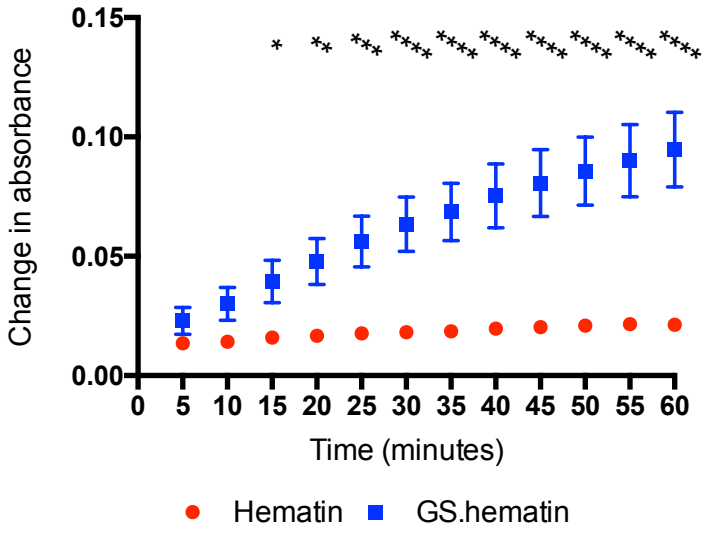

Figure 4-47. Degradation of hematin and GS.hematin over time by 300 µM ascorbic acid. Hematin (10 µM) or GS.hematin (10 µM hematin, 2 mM glutathione) was dissolved in 10 mM phosphate buffer, 20 mM KCl, pH 8 and absorbance recorded at 550 nm (GS.hematin) and 618 nm (hematin), time point 0 minutes. Ascorbic acid was added to a final concentration of 300 µM and absorbance at 550 nm (GS.hematin) and 618 nm (hematin) taken at 5 minute intervals, for 60 minutes. Change in absorbance from time point 0 was plotted against time. Red circles indicate change in absorbance at 618 nm, from time point 0, for hematin solution containing 300 µM ascorbic acid; blue squares indicate change in absorbance at 550 nm, from time point 0, for GS.hematin solution containing 300 µM ascorbic acid. Values are means ± SEM (n=3). Asterisks indicate significant difference (P < 0.05 *, < 0.01 **, < 0.001 ***, < 0.0001 ****) GS.hematin time point 0 vs. GS.hematin individual time points. Where error bars are not visible they are smaller than the point.

In both concentrations of ascorbic acid, GS.hematin degradation continued until the experiment was terminated at 60 minutes when the concentration of hematin was 10 µM. Hematin, both at 1 µM and 10 µM, in the presence of both 100 µM and 300 µM ascorbic acid remained stable and was not degraded or reduced over 60 minutes (Figure 4-46 & 4-47). The initial rate of degradation of GS.hematin at 10 µM hematin was quicker in the presence of 300 µM ascorbic acid compared to 100 µM ascorbic acid (Figure 4-48).

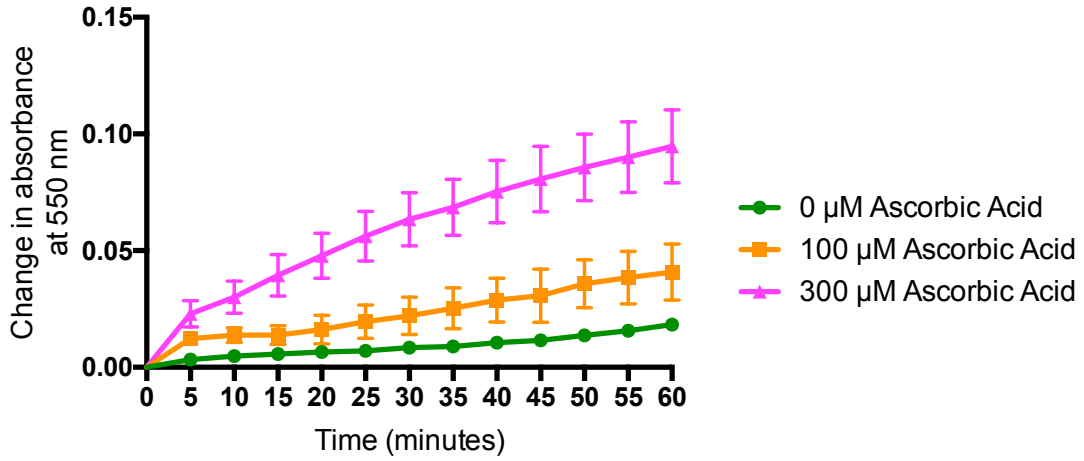

Figure 4-48. Degradation of GS.hematin over time by ascorbic acid. Hematin (10 µM) was dissolved in 10 mM phosphate buffer, 20 mM KCl, 2 mM glutathione, pH 8 and absorbance recorded 550 nm, time point 0 minutes. Ascorbic acid was added at various concentrations, 0 µM (green), 100 µM (orange) and 300 µM (pink) and absorbance at 550 nm taken at 5 minute intervals, for 60 minutes. Change in absorbance from time point 0 was plotted against time. Values are means ± SEM (n=3). Where error bars are not visible they are smaller than the point.

Ascorbic acid is oxidised to dehydroasorbic acid in the presence of oxygen, therefore the degradation of GS.hematin by ascorbic acid could be affected by oxygen. The concentration of oxygen in air is 21% whilst the concentration of oxygen within the cytosol of cells is 5-6% therefore for the experiment to be performed under physiological conditions it should be undertaken in 5% oxygen not 21% oxygen.

4.3.6.3 Hematin and GS.hematin Stability in the Presence of Ascorbic Acid in 5% Oxygen

The overall trend shows that in 5% oxygen, as in air, the GS.hematin complex is degraded by ascorbic acid but hematin alone is not. GS.hematin is significantly degraded by the presence of 100 µM ascorbic acid within 10 minutes in 5% oxygen, and degradation continues throughout the 60 minute experiment. (Figure 4-49).

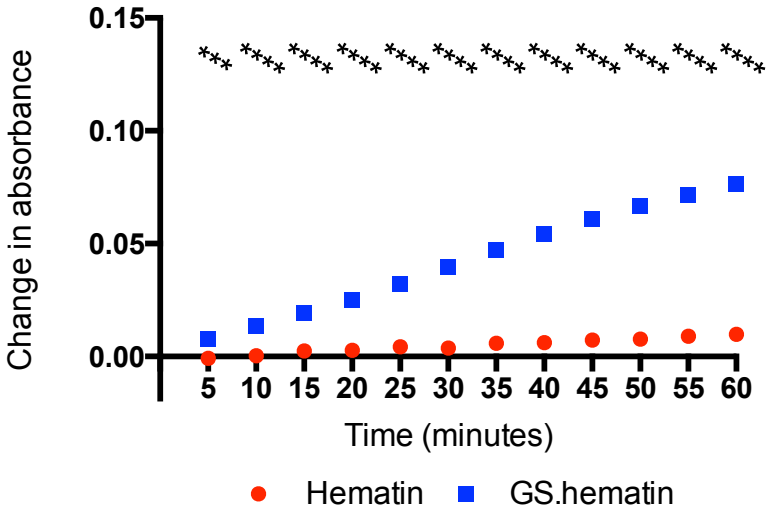

Figure 4-49. Degradation of hematin and GS.hematin over time by 100 μM ascorbic acid in 5 % oxygen. Hematin (10 μM) or GS.hematin (10 μM hematin, 2 mM glutathione) was dissolved in 10 mM phosphate buffer, 20 mM KCl, pH 8 and 90 % N_2, 5 % CO_2, 5 % O_2 bubbled through the solutions for 30 minutes. Absorbance of the solutions was recorded at 550 nm (GS.hematin) and 618 nm (hematin), time point 0 minutes. Ascorbic acid was added to a final concentration of 100 μM and absorbance at 550 nm (GS.hematin) and 618 nm (hematin) taken at 5 minute intervals, for 60 minutes. Change in absorbance from time point 0 was plotted against time. Red circles indicate change in absorbance at 618 nm, from time point 0, for hematin solution containing 100 μM ascorbic acid; blue squares indicate change in absorbance at 550 nm, from time point 0, for GS.hematin solution containing 100 μM ascorbic acid. Values are means ± SEM (n=3). Asterisks indicate significant difference ($P < 0.001$ ***, < 0.0001 ****) GS.hematin time point 0 vs. GS.hematin individual time points. Where error bars are not visible they are smaller than the point.

In the presence of 300 μM ascorbic acid GS.hematin is significantly degraded ($P < 0.001$) within 10 minutes in 5% oxygen and continues to be degraded until the experiment is terminated at 60 minutes. Hematin remains stable throughout the 60 minute incubation and is not degraded or reduced by the higher concentration of ascorbic acid (Figure 4-50).

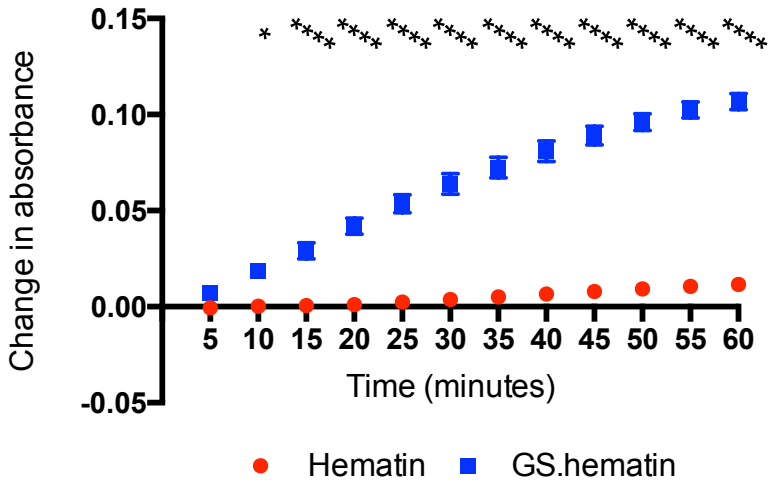

Figure 4-50. Degradation of hematin and GS.hematin over time by 300 μM ascorbic acid in 5 % oxygen. Hematin (10 μM) or GS.hematin (10 μM hematin, 2 mM glutathione) was dissolved in 10 mM phosphate buffer, 20 mM KCl, pH 8 and 90 % N_2, 5 % CO_2, 5 % O_2 bubbled through the solutions for 30 minutes. Absorbance of the solutions was recorded at 550 nm (GS.hematin) and 618 nm (hematin), time point 0 minutes. Ascorbic acid was added to a final concentration of 300 μM and absorbance at 550 nm (GS.hematin) and 618 nm (hematin) taken at 5 minute intervals, for 60 minutes. Change in absorbance from time point 0 was plotted against time. Red circles indicate change in absorbance at 618 nm, from time point 0, for hematin solution containing 300 μM ascorbic acid; blue squares indicate change in absorbance at 550 nm, from time point 0, for GS.hematin solution containing 100 μM ascorbic acid. Asterisks indicate significant difference ($P < 0.05$ *, < 0.0001 ****) GS.hematin time point 0 vs. GS.hematin individual time points. Where error bars are not visible they are smaller than the point.

Unlike in the presence of air (21% oxygen) the initial degradation rate of GS.hematin by ascorbic acid in 5% oxygen does not appear to be dependent on ascorbic acid concentration, change in absorption up to 10 minutes is the same in the presence of 100 μM and 300 μM ascorbic acid (Figure 4-51). However the total degradation of GS.hematin over 60 minutes is less in the presence of 100 μM compared to 300 μM ascorbic acid (Figure 4-51).

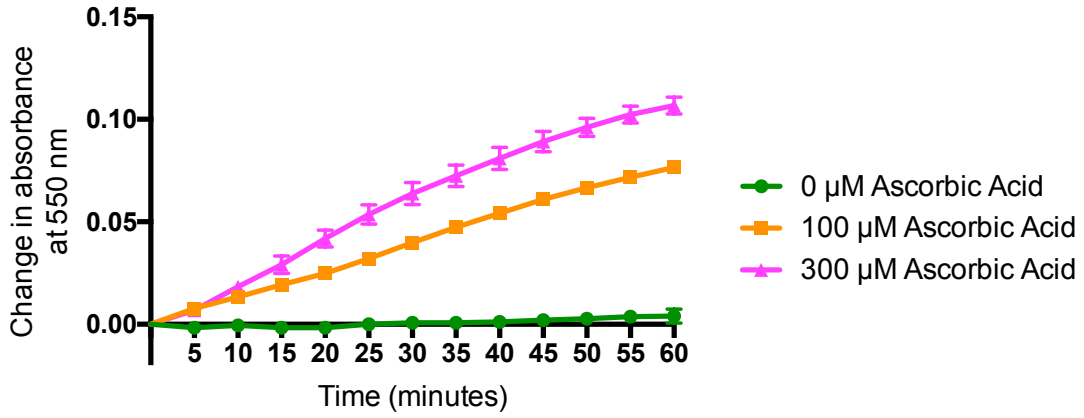

Figure 4-51. Degradation of GS.hematin over time by ascorbic acid in 5 % oxygen. Hematin (10 µM) was dissolved in 10 mM phosphate buffer, 20 mM KCl, 2 mM glutathione, pH 8 and 90 % N_2, 5 % CO_2, 5 % O_2 bubbled through the solutions for 30 minutes. Absorbance of the solutions was recorded at 550 nm, time point 0 minutes. Ascorbic acid was added at various concentrations, 0 µM (green), 100 µM (orange) and 300 µM (pink) and absorbance at 550 nm taken at 5 minute intervals, for 60 minutes. Change in absorbance from time point 0 was plotted against time. Values are means ± SEM (n=3). Where error bars are not visible they are smaller than the point.

GS.hematin degradation over 60 minutes, when incubated with 300 µM ascorbic acid, resulted in an average change in absorbance of 0.1 in both air and 5% oxygen conditions. The degradation of GS.hematin by 100 µM ascorbic acid after 60 minutes resulted in an average change in absorbance of 0.04 in air and 0.08 in 5% oxygen. To determine if the degradation of GS.hematin by ascorbic acid required oxygen the experiment was repeated under nitrogen.

4.3.6.4 GS.hematin Stability in the presence of Ascorbic Acid in Nitrogen

When GS.hematin was incubated under nitrogen conditions with 300 µM ascorbic acid there was no change in absorbance and therefore no degradation of the GS.hematin complex over 60 minutes, unlike when the incubation occurred under air atmosphere or 5% oxygen atmosphere (Figure 4-52). This demonstrates that the degradation of GS.hematin by ascorbic acid requires the presence of oxygen.

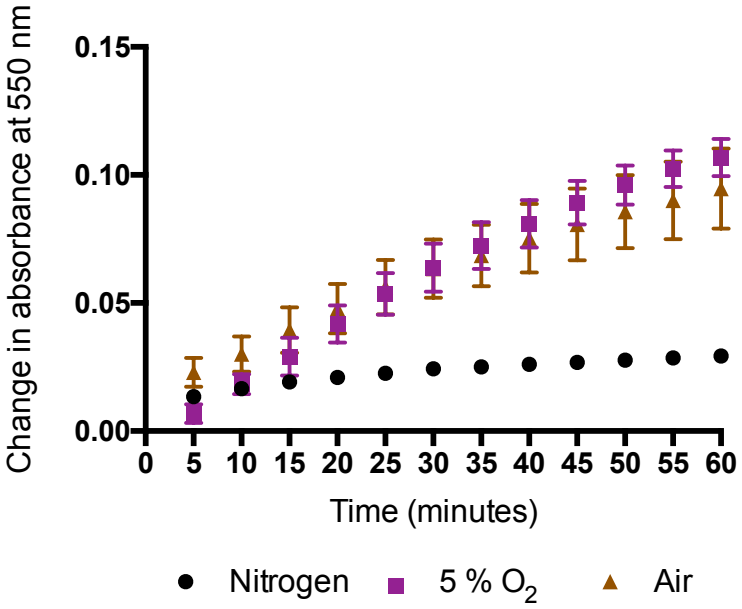

Figure 4-52. Degradation of GS.hematin over time by 300 μM ascorbic acid under different oxygen concentrations. Hematin (10 μM) was dissolved in 10 mM phosphate buffer, 20 mM KCl, 2 mM glutathione, pH 8 and either left for 30 minutes (air, gold triangles), had 100 % N_2 (Nitrogen, black circles) or 90 % N_2, 5 % CO_2, 5 % O_2 (5 % O_2, purple squares) bubbled through the solution for 30 minutes. Absorbance of the solutions was recorded at 550 nm, time point 0 minutes. Ascorbic acid was added to a final concentration of 300 μM and absorbance at 550 nm taken at 5 minute intervals, for 60 minutes. Change in absorbance from time point 0 was plotted against time. Values are means ± SEM (n=3). Where error bars are not visible they are smaller than the point.

The reactions demonstrate that hematin is stable in the presence of physiological concentrations of ascorbic acid. GS.hematin however is degraded by ascorbic acid when present at relatively high cellular concentrations, (10 μM) however at low concentrations (1 μM) the GS.hematin complex is as stable as hematin.

The degradation of high concentrations of GS.hematin by ascorbic acid contradicts the theory that glutathione stabilises hematin thereby protecting the cell from oxidative damage caused by free hematin.

4.4 General Discussion

The significant reduction in hematin partitioning into lipid bilayers, its stability in the presence of H_2O_2 and the continued down regulation of HO-1, when ligated to glutathione, gives weight to the concept that the main species of hematin in the cytosol is the GS.hematin complex.

The formation of GS.hematin affected the partitioning of hematin into prepared liposomes and the plasma membrane of erythrocytes. Formation of the larger, more bulky and less

hydrophobic GS.hematin complex effectively retards hematin partitioning into liposomes and significantly decreases the amount of hematin which partitions into the extracellular face of erythrocyte membranes. Whilst the formation of GS.hematin did decrease hematin partitioning into the erythrocyte plasma membrane the effect was not as dramatic as observed in liposomes. Lipid bilayers are a fluid matrix however the fluidity of the bilayer varies depending on its composition (Ballas & Krasnow, 1980). The prepared liposomes had a more homogenous lipid bilayer compared to that of the plasma membrane of erythrocytes due to the absence of embedded and tethered proteins. The composition of plasma membranes, which consist of approximate equal parts of lipid and protein, result in microdomains occurring within the membrane (Mouritsen & Andersen, 1998; Finean *et al.*, 1978; Tanford, 1980). The microdomains have different properties resulting in a heterogeneous fluidity and curvature of the membrane (Mouritsen & Andersen, 1998; Finean *et al.*, 1978; Tanford, 1980). The heterogeneous nature of the microdomains within the erythrocyte membrane results in sections of the membrane being able to accommodate the insertion of the more bulky GS.hematin complex, which is less well accommodated in the more homogeneous liposomes.

The cytoplasmic face of the plasma membrane contains negatively charged phospholipids and has fewer proteins embedded in the bilayer compared to the extracellular membrane face (Verkleij *et al.,* 1973; Ballas & Krasnow, 1980). This asymmetry means that the negatively charged liposomes are probably a better representation of the cytoplasmic monolayer of erythrocyte plasma membranes. The experiments using negatively charged liposomes indicate that the formation of GS.hematin in the cytosol would drastically decrease hematin partitioning into the cytosolic monolayer of plasma membranes.

Hematin has been shown to be absorbed into Caco-2 cells (Follett *et al.,* 2002) however once inside the cell there is controversy as to how the hematin is processed and in what form the organic iron takes. Size exclusion HPLC of Caco-2 cell lysate showed that both [^{59}Fe]hematin and GS.[^{59}Fe]hematin were present in the cytoplasm of cells incubated with both [^{59}Fe]hematin and GS.[^{59}Fe]hematin, indicating that a portion of the absorbed [^{59}Fe]hematin formed GS.[^{59}Fe]hematin once inside the cytoplasm of the Caco-2 cells.

The expression of HO-1 demonstrated that Caco-2 cells incubated with GS.hematin had significantly less HO-1 expressed compared to cells incubated with hematin alone. This suggests that the GS.hematin complex does not induce HO-1 expression. Cells incubated with glutathione or acetylated cysteine prior to hematin incubation resulted in a decrease

in HO-1 expression compared to cells incubated with only hematin. The decrease in HO-1 expression in cells incubated with glutathione or acetylated cysteine prior to hematin was comparable to HO-1 expression in cells incubated with GS.hematin. The HO-1 expression data suggests that incubating cells with glutathione or acetylated cysteine prior to hematin increases the concentration of glutathione within the cell. If this were not the case the amount of HO-1 expressed in cells pre-incubated with glutathione and acetylated cysteine would not be significantly different then HO-1 expression in cells incubated with only hematin.

All this data is consistent with the concept that GS.hematin is the dominant form of hematin in the cytosol of cells. However the degradation of GS.hematin, at higher concentrations (10 µM), by ascorbic acid does not fit this concept, namely glutathione binds to hematin to protect the cell from the toxic effects of free organic iron.

4.5 Conclusions

Previous studies have shown a decrease in haemolysis when erythrocytes were incubated with hemin and glutathione instead of hemin alone (Sahini *et al.,* 1996). Our studies have shown that in the presence of glutathione hematin partitioning into lipid bilayers is retarded. Therefore it is likely that glutathione reduces haemolysis by reducing hematin partitioning into plasma membranes.

The stability of GS.hematin in the presence of H_2O_2 and the decrease in hematin partitioning into lipid bilayers when hematin is bound to glutathione supports the concept that GS.hematin is the predominant form of organic iron in the cytosol of mammalian cells. The presence of GS.[^{59}Fe]hematin within the lysate of Caco-2 cells also gives weight to this concept. The continued downregulation of HO-1 in Caco-2 cells incubated with GS.hematin and the presence of GS.hematin in the cytoplasm of Caco-2 cells incubated with GS.hematin and hematin provides further indirect evidence for this statement.

The enhanced degradation of the GS.hematin complex in the presence of ascorbic acid in contrast to hematin lone does not readily fit the above general concept, a matter that is considered in more detail in the next chapter (Chapter 5).

5. Discussion

5.1 Distribution and Interaction of Iron with Intracellular Compounds

Whilst hepatocytes store the body's excess iron, in the form of ferritin, the majority of iron, around 65%, is found within erythrocytes. Enterocytes and reticuloendothelial macrophages contain an increased amount of iron compared to other cell types within the human body due to their functions. Enterocytes line the gastrointestinal tract therefore any iron taken up into the body must be transported through enterocytes. If the concentration of iron within the body is high these enterocytes will not release iron from the basal membrane into the blood and therefore a build up of iron occurs in enterocytes (Qioa *et al*., 2012). Enterocytes have the highest turnover rate in the body of any fixed-cell population, between 2 and 6 days, (Mayhew *et al*., 1999) therefore any iron retained within the enterocytes of the duodenum is excreted from the body due to the mechanical shearing of the enterocytes. Reticuloendothelial macrophages contain a large amount of iron due to their role in recycling senescent erythrocytes whilst erythrocytes contain a large amount of iron, in the form of heme as the prosthetic group of haemoglobin.

5.1.1 Hydrogen Peroxide

Hydrogen peroxide (H_2O_2) is found in human tissue due in part to the diet, with instant coffee and black tea containing high concentrations of H_2O_2, (>100 µM) (Halliwell *et al.,* 2000) and in part due to cellular activities including respiration. Hydrogen peroxide is produced through the dismutation of superoxide radical, which can occur both enzymatically and non-enzymatically (Chance *et al*., 1979; Halliwell *et al.,* 2000). Hydrogen peroxide is also produced as a by-product of oxidase enzymes (Halliwell *et* a., 2000), including glycollate and monoamine oxidiases as well as peroxisomal pathway for β-oxidation of fatty acids and therefore the mitochondria is a major source of H_2O_2 (Boveris & Cadenas, 2000). Hydrogen peroxide is freely miscible with water and can easily cross lipid bilayers, thus H_2O_2 can readily partition from the mitochondria into the cytosol of cells. Therefore H_2O_2 is found throughout all cellular compartments of human tissue (Halliwell *et al* 2000). Hydrogen peroxide, in the absence of transition metal ions, is poorly reactive, possessing only mild oxidising and reducing capabilities (Halliwell *et al.,* 2000). However, transition metals, especially iron, render H_2O_2 to become a strong oxidising agent. The Fenton reaction (Equation 1-1) is the interaction between H_2O_2 and iron(II), which results in the production of free radicals. The free radicals interact with various biological molecules, including proteins, DNA and lipids, resulting in the further propagation of free radicals.

Catalase is an enzyme that protects against such free radical damage by degrading H_2O_2, to water and molecular oxygen. More recently H_2O_2 has been shown to be an intracellular signalling molecule (Tang *et al*., 2007; Gough & Cotter, 2011). Within macrophages H_2O_2 induces the secretion of high mobility group box 1 (HMGB1), from the nucleus where it predominantly resides (Tang *et al*., 2007). High mobility group box 1 is a nuclear protein that has recently been identified as a cytokine mediator as well as a transcription and growth factor (Tang *et al*., 2007). When released from the nucleus the extracellular HMBG1 results in a wide range of biological responses including the activation of further macrophages.

5.1.1.1 Hydrogen Peroxide in Mammalian Cells

Enterocytes, reticuloendothelial macrophages and erythrocytes all contain high concentrations of iron and varying concentrations of H_2O_2. Thus iron and H_2O_2 will interact to some degree within these three cell types. Glutathione is an established ligand for cytosolic inorganic labile iron, thereby preventing H_2O_2 from interacting with iron, however the fate of organic iron in these three cell types is not established.

Due to the ingestion of H_2O_2-containing food and drink, the enterocytes in the gastrointestinal (GI) tract are likely to be subjected to higher concentrations of H_2O_2 compared to other cell types. Enterocytes are the cells through which iron enters the body and therefore iron, both organic and inorganic, could come into contact with H_2O_2 in enterocyte cytosol. Inorganic iron is sequestered into ferritin within enterocytes, therefore it would not be available as a substrate for the Fenton reaction. The pathway of organic iron, which is not catabolised by heme oxygenase (HO), in enterocytes is currently unknown. If organic iron taken up by enterocytes was free within the cytosol of the cells it could interact with H_2O_2, through the Fenton reaction, resulting in the production of free radicals. Therefore it is logical that hematin is sequestered in a manner such that it is largely separated from H_2O_2 within enterocytes, in order to maintain the integrity of the cell and to prevent cell death via ferroptosis.

Reticuloendothelial macrophages are phagocytic cells that are activated by H_2O_2 (Tang *et al.* 2006) and produce H_2O_2, from molecular oxygen via an NADPH oxidase complex (Rhee *et al* 2003). This specifically synthesised H_2O_2 is used to degrade material that has been engulfed by the macrophage. Due to the relatively high levels of iron and H_2O_2 within macrophages, macrophages would appear to be prone to ferroptosis. For macrophages not to succumb to ferroptosis they must be able to sequester, or stabilise, the heme iron

which is continually released from the senescent erythrocytes thereby inhibiting the redox cycling of the iron.

Erythrocytes do not contain mitochondria and therefore do not produce H_2O_2 as a biproduct of cellular respiration. The production of H_2O_2 within erythorcytes predominantly comes from the autooxidation of oxyhaemoglobin (Giulivi *et al*., 1994). When oxyhaemoglobin autooxidises O_2^- is produced, and subsequently reduced to H_2O_2 through the catalytic action of superoxide dismutase (Giulivi *et al*., 1994). Due to the high concentration of iron within erythrocytes the probability of the small amount of H_2O_2 interacting with iron is higher then in most cells types and therefore, like enterocytes and macrophages, a system must be in place to stabilise the labile iron pool and inhibit the Fenton reaction.

5.1.1.2 Hydrogen Peroxide in the Presence of Iron in Mammalian Cells

If iron, either organic or inorganic, is not ligated or physically separated from H_2O_2 within mammalian cells the result is the continuous production of free radicals via the Fenton reaction. Cells possess mechanisms to reverse the damage caused by free radicals produced through the Fenton reaction, for example the reduction of lipid peroxides via the enzymatic oxidation of glutathione by glutathione peroxidase 4 (GPX4), (Yang *et al.* 2014). If the production of free radicals outweighs the reduction of lipid peroxides, ferroptosis can occur. The chelation of inorganic iron by various biological molecules, including glutathione, renders it unavailable as a substrate for the Fenton reaction (Hider & Kong 2011; Hider & Kong 2013), therefore protecting the cell from the production of free radicals and ultimately ferroptosis. In contrast little is known about how the organic labile iron pool is prevented from participation in Fenton reactions and subsequent ferroptosis. Lipid membranes (ie vesicles) do not offer an effective barrier. If, however hematin were to be ligated to a compound that stabilised the charge of the iron and sequestered it away from H_2O_2 this could result in the inhibition of the heme induced Fenton reaction. In principle the ligand could be glutathione, as it has been shown to be a ligand for inorganic iron (Hider & Kong 2011; Hider & Kong 2013) and is present throughout all mammalian cells in millimolar concentrations (Kondo *et al.,* 1995; Soboll *et al.,* 1995). If glutathione did ligate hematin, causing organic iron to be unavailable as a substrate for H_2O_2 in the Fenton reaction, then the production of free radicals would cease, and ferroptosis prevented.

5.1.2 Ascorbic Acid

Unlike the majority of animals, humans cannot synthesise ascorbic acid due to a mutation in the gene encoding L-gulonolactone oxidase, and hence it is a vitamin (Du *et al.* 2012; Nishikimi *et al.*, 1994). Ascorbic acid is a water soluble ketolactone molecule with two ionisable hydroxyl groups (Du *et al.* 2012). Ascorbate can undergo two consecutive, one-electron, oxidations resulting in dehydroascorbic acid (DHA) (Du *et al*. 2012). Both ascorbic acid and DHA are absorbed into the body through the enterocytes of the small intestine (Malo & Wilson, 2000). Ascorbic acid is absorbed into enterocytes through Na^+-dependant vitamin C transporters (SVCTs) whilst dehydroascorbic acid is absorbed via Na^+-independent facilitative glucose transporters (GLUTs) and then reduced to ascorbate (Welch *et al.*, 1995). The overall concentration of ascorbate within the body is determined by both intestinal absorption and renal re-absorption.

Ascorbic acid has numerous biological functions all of which rely on the fact that ascorbate is an electron donor (Du *et al.,* 2012). As well as the antiscorbutic properties of ascorbate it also maintains iron in the ferrous state thereby maintaining the activity of collagen hydroxylases, and contributes to the intracellular reducing environment, thereby protecting cells from oxidative damage (Lane & Lawson, 2009; Murad *et al.*, 1981).

5.1.2.1 Ascorbic Acid in Mammalian Cells

Ascorbic acid and DHA are optimally absorbed by the enterocytes lining the ileum and distal segments on the small intestine (Malo & Wilson, 2000) whilst iron is best absorbed into enterocytes in the duodenum and proximal segments of the small intestine. Ascorbate, secreted by enterocytes, is used to reduce lumen ferric inorganic iron to ferrous iron for transport via DMT1 into enterocytes (Pountney *et al*., 1999).

The concentration of ascorbic acid varies between cell types depending on the expression levels of SVCTs and the cell requirement for ascorbate. On average cells contain 300 μM ascorbate (Diem & Lenter, 1970). Neurons have one of the highest concentrations of ascorbate at 10 mM, whilst erythrocytes have on average 60 μM and leucocytes have between 1.2 mM and 4 mM, depending on cell type (Du *et al*., 2012).

Erythrocytes have a relatively low concentration of ascorbic acid compared to the average cell, 60 μM compared to 300 μM (Diem & Lenter, 1970; Du *et al.*, 2012) however erythrocytes play a vital role in recycling ascorbic acid. Erythrocytes express abundant amounts of GLUT1 on their surface thereby rapidly taking up DHA from the plasma (May

1998). The erythrocytes then reduce DHA to ascorbic acid using glutathione as the electron donor, and then slowly releases the recycled ascorbic acid back into the plasma (May 1998).

Macrophages, as phagocytes, produce oxygen radicals as part of their immune response. To control the toxic effects of the oxygen radicals, and maintain their cellular function, macrophages contain a high concentration of antioxidants, including ascorbic acid (Victor *et al*., 2000).

5.1.2.2 Ascorbic Acid in the Presence of Iron in Mammalian Cells

Although erythrocytes do not have a high concentration of ascorbic acid compared to other cell types (Du *et al.* 2012) they contain very high levels of iron. The majority of the iron within erythrocytes is in the form of haemoglobin; around 2% is methaemoglobin (Bowman & Rand, 1980) and the degradation of heme proteins, including haemoglobin, results in the release of small amounts of both hematin and inorganic iron into the cytosol of cells. Enterocytes and macrophages contain relevantly high concentrations of both ascorbic acid and iron therefore the probability of iron, either inorganic or organic, interacting with ascorbic acid in the cytosol of both enterocytes and macrophages is high.

When inorganic iron is released from iron containing proteins or taken up by enterocytes it is quickly sequestered into ferritin or enters the inorganic labile iron pool where glutathione maintains the pool and ensures the inorganic iron remains in the ferrous state (Hider & Kong, 2013). The fate of organic iron, released from degraded heme proteins in erythrocytes and macrophages, or organic iron taken up into enterocytes, is unknown, however if it were to remain free in the cytosol it would quickly oxidise to hematin due to the cytosolic environment. The hematin could then interact with numerous cellular components including ascorbic acid, with the results potentially being detrimental to the cell. In order to inhibit the potential interaction, and possible toxic effects, of hematin and ascorbic acid the sequestering of hematin away from ascorbic acid is desirable. Unlike H_2O_2, ascorbic acid has a slow rate of non-facilitated diffusion across lipid bilayers, and therefore the encapsulation of hematin into vesicles could sequester hematin away from ascorbic acid. However, the sequestering of hematin into a vesicle would not change the highly hydrophobic properties of hematin, therefore hematin would likely partition into the vesicle membrane resulting in the lysis of the membrane and eventual release of hematin back into the cytosol. To prevent this from occurring a ligand that would make hematin less planar and more hydrophilic could reduce the proportion of hematin partitioning into

lipid membranes, ensuring the integrity of the vesicle, and the separation of hematin from ascorbic acid being maintained.

5.2 A Duel Role for Glutathione

For the inorganic labile iron pool (Fe(II)) glutathione is established as a cytosolic buffer, it efficiently prevents auto-oxidation of Fe(II) and so minimises redox action of this iron pool (Hider & Kong, 2011). Unlike the inorganic labile iron pool the nature of the organic labile iron pool is unknown. At the outset of this thesis, the question was asked does glutathione have the same role with the heme cytosolic pool.

5.3 The Search for a Ligand Capable of Ligating Organic Iron

Due to the fluctuations in heme requirement within cells, an organic labile iron pool is required that can be rapidly mobilised and utilised by the cell in order to maintain cellular function. The concentration of organic labile iron within a range of mammalian cells has been estimated to be between 20 nM and 10 μM using various techniques and cell types (Garrick *et al.,* 1999; Hanna *et al.,* 2016). Whether the concentration of 'free' organic iron is 20 nM or 10 μM it must be ligated to inhibit redox cycling between oxidation states thereby controlling the toxic effects of heme iron. Logically the pool would require a ligand that would inhibit the redox cycling ability of organic iron whilst still making it available for cellular processes. Thus the candidate ligand must be able to ligate organic iron however the affinity constant of said ligand must be sufficiently low not to compete with heme-proteins. The ligand must be present at a concentration within the cells, such that even with a relatively weak affinity constant, all labile organic iron would be ligated. The ligand would preferably also be able to increase heme solubility and prevent heme aggregation and precipitation which would increase the bioavailability of heme within the cell (Ponka *et al.,* 2017).

Glutathione concentrations range from 2-8 mM in the cytosol of cells, whilst increasing to 11 mM within the mitochondria, where the final steps of heme synthesis occur (Soboll *et al.,* 1995). Glutathione is a strong reducing agent and a key player in the maintenance of the reducing environment of the cytosol (López-Mirabal & Winther, 2007). It has recently been shown (Kong & Hider, 2011) that glutathione acts as a buffer reservoir for inorganic iron, binding Fe(II) and reducing auto-oxidised inorganic iron back to the ferrous state. In

contrast Silver *et al*. (1985) showed that, rather surprisingly, glutathione did not reduce hematin to heme, instead, in the presence of glutathione organic iron remained in the ferric state. Shviro and Shaklai (1987) elaborated on this interaction by providing spectroscopic evidence for the ligation of glutathione to hemin and deduced it was through the thiol group of glutathione to the iron in hematin. The spectroscopic results in Chapter 2 confirm these previous observations and provide further support for the existence of the glutathione – hematin interaction.

The lack of interaction between glutathione and gallium protoporphyrin provided evidence of the involvement of the 3d orbitals, of iron, in the ligation of glutathione to hematin. Gallium protoporphyrin is in the +3 oxidation state, like hematin, however gallium is not a transition metal. Gallium in the +3 oxidation state contains 10 electrons in the 3d orbitals whilst iron contains only 5. Recently published data (Dereven'kow *et al.,* 2017) provides further evidence for the necessity of partially filled 3d orbitals for the ligation of metal containing tetrapyrrole ring ligation to glutathione. Dereven'kow *et al.,* (2017) demonstrated that cobalamin(III), a corrin structure with cobalt centrally bound via 4 nitrogen atoms, a similar structure to hematin, bound glutathione forming glutathionylcobalamin. Cobalt, like iron, is a transition metal, which in the +3 oxidation state contains 6 electrons in the 3d orbitals meaning, like iron(III) in hematin, cobalt(III) contains only partially filled 3d orbitals. If only the thiol group and 3d orbitals were involved in the ligation of glutathione to hematin, the expectation would be for the affinity constant of cysteine to be in the same order of magnitude to that of glutathione. This however is not the case; with cysteine having an affinity constant at least two orders of magnitude lower then glutathione, $1.6x10^{2}$ M^{-1} compared to $5x10^{4}$ M^{-1}. This significant difference in cysteine and glutathione affinity constants implies the hydrophobic interaction between the peptide backbone, of glutathione, and the planar protoporphyrin ring, of hematin, is involved in the ligation of hematin but glutathione. The hydrophobic interaction between the two molecules results in one face of the highly hydrophobic hematin molecule being shielded from the aqueous cytosolic environment, by glutathione, which is advantageous to hematin and does not occur when ligated to cysteine.

The ligation of hematin by glutathione would protect the cell from the toxic effects of organic iron whilst still maintaining an organic labile iron pool from which heme-proteins could be provided with organic iron. This is because the affinity constant of glutathione for hematin (5×10^{4} M^{-1}), although large enough to ligate <99% of organic iron within the cell,

will not compete with heme-proteins, which can have affinity constants as high as 10^{14} M^{-1} (Hargrove *et al.,* 1996), for heme.

Western Blot analysis of mammalian cells demonstrates a decrease in HO-1 expression resulting from the potential increase in cytosolic glutathione concentrations. This would suggest that hematin absorbed by Caco-2 cells quickly ligates to glutathione, forming GS.hematin. This results in a decrease in labile hematin in the cytosol and subsequently the nucleus. With no increase in hematin within the nucleus the Bach1-Maf heterodimer remains bound to the MARE region of *ho-1* gene, resulting in the continued repression of *ho-1*.

Results from Chapter 4 provide evidence that glutathione protects hematin from degradation by H_2O_2 through the formation of GS.hematin. The increased stability of GS.hematin in the presence of H_2O_2, and the significant retardation of hematin partitioning into liposomes, results in a decrease in free radical production. This ultimately leads to a decrease in lipid peroxidation and oxidative stress. An investigation of glutathione on the stability of haemoglobin in the presence of H_2O_2 concurred with our findings that glutathione protects haemoglobin from degradation by H_2O_2 (Simoni *et al.,* 2009).

5.4 Ferroptosis

Ferroptosis is a unique iron-dependant form of non-apoptotic cell death (Dixon *et al.,* 2012), that is genetically; biochemically and morphologically distant from other cell death modalities (Yang & Stockwell, 2016). Ferroptosis is characterised by the accumulation of lipid-based ROS, resulting from the redox cycling of iron, particularly organic iron, and the absence of the upregulation of apoptotic genes including caspases, BAX and BAK (Dixon *et al.,* 2012; Yang *et al.,* 2014; Yang & Stockwell, 2016). Lipid peroxidation is reversed by reducing the peroxide group via the oxidation of glutathione, a reaction catalysed by glutathione peroxidase 4 (GPX4), a phospholipid hydroperoxidase (Yang *et al.,* 2014) (Figure 5-1). If however, GPX4 activity is downregulated or inhibited the damage is not reversed and instead is compounded by continued production of lipid ROS, resulting in ferroptosis. Using high-throughput screening of small molecule libraries RSL3 and erastin were identified as ferroptosis-inducing compounds (Dixon *et al.,* 2012).

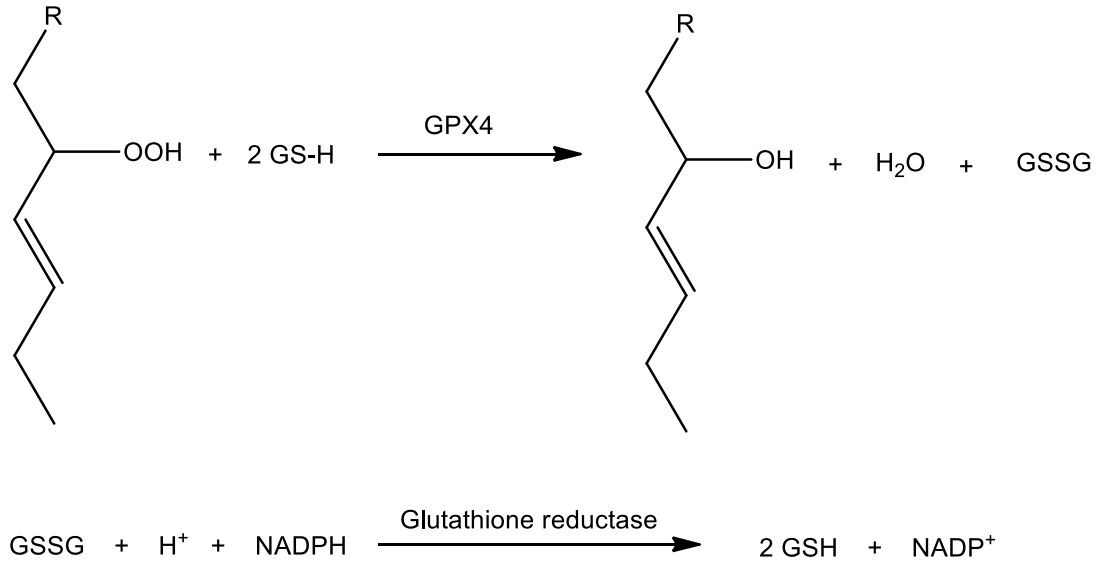

Figure 5-1. Reduction of lipid peroxide by glutathione peroxidase 4. The peroxide group on the lipid is reduced to a hydroxyl group through the oxidation of glutathione, catalysed by glutathione peroxidase 4. Oxidised glutathione is reduced back to reduced glutathione by glutathione reductase and NADPH.

Erastin induced ferroptosis by decreasing cellular concentrations of glutathione, through the inhibition of the cystine/glutamate antiporter, system x_c^- (Dixon *et al.,* 2012 With system x_c^- inhibited, cystine transport into the cell ceases, stopping the *de novo* synthesis of glutathione, due to the lack of cysteine substrate. The continued inhibition of glutathione synthesis, coupled with the perpetual synthesis of oxidants and subsequent requirement for cellular antioxidants, results in the irreversible depletion of glutathione in the cytosol (Yang *et al.,* 2014). RSL3 is another small molecule found through the high throughput screening, that causes ferroptosis through direct binding to GPX4 (Yang *et al*., 2014). Although the mode of action varies between erastin and RSL3 the result is the same, the accumulation of lipid peroxides results from the inhibition of GPX4 and the redox cycling of 'free' iron within the cytosol and plasma membrane. Ferroptosis is a relatively new concept but what research has been conducted has shown that glutathione plays a central role in preventing ferroptosis.

From the various findings presented in section 5.1, we concluded that GS.hematin was the predominant form of iron in the cytosolic organic labile iron pool. Findings in Chapter 4 revealed that although ligation of hematin by glutathione significantly reduced hematin partitioning into erythrocytes membranes, GS.hematin did still partition into the extracellular face of plasma membrane. Thus although it is likely that hematin ligated to glutathione would result in less cellular damage, compared to 'free' organic iron, some damage might still occur which may lead to ferroptosis. These findings suggest that the

original conclusion, that GS.hematin was the predominant form of iron in the organic labile iron pool and protected the cell from redox damage, was not wholly correct. Furthermore conflicting evidence, that GS.hematin was the predominant form of iron in the cytosolic organic labile iron pool, was provided by the observation that enhanced GS.hematin degradation occurred in the combined presence of ascorbic acid and O_2. Ascorbic acid is found in the cytosol of cells, at an average concentration of 300 µM however levels can reach as high as 2 mM in some cells, including the pancreas (Diem & Lentner, 1970). Results in Chapter 4 provided evidence that ascorbic acid degraded GS.hematin, and although the final products of this degradation were not elucidated, the absorbance spectrum of the degraded products confirmed that neither hematin or heme were present in the final solution, suggesting the porphyrin ring had been opened. This is important because destruction of the porphyrin ring will prevent redox cycling.

Thus the combined evidence of GS.hematin partitioning into the plasma membrane of erythrocytes and the degradation of GS.hematin by ascorbic acid and O_2 challenges the original conclusion that GS.hematin is the dominant cytosolic form of organic iron.

5.5 Endosome Transport of Iron – the Possible Involvement of a Heme Chaperone

The last three steps in heme synthesis occur in the mitochondrial matrix, with the last step being the insertion of Fe(II) into PPIX by, the membrane bound, ferrochelatase. The mechanism by which heme is transported out of the mitochondria into awaiting heme-proteins and the cytosol is currently unknown. Taking all the results detailed in this thesis into account, and the fact that organic iron is synthesised as heme, it would suggest that; once synthesised, heme binds to a chaperone to be transported across the mitochondrial membrane into an endosome (Figure 5-2).

Heme would require a chaperone within the endosome to inhibit the partitioning of the highly hydrophobic molecule into the endosome bilayer. Organic iron is synthesised, and likely to be maintained, as heme, whilst glutathione only binds hematin; therefore although found at higher concentrations in the mitochondria, glutathione is unlikely to be the heme chaperone. It has been proposed that the chaperone for heme export from the mitochondria could be the heme-binding protein 1 (HBP1) (Ponka *et al.,* 2017). HBP1 is a 22 kDa protein that binds porphyrins, including heme, with affinity constants in the

micromolar range (Taketani *et al.,* 1998; Jacob Blackmon *et al.,* 2002). HBP1 was originally isolated and purified from the cytosol of mouse liver, however HBP1 is ubiquitously expressed in a wide range of mammalian tissues (Taketani *et al.,* 1998), making it a good candidate for a heme chaperone.

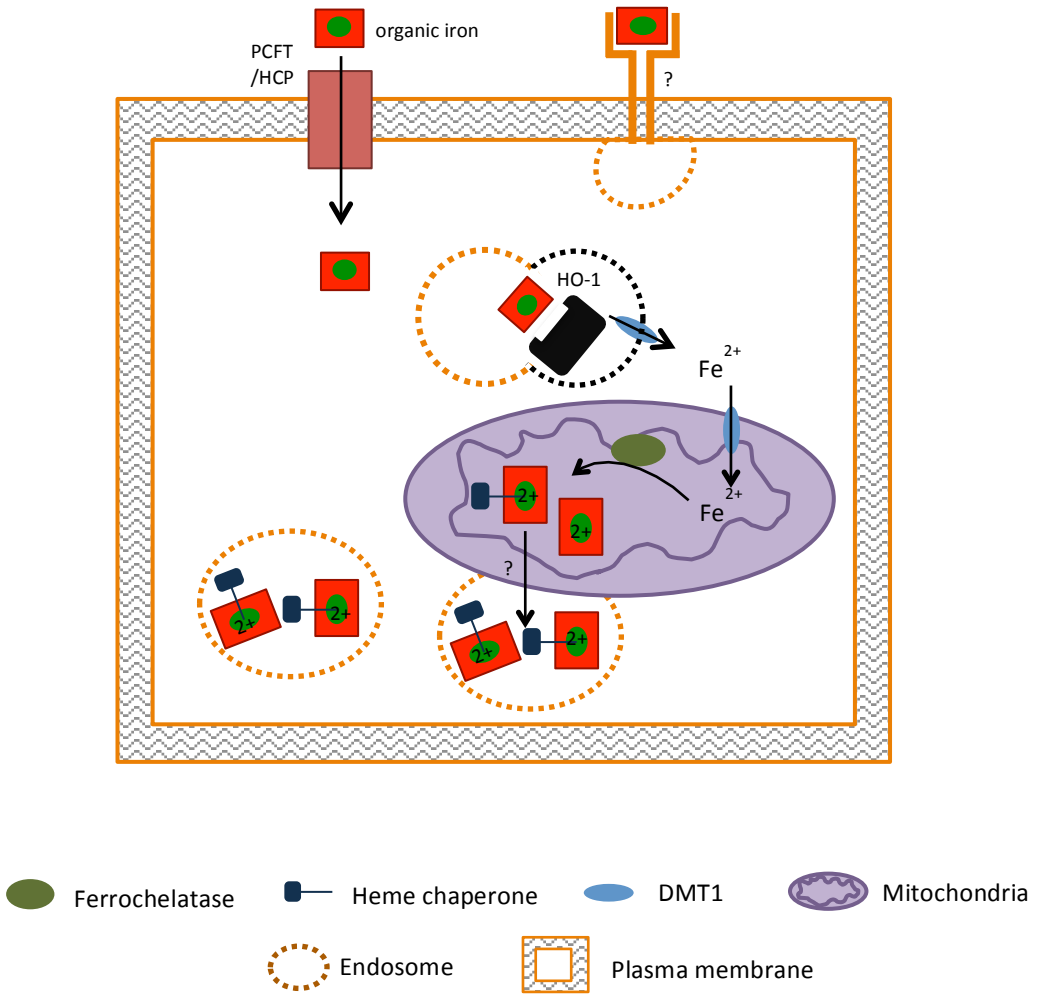

Figure 5-2. Proposed mechanism cellular heme import and mitochondria export. Organic iron transport into cells is proposed to be either via the folate transporter PCFT/HCP1 or through receptor mediated endocytosis. The resulting endosome fuses with a lysosome containing heme oxygenase 1 (HO-1) resulting in the export of inorganic iron into the cytosol via DMT1. The ferrous inorganic iron is transported into the mitochondria via DMT1 where it is incorporated into PPIX by ferrochelatase. The resulting heme is chaperoned out of the mitochondria, by an unknown mechanism, into an endosome. The endosome is released from the mitochondria and transported through the cytosol to heme requiring processes.

Other heme binding proteins include fatty acid-binding protein 1 (FABP1), glutathione *S*-transferases (GSTs) and a 23 kDa heme-binding protein (HBP23). FABP1 is a 14 kDa protein

primarily expressed in the cytoplasm of hepatocytes, containing multiple binding sites, and binds hydrophobic molecules including fatty acids and heme, with affinity for heme in the micromolar range (Vincent & Muller-Eberhard, 1985). Due to the localised expression of FABP1, in the liver, it is unlikely to be the chaperone for heme from mitochondria as heme export from mitochondria is required in all tissues. GSTs are a class of enzyme that functions both as a catalyst, the conjugation of glutathione to xenobiotic substrates and as a general transport protein (Harvey & Beutler, 1982). GSTs have been shown to bind organic iron with micromolar affinity; however experiments were conducted using hemin, rather than heme (Harvey & Beutler, 1982). Published data (Silver & Lukas, 1985) have confirmed that glutathione does not bind heme, only hematin; therefore the likelihood of GSTs binding heme is doubtful, leading to the conclusion that they are unlikely to be the mitochondrial heme export chaperone. HBP23 binds heme with a higher affinity than HBP1, FABP1 and GSTs, ie the nanomolar range (Iwahara *et al.*, 1995). HBP23 has no homology with HBP1 or FABP1 but is highly homologous to stress inducible proteins within mouse macrophages (Iwahara *et al.,* 1995). The homology of HBP23 to oxidative stress inducible proteins suggests an antioxidant role for HBP23 rather than a chaperone role.

5.6 Specific Protective Role of Glutathione

If heme were to partition into the bilayer of the endosome it could lead to endosomal lysis, through lipid peroxidation and loss of bilayer integrity. If this were to happen, or if heme were released from the mitochondria or heme-proteins, directly into the cytosol, it would quickly be auto-oxidised to hematin. If left unligated organic iron would react with H_2O_2 producing free radicals via the Fenton reaction in the cytosol, and partition into lipid membranes resulting in lipid peroxidation (Figure 5-3). However, we suggest that any 'free' heme released within the cytosol, will be oxidised to hematin, and ligated to glutathione in view of the findings reported in Chapter 2. This would significantly reduce the immediate negative effects of 'free' heme in the cytosol (Figure 5-3). The reduction in hematin partitioning into the plasma membrane, and increased stability of GS.hematin in the presence of H_2O_2, would mean the negative effects of organic iron would immediately be reduced. The subsequent degradation of GS.hematin, by the combination of ascorbic

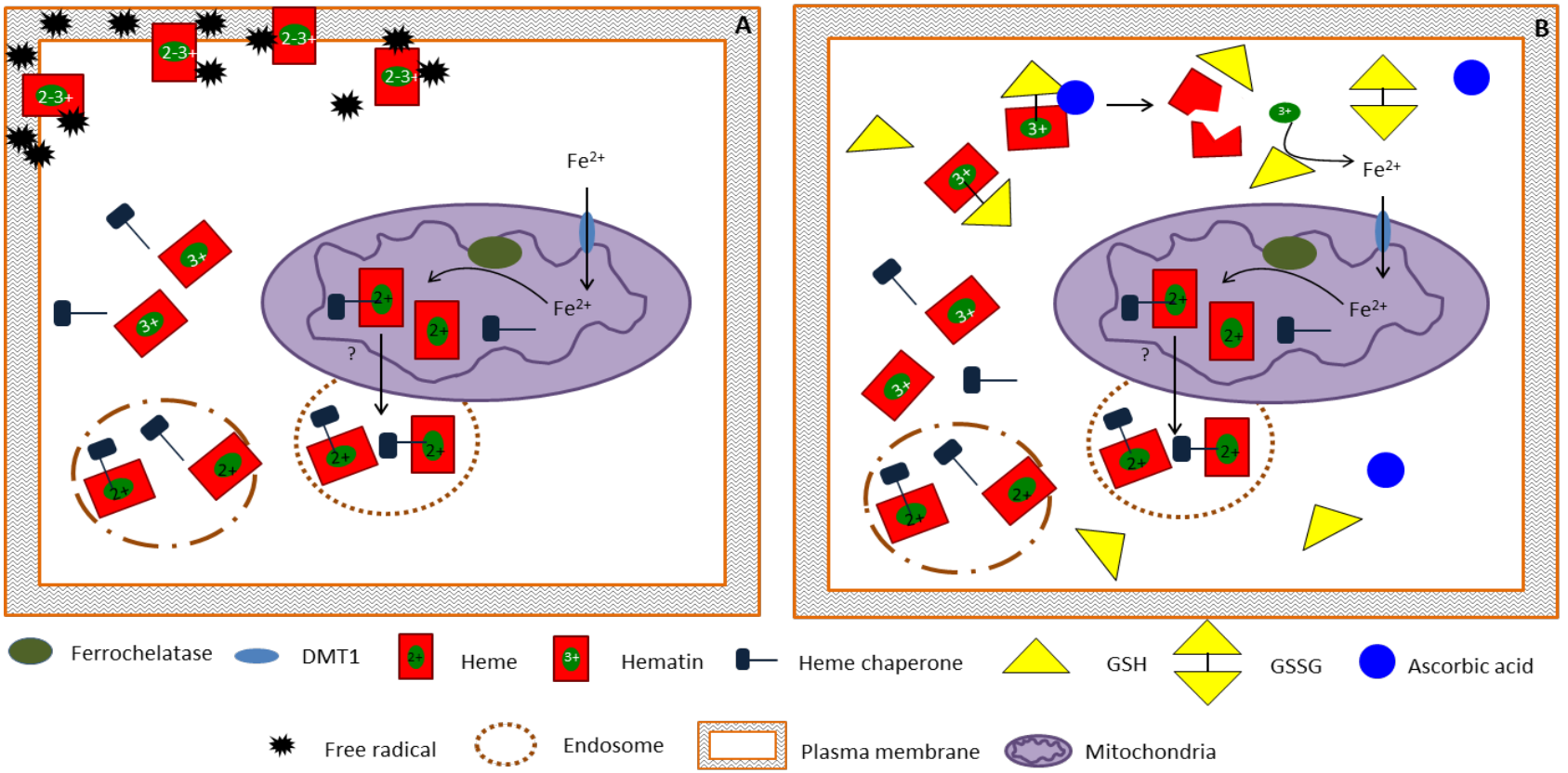

Figure 5-3. Release of heme into the cytosol and subsequent effects. A - Heme synthesised in the mitochondria is chaperoned into a cytosolic endosome. If free heme were to enter the cytosol, through the loss of endosome membrane integrity, and remain unligated it would cause oxidative stress. Heme would quickly auto-oxidise in the cytosol and produce free radicals via the Fenton reaction. Heme would also partition into lipid bilayers resulting in lipid peroxidation. **B –** Release of heme into the cytosol and subsequent ligation with glutathione. GS.hematin inhibits hematin partitioning into the plasma membrane and reaction with H_2O_2. The resulting GS.hematin is degraded by ascorbic acid, likely releasing ferric inorganic iron which is reduced to ferrous iron by glutathione and transported back into the mitochondria for heme synthesis by DMT1.

acid and O_2 in the cytosol, would rapidly eliminate this 'free' hematin, thereby eliminating the root cause of the free radical synthesis, a major contributor to ferroptosis. (Figure 5-3).

5.7 Overview

The concept of endosomes transporting heme throughout the cell, taken in conjunction with the results discussed in this thesis suggests that glutathione protects the cell from oxidative damage caused by free heme by binding to hematin and causing its degradation it in conjunction with ascorbic acid and O_2.

Iron translocation and storage within endosomes is not a new concept. Data supporting the absorption of organic iron by endocytosis, and subsequent translocation of said endosome dates back to 1981 (Parmley *et al*., 1981). More recently, evidence has been published that the transportation of inorganic iron to the mitochondria of maturing erythrocytes, for organic iron synthesis, is also via endosomes (Sheftel *et al.,* 2007; Hamdi *et al.,* 2016). This is in contrast to the prevailing opinion that iron must enter the inorganic labile iron pool, where it diffuses throughout the cytosol, before being transported into the mitochondrial matrix (Ponka *et al.,* 2017). This concept, however, seems rather inefficient considering the size of the cytosol and the mitochondrial requirement for iron. Ponka's group (Sheftel *et al.,* 2007; Hamdi *et al.,* 2016) have provided evidence that endosomes, containing bound transferrin, migrate to the mitochondria where they dock to the mitochondrial membrane and release the inorganic iron within (Sheftel *et al.,* 2007; Hamdi *et al.,* 2016). The endosome only detaches from the mitochondria when a new Fe(II) loaded endosome requires the 'docking site' on the mitochondria (Hamdi *et al.,* 2016).

Heme synthesis is an eight step process. The first step, the formation of aminolevulinic acid from glycine and succinyl-CoA, occurs in the mitochondria. The following four steps, resulting in the formation of coproporphyrinogen III, occur in the cytosol of the cell and the remaining three steps, resulting in the final product, heme, occur in the mitochondrial matrix (Kim *et al*., 2015). The mechanism of translocation of heme from the mitochondrial matrix, where the final stage of heme synthesis occurs, to the cytosol, where it is incorporated into heme proteins, remains unknown. The recent evidence of endosomal delivery of inorganic iron to the mitochondria (Sheftel *et al*., 2007; Hamdi *et al.,* 2016) may hint that a similar system is involved for the export, transportation and storage of heme from the mitochondria to the cytosol. In fact Sheftel *et al.* (2007) concluded that the newly acquired evidence relating to iron transport to the mitochondria, along with previously

published evidence of endosomes trafficking iron to other intracellular compartments, may indicate that iron trafficking in cells in general is achieved via endosomes.

The concept of organic iron being encased in endosomes within the cytosol also fits the evidence of organic iron being absorbed, and transported to the Golgi apparatus, via endocytosis (Parmley *et al*., 1981; Wyllie & Kaufman, 1982). Furthermore evidence has been published relating to other iron sources, including ferritin (Antileo *et al.,* 2013) and nanoparticulate iron (Pereira *et al.,* 2013), being absorbed into enterocytes by endocytosis. The sequestering of organic iron alone into endosomes would merely delay the toxic effects of organic iron rather than inhibiting them. This is because the organic iron would be predicted to partition into the endosome bilayer resulting in the loss of integrity of the bilayer and ultimate release of hematin into the cytosol. To prevent this from happening, organic iron would have to be ligated within the endosome.

The concept proposed of organic iron being isolated from the cytosol by endosomes offers an explanation for the large discrepancy in published concentrations of the organic labile iron pool. The concentration of the organic labile iron pool was calculated to be between 20 and 40 nM when fluorescent probes were used to detect the organic iron (Hanna *et al.,* 2016; Hanna *et al.,* 2017). These probes were either directed to the cytosol or targeted to the nucleus and mitochondria with the addition of a peptide localisation sequence (Hanna *et al.,* 2016). Under these conditions any organic iron that was not present in the cytosol, nucleus or mitochondria would not have been detected. Therefore if organic iron were sequestered within vesicles within the cell the probes would not have detected this portion of cellular organic iron. Garrick *et al.* (1999) used a different technique to observe the organic labile iron pool. Garrick *et al.* (1999) used a chromatography-based system to probe the concentration of labile organic iron within cells. This method was not limited to identifying labile organic iron within the cytosol. Therefore the organic labile iron range that they published, 0.1 µM to 10 µM (Garrick *et al.,* 1999) may reflect both heme free within the cytosol and that sequestered into vesicles or endosomes within the cell.

5.8 Future Work

Whilst the results of this project are conclusive in the affinity and ligation of hematin to glutathione to definitively show the protective role of GS.hematin, further work is required. This includes providing evidence that the ligation of hematin to glutathione decreases

oxidation damage through an oxyblot on cells, with varying concentrations of glutathione, incubated with hematin. The 3-nitrotyrosine assay would be used to detect nitric oxide (NO) levels within cells of various glutathione concentrators, incubation with hematin. Although Western Blot analysis was used to detect HO-1 levels, and provide evidence that glutathione downregulated HO-1 expression qPCR for *ho-1* mRNA would confirm these findings.

GS.[^{59}Fe]hematin was detected in Caco-2 cell lysate using HPLC, however the localisation of the complex within the cell remains unknown. To determine the subcellular location of GS.hematin cells could be cultured in ^{35}S containing medium, meaning any glutathione synthesised within the cell would have ^{35}S incorporated into the molecule. Cells would then be incubated with [^{55}Fe]hematin and after incubation different cellular fractions would be isolated, by centrifuging the cell lysate through a sucrose gradient. The fractions would then be counted for both ^{35}S and ^{55}Fe. If both isotopes were present in stoichiometric amounts it would imply that GS.hematin was formed within that cellular fraction.

5.9 Concluding Remarks

If the integrity of the proposed heme-carrying endosomes is compromised, and heme is released into the cytosol, glutathione will rapidly bind to the auto-oxidised heme, forming GS.hematin. The formation of GS.hematin; reduces the production of free radicals, decreases the partitioning of hematin in to the plasma membrane and promotes heme degradation via ascorbic acid and O_2. Thus the experimental data produced in this thesis does not confirm the role of glutathione, as outlined in Section 5.1, namely that glutathione is the cytosolic buffer for heme, but rather the opposite. Glutathione would appear to still function in a protective capacity against organic iron derived cellular damage, however the manner in which this occurs appears different to that of the buffering role employed for the inorganic iron pool. It is proposed that Glutathione protects the cell from organic iron derived damage via the removal of any non-chaperone-bound heme that has escaped into the cytosol, thereby preventing heme redox cycling and providing protection from ferroptosis.

6 References

Ahad, F., & Ganie, S. A. (2010). Iodine, Iodine metabolism and Iodine deficiency disorders revisited. *Indian Journal of Endocrinology and Metabolism*, *14*, 13–17.

Alderighi, L., Gans, P., Ienco, A., Peters, D., Sabatini, A., & Vacca, A. (1999). Hyperquad simulation and speciation (HySS): a utility program for the investigation of equilibria involving soluble and partially soluble species. *Coordination Chemistry Reviews*, *184*, 311–318.

Alvarez-Hernandez, X., Nichols, G. M., & Glass, J. (1991). Caco-2 cell line: a system for studying intestinal iron transport across epithelial cell monolayers. *Biochimica et Biophysica Acta - Biomembranes, 1070*, 205–208.

Anastácio, A. S., Harris, B., Yoo, H. I., Fabris, J. D., & Stucki, J. W. (2008). Limitations of the ferrozine method for quantitative assay of mineral systems for ferrous and total iron. *Geochimica et Cosmochimica Acta*, *72*, 5001–5008.

Andrews, N. C. (2000). Iron homeostasis: insights from genetics and animal models. *Nature Reviews. Genetics*, *1*, 208–217.

Antileo, E., *et al*. (2013). Endocytic pathway of exogenous iron-loaded ferritin in intestinal epithelial (Caco-2) cells. *American Journal of Physiology. Gastrointestinal and Liver Physiology*, *304*, G655-61.

Arredondo, M., *et al.* (2008). Heme iron uptake by Caco-2 cells is a saturable, temperature sensitive and modulated by extracellular pH and potassium. *Biological Trace Element Research*, *125*, 109–119.

Atkuri, K. R., Mantovani, J. J., Herzenberg, L. A., & Herzenberg, L. A. (2007). N-Acetylcysteine- a safe antidote for cysteine/glutathione deficiency. *Current Opinion in Pharmacology*, *7*, 355–359.

Au, a P., & Reddy, M. B. (2000). Caco-2 cells can be used to assess human iron bioavailability from a semipurified meal. *The Journal of Nutrition*, *130*, 1329–1334.

Azad, B., Cho, C. F., Lewis, J. D., & Luyt, L. G. (2012). Synthesis, radiometal labeling and in vitro evaluation of a targeted PPIX derivative. *Applied Radiation and Isotopes*, *70*, 505–511.

Ballas, S. K., & Krasnow, S. H. (1980). Structure of erythrocyte membrane and its transport functions. *Annals of Clinical and Laboratory Science*, *10*, 209–219.

Bartoszek, M. (2001). Magnetic field effect on hemin. *Physica B: Condensed Matter*, *307*, 217–223.

Beaven, G. H., Chen, S., Albis, A. D., & Gratzer, W. B. (1974). A Spectroscopic Study of the Haemin-Human-Serum-Albumin System. *Eur. J. Biochem, 546*, 539–546.

Behera, R. K., & Theil, E. C. (2014). Moving Fe2+ from ferritin ion channels to catalytic OH centers depends on conserved protein cage carboxylates. *Pnas*, 111, 7925–7930.

Blackmon, B. J., Dailey, T. A., Lianchun, X., & Dailey, H. A. (2002). Characterization of a human and mouse tetrapyrrole-binding protein. *Archives of Biochemistry and Biophysics*, *407*, 196–201.

Boveris, A., & Cadenas, E. (2000). Mitochondrial production of hydrogen peroxide regulation by nitric oxide and the role of ubisemiquinone. *IUBMB Life*, *50*, 245–250.

Bowman, W. and Rand, M. (1980) *Textbook of pharmacology second edition*, London, Blackwell scientific publications.

Breuer, W., Epsztejn, S., & Cabantchik, Z. I. (1995). Iron acquired from transferrin by K562 cells is delivered into a cytoplasmic pool of chelatable iron(II). *Journal of Biological Chemistry*, *270*, 24209–24215.

Breuer, W., Shvartsman, M., & Cabantchik, Z. I. (2008). Intracellular labile iron. International. *Journal of Biochemistry and Cell Biology*, *40*, 350–354.

Brunelle, J. K., et al. (2005). Oxygen sensing requires mitochondrial ROS but not oxidative phosphorylation. *Cell Metabolism*, *1*, 409–414.

Chance, B., Sies, H., & Boveris, A., (1979), Hydroperoxide metabolism in mammalian organs, *Physiological reviews, 59*, 527-605

ChemAxon, www.chemaxon.com/download/marvin-suite, accessed on 30.8.17

Chen, H., et al. (2004). Hephaestin is a ferroxidase that maintains partial activity in sex-linked anemia mice. *Blood*, *103*, 3933–3939.

Conrad, M., Benjamin, B., Williams, H., & Foy, A. (1967). Human Absorption of Hemoglobin-Iron. *Gastroenterology, 53*, 5–10.

Dautry-Varsat, A., Ciechanover, A., & Lodish, H. F. (1983). pH and the recycling of transferrin during receptor-mediated endocytosis. *Pnas*, *80*, 2258–2262.

Dereven'kov, I. A., Makarov, S. V., Shpagilev, N. I., Salnikov, D. S., & Koifman, O. I. (2017). Studies on reaction of glutathionylcobalamin with hypochlorite. Evidence of protective action of glutathionyl-ligand against corrin modification by hypochlorite. *BioMetals*, 1-8.

Devlin, T., (2002). *Biochemistry*, 5th edition, New York, Wiley-Liss. P 564-576

Diem, K. & Lentner, C. (1970). *Documenta Geigy Scientific Tables*, 7th edition, Macclesfield, Geigy pharmaceuticals, p 489-490

Dixon, S. J., et al. (2012). Ferroptosis: An Iron-Dependent Form of Non-Apoptotic Cell Death. *Cell*, *149,* 1060–1072.

Dodge, J. T., & Phillips, G. B. (1967). Composition of phospholipids and of phospholipid fatty acids in human red cells. *Journal of Lipid Research*, *8*, 667–675.

Du, J., Cullen, J. J., & Buettner, G. R. (2012). Ascorbic acid: Chemistry, biology and the treatment of cancer. *Biochimica et Biophysica Acta - Reviews on Cancer*, *1826*, 443–457.

Egyed, A., & Saltman, P. (1984). Iron is maintained as Fe(II) under aerobic conditions in erythroid cells. *Biological Trace Element Research*, *6*, 357–364.

Elmagirbi, A., Sulistyarti, H., & Atikah. (2012). Study of Ascorbic Acid as Iron(III) Reducing Agent for Spectrophotometric Iron Speciation. *Journal of Pure and Applied Chemistry Research*, *1*, 11–17.

Emsley, J. 1998, *The Elements*, 3rd edition, Virginia, Clarendon Press

Emsley, J 2011, *Nature's Building Blocks*, 2nd edition, Oxford, Oxford University Press

Eriksson, S., Graslund, A., Skog, S., Thelander, L., & Tribukait, B. (1984). Cell Cycle-dependent Regulation of Mammalian Ribonucleotide Reductase. *The Journal of Biological Chemistry*, *259*, 11695–11700.

Fidai, I., Wachnowsky, C., & Cowan, J. A. (2016). Glutathione-complexed [2Fe-2S] clusters function in Fe–S cluster storage and trafficking. *JBIC Journal of Biological Inorganic Chemistry*, *21*, 887-901.

Figueroa-Méndez, R., & Rivas-Arancibia, S. (2015). Vitamin C in health and disease: Its role in the metabolism of cells and redox state in the brain. *Frontiers in Physiology*, *6*, 1–11.

Finean, J., Coleman, R., & Michell, R. (1978). *Membranes and their cellular functions*, 2nd edition, Oxford, Blackwell scientific publications, p 37-40

Fischbach, F. A., & Anderegg, J. W. (1965). An X-ray scattering study of ferritin and apoferritin. *Journal of molecular biology*, *14*, 458IN15-473.

Follett, J. R., Suzuki, Y. A., & Lönnerdal, B. (2002). High specific activity heme-Fe and its application for studying heme-Fe metabolism in Caco-2 cell monolayers. *American Journal of Physiology. Gastrointestinal and Liver Physiology*, *283*, G1125-31.

Garcia, M. N., Flowers, C., & Cook, J. D. (1996). The Caco-2 cell culture system can be used as a model to study food iron availability. *Journal of Nutrition*, *126,* 251–258.

Garrick, M. D., Scott, D., Kulju, D., Romano, M. A., Dolan, K. G., & Garrick, L. M. (1999). Evidence for and consequences of chronic heme deficiency in Belgrade rat reticulocytes. *Biochimica et Biophysica Acta - Molecular Cell Research*, *1449*, 125–136.

Giulivi C, Hochstein P & Davies KJ, (1994). Hydrogen peroxide production by red blood cells. *Free radical biology & medicine*, *16*, 123-129

Glahn, R. P., & Van Campen, D. R. (1997). Iron uptake is enhanced in Caco-2 cell monolayers by cysteine and reduced cysteinyl glycine. *The Journal of Nutrition*, *127*, 642–647.

Gorka, A. P., De Dios, A., & Roepe, P. D. (2013). Quinoline drug-heme interactions and implications for antimalarial cytostatic versus cytocidal activities. *Journal of Medicinal Chemistry*, *56*, 5231–5246.

Gough, D. R., & Cotter, T. G. (2011). Hydrogen peroxide: A Jekyll and Hyde signalling molecule. *Cell Death and Disease*, *2*, e213-8.

Granick, S., Sinclair, P., Sassa, S., & Grieninger, G. (1975). Effects by Heme, Insulin, and Serum Albumin on Heme and Protein Synthesis in Chick Embryo Liver Cells Cultured in a Chemically Defined Medium, and a SpectrofluorometricAssay for Porphyrin Composition. *The Journal of Biological Chemistry*, *250*, 1–11.

Grasbeck, R., Kouvonen, I., Lundberg, M., & Tenhunen, R. (1979). An Intestinal Receptor for Heme. *Scandinavian Journal of Haematology*, *23*, 5–9.

Grasbeck, R., Majuri, R., Kouvonen, I., & Tenhunen, R. (1982). Spectral and other studies on the intestinal haem receptor of the pig. *Biochemica et Biophysica Acta*, *700*, 137–142.

Grasset, E., Pinto, M., Dussaulx, E., Zweibaum, A., & Desjeux, J. F. (1984). Epithelial properties of human colonic carcinoma cell line Caco-2: electrical parameters. *Am J Physiol*, *247*, C260-7.

Greenberg, G R; Wintrobe, M. M. (1946). A Labile Iron Pool. *Journal of Biological Chemistry*, *165*, 397–398.

Gunshin, H., et al. (1997). Cloning and characterization of a mammalian proton-coupled metal-ion transporter. *Nature*, *388*, 482–488.

Hallberg, L., Brune, M., & Rossander, L. (1989). Iron absorption in man: inhibition by phytate. *American Journal of Clinical Nutrition*, *49*, 140–144.

Halliwell, B., & Chirico, S. (1993). Lipid peroxidation: its mechanism, measurement, and significance. *The American journal of clinical nutrition*, *57*, 715S-724S.

Halliwell, B., Clement, M. V., & Long, L. H. (2000). Hydrogen peroxide in the human body. *FEBS Letters*, *486*, 10–13.

Hamdi, A., et al. (2016). Erythroid cell mitochondria receive endosomal iron by a "kiss-and-run" mechanism. *Biochimica et Biophysica Acta - Molecular Cell Research, 1863*, 2859–2867.

Hamed, M. Y., Hider, R. C., & Silver, J. (1982). The competition between enterobactin and glutathione for iron. *Inorganica Chimica Acta*, *66*, 13–18.

Han, O., Failla, M. L., Hill, a D., Morris, E. R., & Smith, J. C. (1995). Reduction of Fe(III) is required for uptake of nonheme iron by Caco-2 cells. *The Journal of Nutrition*, *125*, 1291–1299.

Han, O. (2011). Molecular mechanism of intestinal iron absorption. Metallomics : Integrated Biometal, *Science*, *3*, 103–109.

Hanna, D. A., *et al.* (2016). Heme dynamics and trafficking factors revealed by genetically encoded fluorescent heme sensors. *Proceedings of the National Academy of Sciences*, 201523802.

Hanna, D. A., Martinez-Guzman, O., & Reddi, A. R. (2017). Heme Gazing: Illuminating Eukaryotic Heme Trafficking, Dynamics, and Signaling with Fluorescent Heme Sensors. *Biochemistry*, *56*, 1815-1823.

Hargrove, M. S., Barrick, D., & Olson, J. S. (1996). The association rate constant for heme binding to globin is independent of protein structure. *Biochemistry*, *35*, 11293–11299.

Harrison, P. M. (1963). The structure of apoferritin: Molecular size, shape and symmetry from X-ray data. *Journal of Molecular Biology*, *6*, 404–422.

Harvey, J., & Beutler, E. (1982). Binding of heme by glutathione S-transferase: a possible role of the erythrocyte enzyme. *Blood*, *60*, 1227–1230.

He, W., Feng, Y., Li, X., Wei, Y., & Yang, X. (2008). Availability and toxicity of Fe(II) and Fe(III) in Caco-2 cells. *Journal of Zhejiang University SCIENCE B*, *9*, 707–712.

Helm, L., & Merbach, A. E. (2005). Inorganic and bioinorganic solvent exchange mechanisms. *Chemical Reviews*, *105*, 1923–1959.

Hider, R. C*., et al.* (1990). Facilitated uptake of zinc into human erythrocytes. Relevance to the treatment of sickle-cell anaemia. *Biochemical Pharmacology*, *39*, 1005–1012.

Hider, R. C., & Kong, X. L. (2011). Glutathione: A key component of the cytoplasmic labile iron pool. *BioMetals*, *24*, 1179–1187.

Hider, R. C., & Kong, X. (2013). Iron speciation in the cytosol: an overview. *Dalton Trans*, *42*, 3220–3229.

Honarmand Ebrahimi, K., Bill, E., Hagedoorn, P. L., & Hagen, W. R. (2012). The catalytic center of ferritin regulates iron storage via Fe(II)-Fe(III) displacement. *Nat Chem Biol*, *8*, 941–948.

Ibrahim, N. G., Lutton, J. D., & Levere, R. D. (1982). The role of haem biosynthetic and degradative enzymes in erythroid colony development: the effect of haemin. *British journal of haematology*, *50*, 17-28.

Inoue, K., et al. (2008). Functional characterization of PCFT/HCP1 as the molecular entity of the carrier-mediated intestinal folate transport system in the rat model. *American Journal of Physiology: Gastrointestinal and Liver Physiology*, *294*, G660-668.

Iwahara, S. ichiro, Satoh, H., Song, D. X., Webb, J., Burlingame, A. L., Nagae, Y., & Muller-Eberhard, U. (1995). Purification, Characterization, and Cloning of a Heme-Binding Protein (23 kDa) in Rat Liver Cytosol. *Biochemistry*, *34*, 13398–13406.

Jacobs, A. (1977). Low Molecular Weight Intracelular Iron Transport Compounds. *Blood*, *50*, 433–439.

Johnson, L. (1987). *Physiology of the gastrointestinal tract volume 2*. 2nd edition, New York, Raven press, p 1437-1453

Kakhlon, O., & Cabantchik, Z. I. (2002). The labile iron pool: Characterization, measurement, and participation in cellular processes. *Free Radical Biology and Medicine*, *33*, 1037–1046.

Kalgaonkar, S., & Lönnerdal, B. (2008). Effects of dietary factors on iron uptake from ferritin by Caco-2 cells. *The Journal of Nutritional Biochemistry*, *19*, 33–9.

Keel, S. B., et al. (2008). A Heme Export Protein is Required for Red Blood Cell Differentiation and Iron Homeostasis. *Science*, *506*, 825–829.

Khan, A. A., & Quigley, J. G. (2011). Control of intracellular heme levels: Heme transporters and heme oxygenases. *Biochimica et Biophysica Acta - Molecular Cell Research*, *1813*, 668–682.

Kidane, T. Z., Sauble, E., & Linder, M. C. (2006). Release of iron from ferritin requires lysosomal activity. *American Journal of Physiology. Cell Physiology*, *291*, C445-55.

Kim, H. R., Won, S. J., Fabian, C., Kang, M. G., Szardenings, M., & Shin, M. G. (2015). Mitochondrial DNA aberrations and pathophysiological implications in hematopoietic diseases, chronic inflammatory diseases, and cancers. *Annals of Laboratory Medicine*, *35*, 1–14.

Kirschner-Zilber, I., Rabizadeh, E., & Shaklai, N. (1982). The interaction of hemin and bilirubin with the human red cell membrane. *Biochimica et Biophysica Acta - Biomembranes*, *690*, 20-30.

Knutson, M. D., Vafa, M. R., Haile, D. J., & Wessling-Resnick, M. (2003). Iron loading and erythrophagocytosis increase ferroportin 1 (FPN1) expression in J774 macrophages. *Blood*, *102*, 4191–4197.

Kondo, T., Dale, G. L., & Beutler, E. (1995). [8] Thiol transport from human red blood cells. *Methods in enzymology*, *252*, 72-82.

Korolnek, T., & Hamza, I. (2015). Macrophages and iron trafficking at the birth and death of red cells. *Blood*, *125*, 2893–2897.

Kruszewski, M. (2003). Labile iron pool: The main determinant of cellular response to oxidative stress. *Mutation Research - Fundamental and Molecular Mechanisms of Mutagenesis*, *531*, 81–92.

Kuban, R. J., et al. (1998). The iron ligand sphere geometry of mammalian 15-lipoxygenases. *The Biochemical Journal*, *332*, 237–242.

Kumar, S., & Bandyopadhyay, U. (2005). Free heme toxicity and its detoxification systems in human. *Toxicology Letters*, *157*, 175–188.

Kumar, C., *et al.* (2011). Glutathione revisited: a vital function in iron metabolism and ancillary role in thiol-redox control. *The EMBO Journal*, *30*, 2044–2056.

Laftah, A. H., Latunde-Dada, G. O., Fakih, S., Hider, R. C., Simpson, R. J., & McKie, A. T. (2009). Haem and folate transport by proton-coupled folate transporter/haem carrier protein 1 (SLC46A1). *The British Journal of Nutrition*, *101*, 1150–6.

Lane, D. J. R., & Lawen, A. (2009). Ascorbate and plasma membrane electron transport-Enzymes vs efflux. *Free Radical Biology and Medicine*, *47*, 485–495.

Lange, H., Kaut, A., Kispal, G., & Lill, R. (2000). A mitochondrial ferredoxin is essential for biogenesis of cellular iron-sulfur proteins. *Pnas*, *97*, 1050–5.

Layrisse, M., Martínez-Torres, C., Leets, I., Taylor, P., & Ramírez, J. (1984). Effect of histidine, cysteine, glutathione or beef on iron absorption in humans. *The Journal of Nutrition*, *114*, 217–223.

Le Blanc, S., Garrick, M. D., & Arredondo, M. (2012). Heme carrier protein 1 transports heme and is involved in heme-Fe metabolism. *AJP: Cell Physiology*, *302*, C1780–C1785.

Leong, W.-I., & Lönnerdal, B. (2004). Hepcidin, the recently identified peptide that appears to regulate iron absorption. *The Journal of Nutrition*, *134*, 1–4.

Li, T., Bonkovsky, H. L., & Guo, J. (2011). Structural analysis of heme proteins: implications for design and prediction. *BMC Structural Biology*, *11*, 13.

Lill, R., & Mühlenhoff, U. (2008). Maturation of iron-sulfur proteins in eukaryotes: mechanisms, connected processes, and diseases. *Annual Review of Biochemistry*, *77*, 669–700.

Lill, R., et al. (2012). The role of mitochondria in cellular iron-sulfur protein biogenesis and iron metabolism. *Biochimica et Biophysica Acta - Molecular Cell Research*, *1823*, 1491–1508.

López-Mirabal, H. R., & Winther, J. R. (2008). Redox characteristics of the eukaryotic cytosol. *Biochimica et Biophysica Acta - Molecular Cell Research*, *1783*, 629–640.

Lushchak, V. I. (2012). Glutathione Homeostasis and Functions: Potential Targets for Medical Interventions. *Journal of Amino Acids*, *2012*, 1–26.

Ma, Y., Abbate, V., & Hider, R. C. (2015). Iron-sensitive fluorescent probes: monitoring intracellular iron pools. *Metallomics*, *7*, 212–222.

Malo, C., & Wilson, J. X. (2000).Glucose modulates vitamin C transport in adult human small intestinal brush border membrane vesicles. J. Nutr. 130, 63–69.

Maret, W., & Wedd, A., (2014), *Binding, Transport and Storage of Metal Ion in Biological Cells*, Cambridge, Royal society of chemistry, 193-194

Martell, A. E., & Hancock, R. D. (2013). *Metal complexes in aqueous solutions*. Berlin, Springer Science & Business Media.

Martinez, S., & Hausinger, R. P. (2015). Catalytic mechanisms of Fe(II)- and 2-Oxoglutarate-dependent oxygenases. *Journal of Biological Chemistry*, *290*, 20702–20711.

May, J. M. (1998). Ascorbate function and metabolism in the human erythrocyte. *Frontiers in Bioscience : A Journal and Virtual Library*, *3*, d1-10.

Mayhew TM, Myklebust R, Whybrow A, & Jenkins R, (1999). Epithelial integrity, cell death and cell loss in mammalian small intestine. *Histol Histopathol*, *14***,** 257–267

McKie, A. et al. (2000) A novel duodenal iron-regulated transporter, IREG1, implicated in the basolateral transfer of iron to the circulation. *Molecular cell, 5*, 299-309.

Mergler, B. I., Roth, E., Bruggraber, S. F. A., Powell, J. J., & Pereira, D. I. A. (2012). Development of the Caco-2 model for assessment of iron absorption and utilisation at supplemental levels. *Journal of Pharmacy and Nutrition Sciences*, *2*, 26–33.

Morley, C. G. D., & Bezkorovainy, A. (1983). Identification of the iron chelate in hepatocyte cytosol. *IRCS medical science-biochemistry*, *11*, 1106-1107.

Mouritsen, O. & Andersen, S. (1998). *In search of a new biomembrane model*, Copenhagen, Biol. Skr. Dan. Vid. Selsk,

Muller-Eberhard, U., & Fraig, M. (1993). Bioactivity of heme and its containment. American *Journal of Hematology*, *42*, 59–62.

Murad, S., Grove, D., Lindberg, K. A., Reynolds, G., Sivarajah, A., & Pinnell, S. R. (1981). Regulation of collagen synthesis by ascorbic acid. *Proceedings of the National Academy of Sciences of the United States of America*, *78*, 2879–82.

Murphy, T. H., Miyamoto, M., Sastre, A., Schnaar, R. L., & Coyle, J. T. (1989). Glutamate toxicity in a neuronal cell line involves inhibition of cystine transport leading to oxidative stress. *Neuron*, *2*, 1547–1558.

Nagababu, E., & Rifkind, J. M. (2000). Reaction of Hydrogen Peroxide with Ferrylhemoglobin : Superoxide Production and Heme Degradation Reaction of Hydrogen Peroxide with Ferrylhemoglobin : Superoxide Production and Heme Degradation. *Biochemistry*, *39*, 12503–12511.

Nagababu, E. & Rifkind, J. (2005). Heme Degradation by Reactive Oxygen Species. *Analytical Chemistry*, *7*, 804–813.

Nemeth, E., et al. (2004). Hepcidin Regulates Cellular Iron Efflux by Binding to Ferroportin and Inducing Its Internalization. *Science*, *306*, 2090–2093.

Nishikimi, M., Fukuyama, R., Minoshima, S., Shimizu, N., & Yagi, K. (1994). Cloning and chromosomal mapping of the human nonfunctional gene for L-gulono-gamma-lactone oxidase, the enzyme for L-ascorbic acid biosynthesis missing in man. *The Journal of Biological Chemistry*, *269*, 13685–13688.

Noyer, C. M., Immenschuh, S., Liem, H. H., Muller-Eberhard, U., & Wolkoff, A. W. (1998). Initial heme uptake from albumin by short-term cultured rat hepatocytes is mediated by a transport mechanism differing from that of other organic anions. *Hepatology*, *28*, 150–155.

Ogawa, K., *et al.* (2001). Heme mediates derepression of Maf recognition element through direct binding to transcription repressor Bach1. *EMBO Journal*, *20*, 2835–2843.

Ohgami, R. S.et al. (2005). Identification of a ferrireductase required for efficient transferrin- dependent iron uptake in erythroid cells. *Nature genetics*, *37*, 1264.

Pan, B. T., & Johnstone, R. M. (1983). Fate of the transferrin receptor during maturation of sheep reticulocytes in vitro: Selective externalization of the receptor. *Cell*, *33*, 967–978.

Pandey, A., Pain, J., Ghosh, A. K., Dancis, A., & Pain, D. (2015). Fe-S cluster biogenesis in isolated mammalian mitochondria: Coordinated use of persulfide sulfur and iron and requirements for GTP, NADH, and ATP. *Journal of Biological Chemistry*, *290*, 640–657.

Parmley, R. T., Barton, J. C., Conrad, M. E., Austin, R. L., & Holland, R. M. (1981). Ultrastructural cytochemistry and radioautography of hemoglobin-iron absorption. *Experimental and Molecular Pathology*, *34*, 131–144.

Pereira, D. I. A., *et al*. (2013). Caco-2 cell acquisition of dietary iron(III) invokes a nanoparticulate endocytic pathway. *PLoS ONE*, *8*, 1–12.

Pereira, D. I. A., Lederer, B., & Powell, J. J. (2015). A balanced salt solution that prevents agglomeration of nano iron oxo - hydroxides in serum - free cellular assays. *Mater . Res., 2*, 015403

Petrat, F., Rauen, U., & de Groot, H. (1999). Determination of the chelatable iron pool of isolated rat hepatocytes by digital fluorescence microscopy using the fluorescent probe, phen green SK. *Hepatology*, *29*, 1171-1179.

Petrat, F., Weisheit, D., Lensen, M., de Groot, H., Sustmann, R., & Rauen, U. (2002). Selective determination of mitochondrial chelatable iron in viable cells with a new fluorescent sensor. *The Biochemical Journal*, *362*, 137–147.

Petry, N., Egli, I., Gahutu, J. B., Tugirimana, P. L., Boy, E., & Hurrell, R. (2014). Phytic Acid Concentration Influences Iron Bioavailability from Biofortified Beans in Rwandese Women with Low Iron Status 1 , 2. *The Journal of Nutrition*, *144*, 1681–1687.

Phelps, D. T., Deneke, S. M., Daley, D. L., & Fanburg, B. L. (1992). Elevation of glutathione levels in bovine pulmonary artery endothelial cells by N-acetylcystein. *American Journal of Respiratory Cell and Molecular Biology*, *7*, 293–299.

Pigeon, C., *et al.* (2001). A New Mouse Liver-specific Gene, Encoding a Protein Homologous to Human Antimicrobial Peptide Hepcidin, Is Overexpressed during Iron Overload. *Journal of Biological Chemistry*, *276*, 7811–7819.

Pinter, T. B., Dodd, E. L., Bohle, D. S., & Stillman, M. J. (2012). Spectroscopic and theoretical studies of Ga (III) protoporphyrin-IX and its reactions with myoglobin. *Inorganic chemistry*, *51*, 3743-3753.

Ponka, P. (1997). Tissue-specific regulation of iron metabolism and heme synthesis: distinct control mechanisms in erythroid cells. *Blood*, *89*, 1–25.

Ponka, P., Sheftel, A. D., English, A. M., Scott Bohle, D., & Garcia-Santos, D. (2017). Do Mammalian Cells Really Need to Export and Import Heme? *Trends in Biochemical Sciences*, *0*, 1–12.

Pountney, D. J., Raja, K. B., Simpson, R. J., & Wrigglesworth, J. M. (1999). The ferric-reducing activity of duodenal brush-border membrane vesicles is associated with a b-type haem. *BioMetals*, *12*, 53–62.

Prashanth, L., Kattapagari, K. K., Chitturi, R. T., Baddam, V. R. R., & Prasad, K. (2015). A review on role of essential trace elements in health and disease. *Journal of Dr. NTR University of Health Sciences*, *4*, 75.

Qiao, B., *et al.* (2012). Hepcidin-induced endocytosis of ferroportin is dependent on ferroportin ubiquitination. Cell Metabolism, 15, 918–924.

Qiu, A., *et al*. (2006). Identification of an Intestinal Folate Transporter and the Molecular Basis for Hereditary Folate Malabsorption. *Cell, 127*, 917–928.

Quigley, J. G., *et al.* (2004). Identification of a human heme exporter that is essential for erythropoiesis. *Cell, 118*, 757–766.

Rao, B. S., & Rao, K. S. (1992). Studies on the role of iron binding ligands and the intestinal brush border receptors in iron absorption. *Indian journal of biochemistry & biophysics*, *29*, 214-218.

Reed, J. R., Huber, W. J., & Backes, W. L. (2010). Human heme oxygenase-1 efficiently catabolizes heme in the absence of biliverdin reductase. *Drug Metabolism and Disposition, 38*, 2060–2066.

Reichstein, E., & Blostein, R. (1975). Arrangement of human erythrocyte membrane proteins. *J Biol Chem, 250*, 6256–6263.

Richman, P., & Meister, A. (1974). Regulation of y-Glutamyl-Cysteine Synthetase bv Nonallosteric Feedback Inhibition by Glutathione. *Biological Chemistry, 250,* 1422–1427.

Rhee, S. G. (2003). Cellular Regulation by Hydrogen Peroxide. *Journal of the American Society of Nephrology*, *14*, 211S–215.

Riss, T. L., *et al.* (2016). *Assay Guidance Manual*, (Internet), Eli Lilly & Company and the National Centre for Advancing Translations Sciences, p 356-360

Ross, S. L., *et al.* (2012). Molecular mechanism of hepcidin-mediated ferroportin internalization requires ferroportin lysines, not tyrosines or JAK-STAT. *Cell Metabolism, 15*, 905–917.

Ryter, S., & Tyrrell, R. M. (2000). The heme synthesis and degradation pathways: role in oxidant sensitivity. *Science, 28*, 289–309.

Sahini, V. E., Dumitrescu, M., Volanschi, E., Birla, L., & Diaconu, C. (1996). Spectral and interferometrical study of the interaction of haemin with glutathione. *Biophysical Chemistry, 58*, 245–253.

Salovaara, S., Sandberg, A.-S., & Andlid, T. (2002). Organic acids influence iron uptake in the human epithelial cell line Caco-2. *Journal of Agricultural and Food Chemistry, 50,* 6233–6238.

Sandberg, A. S. (2010). The use of Caco-2 cells to estimate Fe absorption in humans—a critical appraisal. *International Journal for Vitamin and Nutrition Research, 80,* 307.

Sato, H., Ido, K. I., & Kimura, K. (1994). Simultaneous separation and quantification of free and metal-chelated protoporphyrins in blood by three-dimensional HPLC. *Clinical Chemistry, 40*, 1239–1244.

Scotto, A. W., Changs, L. L., & Beattie, D. S. (1982). The Characterization and Submitochondrial Localization of S-Aminolevulinic Acid Synthase and an Associated Amidase in Rat Liver Mitochondria Using an Improved Assay for Both Enzymes. *The Journal of Biological Chemistry, 258,* 81–90.

Shannon, R. D. (1976). Revised effective ionic radii and systematic studies of interatomic distances in halides and chalcogenides. *Acta Crystallographica Section A, 32*, 751–767.

Sharp, P., Kaila Srai, S., & Subramaniam, N. (2007). Molecular mechanisms involved in intestinal iron absorption. *World J Gastroenterol World Journal of Gastroenterology World J Gastroenterol, 13,* 4716–4724.

Shayeghi, M., *et al.* (2005). Identification of an intestinal heme transporter. *Cell, 122*, 789–801.

Sheftel, A. D., Zhang, A. S., Brown, C., Shirihai, O. S., & Ponka, P. (2007). Direct interorganellar transfer of iron from endosome to mitochondrion. *Blood*, *110*, 125–132.

Shviro, Y., & Shaklai, N. (1987). Glutathione as a scavenger of free hemin. A mechanism of preventing red cell membrane damage. Biochemical Pharmacology, 36, 3801–3807.

Sievers, G., Hakli, H., Luhtala, J., & Tenhunen, R. (1987). Optical and ERP spectroscopy studies on heme arginate, a new compound used for the treatment of porphyria. *Chem Biol. Interactions, 63*, 105–114.

Silva, A. M. N., Kong, X., Parkin, M. C., Cammack, R., & Hider, R. C. (2009). Iron(iii) citrate speciation in aqueous solution. *Dalton Transactions*, 8616.

Silver, J., & Lukas, B. (1985). Studies on the reactions of ferric iron with glutathione and some related thiols. Part IV. A study of the reaction of glutathione with PPIX iron(III). *Inorganica Chimica Acta, 106,* 7–12.

Simoni, J., Villanueva-Meyer, J., Simoni, G., Moeller, J. F., & Wesson, D. E. (2009). Control of oxidative reactions of hemoglobin in the design of blood substitutes: Role of the ascorbate-glutathione antioxidant system. *Artificial Organs, 33*, 115–126.

Simpson, R. J., & Mohamad-chaffer, A. (1998). Glutahtione and duodenal reduction and absorption of iron. *Biochemical Society Transactions, 26*, S352.

Singer, A. S. J., & Nicolson, G. L. (1972). The Fluid Mosaic Model of the Structure of Cell Membranes. *Science, 175*, 720–731.

Sjoberg, B.-M., Reichard, P., Graslund, A., & Ehrenberg, A. (1978). The yrosine free radical in ribonucleotide reductase from E. coli. *The Journal of Biological Chemistry, 253,* 6863–6865.

Snider, M. D., & Rogers, D. C. (1985). Intracellular movement of cell surface receptors after endogliosis: resialylation of asial-transferin receptor in human erythroleukemia cells. *J. Cell Biol., 100*, 826–836.

Soboll, S., *et al.* (1995). The content of glutathione and glutathione S-transferases and the glutathione peroxidase activity in rat liver nuclei determined by a non-aqueous technique of cell fractionation. *The Biochemical Journal, 311*, 889–94.

Soe-Lin, S., Apte, S. S., Mikhael, M. R., Kayembe, L. K., Nie, G., & Ponka, P. (2010). Both Nramp1 and DMT1 are necessary for efficient macrophage iron recycling. *Experimental Hematology, 38*, 609–617.

Stadtman, E. R. (1992). Protein oxidation and aging. *Science, 257*, 1220-1224.

Stadtman, E. R. (1993). Oxidation of free amino acids and amino acid residues in proteins by radiolysis and by metal-catalyzed reactions. *Annual review of biochemistry, 62*, 797-821.

Stookey, L. L. (1970). Ferrozine a new spectrophotometric reagent for iron. *Analytical Chemistry, 42*, 779–781.

Sun, J., *et al.* (2002). Hemoprotein Bach1 regulates enhancer availability of heme oxygenase-1 gene. *EMBO Journal, 21*, 5216–5224.

Tailor, C. S., Willett, B. J., & Kabat, D. (1999). A putative cell surface receptor for anemia-inducing feline leukemia virus subgroup C is a member of a transporter superfamily. *Journal of Virology, 73*, 6500–6505.

Taketani, S., Adachi, Y., Ishii, T., & Chem, J. B. (1998). Molecular Characterization of a Newly Identified Heme-binding Protein Induced during Differentiation of urine erythroleukemia cells. *The Journal of Biological Chemistry*, *273*, 31388–31394.

Tanford, C. (1980). *The hydrophobic effect formation of micelles and biological membranes*, New Jersey, John Wiley & Sons, Inc., p 200-201

Tang, D., Shi, Y., Kang, R., Li, T., Xiao, W., Wang, H., & Xiao, X. (2006). Hydrogen peroxide stimulates macrophages and monocytes to actively release HMGB1. *Journal of Leukocyte Biology*, *81*, 741–747.

Tangerås, A. (1984). Separation of haem compounds by reversed-phase liquid chromatography and its application in the assay of ferrochelatase activity. *Journal of Chromatography, 310*, 31–39.

Tenhunen, R., Marver, H. S., & Schmid, R. (1968). The enzymatic conversion of heme to bilirubin by microsomal heme oxygenase. *Pnas*, *61,* 748–755.

Tenhunen, R., Gräsbeck, R., Kouvonen, I., & Lundberg, M. (1980). An intestinal receptor for heme: Its partial characterization. *International Journal of Biochemistry, 12*, 713–716.

Topf, M., Sandala, G. M., Smith, D. M., Schofield, C. J., Easton, C. J., & Radom, L. (2004). The unusual bifunctional catalysis of epimerization and desaturation by carbapenem synthase. *Journal of the American Chemical Society, 126*, 9932–9933.

Trewick, S. C., Henshaw, T. F., Hausinger, R. P., Lindahl, T., & Sedgwick, B. (2002). Oxidative demethylation by Escherichia coli AlkB directly reverts DNA base damage. *Nature, 419*, 174–178.

Uc, A., Stokes, J. B., & Britigan, B. E. (2004). Heme transport exhibits polarity in Caco-2 cells: evidence for an active and membrane protein-mediated process. *American Journal of Physiology. Gastrointestinal and Liver Physiology, 287*, G1150-7.

Victor, V. V., Guayerbas, N., Puerto, M., Medina, S., & De La Fuente, M. (2000). Ascorbic acid modulates in vitro the function of macrophages from mice with endotoxic shock. *Immunopharmacology*, *46*, 89–101.

Vaillancourt, F. H., Yeh, E., Vosburg, D. a, O'Connor, S. E., & Walsh, C. T. (2005). Cryptic chlorination by a non-haem iron enzyme during cyclopropyl amino acid biosynthesis. *Nature, 436*, 1191–1194.

Verkleij, A. J., *et al.* (1973). The asymmetric distribution of phospholipids in the human red cell membrane. A combined study using phospholipases and freeze-etch electron microscopy. *Biochimica et Biophysica Acta – Biomembranes, 323*, 178–193.

Vincent, S. (1989). Oxidative effects of heme and porphyrins on proteins and lipids. *Seminars in Hematology, 26*, 105–113.

Vincent, S. H., & Muller-Eberhard, U. (1985). A protein of the Z class of liver cytosolic proteins in the rat that preferentially binds heme. *Journal of Biological Chemistry*, *260*, 14521–14528.

Vulpe, C. D., *et al.* (1999). Hephaestin, a ceruloplasmin homologue implicated in intestinal iron transport, is defective in the sla mouse. *Nature Genetics, 21*, 195–199.

Walsh, R., Kaldor, I., Brading, I., & George, E. (1955). The availability of iron in meat : some experiments with radioactive iron. *Australasian Annals of Medicine, 4*, 272–276.

Wanders, R. J. A., Komen, J., & Ferdinandusse, S. (2011). Phytanic acid metabolism in health and disease. *Biochimica et Biophysica Acta - Molecular and Cell Biology of Lipids, 1811,* 498–507.

Welch, R. W., Wang, Y., Crossman, A., Park, J. B., Kirk, K. L., & Levine, M. (1995). Accumulation of vitamin C (ascorbate) and its oxidized metabolite dehydroascorbic acid occurs by separate mechanisms. *Journal of Biological Chemistry*.

West, A. R., & Oates, P. S. (2008). Mechanisms of heme iron absorption: Current questions and controversies. *World Journal of Gastroenterology, 14*, 4101–4110.

Whitehead, M. W., Thompson, R. P., & Powell, J. J. (1996). Regulation of metal absorption in the gastrointestinal tract. *Gut*, *39*, 625–628.

Williams, R. J. P. (1982). Free manganese(II) and iron(II) cations can act as intracellular cell controls. *FEBS Letters, 140*, 3–10.

Winterbourn, C. C., McGrath, B. M., & Carrell, R. W. (1976). Reactions involving superoxide and normal and unstable haemoglobins. *The Biochemical Journal, 155*, 493–502.

Winterbourn, C. C. (1995). Toxicity of iron and hydrogen peroxide: the Fenton reaction. *Toxicology Letters, 82–83*, 969–974.

Worthington, M. T., Cohn, S. M., Miller, S. K., Luo, R. Q., & Berg, C. L. (2001). Characterization of a human plasma membrane heme transporter in intestinal and hepatocyte cell lines. *American Journal of Physiology. Gastrointestinal and Liver Physiology, 280,* G1172–G1177.

Wyllie, J., & Kaufman, N. (1982). An electron microscopic study of heme uptake by rat duodenum. *Laboratory Investigation, 47*, 471–476.

Yamaguchi, A., Akasaka, T., Ono, N., Someya, Y., Nakatani, M., & Sawai, T. (1992). Metal-tetracycline/H+ antiporter of escherichia coli encoded by transposon Tn10. *Journal of Biological Chemistry, 267*, 7490–7498.

Yamashiro, D. J., Tycko, B., Fluss, S. R., & Maxfield, F. R. (1984). Segregation of Transferrin to a Mildy Acidic (pH 6.5) Para-Golgi Compartment in the Recycling Pathway. *Cell, 37*, 789–800.

Yang, Z., et al. (2010). Kinetics and specificity of Feline Leukemia Virus Subgroup C Receptor (FLVCR) export function and its dependence on hemopexin. *Journal of Biological Chemistry, 285,* 28874–28882.

Yang, W. S., *et al.* (2014). Regulation of ferroptotic cancer cell death by GPX4. *Cell*, *156*, 317–331.

Yang, W. S., & Stockwell, B. R. (2016). Ferroptosis: Death by Lipid Peroxidation. *Trends in Cell Biology, 26,* 165–176.

Zhao, N., & Enns, C. (2012). Iron transport machinery of human cells: Players and their interactions. *Current Topics in Membranes, 69*, 67–93.

Zhong, J. L., Yiakouvaki, A., Holley, P., Tyrrell, R. M., & Pourzand, C. (2004). Susceptibility of skin cells to UVA-induced necrotic cell death reflects the intracellular level of labile iron. *Journal of Investigative Dermatology, 123*, 771–780.

Appendix A – Ferrozine Experiment

Methodology

Influence of Amino Acids, Ascorbic Acid and Glutathione on Hematin Absorption Analysed by Ferrozine Assay

Cells were seeded in 6 well plates (6 well cell culture cluster plates, Corning, New York, USA). The experiment was conducted in triplicate. Each experimental treatment was performed in triplicate for each replication of the experiment. The triplicates were averaged and the mean values were used for statistical analysis.

Formulation of Uptake Solutions

Stock solutions of hematin (100 mM) in 0.1 N NaOH and iron(II) chloride (100 mM) in ddH_2O were prepared immediately prior to use. Stock solutions of glutathione (910 mM), cysteine (910 mM), ascorbic acid (80 mM), arginine (910 mM), histidine (290 mM) and glycine (910 mM) were made in 200 mM potassium phosphate buffer (pH 8) and adjusted to pH 8 with 0.1 N NaOH.

Hematin uptake solutions in phenol free MEM supplemented with a final concentration of 66.7 mM potassium phosphate buffer contained 2 mM hematin, and either 91 mM glutathione, 91 mM cysteine, 8 mM ascorbic acid, 91 mM arginine, 91 mM histidine, 91 mM glycine or no additive.

Iron(II) chloride uptake solution in phenol free MEM supplemented with a final concentration of 66.7 mM potassium phosphate buffer contained 2 mM $FeCl_2$.

All solutions were prepared immediately prior to use and filter-sterilised through 0.22-µm filters.

Incubation with Hematin or $FeCl_2$

MEM was aspirated from each well after 16 hours and monolayers were washed once with phenol free MEM. Uptake solution (1 mL of each, nine in total) was added to each well and monolayers were incubated for 1 hour at 37^{o}C, 5% CO_2, 95% air atmosphere. Medium was aspirated from monolayers and cells were washed twice with PBS (150 µL). Cells were collected and disrupted with HEPES saline (10 mM HEPES pH 7.4, 0.9% (w/v) sodium chloride) (160 µL) and a cell scraper, the resulting digested cells were collected.

Ferrozine Assay

The digested cells (90 µL) were added to 20% (w/v) trichloroacetic acid in 4% (w/v) sodium pyrophosphate (200 µL) and boiled for 5 minutes. Samples were centrifuged at 12,000 rpm for 5 minutes. Supernatant (200 µL), was added to Ferrozine solution, (38.3 mM sodium ascorbate, 1.3 mM ferrozine, 1.4 M sodium acetate) (600 µL), incubated for 10 minutes, plated in triplicate in a 96-well plate and absorbance measured at 562 nm (Bio-Tek ELx800 plate reader).

Protein Assay

The protein content of the digested cells was determined using BioRad DC Protein Assay Kit. Solution S (40 µL) was added to 2 mL of solution A, forming solution X. The digested cells were diluted one in four in ddH_2O, and added (40 µL) to solution X (40 µL), solution B (320 µL) was then added to the lysate-solution X mix and left to incubate at room temperature for 10 minutes. The protein assay solution (100 µL) was plated in triplicate in a 96-well plate and absorbance read at 750 nm on a spectrophotometric plate reader. Standards using BSA dissolved in water were run and a standard curve drawn with lineal regression in GraphPad Prism. The mean absorbance for each sample and the protein standard curve was used to determine the amount of protein in each sample.

Statistical Analysis of Iron Absorption

The amount of hematin or $FeCl_2$ absorbed into cells (nmol) per µg protein was calculated from the mean of each experimental repeat. The mean value with standard error of the mean (SEM) plotted for each condition in GraphPad Prism. A 1-way ANOVA in GraphPad Prism, with alpha set at 0.05, was conducted on the mean repeat values to determine if there was a significant difference in hematin (or $FeCl_2$) absorbed from each condition compared to cells incubated with only hematin.

Results

Detection of Iron Absorbed into Caco-2 cells by Ferrozine Assay

There was no significant difference in the amount of iron (organic or inorganic) associated with the Caco-2 cells, over one hour, when comparing inorganic iron source ($FeCl_2$) to organic iron source (hematin). Cells incubated with $FeCl_2$ had 1.8 iron µmol/µg protein of iron associated with the monolayer whilst cells incubated with hematin had 1.5 µmol iron/µg protein (Figure 3-5). The addition of ascorbic acid, cysteine, arginine, histidine or glycine had no significant effect on the amount of hematin associated with the monolayer (Figure 3-5). However the presence of glutathione within the uptake medium significantly

($P < 0.05$) increased the amount of hematin associated with the monolayers, to 3.9 μmol iron/μg protein, compared to cells that were incubated with hematin only (Figure A-1). This would indicate that the GS.hematin complex significantly increased the amount of hematin associated with the enterocytes whist the presence of cysteine, which also contains a thiol group, appreciably increased hematin association.

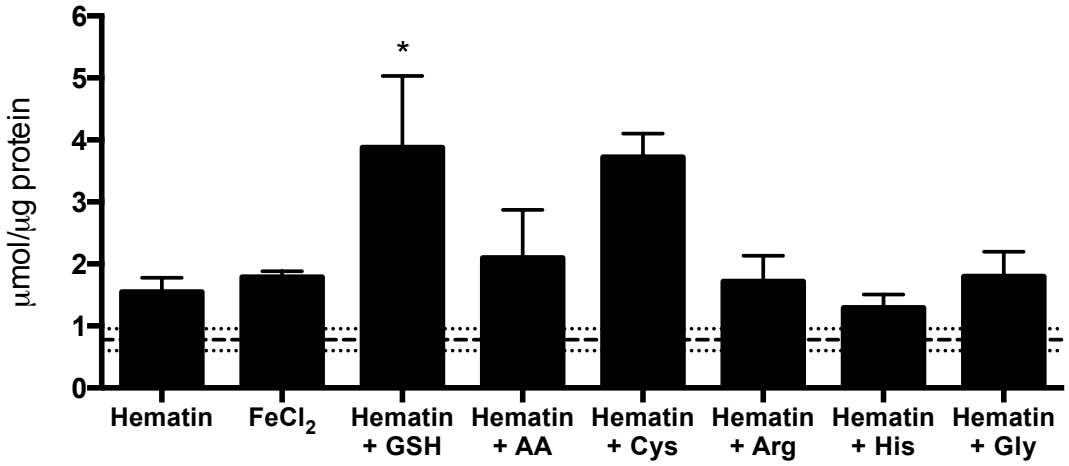

Figure A-1. Influence of amino acids, glutathione and ascorbic acid on cell associated iron detected by ferrozine assay. Caco-2 cell monolayers were grown for 14 days in 12-well plates at 37 ^{o}C, 95 % air, 5 % CO_2, depleted of iron for 16 hours then incubated with either 2 mM $FeCl_2$ and 900 μM ascorbic acid or 2 mM hematin alone or supplemented with glutathione (GSH), cysteine (Cys), arginine (Arg), histidine (His) or glycine (Gly) at 91 mM or ascorbic acid (AA) at 8 mM for 1 hour at 37 ^{o}C, 95 % air, 5 % CO_2. Monolayers were washed 3 times and cells collected for detection of iron. Negative control contained no hematin or $FeCl_2$ in uptake solution and the mean (- - -) ± SEM (˙ ˙ ˙) is plotted on the graph. Values are means ± SEM (n=3 experimental triplicates). Asterisks indicate significant difference in iron cell content ($P < 0.05$ *) hematin vs. each condition.

The principle of the ferrozine assay is based on the change in electron configuration, and resulting change in absorption, of ferrozine molecules when chelated to ferrous inorganic iron (Stookey 1970). Hematin, is a more complex molecule then inorganic iron, consisting of ferric inorganic iron bound to the centre of protoporphyrin IX. Therefore the samples require processing, to release and oxidise the iron, prior to detection by ferrozine. The process by which iron is extracted, oxidised and subsequently chelated by three ferrozine molecules, from hematin, is not efficient and requires several different conditions. This could account for the erroneous results recorded on hematin association with Caco-2 cells detected using the ferrozine assay (Figure A-1). The lack of sensitivity of the machinery and protocol could also contribute to the erroneous results.

The high concentration of iron, both organic and inorganic, required to produce results from the ferrozine assay mean that precipitation of the iron from the uptake solutions is

highly likely. Precipitated iron will settle on the membrane of the Caco-2 cell monolayer and would not be washed off by PBS. This results in the precipitated iron being collected with the cells and contributing to the amount of iron detected within the samples. This would cause inaccuracy in the recorded amount of iron associated with the Caco-2 cells as not only does the sample contain iron within the cell, iron associated with the Caco-2 membrane but also iron which has precipitate and settled at the bottom of the well.

Taking the above issues into consideration the decision was made to use radioactive hematin ([^{59}Fe]hematin) for all future experiments investigating hematin and Caco-2 interaction. The lower concentration of hematin and $FeCl_2$ required for experiments using [^{59}Fe]hematin or $^{59}FeCl_2$ meant a lower possibility of iron precipitation and the single step to collect and analyse the amount of iron associated with the Caco-2 cells should result in more accurate readings.